University of New Orleans
ScholarWorks@UNO

University of New Orleans Theses and Dissertations | Dissertations and Theses

12-15-2007

Long-Term Ambient Noise Statistics in the Gulf of Mexico

Mark Alan Snyder
University of New Orleans

Follow this and additional works at: https://scholarworks.uno.edu/td

Recommended Citation

Snyder, Mark Alan, "Long-Term Ambient Noise Statistics in the Gulf of Mexico" (2007). *University of New Orleans Theses and Dissertations*. 595.
https://scholarworks.uno.edu/td/595

This Dissertation is protected by copyright and/or related rights. It has been brought to you by ScholarWorks@UNO with permission from the rights-holder(s). You are free to use this Dissertation in any way that is permitted by the copyright and related rights legislation that applies to your use. For other uses you need to obtain permission from the rights-holder(s) directly, unless additional rights are indicated by a Creative Commons license in the record and/or on the work itself.

This Dissertation has been accepted for inclusion in University of New Orleans Theses and Dissertations by an authorized administrator of ScholarWorks@UNO. For more information, please contact scholarworks@uno.edu.

Long-Term Ambient Noise Statistics in the Gulf of Mexico

A Dissertation

Submitted to the Graduate Faculty of the
University of New Orleans
in partial fulfillment of the
requirements for the degree of

Doctor of Philosophy
In
Engineering and Applied Science

by

Mark Alan Snyder

B.S. University of Illinois, 1981
M.S. University of New Orleans 1986

December 2007

Acknowledgements

I want to thank my Dissertation Committee members for their valuable and insightful comments and the guidance they provided during the writing of this dissertation as well as the teaching and mentoring they provided during many classes over the years: my Committee Chairs Dr. George E. Ioup and Dr. Stanley A. Chin-Bing, and the members Dr. Juliette W. Ioup, Dr. Joseph E. Murphy from the Department of Physics (University of New Orleans), Dr. Vesselin P. Jilkov from the College of Engineering (University of New Orleans), and Dr. Anthony I. Eller from Science Applications International Corporation.

I also want to thank my wife Marlene and my daughters Elizabeth and Victoria for their love, support and patience with me during the long process of finishing this dissertation.

I am grateful that my employer, the Naval Oceanographic Office, supported me during this endeavor. This included ship cruises to deploy and recover the EARS buoys, as well as the time to do the processing and analysis of the data.

I also want to thank Dr. Peter A. Orlin of the Naval Oceanographic Office and Dr. Anthony I. Eller from my Dissertation Committee for their computer software support. Dr. Orlin wrote the MATLAB © code that was used to process the raw acoustic data and produce the spectrogram and percentile plots. Dr. Eller wrote the MATLAB © code that was used to calculate the fluctuation spectra of the data and produce the coherence time and distribution of variance plots.

Josette Fabre of the Naval Research Laboratory at Stennis Space Center was very helpful in running the Historical Temporal Shipping Data Base Vessel Motion Simulation (HVMS) model within the Dynamic Ambient Noise Model (DANM) and producing plots of the shipping lanes in the Gulf of Mexico.

Finally, I want to thank and dedicate this dissertation to my parents, Harriet M. Snyder and the late Richard G. Snyder. They have given me strong support and encouragement throughout my life and instilled in me a love for learning. My father was an outstanding high-school math teacher, and sparked my interest in math and science.

Table of Contents

List of Figures

List of Tables

Nomenclature and Abbreviations

BWF – Beaufort Wind Force

dB – decibel

CDF – Cumulative Distribution Function

CEP – Cumulative Exceedance Probability

CT – Coherence Time

CTD – Conductivity Temperature Depth

dof – degrees of freedom

DSCA – Deep Sound Channel Axis

EARS – Environmental Acoustic Recording System

FFT – Fast Fourier Transform

IAT – Inter-Arrival Time

JD – Julian Date

μPa – micropascal

MLD – Mixed Layer Depth

NAVOCEANO – Naval Oceanographic Office

NDBC – National Data Buoy Center

NOAA – National Oceanic and Atmospheric Administration

PDF – Probability Density Function

PSD – Power Spectral Density

XBT – Expendable BathyThermograph

Abstract

Long-term omni-directional ambient noise was collected at several sites in the Gulf of Mexico during 2004 and 2005. The Naval Oceanographic Office deployed bottom moored Environmental Acoustic Recording System (EARS) buoys approximately 159 nautical miles south of Panama City, Florida, in water depths of 3200 meters. The hydrophone of each buoy was 265 meters above the bottom. The data duration ranged from 10-14 months. The buoys were located near a major shipping lane, with an estimated 1.5 to 4.5 ships per day passing nearby. The data were sampled at 2500 Hz and have a bandwidth of 10-1000 Hz.

Data are processed in eight 1/3-octave frequency bands, centered from 25 to 950 Hz, and monthly values of the following statistical quantities are computed from the resulting eight time series of noise spectral level: mean, median, standard deviation, skewness, kurtosis and coherence time.

Four hurricanes were recorded during the summer of 2004 and they have a major impact on all of the noise statistics. Noise levels at higher frequencies (400-950 Hz) peak during extremely windy months (summer hurricanes and winter storms). Standard deviation is least in the region 100-200 Hz but increases at higher frequencies, especially during periods of high wind variability (summer hurricanes). Skewness is positive from 25-400 Hz and negative from 630-950 Hz. Skewness and kurtosis are greatest near 100 Hz. Coherence time is low in shipping bands and high in weather bands, and it peaks during hurricanes.

The noise coherence is also analyzed. The 14-month time series in each 1/3-octave band is highly correlated with other 1/3-octave band time series ranging from 2 octaves below to 2 octaves above the band's center frequency. Spatial coherence between hydrophones is also analyzed for hydrophone separations of 2.29, 2.56 and 4.84 km over a 10-month period. The noise field is highly coherent out to the maximum distance studied, 4.84 km.

Additionally, fluctuations of each time series are analyzed to determine time scales of greatest variability. The 14-month data show clearly that variability occurs primarily over three time scales: 7-22 hours (shipping-related), 56-282 hours (2-12 days, weather-related) and over an 8-12 month period.

Keywords

Ambient noise, autocorrelation, acoustics, coherence, correlation, fluctuations, Fourier transform, Gulf of Mexico, hurricanes, kurtosis, long-term, omni-directional, percentiles, power spectral density, probability density functions, shipping noise, skewness, spectrogram, standard deviation, statistics, underwater, variability, variance, wave height, weather noise, wind speed.

Chapter 1
Introduction and Overview

1.1 Introduction

Recent advances in technology have made it easier to record ambient noise in the ocean for long time periods. The Naval Oceanographic Office has been deploying Environmental Acoustic Recording System (EARS) buoys to record long-term ambient noise in the ocean since 1996. In 2004 and 2005 seven EARS buoys of a new design were deployed in the Gulf of Mexico in order to compare their performance to EARS buoys of an older design. One of these bottom-mounted, omni-directional buoys was deployed in April 2004 in a location with a water depth of around 3200 meters; the hydrophone depth was around 2935 meters (the hydrophone was moored about 265 meters above the bottom). In August 2004 this buoy was recovered, four months of data were retrieved, and this buoy plus six others were deployed for another ten months. They recorded continuously until their final recovery in May 2005. The recovered data are of high quality, and consist of almost fourteen months (with a two day gap in August 2004) of continuous recording at one buoy location at a sampling rate of 2500 Hz and almost ten months at six nearby locations. The data have a useful bandwidth of 10-1000 Hz.

Two principal sources of underwater ambient noise in the band 10-1000 Hz include noise from wind and shipping [Wenz, 1962]. Distant shipping traffic is a principal source of noise in the region of 10 to 300 Hz; see Figure 1.1. Although shipping energy is dominant in the 10-300 Hz region, shipping noise extends well beyond 500 Hz, especially for nearby or extremely loud ships [Hall, 2004]. Ambient noise in the region of about 300 Hz and above is dominated by weather (as measured by wave height or wind speed) [Wenz, 1962]. As can be seen from Figure 1.1, shipping noise can be important at high frequencies when weather noise is low, and weather noise can be important at low frequencies when shipping noise is low.

1.2 Overview

The goal of this dissertation research is how best to characterize the ambient noise in long-term data sets, and how to quantify the contributions of the wind and shipping sources in

the band 10 – 1000 Hz. This includes describing the overall background noise distribution (the long period fluctuations in the data due to weather and distant shipping) as well as the discrete shipping noise distribution (the short period fluctuations in the data due to nearby ships).

Chapter 2 discusses the methodology used to process the data.

Chapter 3 is a summary of the environmental conditions in the region of the Gulf of Mexico near the EARS buoys. It includes a discussion of historical data as well as data collected during the EARS deployment cruise of August 2004.

Chapter 4 provides a detailed examination of the monthly statistics from April 2004 to May 2005. MATLAB © is used to analyze the monthly data over eight 1/3-octave frequency bands, centered at the following frequencies: 25, 50, 100, 200, 400, 630, 800 and 950 Hz. The following statistical quantities are computed monthly at each frequency: mean, median, standard deviation, skewness, kurtosis, coherence time and the 10^{th} and 90^{th} percentiles. Trends in the data (plotted versus time and frequency) are discussed.

Chapter 5 provides an examination of the long-term statistical trends in the data. This includes an analysis of each of the fourteen month time series at each of the eight 1/3-octave bands, focused on the long term variability as a function of frequency. This enables a comparison of month-to-month variability versus long-term (seasonal and annual) variability. Shipping and weather processes have distinctly different variability time scales. There is also an attempt to classify each fourteen month probability density function (PDF) in each frequency band. The shape of each PDF is determined by the relative contributions of shipping and weather noise in each band.

Chapter 6 discusses threshold crossing statistics. The monthly time series for each of the frequency bands are analyzed for their peaks and troughs. The ordered statistics concerning the peaks and troughs are important because they describe the temporal variation of the noise. The following statistical quantities are computed for the peaks and troughs: peaks/troughs per day, peak/trough duration (time above/below a specified threshold), and peak/trough inter-arrival times (intervals between peaks/troughs). Two types of thresholds are investigated. One is an absolute threshold for each frequency band and month: the 10^{th} percentile for troughs and the 90^{th} percentile for peaks. The second is a relative threshold, based on a six hour running average of the data and the monthly standard deviation in each frequency band.

In Chapter 7 the coherence (spatial, temporal, and frequency) of the ambient noise field is investigated. The coherence time and frequency correlation coefficient are computed and compared at three EARS buoys over a ten month period. An additional four months of data are analyzed at one location. The spatial coherence between the three EARS buoys is analyzed for hydrophone separations of 2.29, 2.56, and 4.84 km over a ten month period.

In Chapter 8 the average noise measured by the EARS buoys is compared to the weather and shipping noise results of Wenz and others (Figure 1.1). The National Oceanic and Atmospheric Administration (NOAA), through the National Data Buoy Center (NDBC), operates a network of weather buoys in the Gulf of Mexico [National Data Buoy Center, 2007]. Two NDBC buoys close to the EARS buoys recorded wind speed and wave height data for the entire EARS data acquisition period (Figure 1.2). The wind and wave data are separated into monthly time series. This allows for monthly comparisons of wind speed, wave height and ambient noise levels at the EARS locations.

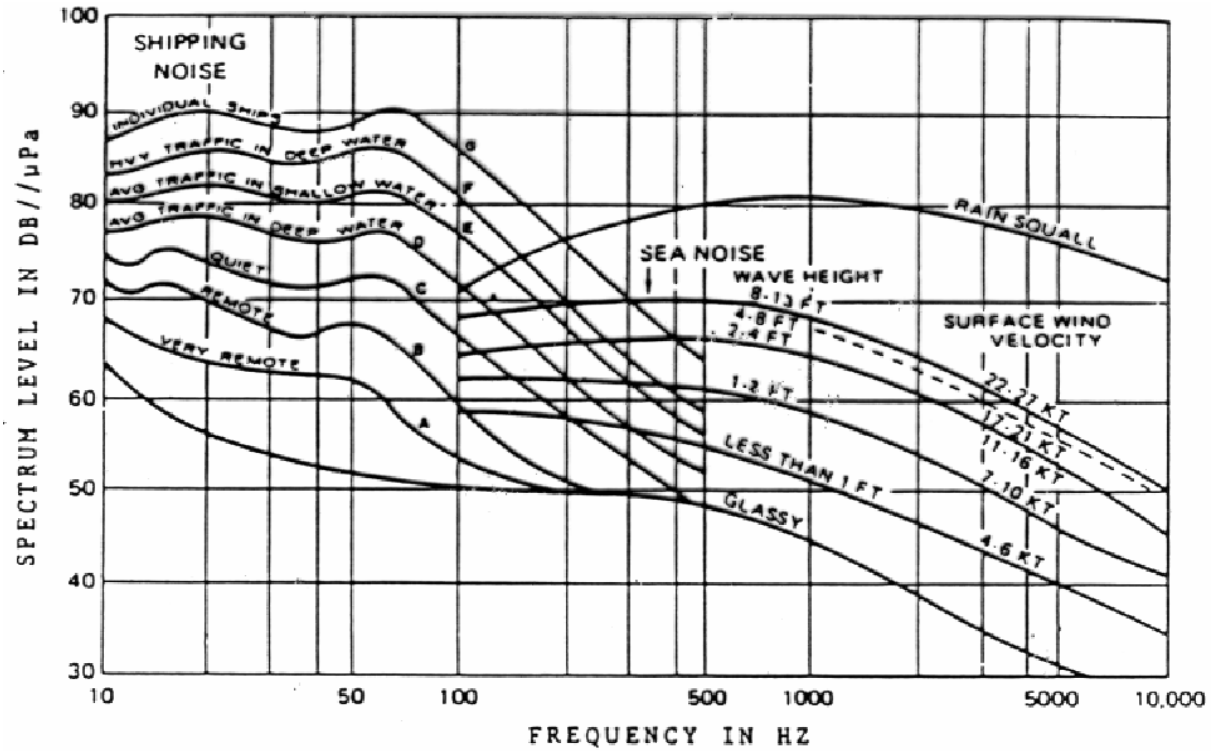

Figure 1.1 Wenz curves.

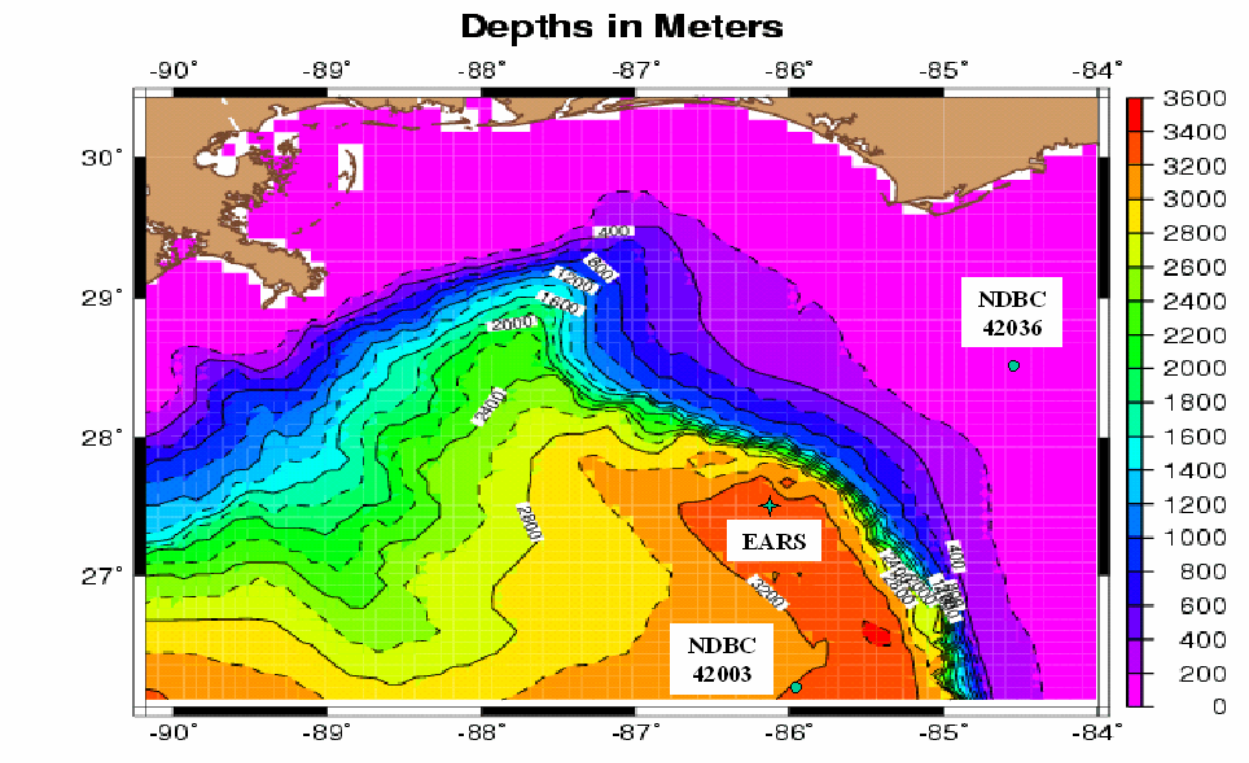

Figure 1.2 Gulf of Mexico bathymetry and location of EARS buoys and NDBC weather buoys.

Chapter 9 discusses the results of a comparison of day versus night ambient noise data. Four months representing the four seasons are analyzed to look for any diurnal variability in the data. The data in each frequency band are separated into day and night periods for each month and the following statistical parameters are computed: the mean, standard deviation, and skewness.

Conclusions are discussed in chapter 10. Section 10.1 contains a summary of the monthly statistics. The passage of four hurricanes during the summer of 2004 (three during the month of September) had a major impact on all of the statistical quantities measured, which are summarized in section 10.2. The statistics computed over the entire fourteen month period are discussed in section 10.3, followed by the threshold crossing results in section 10.4. The coherence of the ambient noise field is summarized in section 10.5. The comparison of day versus night noise data is discussed in section 10.6. Current research in this area is described in section 10.7. Section 10.8 discusses a proposed ambient noise model for this region of the Gulf of Mexico that is based on all of these observations. The chapter concludes with some suggestions for future work.

Appendix A provides the fourteen monthly spectrograms at site EARS A1. Each spectrogram displays the noise level (in dB re 1 μPa^2 per Hz) as a function of time and frequency. The spectrograms have a time resolution of ten minutes and a frequency resolution of 1 Hz.

Appendix B provides the fourteen monthly percentile plots at site EARS A1. Each plot displays the average noise power (in dB re 1 μPa^2 per Hz) calculated in each 1/3-octave frequency band from 16 Hz to 950 Hz. Five percentiles are plotted: the 10^{th}, 25^{th}, 50^{th}, 75^{th} and 90^{th} percentiles are displayed as a function of frequency.

Appendix C contains monthly plots of the average power (in dB re 1 μPa^2 per Hz) in the 900 to 1000 Hz band at site EARS A1, computed every ten minutes. Each plot also shows the six hour running average power, as well as the monthly mean level, the monthly 10^{th} percentile and the monthly 90^{th} percentile.

Appendix D provides the fourteen monthly significant wave height measurements (in meters) at the two NDBC weather buoys. The wave measurements were made hourly and have a high correlation with the measured EARS noise levels in the higher frequency bands.

Appendix E contains a copyright permission letter.

Appendix F contains a summary of the statistical definitions used in this document.

Chapter 2
Methodology

The EARS buoy at site A1 was deployed on 03 April 2004. On 02 August 2004 this buoy was recovered, the data were downloaded, and the buoy was redeployed. Six other buoys (designated A2-A7) were also deployed at this time. Each of the buoys A2-A7 was deployed on a circle of approximate radius 2.5 km, with A1 at the center of the circle. Each of the seven EARS buoys then recorded continuously until 23 May 2005 when all of the buoys were recovered. Upon recovery, site A1 had collected data for 14 months (from April 2004 to May 2005, 11 complete months and 3 partial months) or a total of 412 days of uncorrupted data. The EARS buoys at the other sites (A2-A7) collected data from August 2004 to May 2005, or a total of approximately 10 months of data. Most of this dissertation will deal with the 14 months of data collected at site A1. However, the data from sites A3 and A6 are used in section 7.1 on spatial coherence.

The EARS buoys each used a High Tech HT1-90-U hydrophone with a sensitivity of -197 dB reference 1 volt per micropascal. The system gain was 35 dB. The clipping level was 156 dB reference 1 micropascal. The A/D sampling rate was 2500 Hz. The data have a useful bandwidth of 10-1000 Hz, limited at each end by filter roll-off and aliasing[1]. The gain in the 10 Hz to 1000 Hz passband was flat to within ±0.5 dB.

At site A1, raw data were sampled continuously for fourteen months at 2500 Hz. Time periods corrupted by clipping and spinning of the hard disks inside the EARS buoy are removed during processing; see Figure 2.1. The remaining data are processed using the Bartlett method with a Hann window [Stoica and Moses, 1997] and a 2048-point non-overlapping Fast Fourier Transform (FFT), corresponding to 0.82 seconds of data. A 0.82 second segment of data is read in and multiplied by a Hann window in the time domain. A 2048-point FFT is computed for this segment and then the periodogram estimate is calculated. This process is repeated 732 times for each 10 minute segment of raw data (732 x 0.82 seconds = 10 minutes). The 732 resulting periodograms are then averaged, using a 90% acceptance factor. (At least 659 out of the 732 segments of data had to contain valid data for the 10 minute average periodogram to be accepted.

[1] The raw data from 1000-1250 Hz are potentially aliased and therefore not used in this analysis.

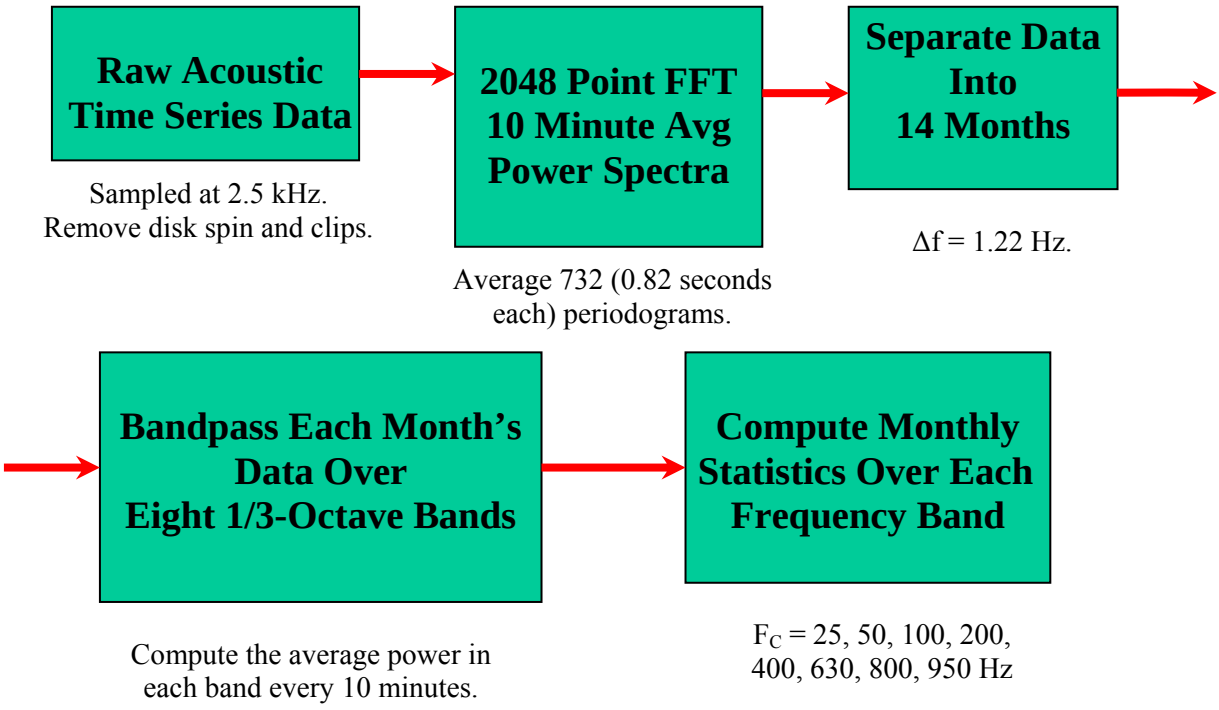

Figure 2.1 Data processing.

Using this criterion, every 10 minute period for the entire 14 months was accepted.) Each 10 minute average result is converted to decibels (dB). (All noise levels in this dissertation are computed as spectrum levels, with units of dB reference 1 micropascal[2] per Hz.[2]) This yields the Power Spectral Density (PSD) estimate for this 10 minute segment of data. This process is repeated for the next 10 minute segment of data (with no overlap) until the entire fourteen month data set is processed. At this point the processed data have a frequency resolution given by Δf = 2500Hz / 2048 = 1.22 Hz.

The data are then separated into 14 monthly intervals, and each month's data are separated into eight 1/3-octave frequency bands. Table 2.1 shows the third-octave bandwidths for each center frequency, F_c. The first seven values, from 25-800 Hz, are standard 1/3-octave center frequencies. The last value, 950 Hz, is chosen as the approximate geometric mean

[2] The ambient noise level is the intensity in decibels of the ambient noise measured by an omnidirectional hydrophone and referenced to the intensity of a plane wave having a root mean square (rms) pressure of 1 μPa [Urick, 1983]. Although the noise may be measured in different frequency bands, noise levels are always reduced to a 1-Hz frequency band, and are then denoted as ambient noise spectrum levels.

frequency of the band 900-1000 Hz. The raw data from 1000-1250 Hz are potentially aliased and therefore are not used in this analysis.

Center Frequency F_c (Hz)	1/3-Octave Bandwidth (Hz)
25	22-28
50	45-56
100	90-112
200	180-224
400	355-450
630	560-710
800	710-900
950	900-1000

Table 2.1 Third-octave center frequencies and bandwidths.

The 1/3-octave[3] bands are processed using the Daniell method [Stoica and Moses, 1997]. The PSD estimate for a 10 minute segment of data (with a frequency resolution of 1.22 Hz) is retrieved and the dB values at each frequency are converted back to power units (μPa^2). The power values are averaged in the frequency domain within the appropriate 1/3-octave band limits (Table 2.1). After the average power in μPa^2 for each 1/3-octave band is determined, the result is converted back to dB. At this point in the processing one number represents the average power (in dB re 1 μPa^2 per Hz) in each 1/3-octave band for this 10 minute segment of data. This process is repeated for all 10 minute segments in a month. The monthly statistics are then computed for each 1/3-octave band. A thirty day month contains approximately 4320 data points for each 1/3-octave band. The final fourteen month time series for the eight 1/3-octave bands contains 59,365 data points each.

[3] Noise energy is typically separated into various frequency bands for frequency domain analysis. Octave bands cover a 2-to-1 range of frequencies. For a more detailed analysis of the distribution of noise energy as a function of frequency, still narrower bands are used. One-third octave bands split the octave into three parts. Ten such filters can be arranged to cover a 10-to-1 frequency range. The preferred center frequencies F_C for such a series would be, for example, 100, 125, 160, 200, 250, 315, 400, 500, 630 and 800 Hz. The next series would start with 1000 Hz as the center frequency, and would continue by multiplying each number in the previous series by 10: 1000, 1250, 1600, … The lower frequency in a 1/3-octave band is $2^{-1/6} F_C$ while the upper frequency is given by $2^{1/6} F_C$. The bandwidth for each 1/3-octave band is $(2^{1/6} - 2^{-1/6})F_C = 23\%$ of the center frequency [Peterson and Gross, 1972].

Chapter 3
Environmental Conditions

This chapter is a summary of the environmental conditions in the region of the EARS buoys. The information in section 3.1 was obtained mainly from two NAVOCEANO publications, "Environmental-Acoustics Atlas of the Caribbean Sea and Gulf of Mexico, Volumes I and II (Marine Acoustics and Marine Environment)" [NAVOCEANO, 1972]. Section 3.2 contains environmental data recorded during one of the EARS deployment cruises in August 2004.

3.1 Historical Environmental Conditions

The average depth of the Gulf of Mexico is 1615 meters, while the deepest depth is 4384 meters (in the Sigsbee Deep region). The Gulf of Mexico basin resembles a deep basin with a broad shallow rim. Approximately 38% of the Gulf consists of shallow intertidal areas. The continental shelf waters (<200 meters deep) represent 22% of the Gulf while the continental slope waters (200 – 3000 meters deep) comprise 20% of the Gulf. Abyssal areas (deeper than 3000 meters) make up the final 20% [http://www.edc.uri.edu/lme/text/gulf-of-mexico]. The EARS buoys were located in an abyssal area where the water depth was 3200 meters. Table 3.1 summarizes the water depths in the Gulf of Mexico.

Area	Water Depth (meters)	% of Total Area
Intertidal	Shallow	38
Continental shelf	< 200	22
Continental slope	200 - 3000	20
Abyssal	> 3000	20

Table 3.1 Water depths in the Gulf of Mexico.

The Mexican Basin region (near the West Florida Escarpment) is characterized by a mud bottom consisting mostly of clay with some silt. A nearby bottom sediment core shows 80% clay and 20% silt. This yields a high bottom loss of 4-5 for this area on a scale of 1-5, with 1 = low loss and 5 = high loss. For grazing angles between about 50° and 90°, the estimated

bottom loss at 100 Hz is 12-14 dB/bounce, at 500 Hz is 14-16 dB/bounce, and at 1000 Hz is 14-18 dB/bounce. Shallower grazing angles have less loss.

There is a major shipping lane that runs from the Straits of Florida and Cuba to New Orleans that passes nearby the EARS buoys (Figure 3.1). This shipping lane is characterized as "very heavy", meaning more than 5 ships per day. (Heavy is considered 3-5 ships per day, moderate is 2-3 ships per day, and light is 1-2 ships per day.)

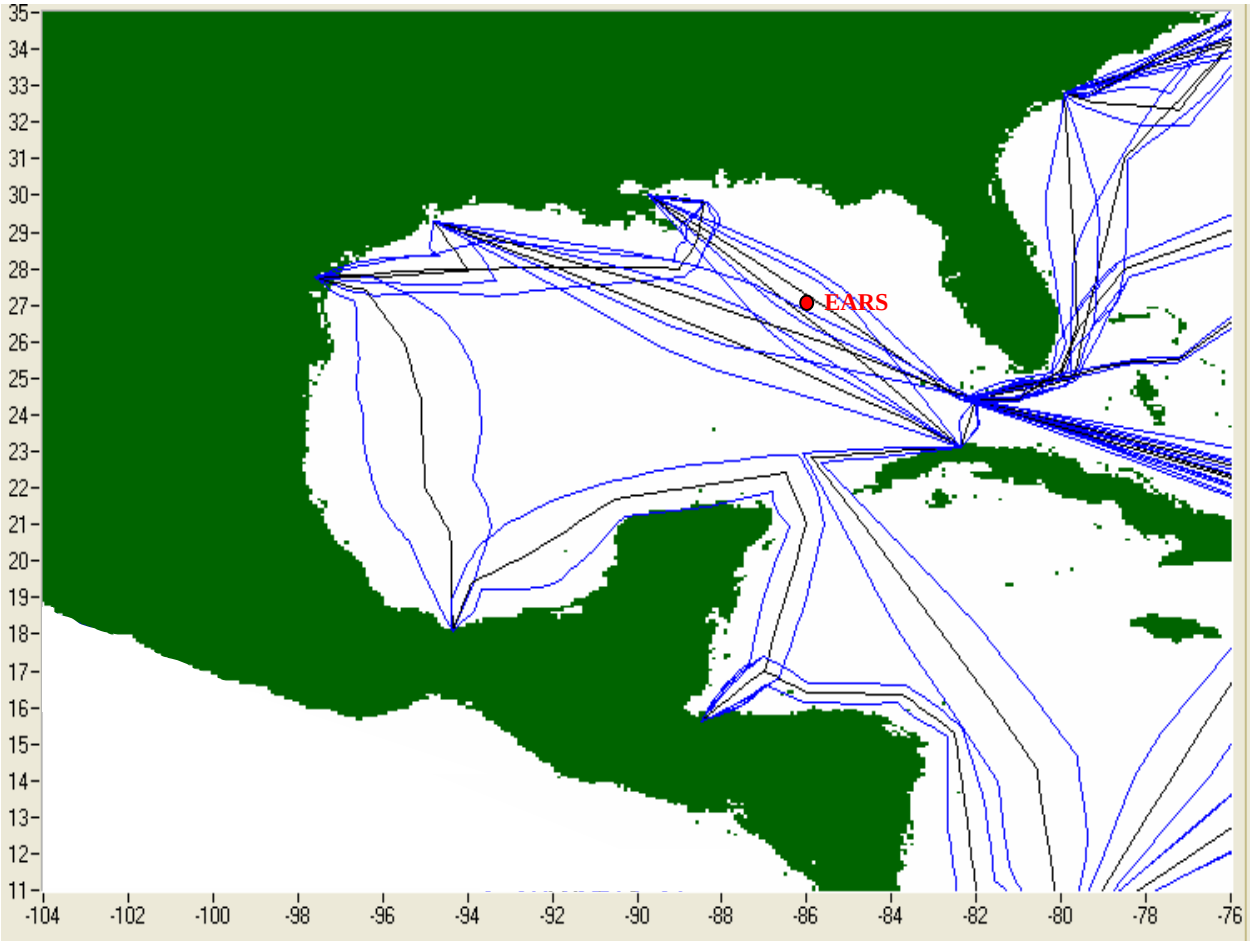

Figure 3.1 Shipping lanes in the Gulf of Mexico.

Ambient noise in the Gulf of Mexico is dominated by shipping noise and seismic exploration [Shooter, 1982]. But the seismic exploration activity (including oil rigs and support boats) is concentrated more in the western Gulf of Mexico, south of Louisiana and Texas, and occurs only occasionally in the eastern Gulf of Mexico where the EARS buoys were located.

The oil platform drilling activity to the west of the EARS buoys is a possible noise source if the drilling noise can be propagated without high transmission loss to the EARS hydrophones.

Historically, wind noise is loudest in the fall and winter (October and January), medium in the spring (April), and quietest during the summer (July). This corresponds to highest wind speeds in the fall and winter and lowest wind speeds in the summer (neglecting tropical storm activity). High wind speeds in the fall and winter cause deeper mixed layer depths (MLD). The MLD is generally shallow in the summer due to low wind speeds, but the summer MLD can become deeper in August and September if it is an active tropical storm season. Typical MLDs are 250 ft (November-February), 225 ft (March), 200 ft (April), 150 ft (May), <100 ft (June-August), 125 ft (September) and 175 ft (October).

For most surface ships, the effective source of the radiated noise is between 10 - 30 ft (3 – 9 m) below the surface [Wenz, 1962]. If the mixed layer is at least 30 ft thick, it has the potential to trap some of the energy radiated by surface ships. Frequencies above a cutoff frequency will be trapped in the mixed layer[1]; frequencies below the cutoff frequency will not be trapped. One expression for the cutoff frequency f_{co} in the mixed layer is[2]

$$f_{co} = 1.1 \times 10^{6} \; H^{-3/2} \qquad \text{Equation 3.1}$$

where H = mixed layer depth in feet and f_{co} is the cutoff frequency in Hz [Urick, 1983].

Table 3.2 shows the following approximate cutoff frequencies for MLDs ranging from 100 ft to 250 ft:

Mixed Layer Depth (ft)	**Cutoff Frequency f_{co} (Hz)**
100	1100
150	600
200	400
250	300

Table 3.2 Mixed layer depths and cutoff frequencies.

[1] The MLD is the depth with the maximum near surface temperature. The sonic layer depth (SLD) is the depth with the maximum near surface sound speed. The SLD occurs at the bottom of the mixed layer, and forms the upper boundary of the deep sound channel (DSC) [NAVOCEANO, 1999].

[2] This assumes the average sound speed in the mixed layer is 5100 ft/s (1550 m/s). This was the surface sound speed measured by a nearby CTD; see section 3.2.

(The cutoff is not sharp, so the values have been rounded to the nearest 100 Hz.) This means that frequencies of about 300 Hz and above will be trapped in the mixed layer during windy time periods (fall, winter and during tropical storm activity) while frequencies of about 1100 Hz and above will be trapped in the mixed layer during low wind conditions (early summer). Since most of the noise due to surface shipping is concentrated in frequencies below 300 Hz, this means that most low frequency shipping noise will not be trapped at any time during the year. Most of the shipping noise will escape the mixed layer. Energy from nearby ships will be propagated via direct and bottom bounce propagation paths.

However, energy from distant ships located in shallow water (such as in shelf regions near Florida, Alabama, Mississippi, Louisiana and possibly as far away as Texas, Mexico and Cuba) may be able to travel long distances with little attenuation if the energy is trapped in the deep sound channel[3]. This phenomenon is called downslope enhancement [NAVOCEANO, 1999] and consists of sound energy travelling via bottom bounce propagation in shallow water being converted to deep sound channel propagation in deep water. Also known as the megaphone effect [Urick, 1984], energy from coastal shipping can be an important contribution to the noise field at a hydrophone located in the deep sound channel [Carey, 1986 and Wagstaff, 1981]. The amount of noise received depends on the density of shipping, the slope of the shelf, the bottom properties of the slope and the near-surface characteristics of the shelf waters. Other sound sources such as wind-induced noise can have the same effect [Carey, 1986]. This noise enhancement can also be produced by a range-dependent sound speed profile. This can occur in frontal regions, such as across the Loop Current in the Gulf of Mexico [Urick, 1984].

The average annual depth of the deep sound channel axis (DSCA)[4] is about 850 meters, varying from 800-1000 meters. The EARS hydrophones were located at depths of around 2935 meters, or about 2000 meters below the DSCA. It is possible for distant shipping noise to be received by the EARS hydrophones if the shipping noise enters the deep sound channel via downslope enhancement. The EARS buoys were located in the deepest part of the Mexican Basin, which is basically a bowl. Distant shipping noise could come from any direction and be funnelled downslope into the bowl and be received by the deep EARS hydrophones.

[3] A sound channel is located on a sound speed profile where a negative sound speed gradient is followed by a positive sound speed gradient. The sound channel axis is located at the sound speed minimum between the two gradients. Sound channels can trap acoustic energy between their upper and lower boundaries.
[4] The DSCA is located at the depth of the minimum sound speed on the entire sound speed profile.

The average critical depth[5] in the winter is 3750 meters while in the summer it is 4210 meters. Because of this, the entire Gulf of Mexico is bottom-limited year-round; no convergence zone[6] propagation is possible because the Gulf of Mexico is too shallow[7]. (The water depth near the EARS buoys was 3200 meters.) Consequently, distant shipping noise will not be able to travel to the EARS buoys via convergence zone propagation.

Historically, ambient noise data recorded by bottom-mounted hydrophones (such as EARS) are usually quieter than ambient noise levels recorded by shallow hydrophones (such as sonobuoys or towed arrays). Shallow hydrophones tend to be located within the mixed layer and generally record higher noise levels due to frequencies trapped in the mixed layer and the closer proximity of noise sources such as shipping and weather. Hence, the noise levels recorded by EARS might be expected to be somewhat lower than the levels recorded by shallow hydrophones located in the same region of the Gulf of Mexico during the same time period.

The Loop Current flows in the vicinity of the EARS buoys. This front can have a major impact on sound propagation. The surface water temperature is warmer to the north of the Loop Current and colder to the south, which causes the surface sound speed to be higher to the north. The MLD and DSCA can also change abruptly from one side of a front to the other, causing a range-dependent sound speed profile. In addition, as the Loop Current meanders, it can spin off warm core rings (eddies) near the EARS buoys. A warm core ring is a rotating, drifting mass of warm water that can be formed north of the Loop Current. Since a ring is a circular front, it can also have a major impact on sound propagation.

[5] Critical depth is the depth below the DSCA where the sound speed is equal to the surface or near surface sound speed maximum. The critical depth is generally the lower boundary of the deep sound channel. In bottom-limited areas the ocean bottom is the lower boundary of the deep sound channel.
[6] Convergence zone propagation is a long range acoustic path with little transmission loss.
[7] Depth excess is defined as the bottom depth minus the critical depth. At least 1200 ft (366 m) of depth excess is required to support convergence zone propagation [NAVOCEANO, 1972].

3.2 Environmental Data from August 2004

While the EARS buoys were being deployed on 02 August 2004, environmental data were collected in the region of the EARS buoys. A total of seven expendable bathythermograph (XBT) surveys and one conductivity temperature depth (CTD) survey were recorded. Figure 3.2 shows the locations of the CTD and XBT surveys with respect to the EARS buoys. Figure 3.3 shows the CTD and XBT temperature data from 0 to 900 m, and Figure 3.4 shows the sound speed profile obtained from the CTD near the site of EARS A1. Figure 3.5 shows the temperature, salinity and sound speed values as measured by this CTD from 0 to 3000 m.

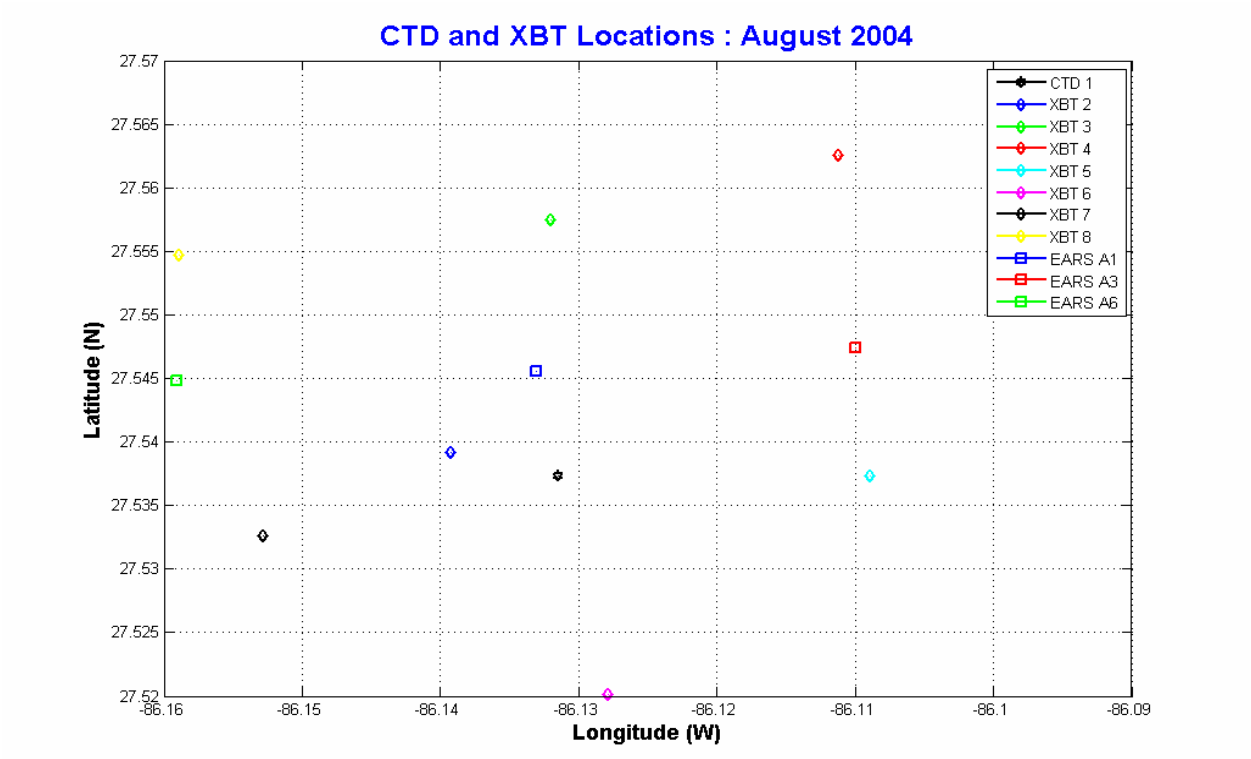

Figure 3.2 CTD and XBT locations from August 2004.

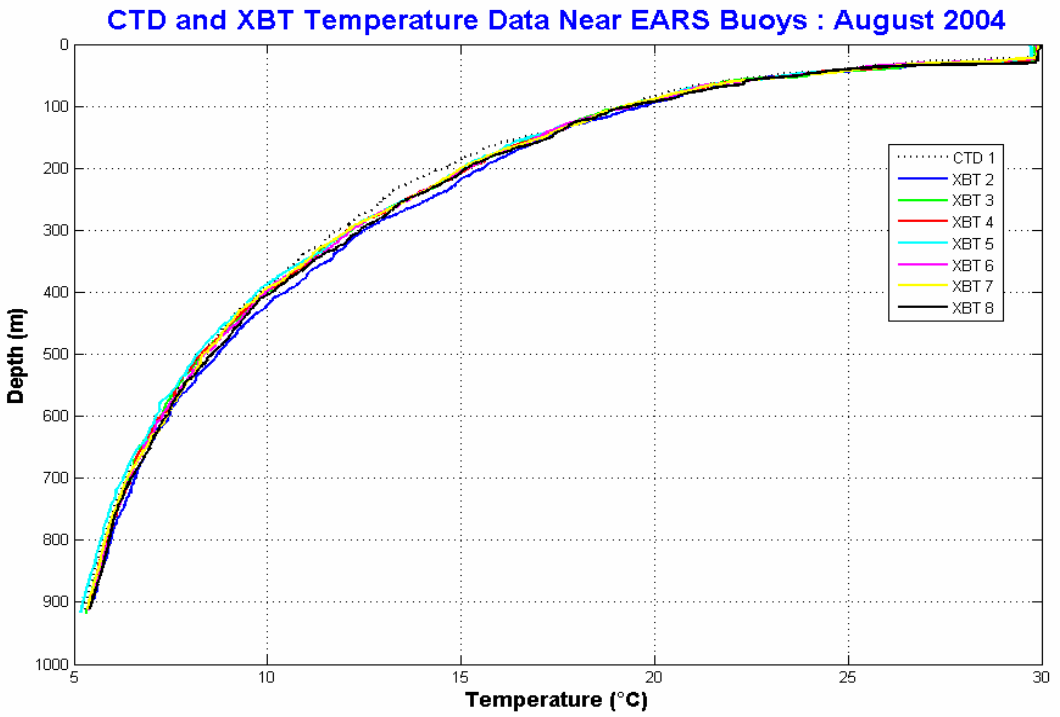

Figure 3.3 CTD and XBT temperature data from August 2004.

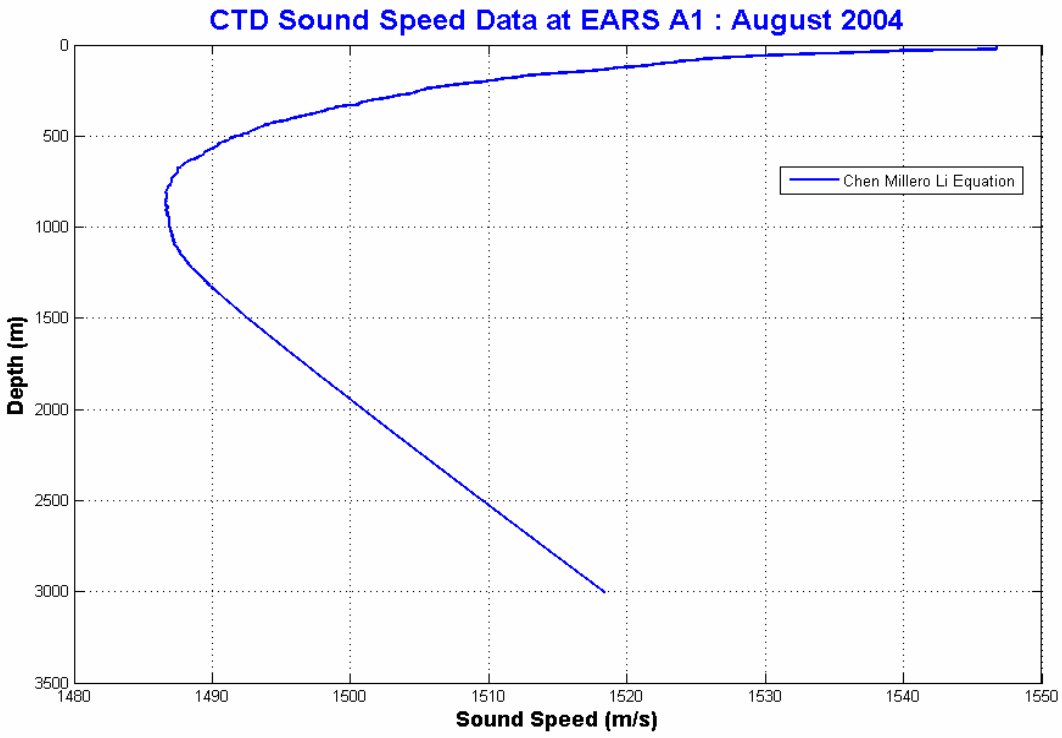

Figure 3.4 Sound speed profile near EARS A1.

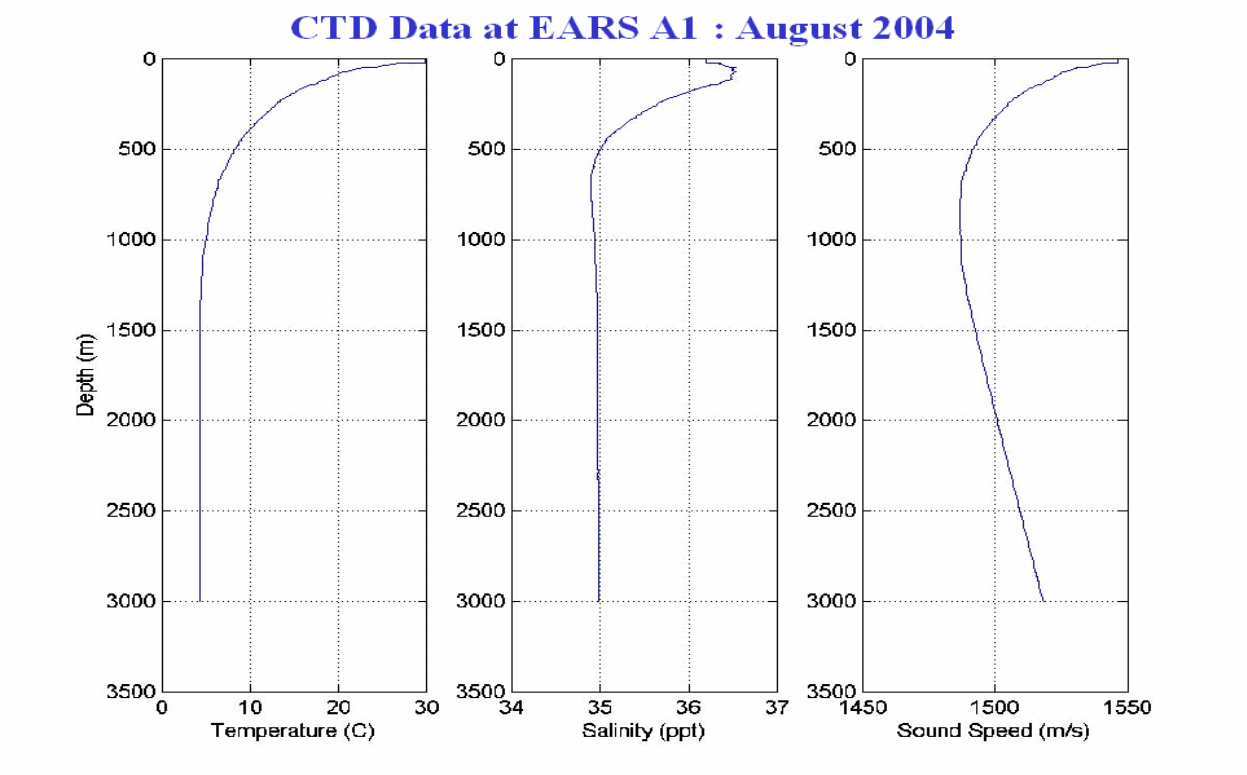

Figure 3.5 CTD data near EARS A1 from August 2004.

The MLDs obtained from these eight temperature measurements ranged from 20 – 30 m (66 – 100 ft) in the vicinity of the EARS buoys. The surface sound speed was 1547 m/s, and the DSCA was at 850 m. These results for MLD, surface sound speed and DSCA are in complete agreement with historical averages. The sound speed profile was strongly downward refracting, and it was obviously bottom-limited in this area. The deepest MLD recorded (30 m) is only capable of trapping frequencies of 1100 Hz and above. Since the EARS bandwidth was 10 – 1000 Hz, none of the energy in the EARS bandwidth would be trapped in the mixed layer during these summer conditions. All energy from ships travelling in the vicinity of the EARS buoys would escape the surface duct and travel via bottom bounce propagation paths.

From the sound speed profile (Figure 3.4), the estimated boundaries of the deep sound channel near the EARS buoys were 100 to 3200 meters. Since the EARS hydrophones were located at 2935 meters, they were well within the deep sound channel and capable of exploiting the megaphone effect (downslope enhancement) mentioned earlier.

Chapter 4
Monthly Statistics

In this chapter the monthly statistics at each of the eight 1/3-octave center frequencies are discussed. These include the trends observed, both as a function of month as well as frequency band. The following quantities are analyzed: mean, median, standard deviation, skewness, kurtosis, coherence time, and the spread[1] of the data.

The monthly mean ambient noise values peak at 25 and 50 Hz, then decrease with increasing frequency out to 950 Hz (Figures 4.1 to 4.3). Most frequency bands appear to have a cycle of about one year, based on the monthly mean values. Figures 4.4 to 4.11 show the ambient noise at the eight 1/3-octave center frequencies (25 – 950 Hz) versus month from April 2004 to May 2005. Each of these figures shows how the mean, median, 10^{th} percentile and 90^{th} percentile values vary in each frequency band with month. The low frequencies (25 – 100 Hz) peak during March 2005 and are minimum during the hurricane month of September 2004. High frequencies (400 – 950 Hz) are loudest during September 2004 and during the winter months of November, December and January due to high average wind speeds during these months. Conversely, the high frequencies are quietest during the summer months of June through August of 2004 due to low average wind speeds during these months.

[1] The spread of the data is defined as the range of the data (in dB) from the 10^{th} percentile to the 90^{th} percentile. All of the statistical terms used in this dissertation are defined in Appendix F.

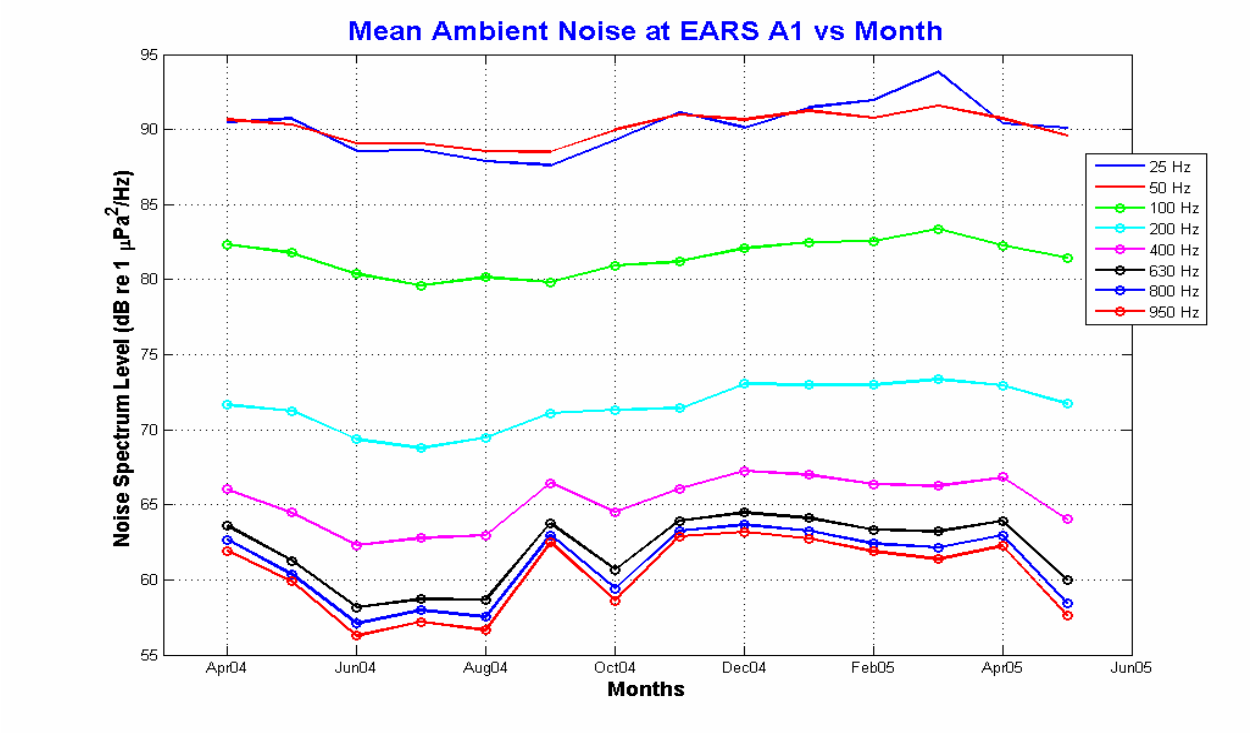

Figure 4.1 Mean ambient noise vs. month.

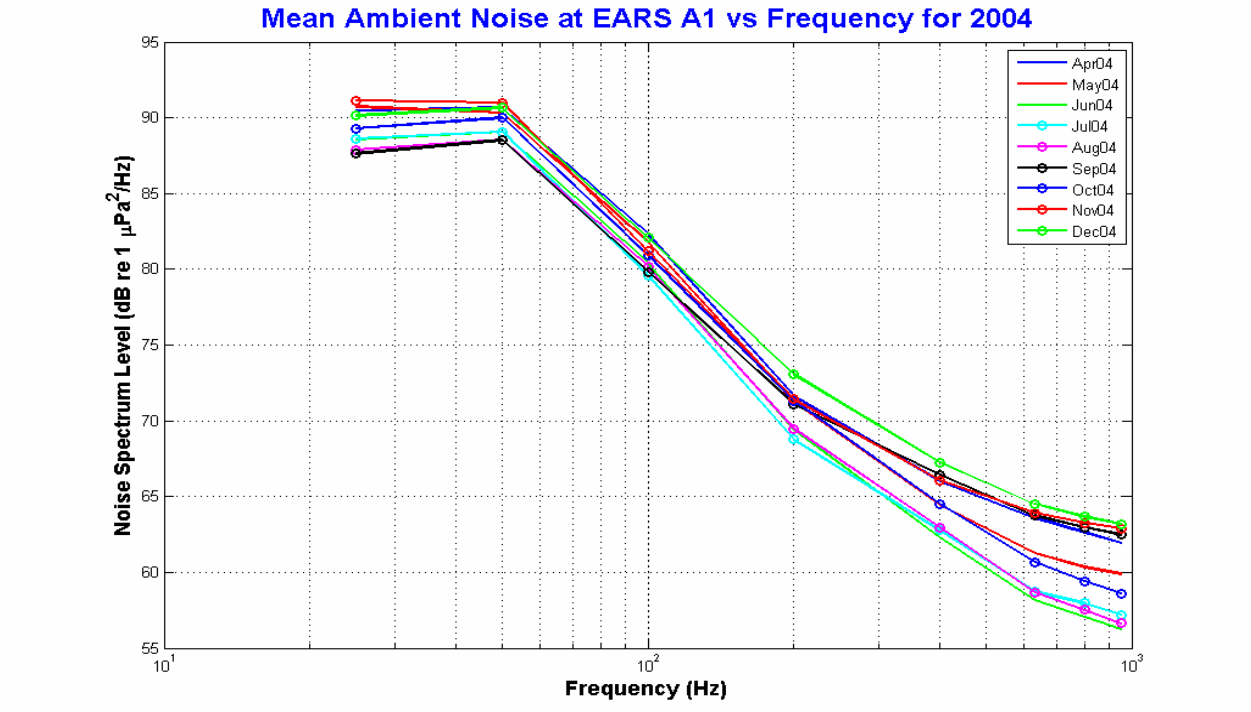

Figure 4.2 Mean ambient noise vs. frequency for 2004.

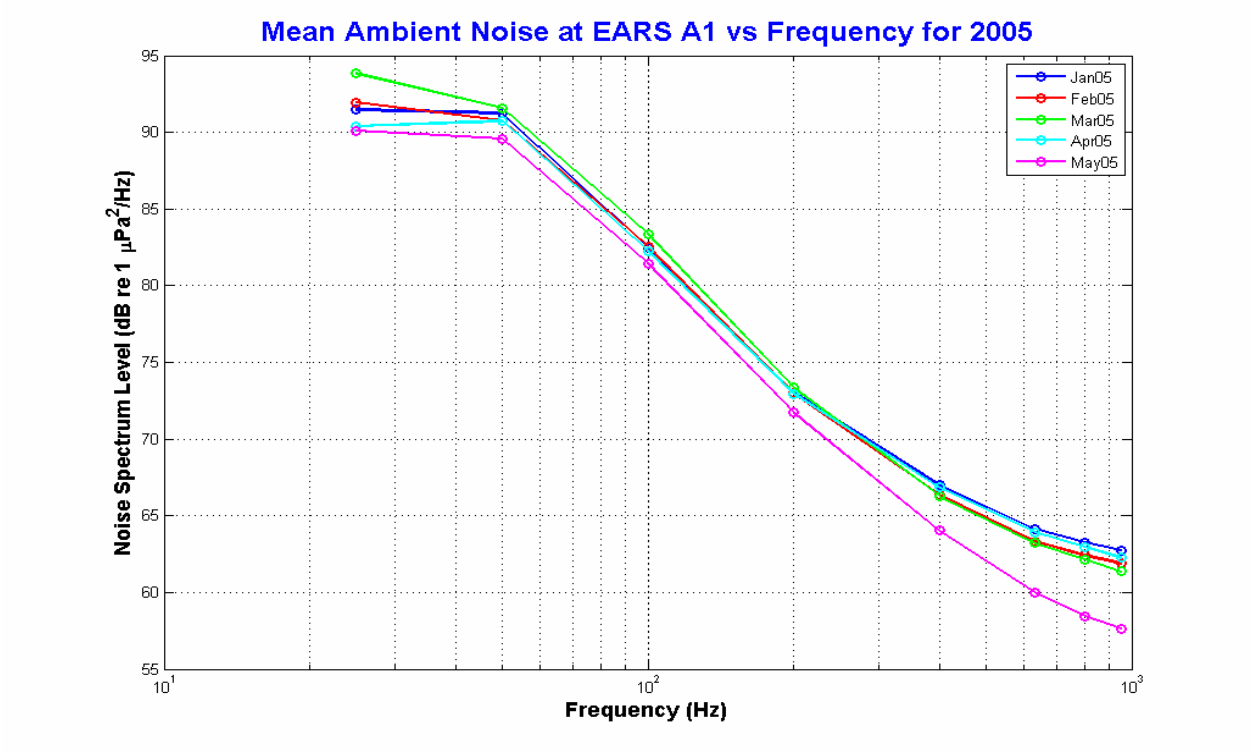

Figure 4.3 Mean ambient noise vs. frequency for 2005.

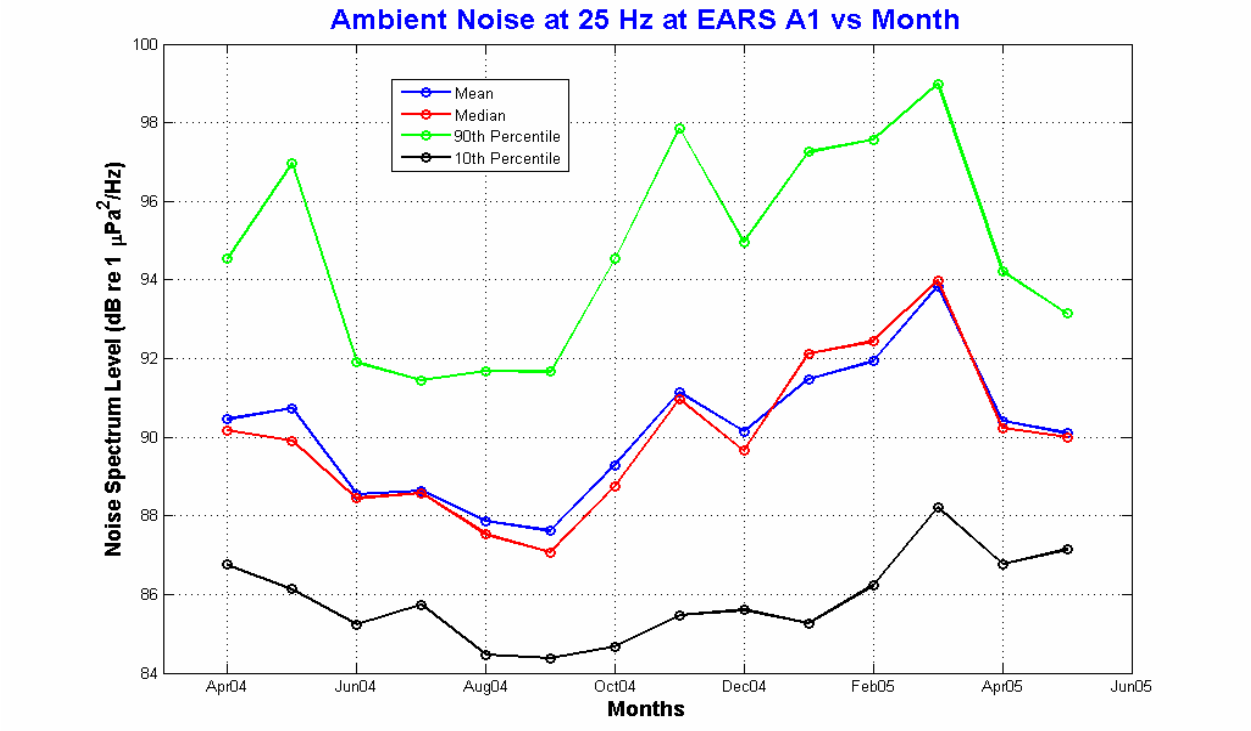

Figure 4.4 Ambient noise at 25 Hz vs. month.

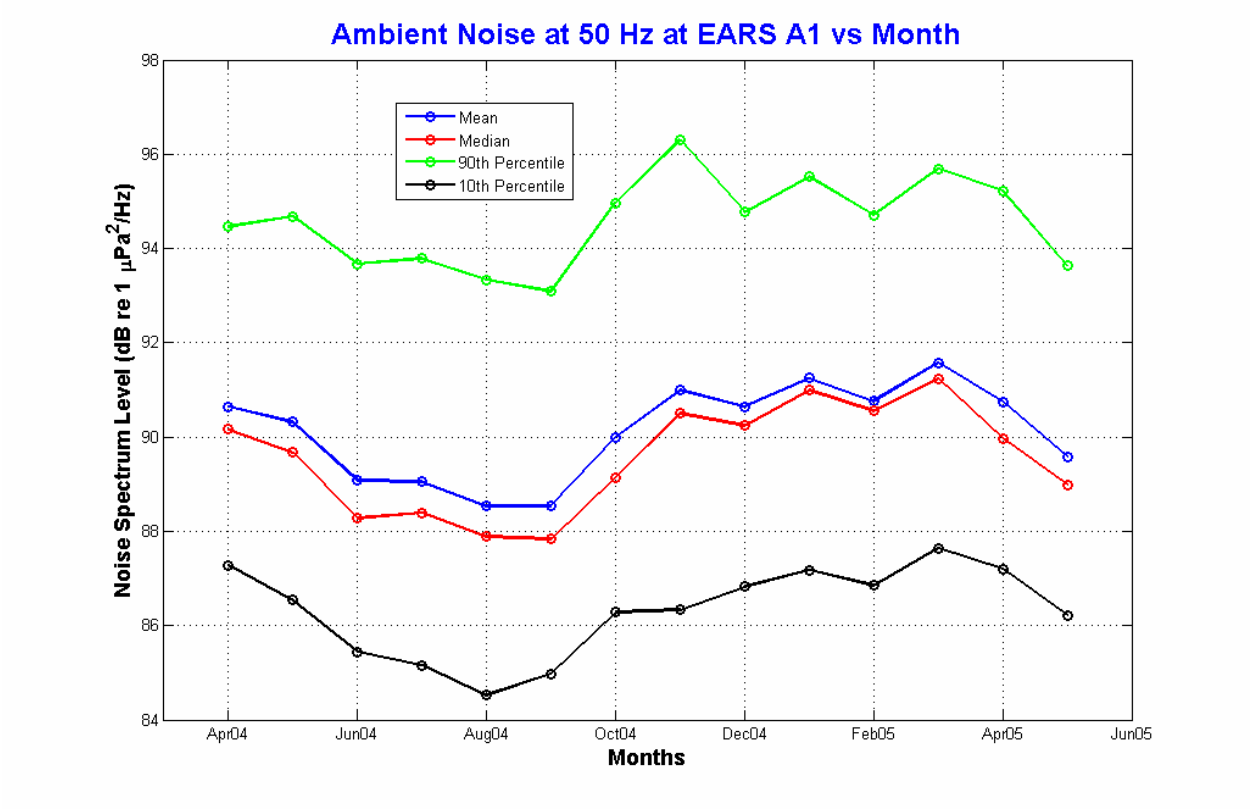

Figure 4.5 Ambient noise at 50 Hz vs. month.

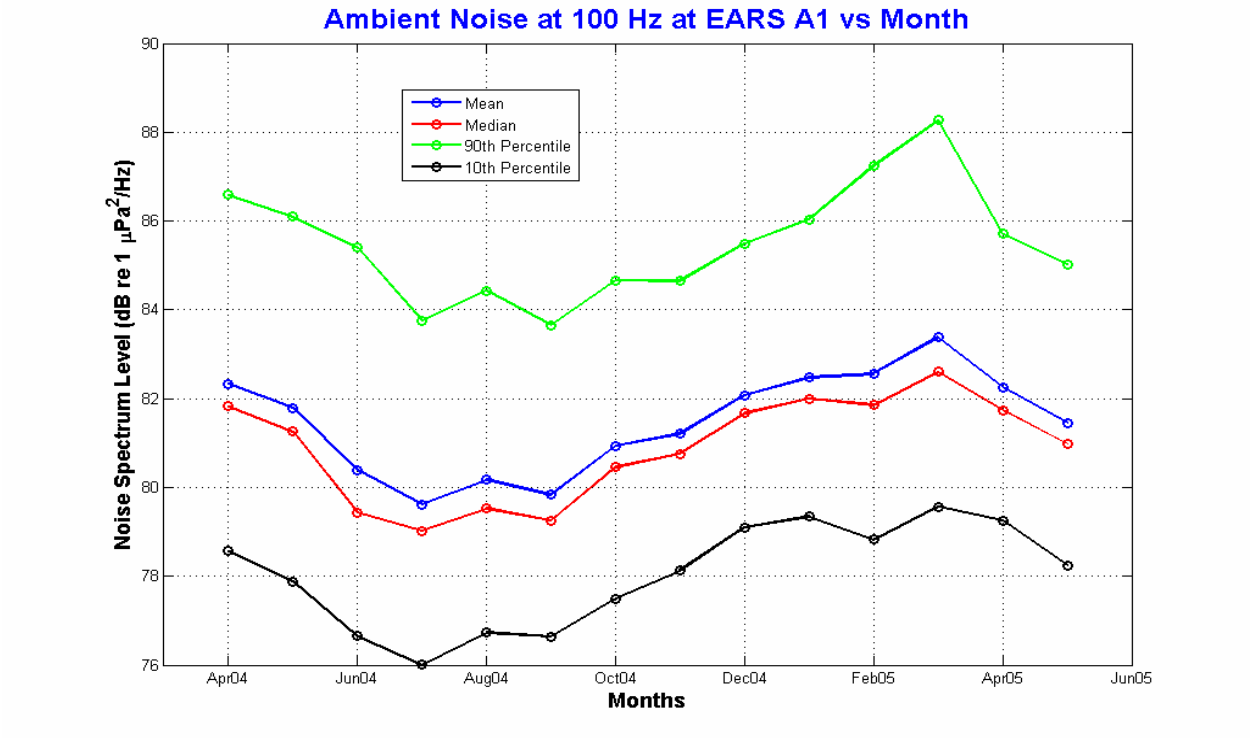

Figure 4.6 Ambient noise at 100 Hz vs. month.

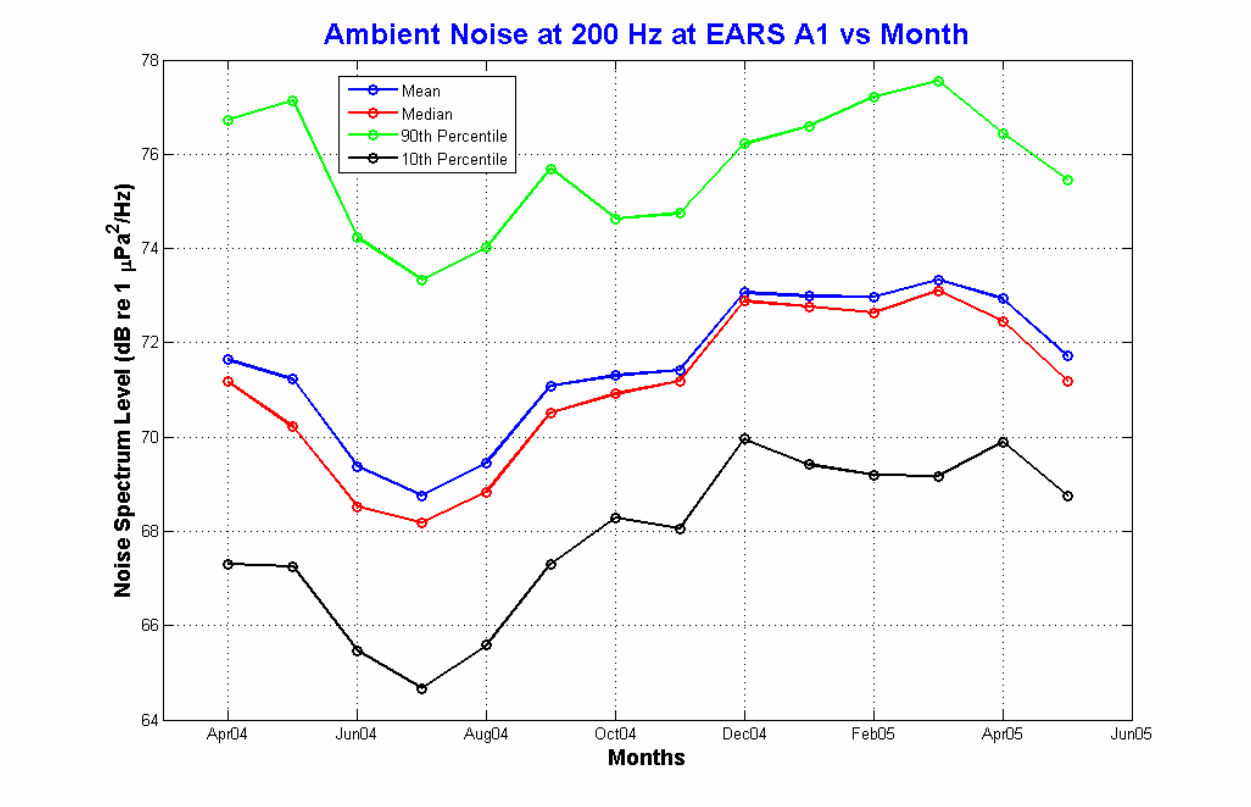

Figure 4.7 Ambient noise at 200 Hz vs. month.

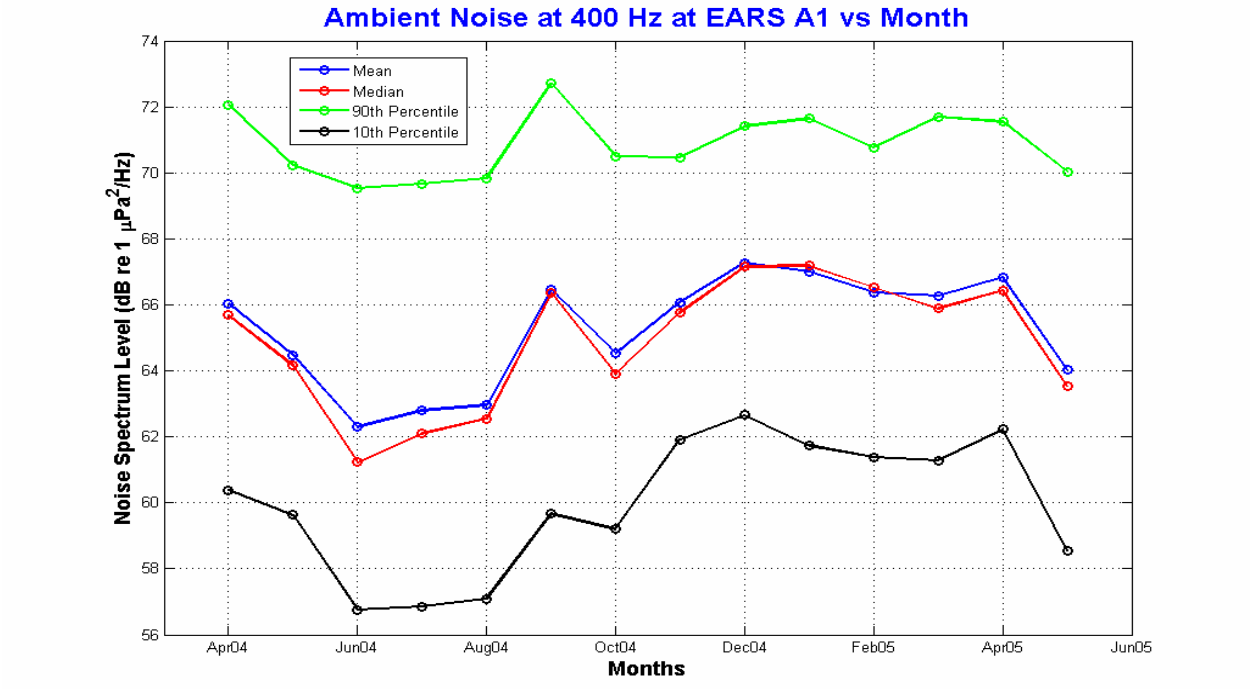

Figure 4.8 Ambient noise at 400 Hz vs. month.

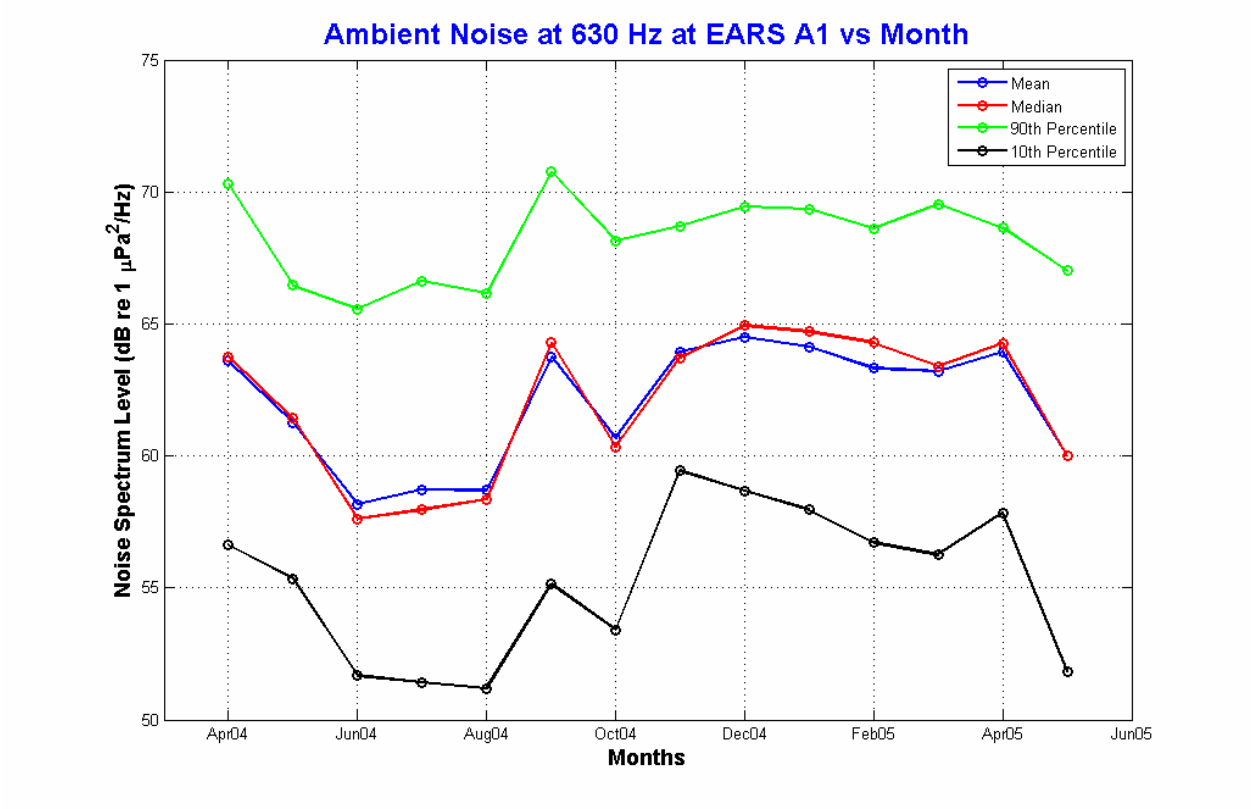

Figure 4.9 Ambient noise at 630 Hz vs. month.

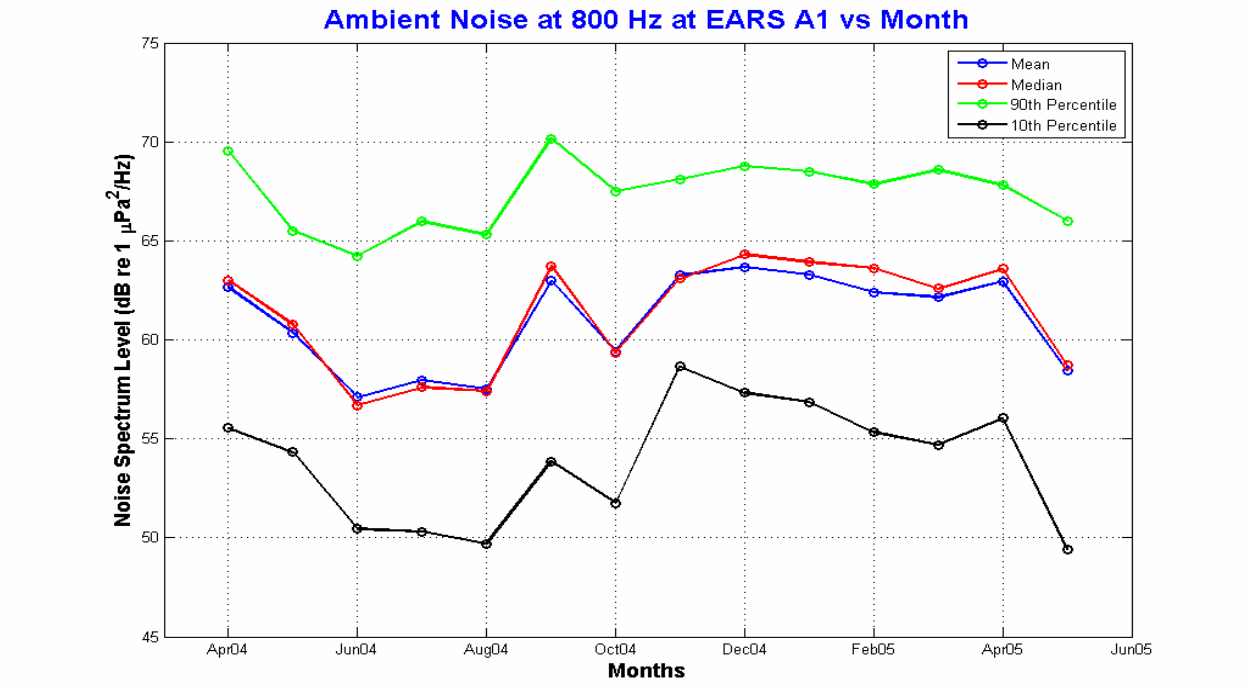

Figure 4.10 Ambient noise at 800 Hz vs. month.

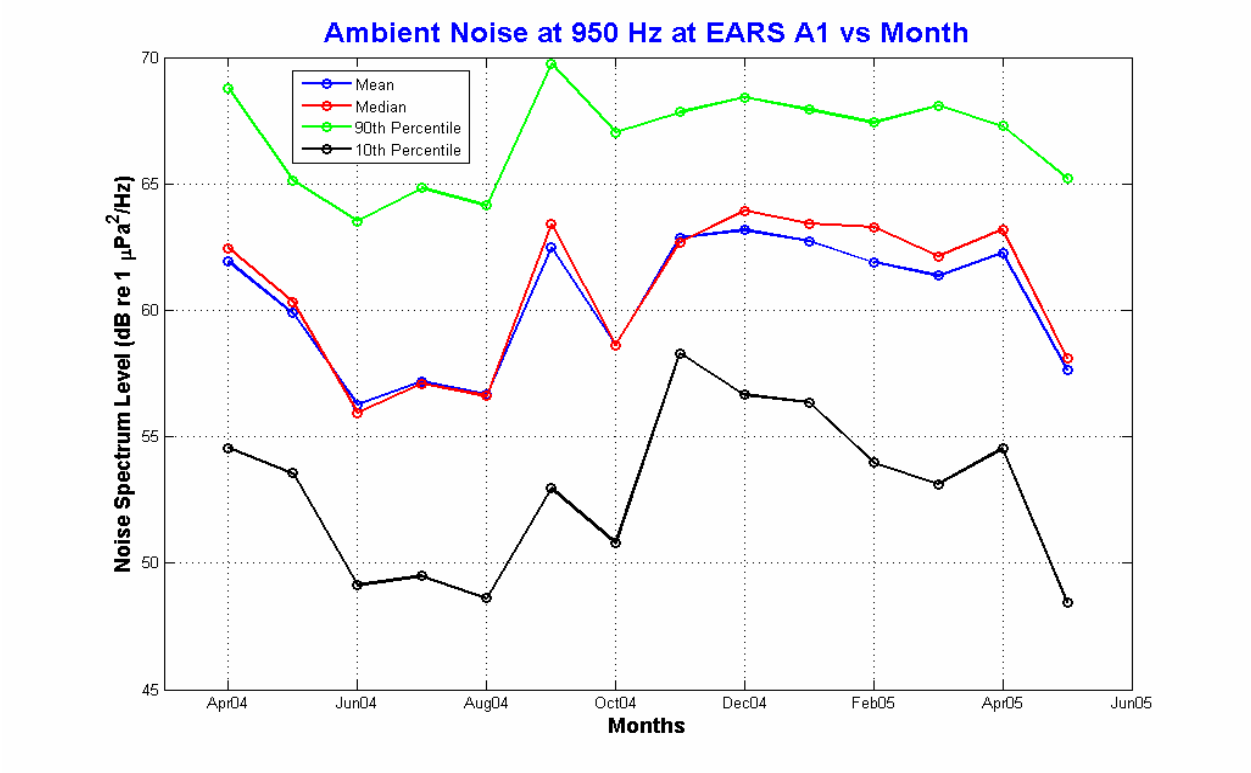

Figure 4.11 Ambient noise at 950 Hz vs. month.

The mean and median monthly values at each frequency never differ by more than 1.5 dB (Figure 4.12). The mean value is generally larger than the median value at low frequencies (25 - 400 Hz), which corresponded with monthly time series having positive skewness. Exceptions occur at 25 Hz from January to March of 2005 and at 400 Hz from January to February of 2005.

The median value is generally larger than the mean value at high frequencies (630 - 950 Hz), which corresponded with monthly time series having negative skewness. This was always the case during months with high average wind speeds. The months of June through August 2004 had low average wind speeds, which appears to have produced positive skewness and resulted in the mean values exceeding the median values at high frequencies.

The spread of the data, as determined by subtracting the 10^{th} percentile value from the 90^{th} percentile value in dB for each 1/3-octave band, is shown in Figure 4.13. The data has the highest spread at the higher frequencies, especially from 630 – 950 Hz during July – October 2004 and May 2005. The spread is usually smallest in the region 100 – 200 Hz. The spread is reduced at high frequencies (400 – 950 Hz) during November 2004, which had low standard deviations over the same band of frequencies.

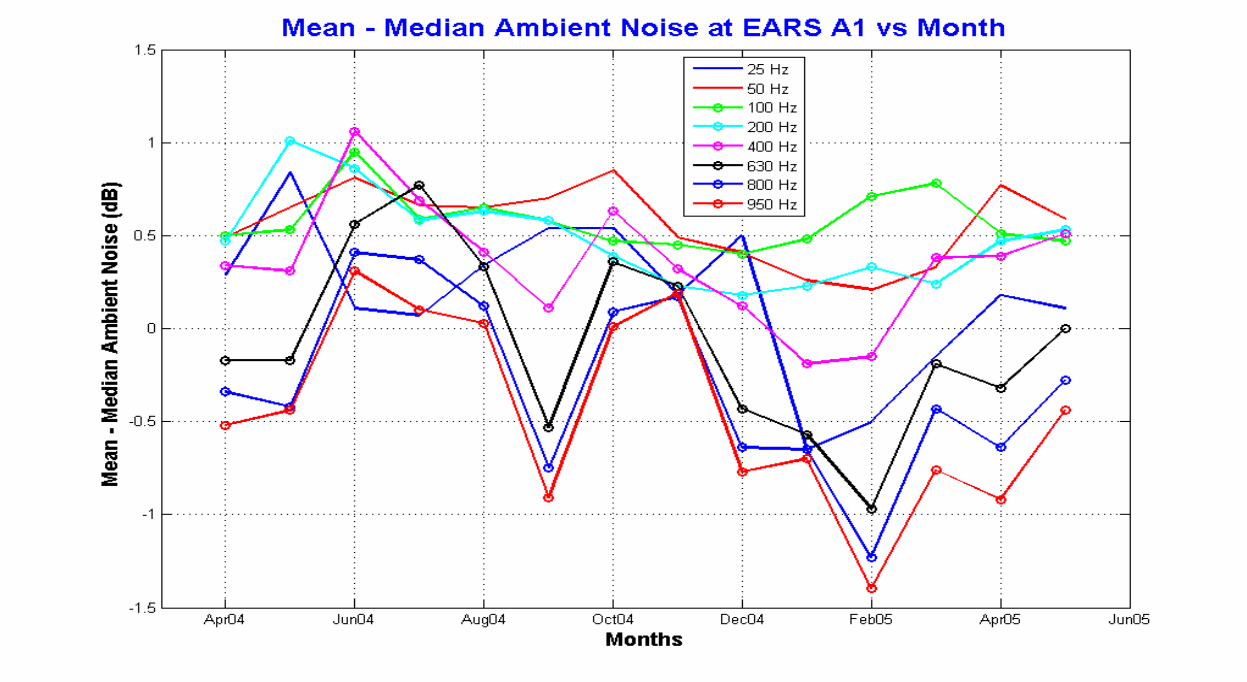

Figure 4.12 Mean – median ambient noise vs. month.

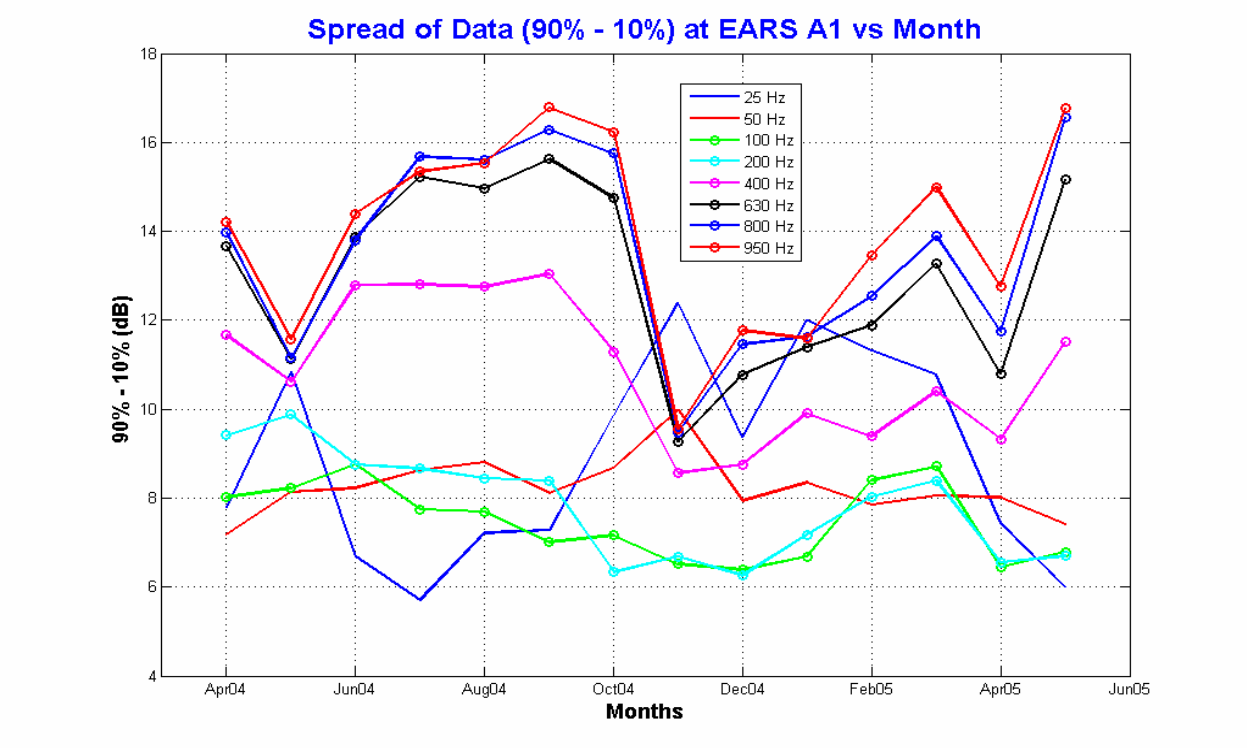

Figure 4.13 Spread of data (90% - 10%) vs. month.

Figure 4.14 shows a plot of the spread of the data (90% minus 10% levels) expressed as a multiple of the standard deviation (σ) for each 1/3-octave band. (The spread in σ units equals the spread in dB divided by the standard deviation (σ) in dB for each 1/3-octave band.) The spread in σ units ranges from a low value of 2.13 to a high value of 2.67. For comparison, the spread in σ units between the 90th and 10th percentiles of a Gaussian distribution is 2.56 σ [Li, 1999].

The standard deviation (Figures 4.15 to 4.17) tends to be high at low frequencies (25 Hz), is smallest near 100 – 200 Hz, and increases to high values again at high frequencies (630 – 950 Hz). The highest standard deviations occur during September 2004 from 630 – 950 Hz due to the high wind speed variability during the hurricanes. The same pattern (although not as pronounced) is observed during May 2005.

The month of November 2004 is characterized by very low values of the standard deviation from 400 – 950 Hz (all about 3.6 dB). The minimum noise levels in this band of frequencies jumps abruptly from October to November, as can be seen in the 10th percentile values in Figures 4.8 to 4.11, and in the greatly reduced spread of the data during November (Figure 4.13). This can also be seen in Appendix B, Figure B.8, which shows the November percentiles "bunched up" at high frequencies as compared to the more spread out percentiles at adjacent months (Figures B.7 and B.9).

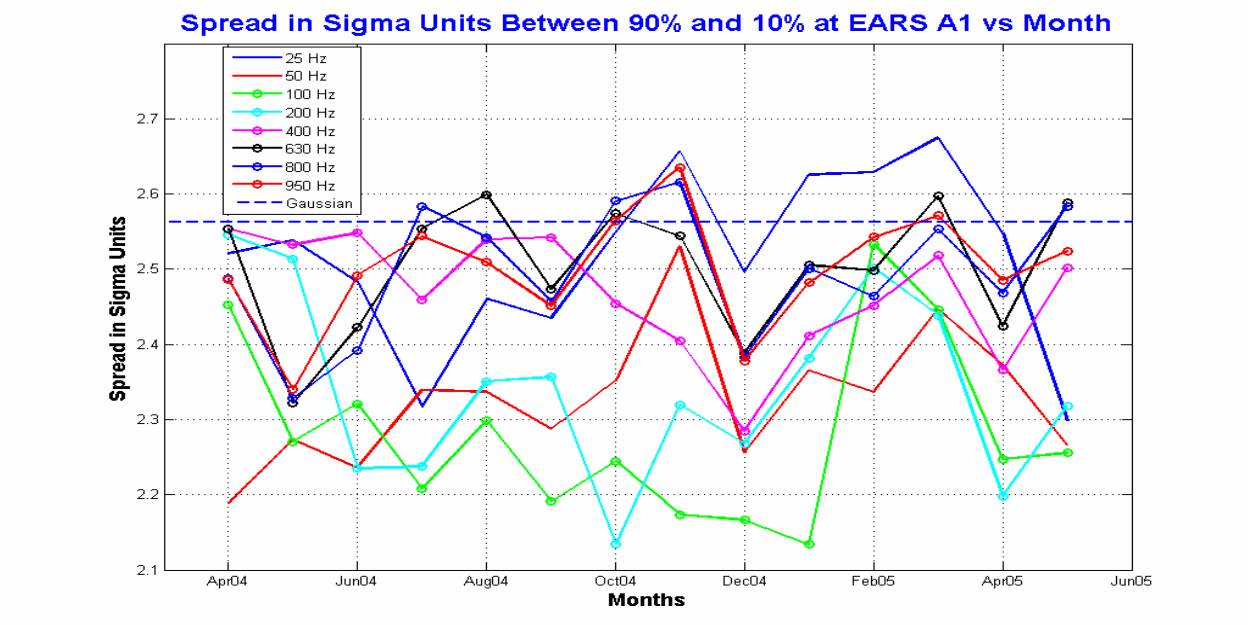

Figure 4.14 Spread of data in sigma units vs. month.

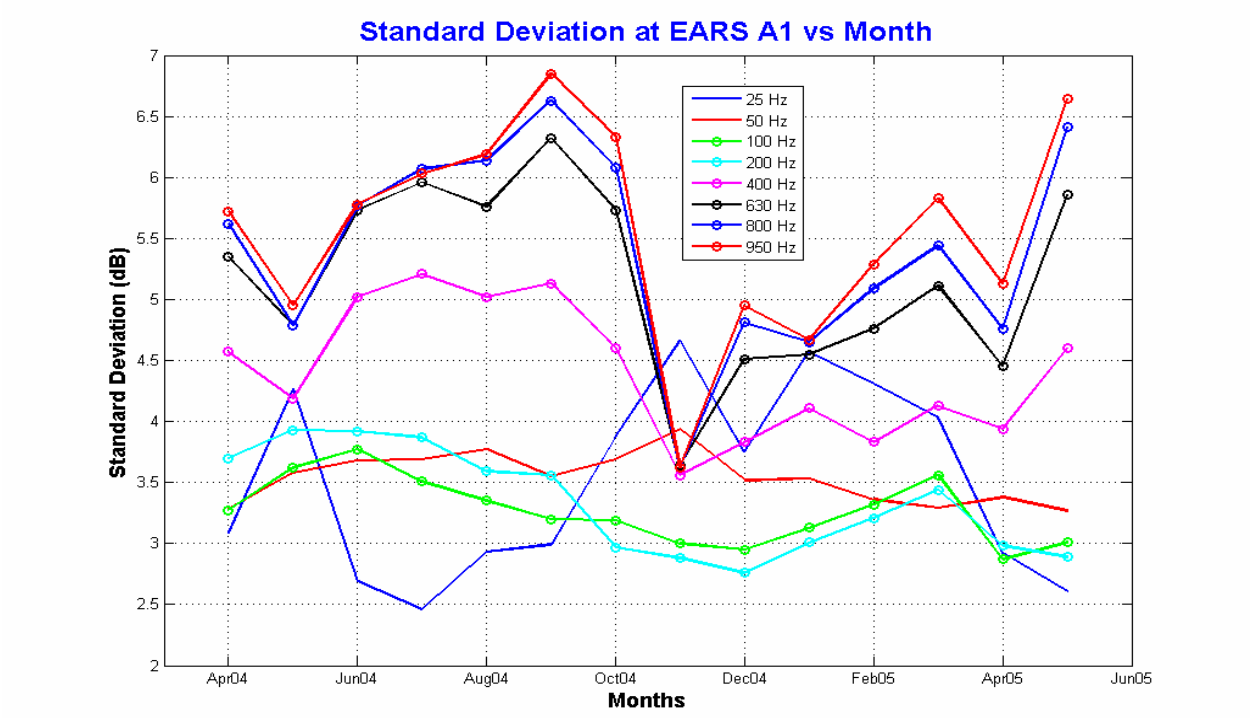

Figure 4.15 Standard deviation vs. month.

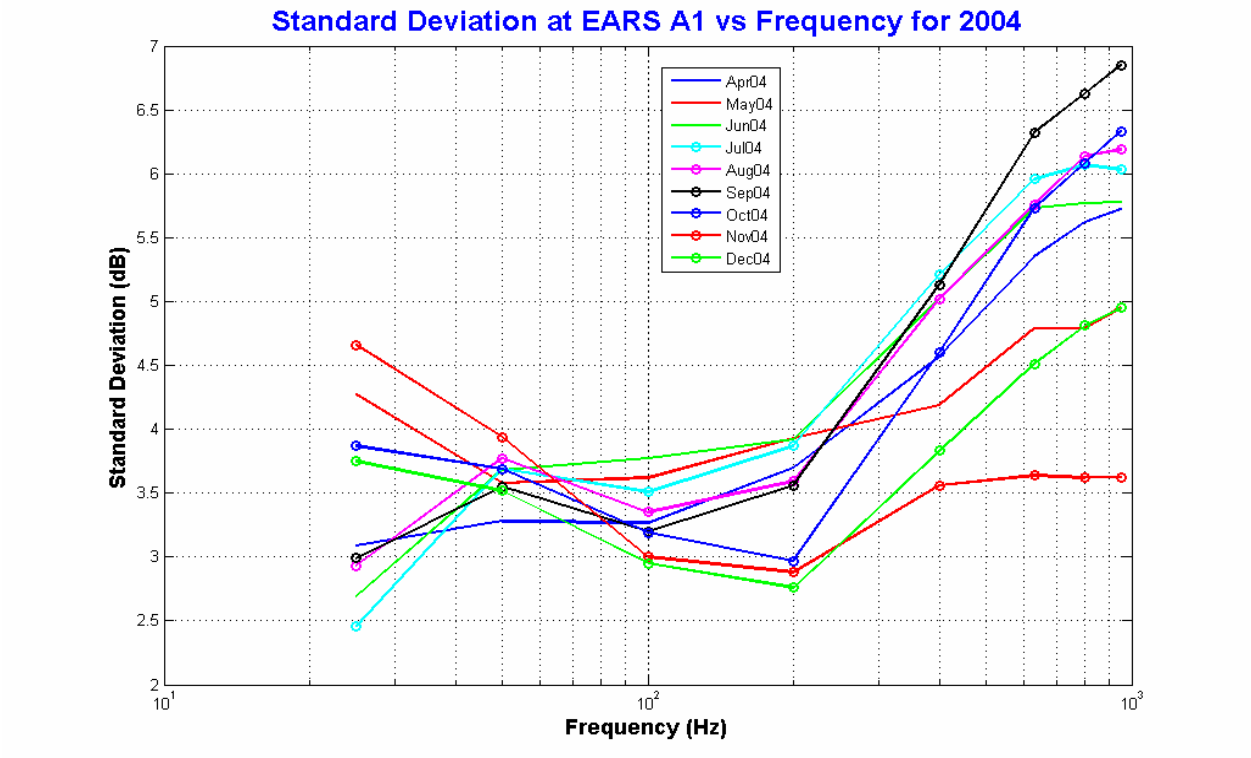

Figure 4.16 Standard deviation vs. frequency for 2004.

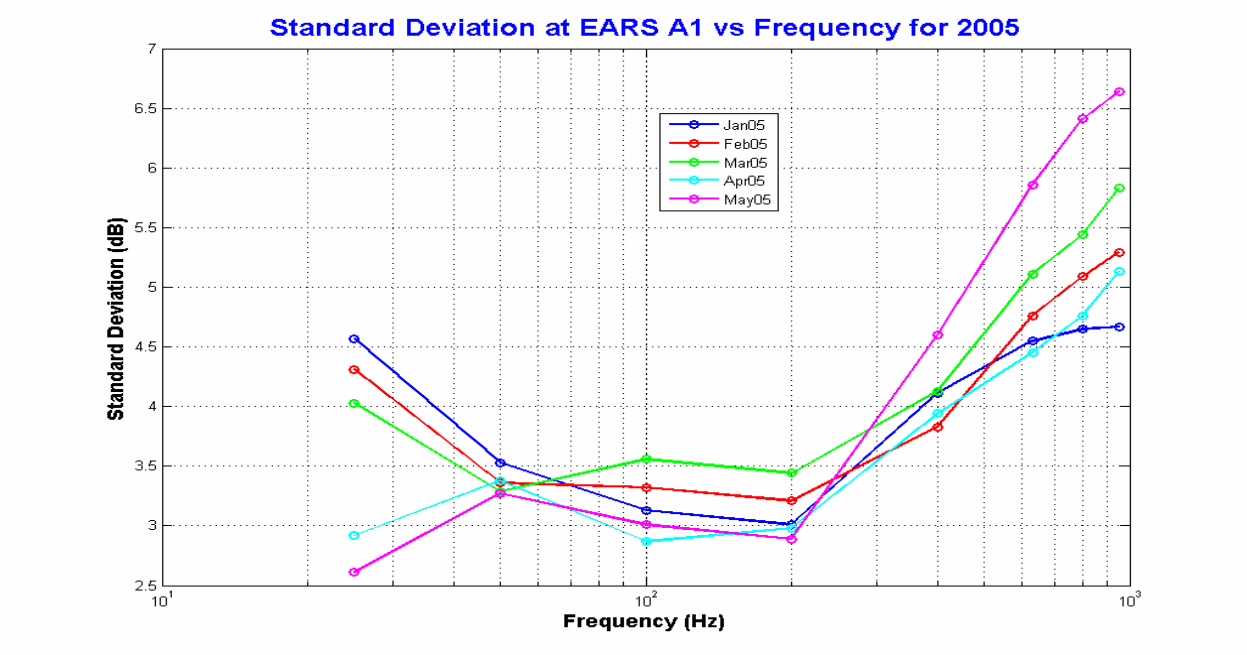

Figure 4.17 Standard deviation vs. frequency for 2005.

The skewness (Figures 4.18 to 4.20) tends to be low at low frequency (25 Hz), increasing to a maximum at 100 Hz, and then decreasing again at higher frequencies, with the lowest values at 950 Hz. The skewness is always positive (skewed towards peaks) from 25 - 400 Hz, except at 25 Hz during January – March 2005. Since shipping noise dominates low frequencies, the region 25 - 400 Hz is dominated by shipping peaks, which contribute to the high amplitude tails (louder decibel values) of a PDF and make the skewness positive.

Weather noise dominates high frequencies, so the region 630 - 950 Hz is dominated by weather. The average weather in a month determines the skewness in that month at higher frequencies. The skewness is usually negative (skewed towards troughs) from 630 - 950 Hz, especially in months with high average wind speeds. Of the 14 months analyzed, 11 months had average wind speeds of 9 knots or greater, and these months are generally negatively skewed in the region of 630 - 950 Hz. The skewness is positive from 630 - 950 Hz when the monthly average wind speed is low, such as occurred during June to August 2004 (when the monthly average wind speed ranged from 7.3 to 7.8 knots). (In general, the skewness is positive when the mean is greater than the median and negative when the median is greater than the mean.) The most negative values of skewness at 630 - 950 Hz occur during February 2005, a very windy month with an average wind speed of 12.1 knots.

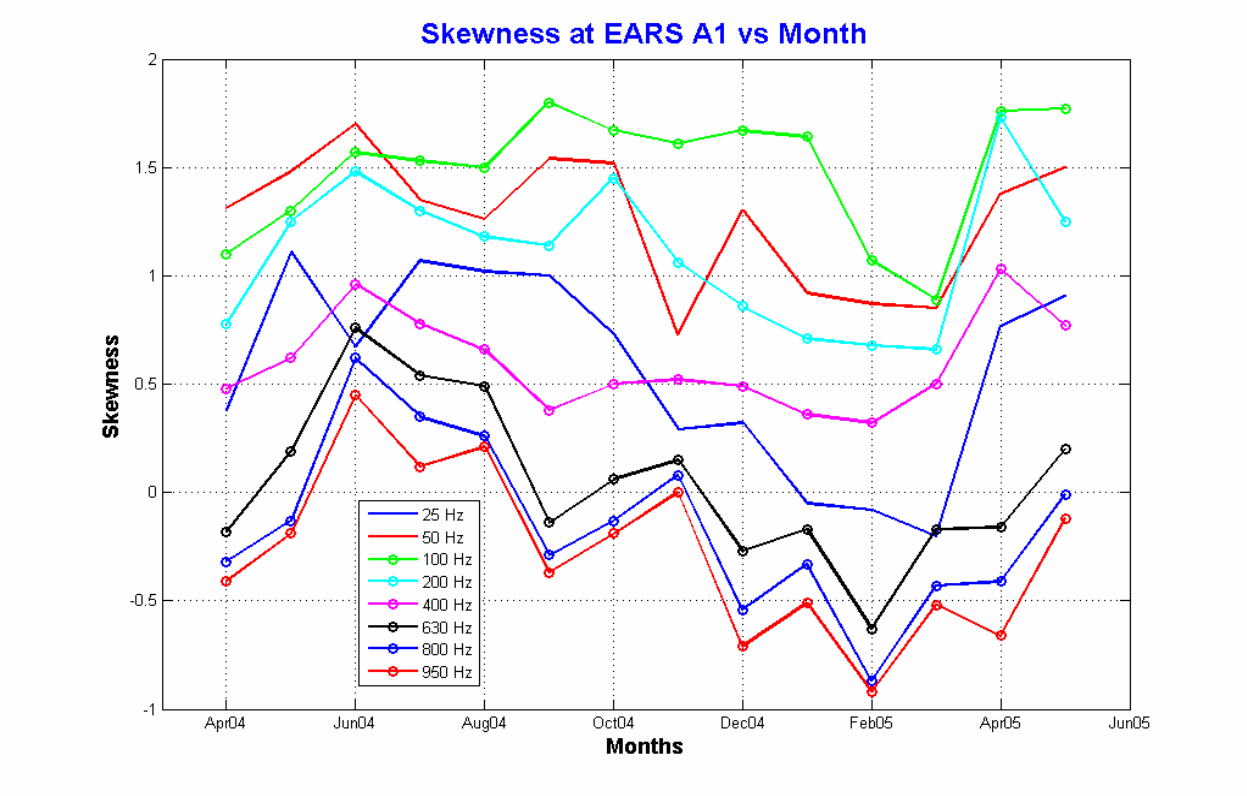

Figure 4.18 Skewness vs. month.

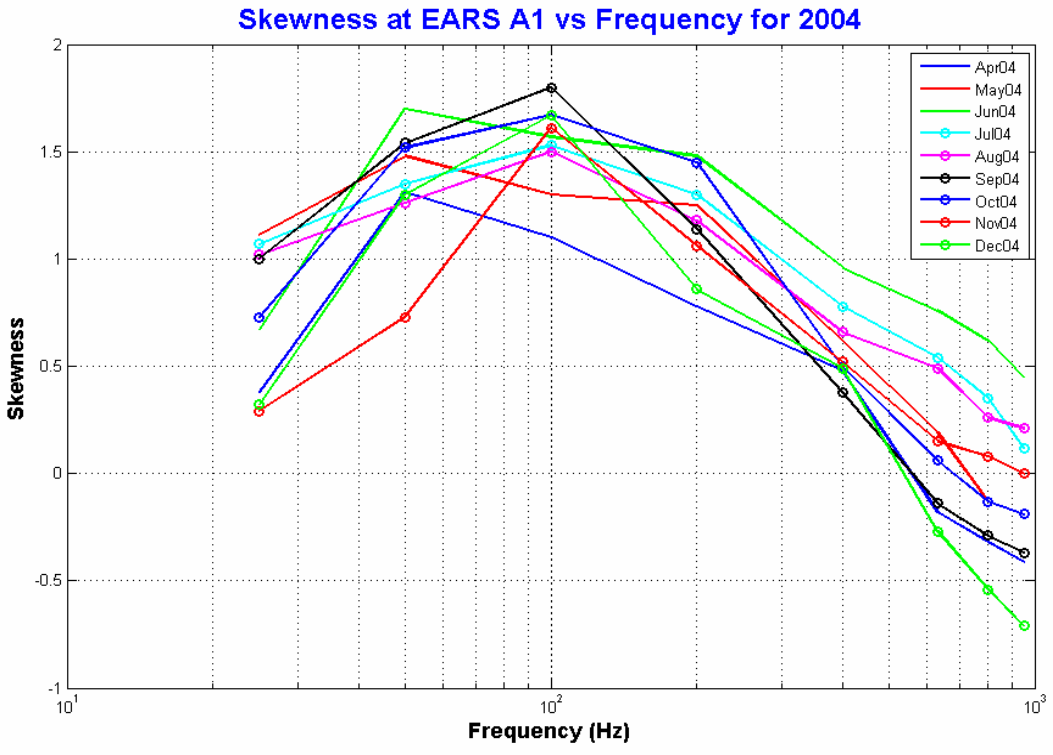

Figure 4.19 Skewness vs. frequency for 2004.

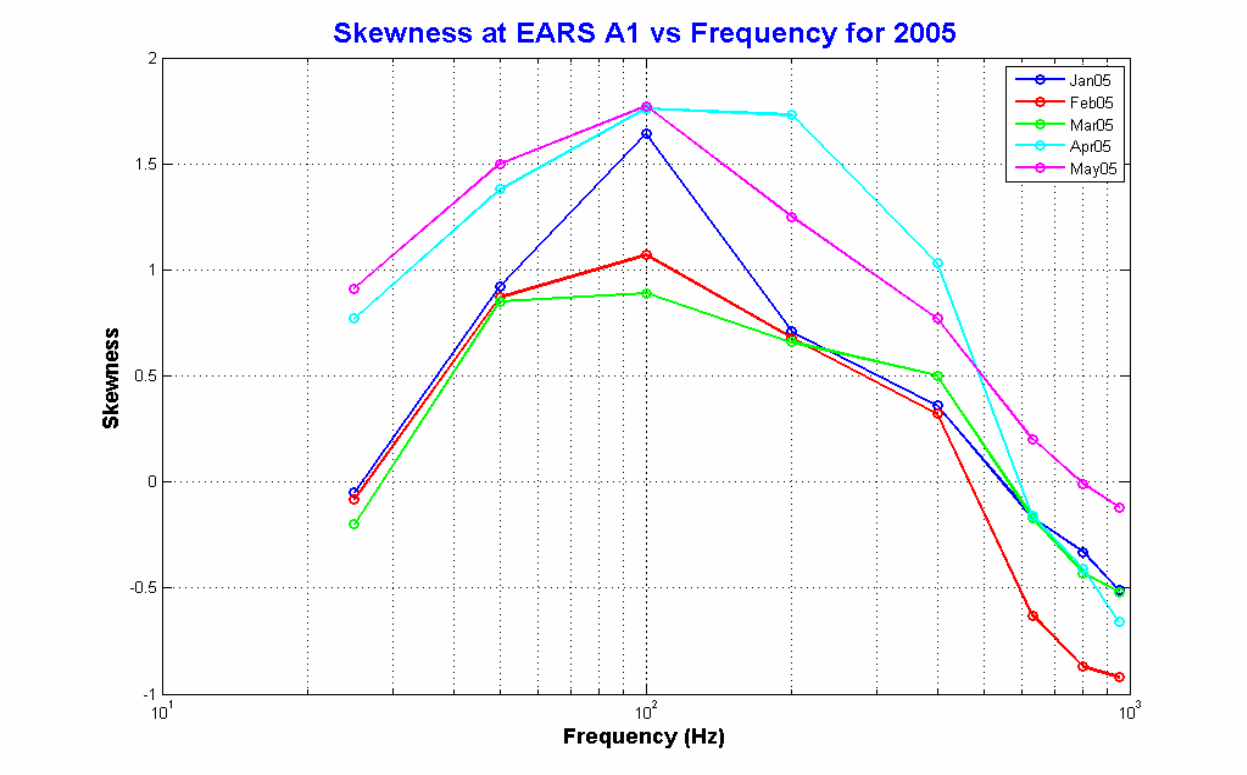

Figure 4.20 Skewness vs. frequency for 2005.

A good example showing how wind speeds influence the skewness is shown in Figure 4.21. This figure compares the histograms at 950 Hz during June 2004 and January 2005. June 2004 was a calm month with an average wind speed of 7.4 knots while January 2005 was a very windy month with an average wind speed of 13.0 knots. The low average wind speeds during June contribute more energy to the "quiet side" (i.e., low dB side) of the PDF at high frequencies. The mean noise at 950 Hz during June was 56.26 dB. Conversely, the high average wind speeds during January contribute more energy to the "loud side" (i.e., high dB side) of the PDF at high frequencies. The mean noise at 950 Hz during January was 62.73 dB. Thus, the average noise level during January was 6.47 dB louder than the average noise level during June. Even more striking is the change in the mode. For June the mode is about 56 dB, while for January the peak value of the PDF is about 65 dB, an increase of 9 dB. Low wind speeds during June cause the mode to occur at a lower value with respect to the range of the data and cause the skewness to be positive (0.45 for June). High wind speeds during January cause the mode to occur at a higher value with respect to the range of the data and cause the skewness to be negative (-0.51 for January).

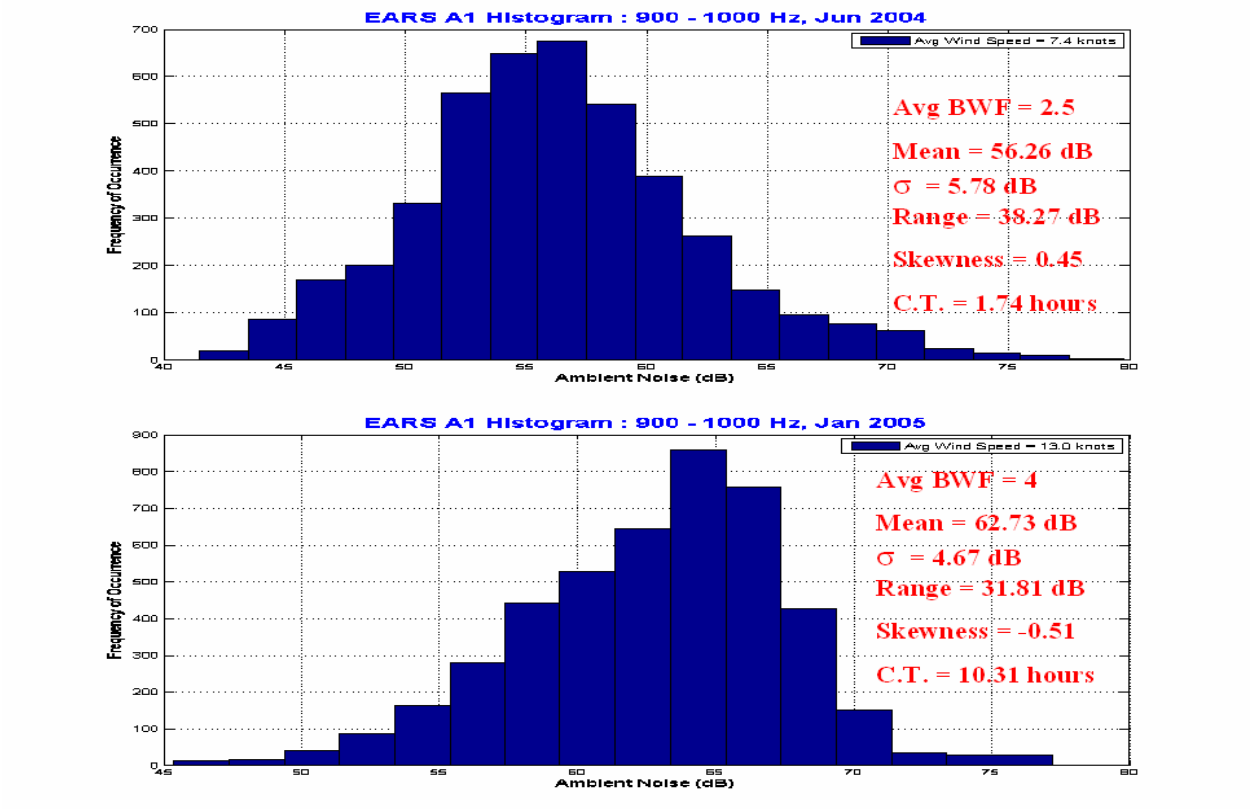

Figure 4.21 Histograms at 950 Hz during June 2004 and January 2005.

The kurtosis (Figures 4.22 to 4.24) tends to be low at 25 Hz, peaks at 100 Hz and decreases again at higher frequencies. Values of kurtosis in the weather band of 630 – 950 Hz tend to be between 3 and 4, generally near 3 (the kurtosis of a Gaussian distribution). Conversely, the values of kurtosis in the shipping band of 25 - 200 Hz tend to be higher, reaching a maximum value of 9.5 at 100 Hz.

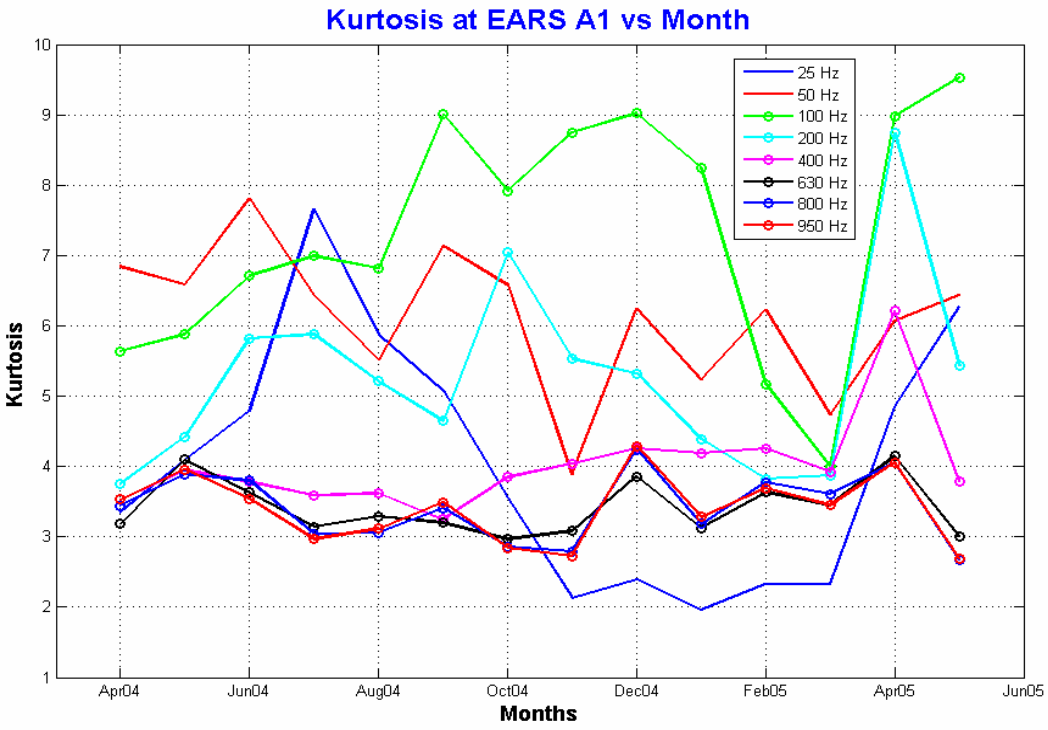

Figure 4.22 Kurtosis vs. month.

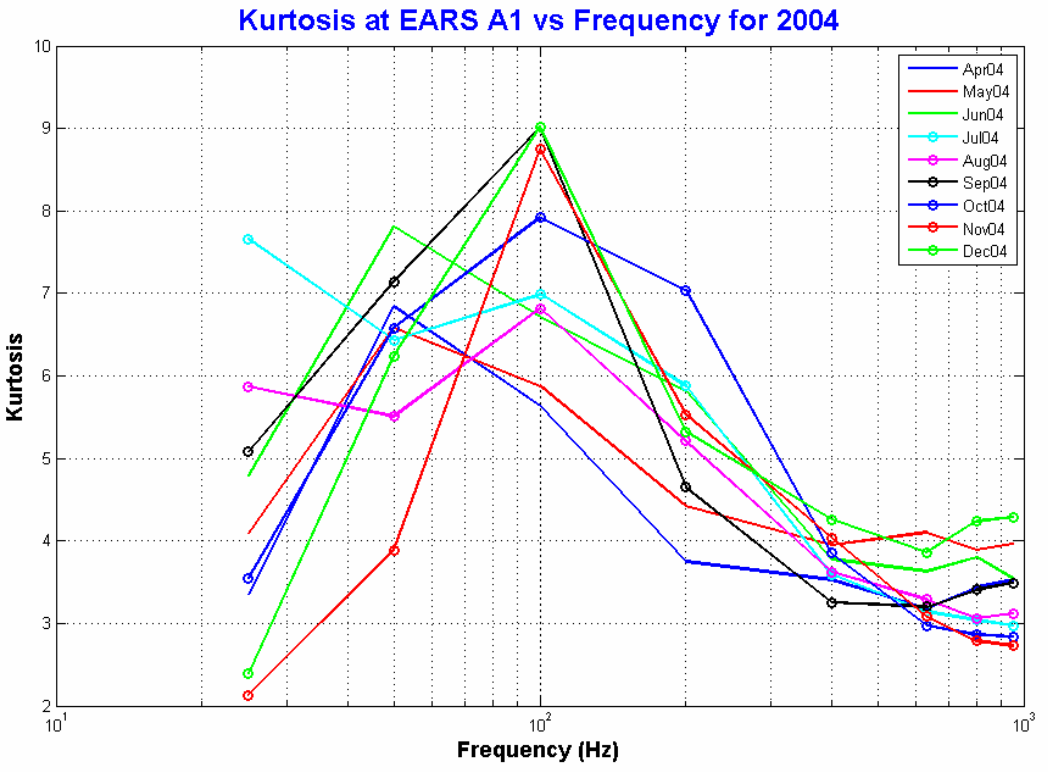

Figure 4.23 Kurtosis vs. frequency for 2004.

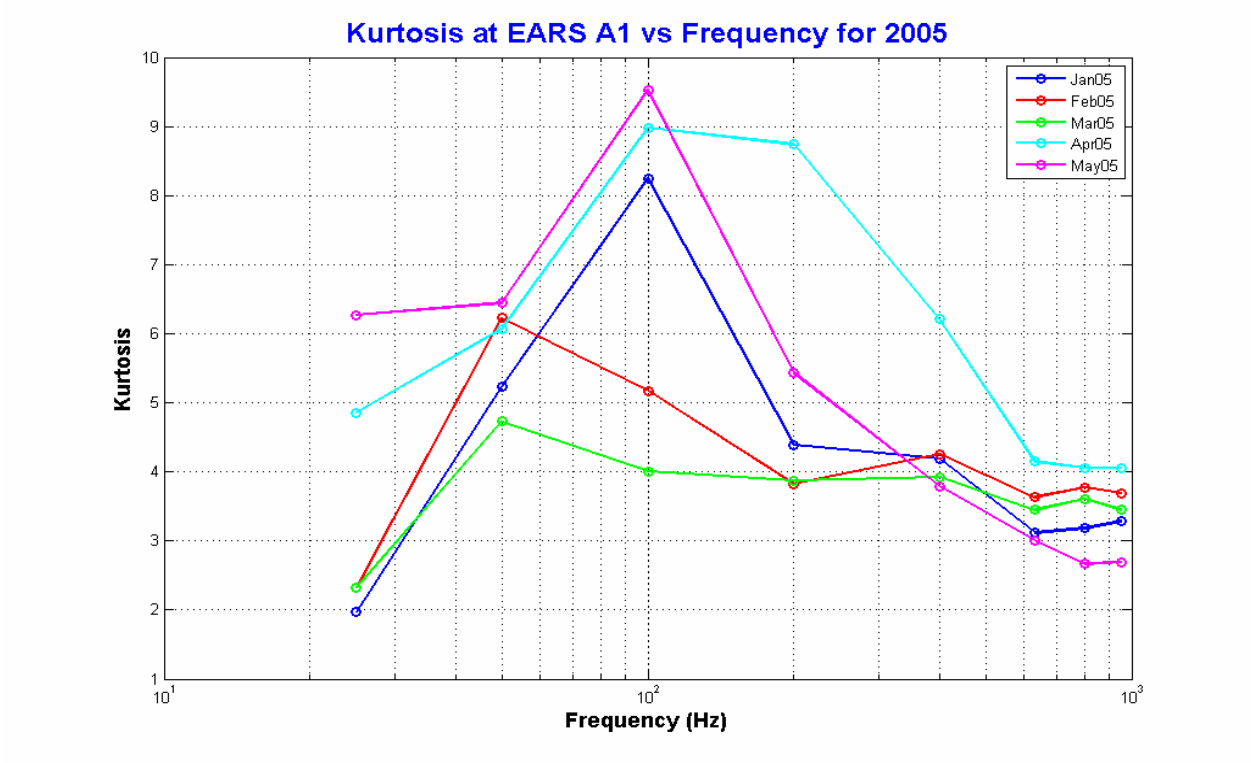

Figure 4.24 Kurtosis vs. frequency for 2005.

The temporal coherence of the noise field was analyzed by computing the autocorrelation function for each of the eight 1/3-octave band time series for each month. The time for the autocorrelation to fall to e^{-1} of its central (zero-lag) value is called the coherence time.[2] The coherence time is a measure of the effective width of the autocorrelation function, or how long a time series is coherent with itself. The coherence times (Figures 4.25 to 4.27) range from a low value of about 1 hour to a high value of about 33 hours. The coherence time is generally low at low frequencies in the shipping band (25 - 400 Hz) year-round, and at higher frequencies in the weather band (630 - 950 Hz) when the average monthly wind speed is low (such as June through August of 2004). It is generally high at higher frequencies (630 - 950 Hz) when the average monthly wind speed is high. The highest values are observed during the hurricane month of September 2004 at all frequencies above 200 Hz, with the maximum being 32.66 hours at 950 Hz. During 2005 the highest values for coherence time are observed during May at higher frequencies; the peak value is about 18 hours at 950 Hz.

[2] Some authors call this the *correlation time* or the *decorrelation time*.

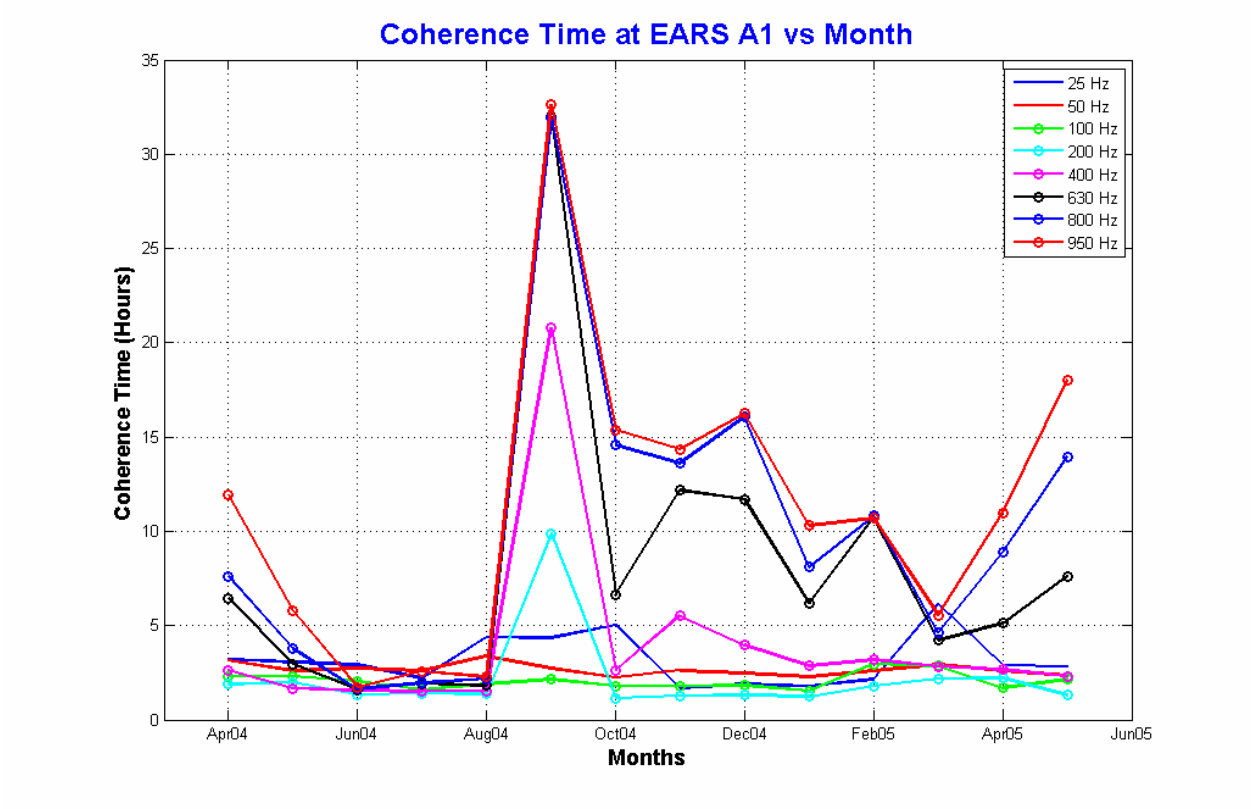

Figure 4.25 Coherence time vs. month.

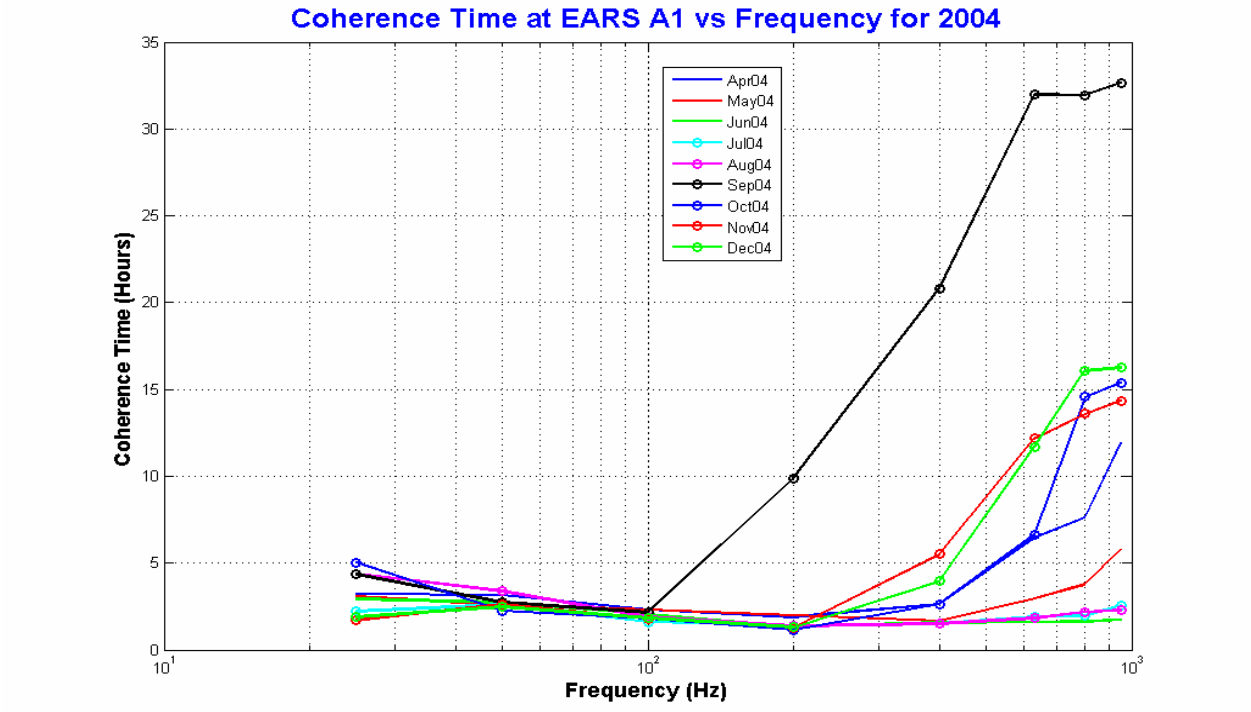

Figure 4.26 Coherence time vs. frequency for 2004.

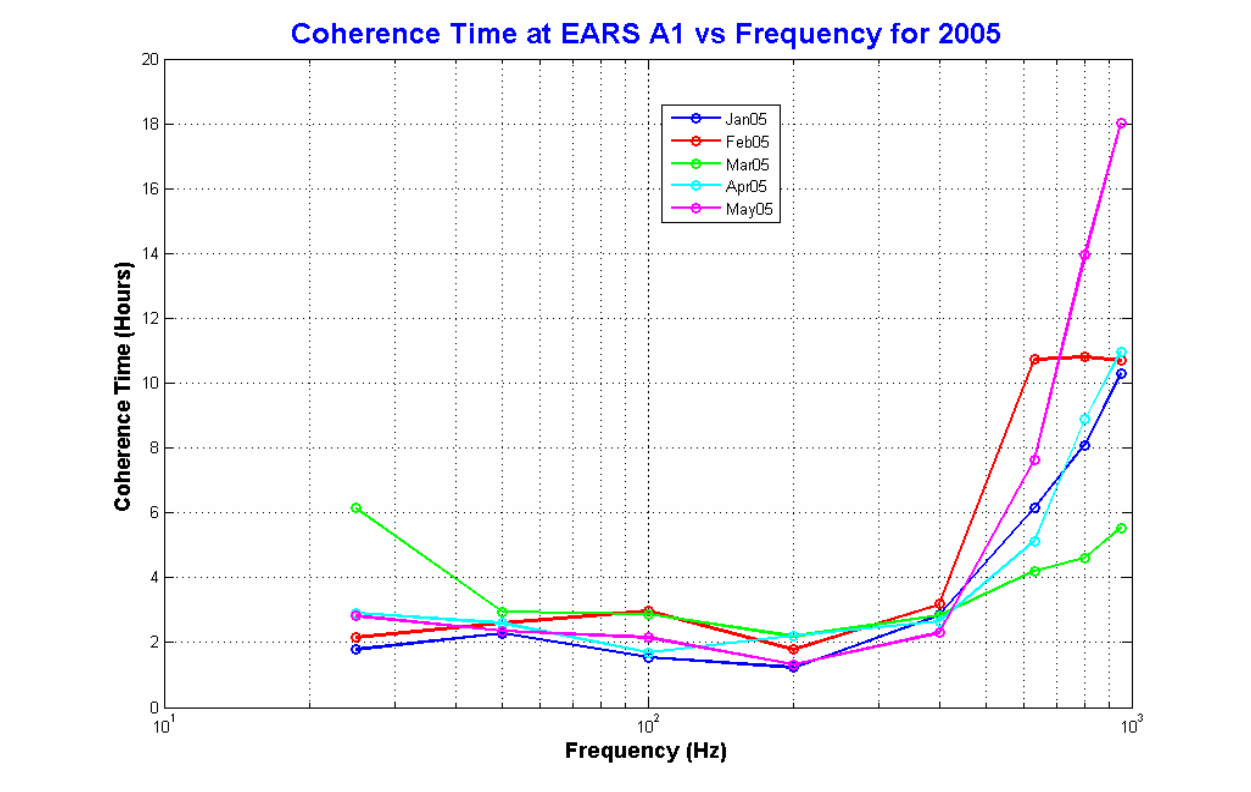

Figure 4.27 Coherence time vs. frequency for 2005.

Chapter 5
Long-Term Statistics

5.1 Fourteen Month Statistics

In this chapter the entire fourteen month time series at each of the eight 1/3-octave center frequencies is discussed. The mean values (Figure 5.1) for the fourteen month period peak at 25 Hz and 50 Hz, and then decrease with increasing frequency out to 950 Hz. Figure 5.1 also shows the median, 90th percentile and 10th percentile values for the entire time period. The fourteen month mean and median values at each frequency never differ by more than 0.8 dB. The mean value is larger than the median value from 25-400 Hz, while the median value is greater from 630-950 Hz.

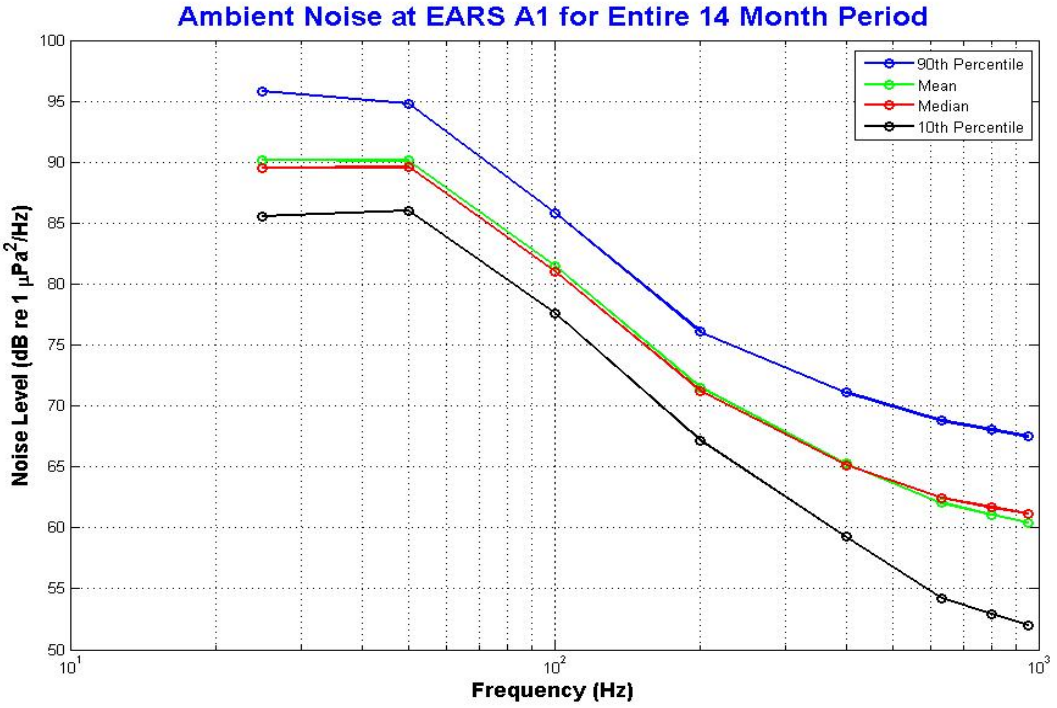

Figure 5.1 Ambient noise for entire 14 month period.

The spread of the data, as determined by subtracting the 10th percentile value from the 90th percentile value for each 1/3-octave band, is shown in Table 5.1. This number was divided by the standard deviation (σ) for each 1/3-octave band to compute the spread in σ units.

F_c (Hz)	90% - 10% (dB)	Spread in σ units
25	10.26	2.58
50	8.80	2.39
100	8.24	2.37
200	8.90	2.43
400	11.84	2.50
630	14.56	2.56
800	15.11	2.54
950	15.50	2.53

Table 5.1 Spread of data for entire 14 month period.

As can be seen in Table 5.1 and Figure 5.1, the spread of the data is rather large at 25 Hz, decreases to a minimum at 100 Hz, and then increases again at higher frequencies. Note how the spread in σ units varies from a low value of 2.37 at 100 Hz to a high value of 2.58 at 25 Hz. For comparison, the spread in σ units for a Gaussian distribution is 2.56 σ [Li, 1999].

The standard deviation for the entire fourteen month period is shown in Figure 5.2. The standard deviation is relatively high (3.97 dB) at 25 Hz and at higher frequencies (greater than 4.0 dB from 400-950 Hz) but is smallest in the region 50-200 Hz. The minimum standard deviation value is 3.47 dB at 100 Hz. The minimum at 100 Hz agrees with the minimum spread of the data shown in Table 5.1.

The skewness for the entire fourteen month period is shown in Figure 5.3. The skewness is positive (skewed towards peaks) from 25-400 Hz but negative (skewed towards troughs) from 630-950 Hz.[1] This is expected. Since shipping noise dominates low frequencies, the region 25-400 Hz is dominated by shipping peaks, which contribute to the high amplitude tails (louder decibel values) of a probability density function (PDF) and make the skewness positive. Weather noise dominates high frequencies, so the region 630-950 Hz is dominated by weather. Of the fourteen months analyzed, eleven months had average wind speeds of 9 knots or greater, and these months were generally negatively skewed in the region of 630 - 950 Hz. The average

[1] In general, the skewness is positive when the mean is greater than the median and negative when the median is greater than the mean.

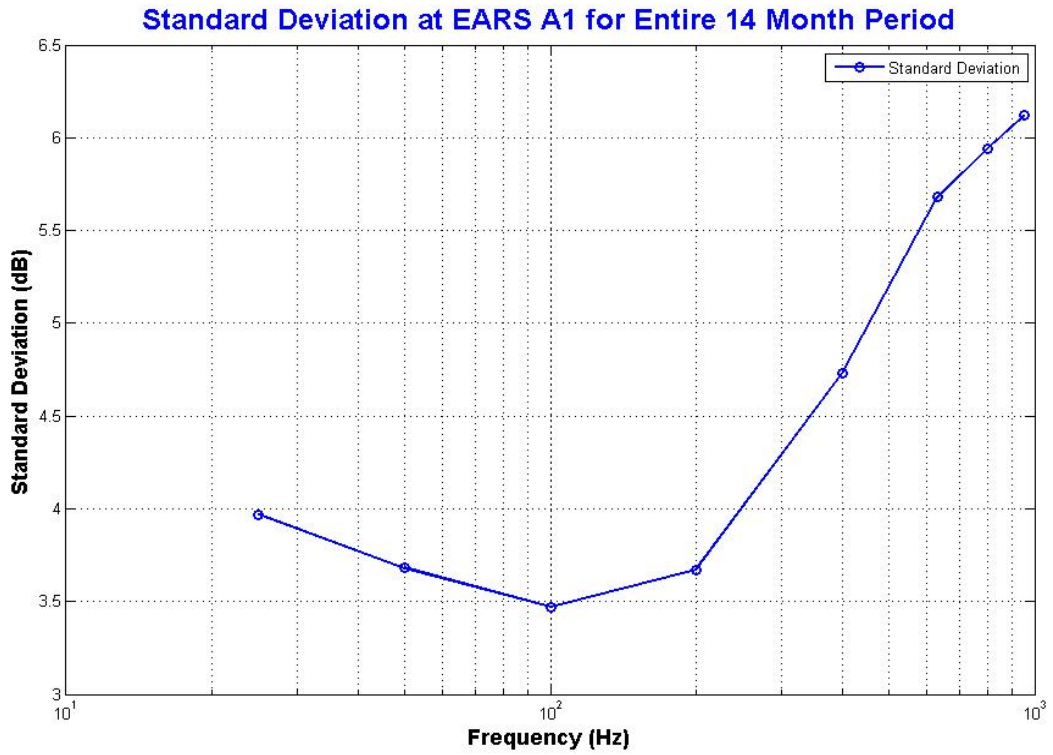

Figure 5.2 Standard deviation for entire 14 month period.

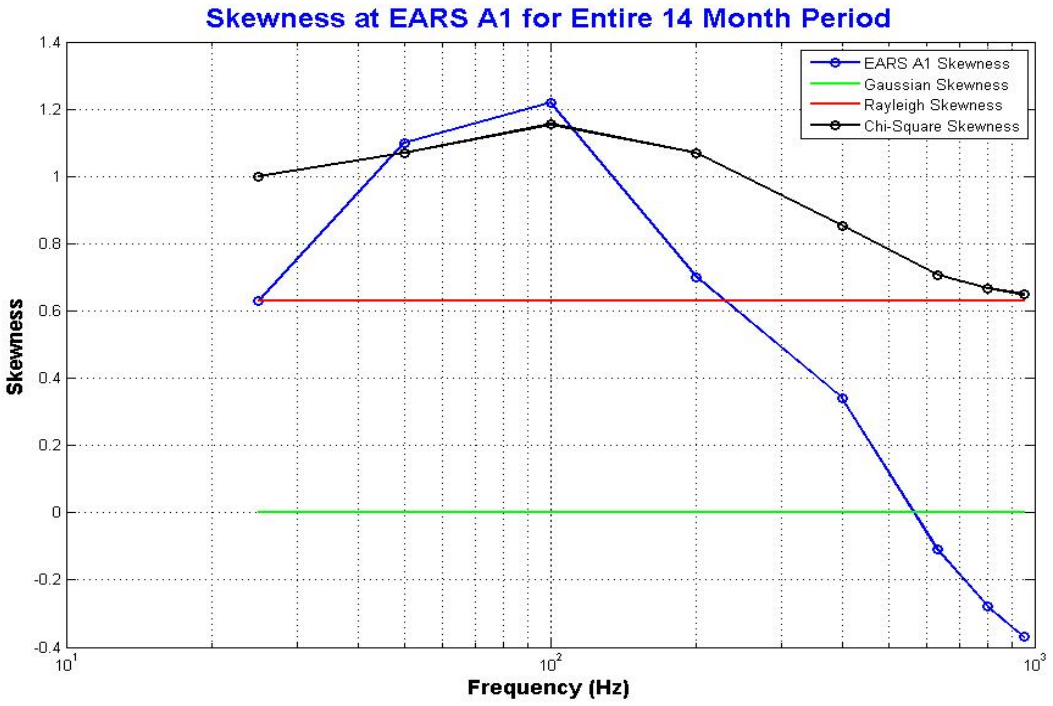

Figure 5.3 Skewness for entire 14 month period.

wind speed for the entire fourteen month period is 11.3 knots, which causes the skewness in the region 630-950 Hz to be negative.

The kurtosis for the entire fourteen month period is shown in Figure 5.4. The kurtosis is low at 25 Hz, peaks in the region 50-400 Hz and settles down to values near 3 from 630-950 Hz. (The kurtosis of a Gaussian distribution is 3.)

The coherence time for the entire fourteen month period is shown in Figure 5.5. The coherence time is low (2.52-3.71 hours) at low frequencies (25-400 Hz) due to shipping variability but high (14.54-21.01 hours) at high frequencies (630-950 Hz) due to wind variability.

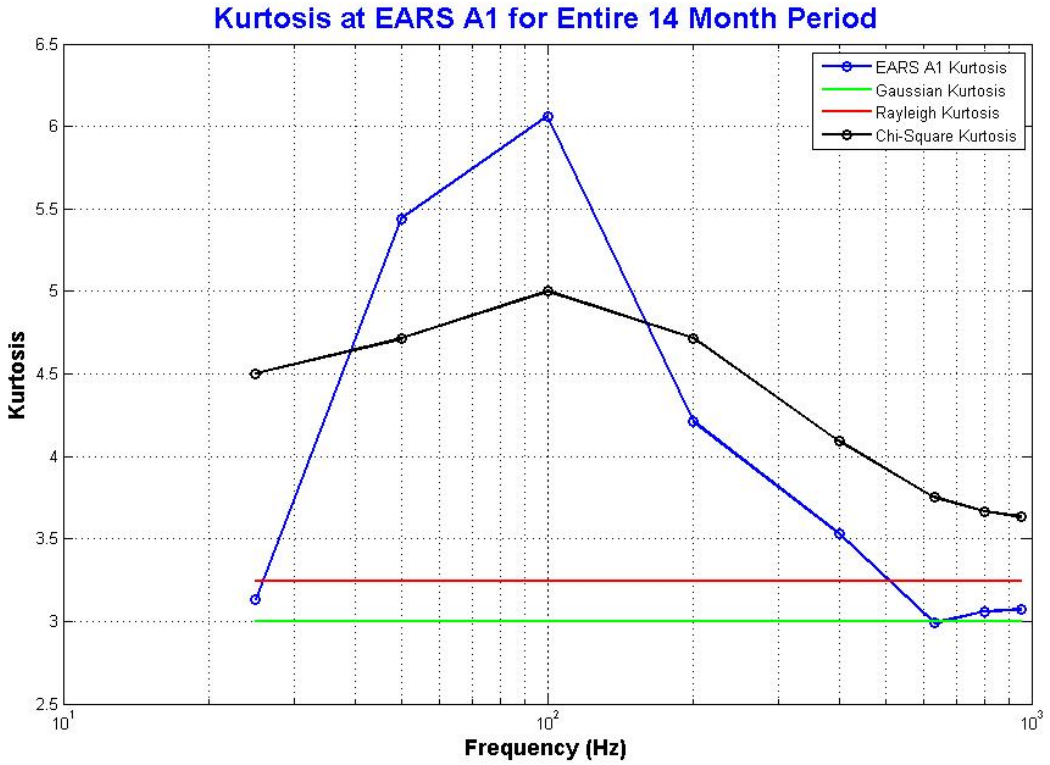

Figure 5.4 Kurtosis for entire 14 month period.

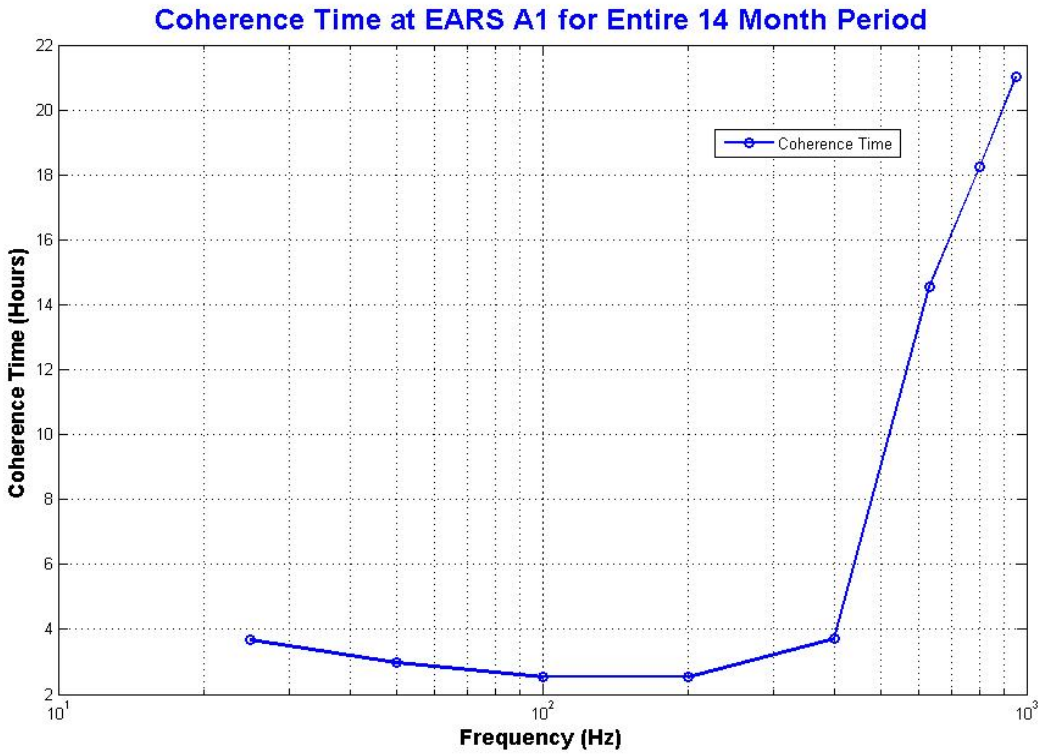

Figure 5.5 Coherence time for entire 14 month period.

5.2 Probability Density Functions

It is obvious from the results of Chapter 4 that the processes producing the noise are not stationary. All four moments, the mean, standard deviation, skewness and kurtosis, vary considerably from month to month. There are obvious long-term trends in the data, which are especially evident in Figure 4.1. The histograms in a given frequency band sometimes vary significantly from month to month. But it seems of interest to see if each long-term histogram, based on fourteen months of data, follows any patterns in each frequency band.

Many theoretical ambient noise studies assume the ambient noise is Gaussian and stationary over short time periods. Nearby shipping noise has been found to be non-Gaussian, while much of the data with no obvious ship or biological sources present has been found to be Gaussian [Arase and Arase, 1968]. Arase and Arase found more than half of their data sets to be Gaussian, and their data to be stationary for less than 3 minutes.

Urick described a noise model that assumed Gaussian noise was input to a conventional sonar processor [Urick, 1977]. He showed that the output of the processor can be represented as *n* independent samples of the Gaussian input. The sum of the squares of *n* independent samples of a Gaussian random variable has a Chi-Square probability density function (PDF) with *n* degrees of freedom. A Chi-Square random variable is a good model for the total power of a signal that has *n* independent components [Li, 1999]. Urick pointed out that a Chi-Square PDF with $n = 2$ is the same as a Rayleigh PDF, and that as *n* approaches infinity, the Chi-Square PDF approaches a Gaussian PDF. Thus, it seems instructive to see if any of the long-term PDFs could be characterized as Gaussian, Chi-Square or Rayleigh.

An attempt has been made to classify the PDF in each frequency band. The shape of each PDF is determined by the relative contributions of shipping and weather noise in each band. Figures 5.6 to 5.13 show the time series and histograms for the entire fourteen month period for each frequency band, from 25 to 950 Hz. Each figure also displays the skewness determined for that frequency band.

At 25 Hz (Figure 5.6) the PDF appears to match a Rayleigh distribution. The first three moments match a Rayleigh distribution with Rayleigh parameter $\sigma_R = 6.0597$ dB.

With this choice of σ_R, the first two moments (the mean and the variance) match exactly. The third moment matches as well: the measured skewness is 0.63, yielding excellent agreement with the skewness of a Rayleigh[2] distribution, 0.6311. The fourth moments are close: the measured kurtosis is 3.13, compared to 3.2451, the kurtosis of a Rayleigh distribution.

---

[2] A Rayleigh distribution has the PDF $f(x) = \frac{x}{\sigma_R^2} e^{\frac{-x^2}{2\sigma_R^2}}$ *for* $x > 0$.

It has a mean value of $\sqrt{\frac{\pi}{2}}\sigma_R$ and a variance of $(2-\frac{\pi}{2})\sigma_R^2$. It has a skewness of 0.6311 and a kurtosis of 3.2451 [Evans, 2000]. A Rayleigh distribution shifted to the right by an amount "*a*" has a mean value of $a + \sqrt{\frac{\pi}{2}}\sigma_R$. The values for the second, third and fourth moments remain unchanged.

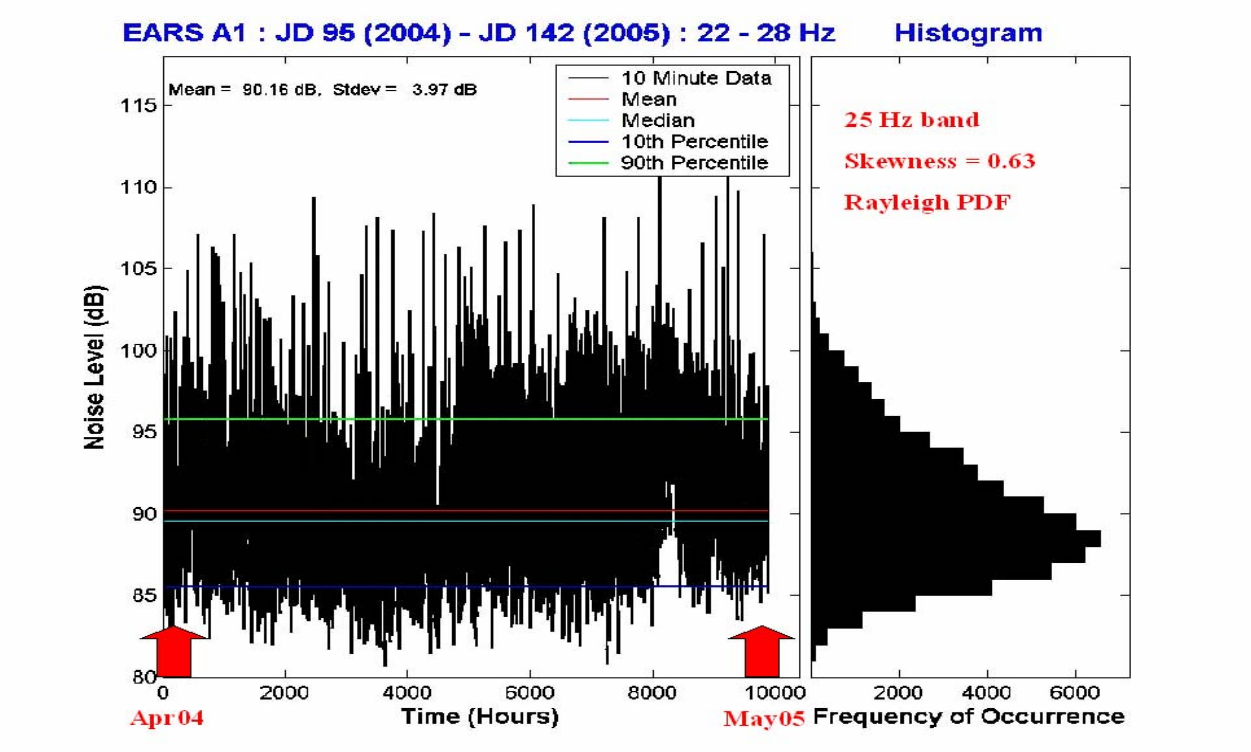

Figure 5.6 Time series and histogram at 25 Hz for entire 14 month period.

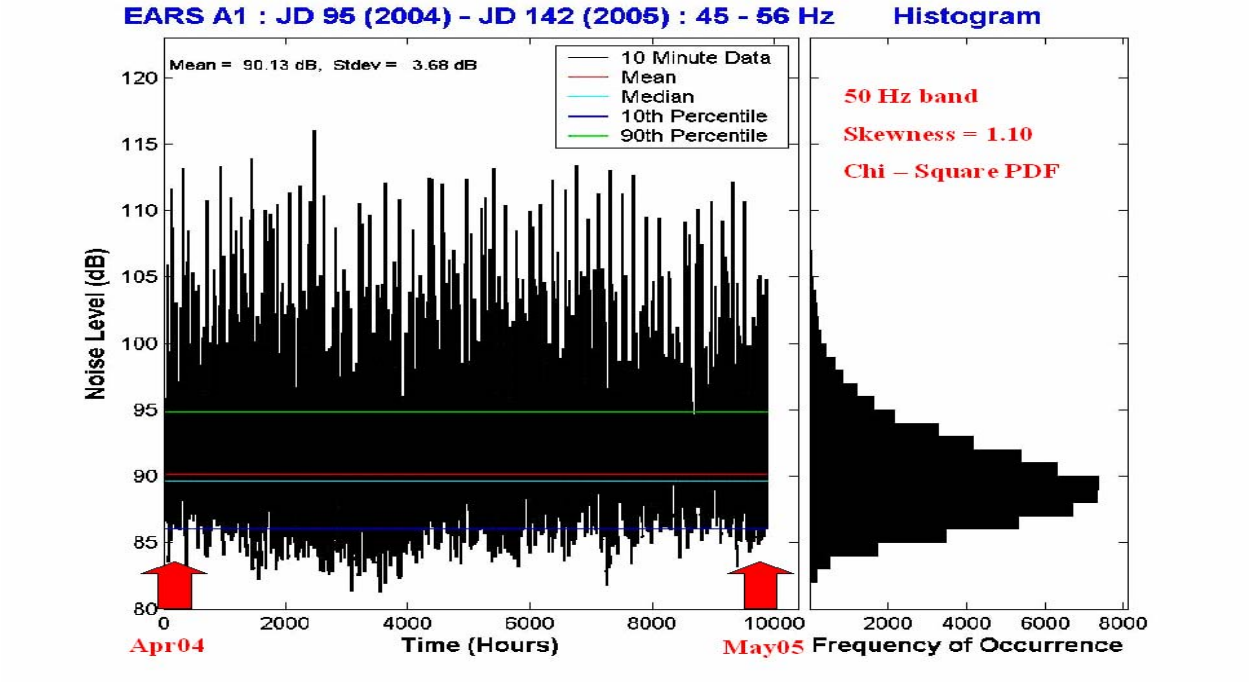

Figure 5.7 Time series and histogram at 50 Hz for entire 14 month period.

At 50 Hz (Figure 5.7) the PDF appears to match a Chi-Square[3] distribution. The first three moments match a Chi-Square distribution with $n = 7$ degrees of freedom (dof). With this choice of dof, the first two moments (the mean and the variance) match exactly. The third moments match as well: the measured skewness is 1.10, yielding very good agreement with the skewness of a Chi-Square distribution with 7 degrees of freedom, 1.07. The fourth moments don't match: the measured kurtosis is 5.44, compared to 4.71, the kurtosis of a Chi-Square distribution with 7 degrees of freedom.

At 100 Hz (Figure 5.8) the PDF also appears to match a Chi-Square distribution. The first two moments match a Chi-Square distribution with $n = 6$ degrees of freedom. With this choice of dof, the first two moments (the mean and the variance) match exactly. The third moments match approximately: the measured skewness is 1.22, yielding pretty good agreement with the skewness of a Chi-Square distribution with 6 degrees of freedom, 1.15. The fourth moments don't match: the measured kurtosis is 6.06, compared to 5.00, the kurtosis of a Chi-Square distribution with 6 degrees of freedom.

At 200 Hz (Figure 5.9) the PDF appears to match a Rayleigh distribution. The first two moments match a Rayleigh distribution with Rayleigh parameter $\sigma_R = 5.5965$ dB. With this choice of σ_R, the first two moments (the mean and the variance) match exactly. The third moments match as well: the measured skewness is 0.70, yielding pretty good agreement with the skewness of a Rayleigh distribution, 0.6311. The fourth moments don't match: the measured kurtosis is 4.21, compared to 3.2451, the kurtosis of a Rayleigh distribution.

At 400 Hz the PDF could be made to match either a Rayleigh or a Chi-Square distribution by matching the first two moments, but the third and fourth moments don't match. The first two moments match a Rayleigh distribution with Rayleigh parameter $\sigma_R = 7.2239$ dB. But the measured skewness is 0.34, not matching the skewness of a Rayleigh distribution,

---

[3] A Chi-Square distribution has the PDF $f(x) = \frac{2^{-\frac{n}{2}}}{\Gamma(\frac{n}{2})} x^{\frac{n-2}{2}} e^{-\frac{x}{2}}$ *for* $x > 0$.

It has a mean value of n and a variance of $2n$. It has a skewness of $\sqrt{\frac{8}{n}}$ and a kurtosis of $3 + 12/n$ [Evans, 2000]. A Chi-Square distribution shifted to the right by an amount "a" has a mean value of $a + n$. The values for the second, third and fourth moments remain unchanged.

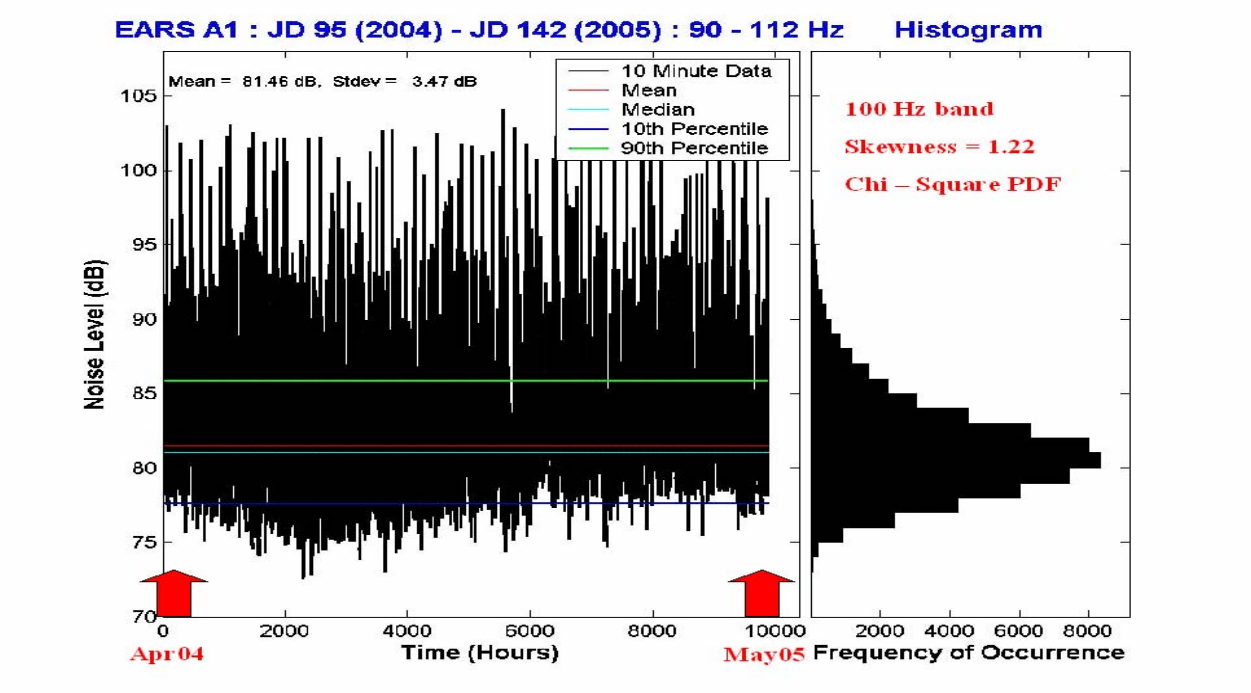

Figure 5.8 Time series and histogram at 100 Hz for entire 14 month period.

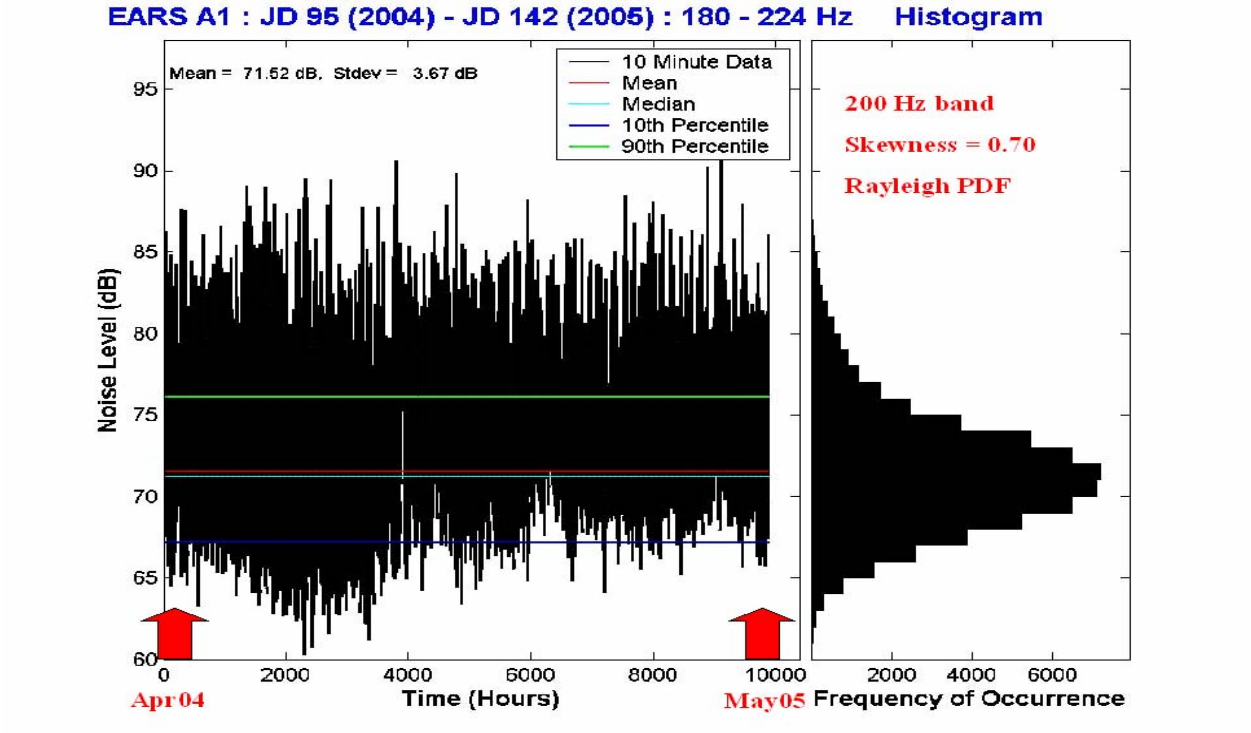

Figure 5.9 Time series and histogram at 200 Hz for entire 14 month period.

0.6311. The fourth moments also don't match: the measured kurtosis is 3.53, compared to 3.2451, the kurtosis of a Rayleigh distribution.

The first two moments match a Chi-Square distribution with $n = 11$ degrees of freedom. With this choice of dof, the first two moments (the mean and the variance) match exactly. But the measured skewness is 0.34, not matching the skewness of a Chi-Square distribution with 11 degrees of freedom, 0.85. The fourth moments also don't match: the measured kurtosis is 3.53, compared to 4.09, the kurtosis of a Chi-Square distribution with 11 degrees of freedom.

The PDFs from 630-950 Hz are complicated by the effects of weather and do not fit simple distributions. In particular, they have negative values for skewness. Distributions such as Rayleigh or Chi-Square have positive skewness so they don't match the PDFs at the higher frequencies. They also don't match a Gaussian distribution, which has a skewness of 0.

Table 5.2 summarizes the best-fit distributions for 25-200 Hz for the entire fourteen month period.

F_c (Hz)	Best-Fit Distribution	Comments
25	Rayleigh	$\sigma_R = 6.0597$ dB
50	Chi-Square	n = 7
100	Chi-Square	n = 6
200	Rayleigh	$\sigma_R = 5.5965$ dB

Table 5.2 Best-fit distributions for entire 14 month period.

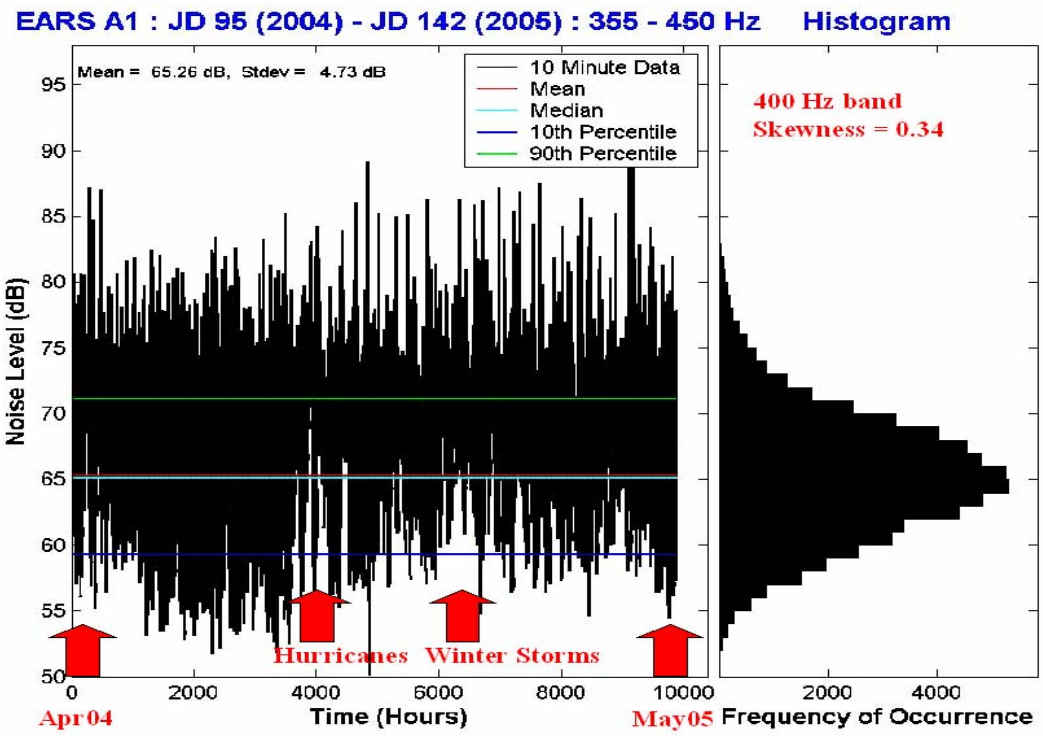

Figure 5.10 Time series and histogram at 400 Hz for entire 14 month period.

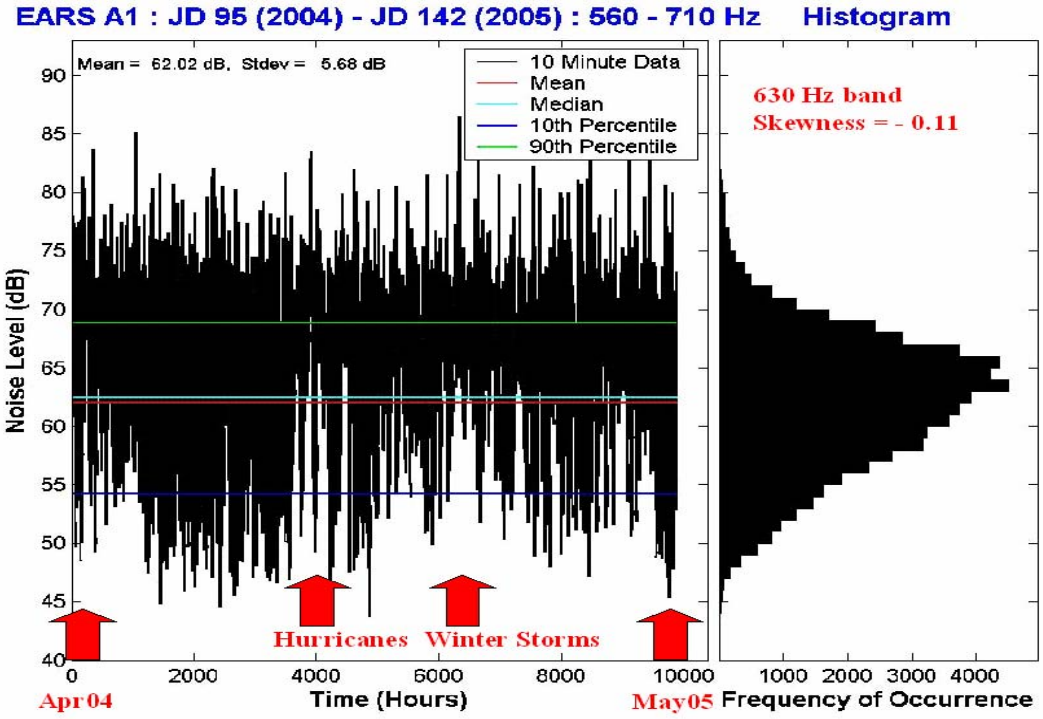

Figure 5.11 Time series and histogram at 630 Hz for entire 14 month period.

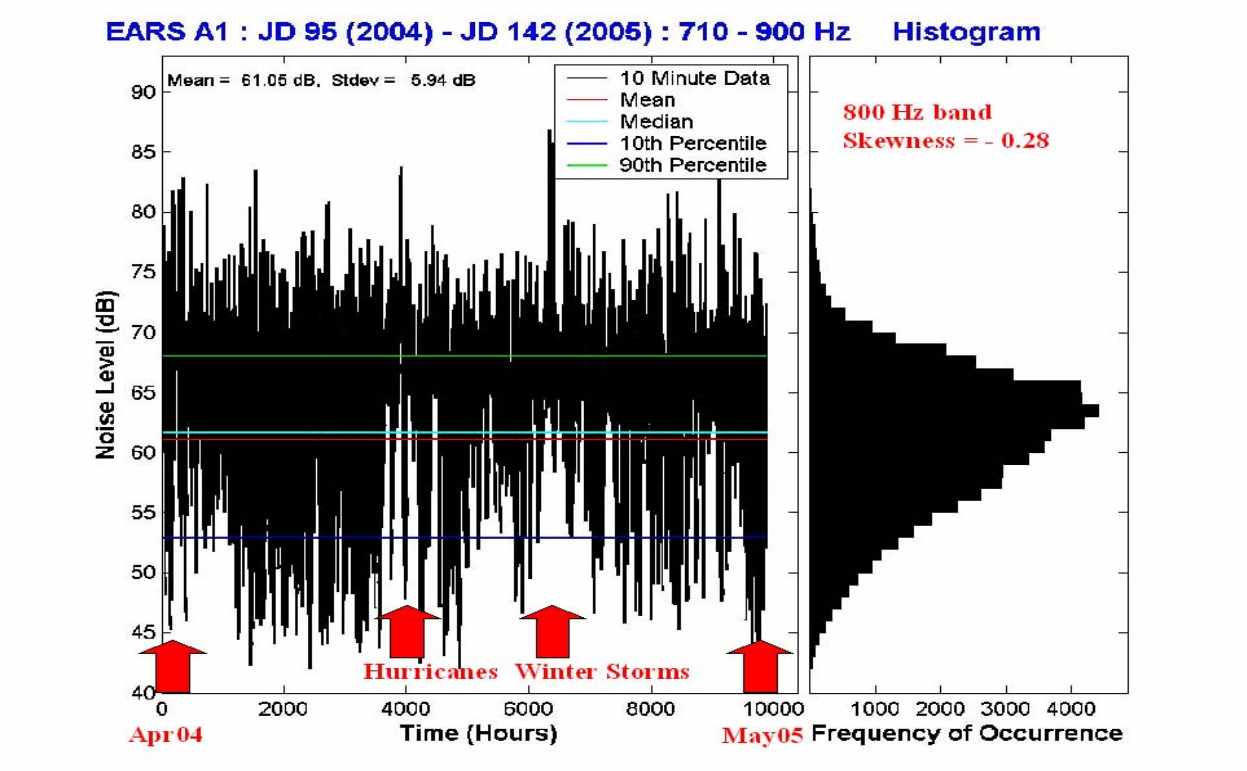

Figure 5.12 Time series and histogram at 800 Hz for entire 14 month period.

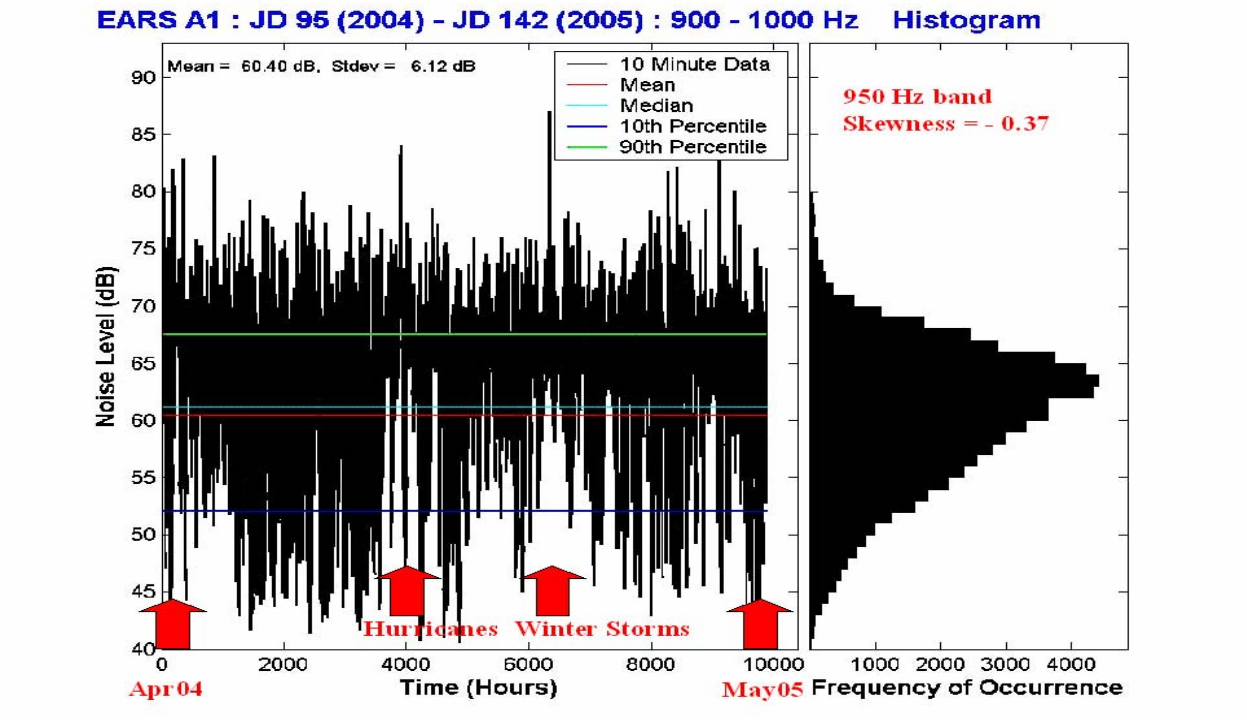

Figure 5.13 Time series and histogram at 950 Hz for entire 14 month period.

5.3 Variability Time Scales

The level of the ambient noise background at a fixed location in the ocean varies with time because of the time variability of the sources of noise. This time variability covers a wide scale, from very fast (short period) phenomena, such as transients from breaking waves, nearby ships and biological sources, to the very slow (long period) phenomena, such as weather and climate changes [Urick, 1984].

The variability of a noise time series X(t) can be expressed in terms of its fluctuation (power) spectrum S(ω), which gives the fluctuation power per unit frequency band as a function of frequency. These spectra can be useful in revealing the sources of the noise fluctuations. The fluctuation spectrum contains information about the power content of the different frequencies making up the time series and displays the dominant fluctuations and their associated periods or frequencies[4].

For each fourteen month time series, the fourteen month mean value was computed and subtracted from every sample, making the resulting time series X(t) zero mean (μ = 0). The autocorrelation function $R(\tau)$ was computed (see Appendix F):

$$R(\tau) = E[X(t+\tau)X(t)] \qquad \text{Equation 5.1}$$

Equivalently, $R(\tau)$ is the inverse Fourier transform of the power spectral density S(ω) :

$$R(\tau) = \int_{-\infty}^{\infty} S(\omega) e^{+i\omega\tau} d\omega \qquad \text{Equation 5.2}$$

The power spectral density or power spectrum $S(\omega)$ is the Fourier transform of the autocorrelation function:

$$S(\omega) = \frac{1}{2\pi} \int_{-\infty}^{\infty} R(\tau) e^{-i\omega\tau} d\tau \qquad \text{Equation 5.3}$$

[4] Since the power spectrum is the Fourier transform of the autocorrelation function, they are equivalent ways of describing the fluctuation time scale. The autocorrelation function is more useful in determining the coherence time of a time series [Bracewell, 2000 and Urick, 1982].

Now, the variance of a time series is given by

$$\text{variance} = \sigma^2 = E[X^2] - \mu^2 \qquad \text{Equation 5.4}$$

Since X(t) is zero mean, $\sigma^2 = E[X^2]$. Substituting $\tau = 0$ in Equation 5.1 yields

$$R(0) = E[X(t)^2] = E[X^2] = \sigma^2 = \text{variance} \qquad \text{Equation 5.5}$$

Substituting $\tau = 0$ in Equation 5.2 and using Equation 5.5 yields

$$R(0) = \int_{-\infty}^{\infty} S(\omega)\, d\omega = \sigma^2 = \text{variance} \qquad \text{Equation 5.6}$$

Equation 5.6 says that the area under the power spectral density (PSD) function is equal to the variance.

The fluctuation spectrum of each fourteen month time series has been computed. The results are plotted as a function of period (vice frequency) and are shown in Figures 5.14 to 5.21, from 25 Hz to 950 Hz. These plots show how the energy associated with variability is spread over long and short time scales and is termed the "distribution of variance" for that frequency band. In these plots, each vertical bar represents the variance in each 1/10-decade[5] frequency band. From Equation 5.6, the sum of all the vertical bars equals the total variance for that frequency band. Also plotted on each distribution of variance graph is a red curve showing a 1st order Gauss-Markov[6] process.

At low frequencies, most of the variability is in time scales near 10 hours. This can be seen in Figures 5.14 through 5.18, which display the distribution of variance for the shipping bands of 25 to 400 Hz.

[5] A decade is a factor of 10 in frequency, while an octave is a factor of 2 in frequency. Since $10^1 \approx 2^{3.32}$, 1.0 decade ≈ 3.32 octaves, or 0.1 decade ≈ 0.332 octaves ≈ 1/3 octave. So a 1/10-decade band and a 1/3-octave band are almost equal.

[6] A 1st order Gauss-Markov process is well characterized by 3 parameters: the mean, variance and coherence time of the process. Such a process also has an exponentially-decaying autocorrelation function. See Table 5.3.

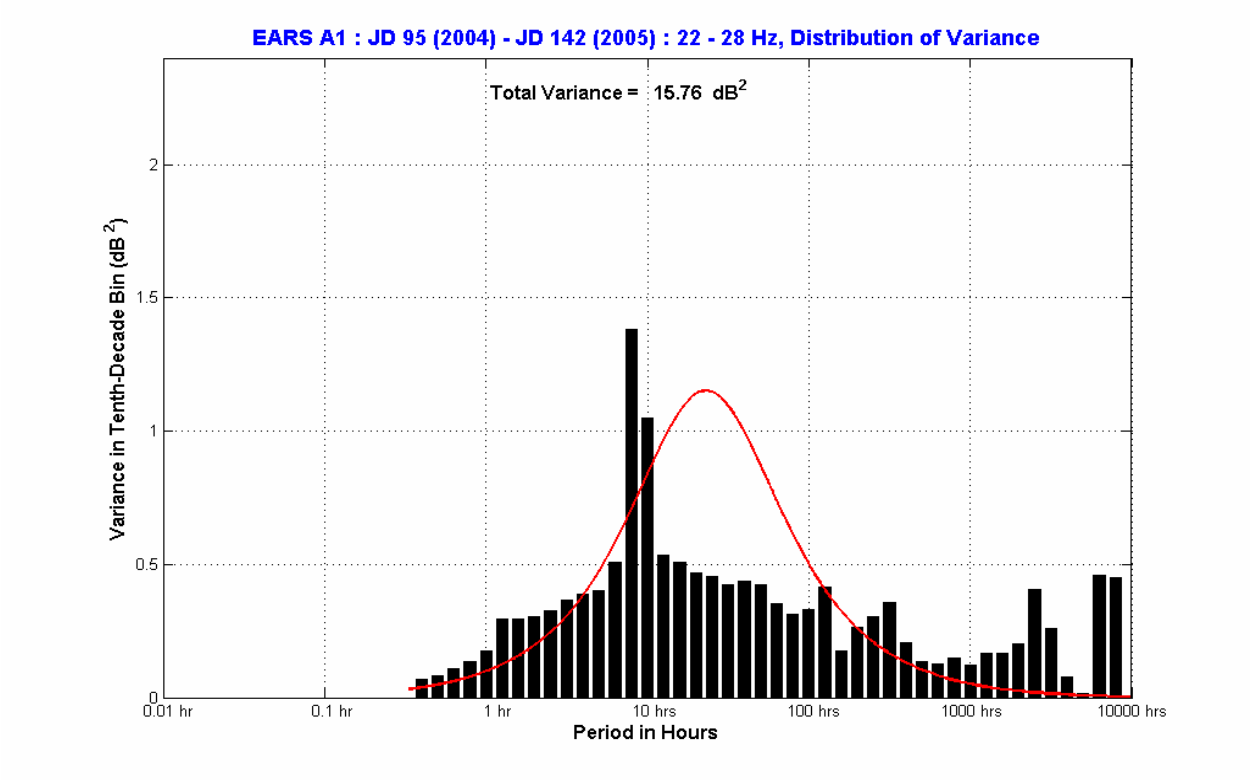

Figure 5.14 Distribution of variance at 25 Hz for entire time period.

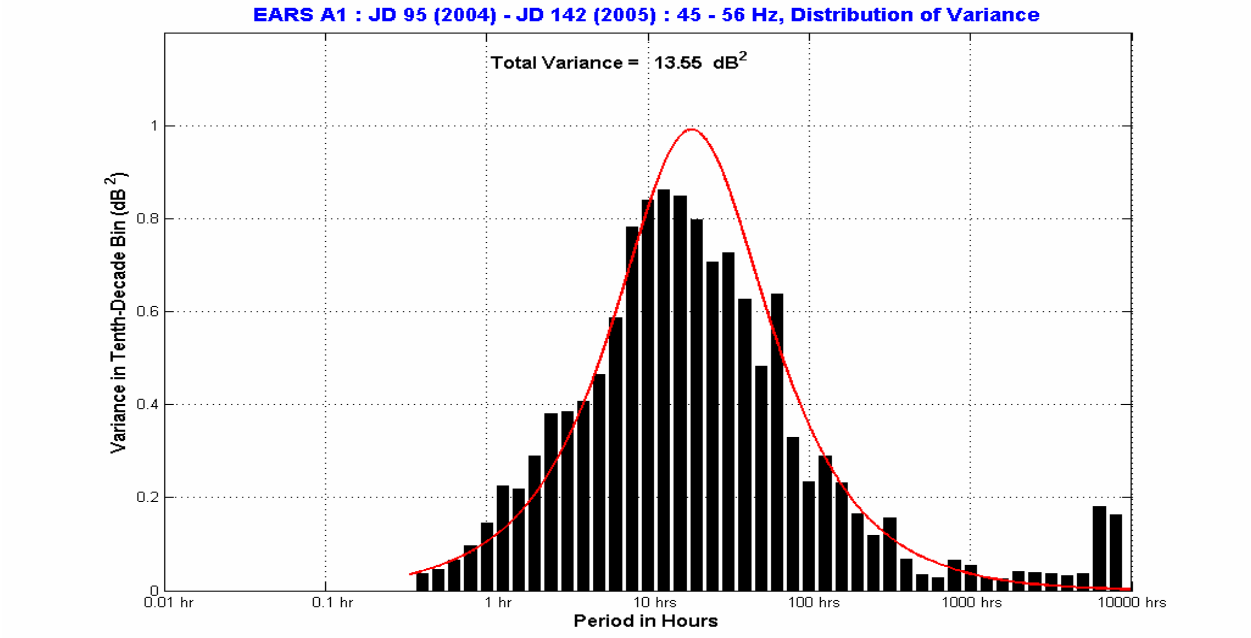

Figure 5.15 Distribution of variance at 50 Hz for entire time period.

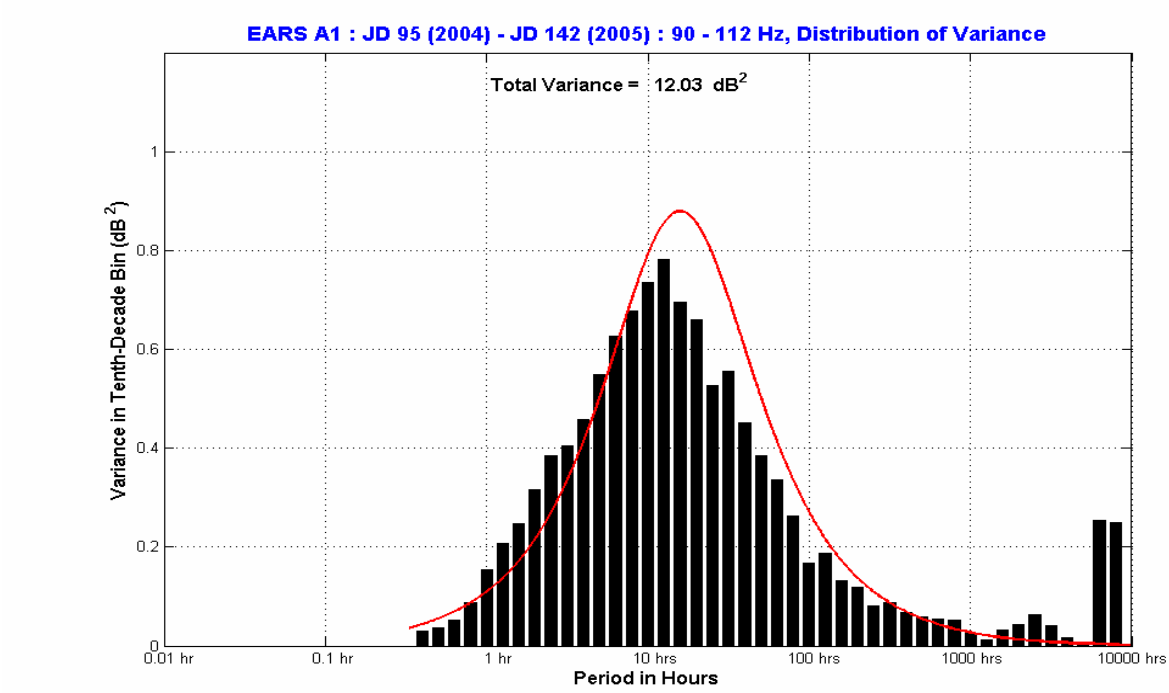

Figure 5.16 Distribution of variance at 100 Hz for entire time period.

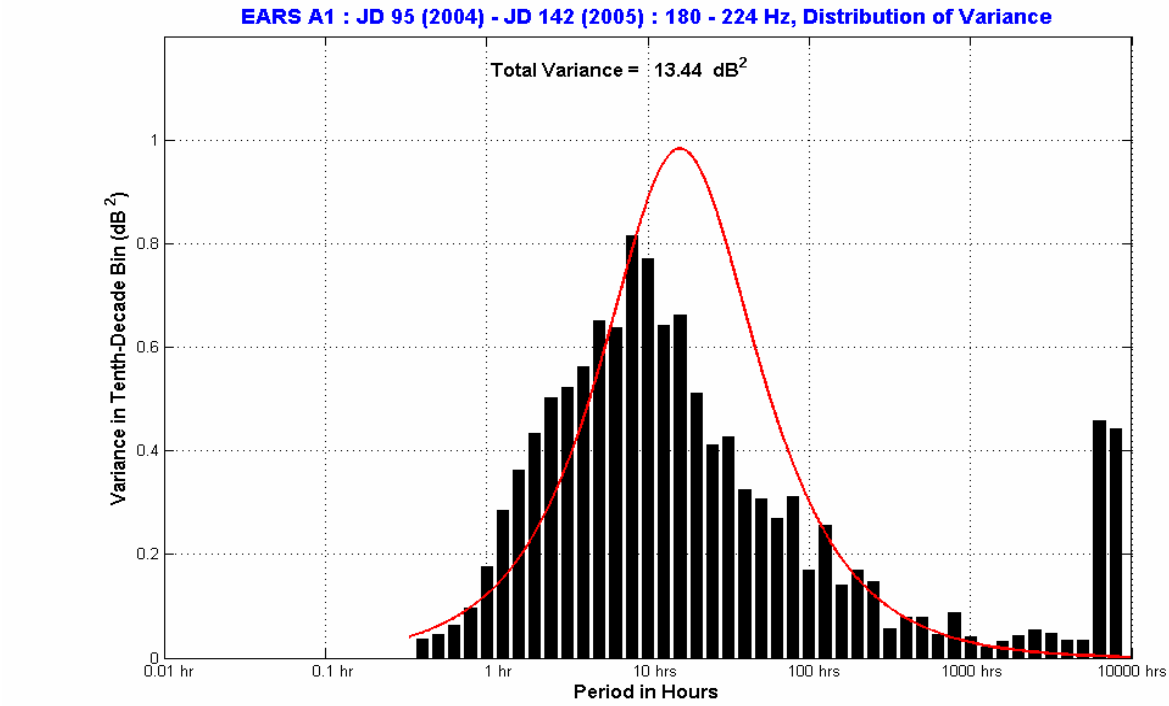

Figure 5.17 Distribution of variance at 200 Hz for entire time period.

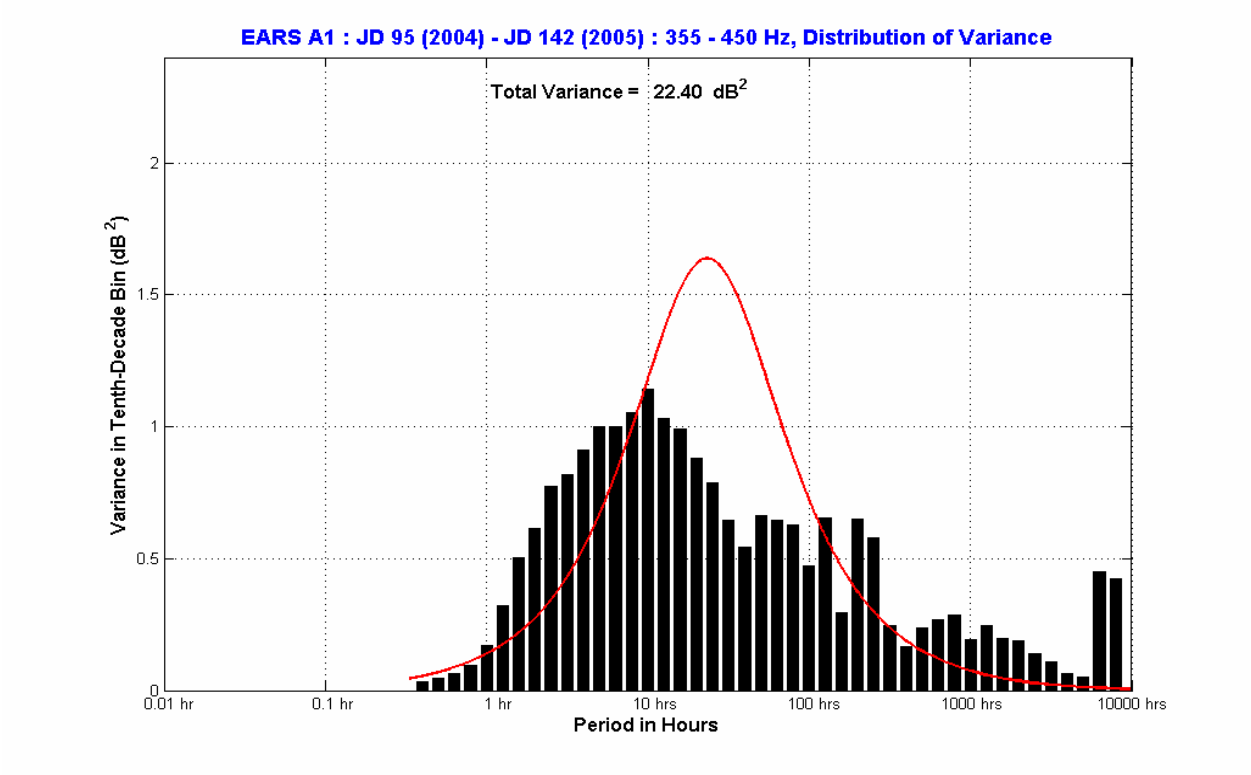

Figure 5.18 Distribution of variance at 400 Hz for entire time period.

But in the higher frequency weather bands (630 to 950 Hz), most of the variability is in time scales near 100 hours (about 4 days; see Figures 5.19 to 5.21). The higher frequency bands still showed variability near 10 hours, but more of the variance energy starts shifting to longer time scales as long period weather processes start to dominate short period shipping processes.

All frequency bands show energy at time scales near 10,000 hours (about 1.1 years), which is the longest period that can be observed in a fourteen month data set. This is consistent with the one year cycle observed in Figure 4.1, which displays the mean noise levels for all fourteen months for all 8 frequency bands.

Long period variations in ambient noise have been measured with periods ranging from several months to a year. The temperature structure of the ocean obviously changes with the seasons. The changing temperatures can affect the fish and marine mammal populations. The seasonal changes in wind speed will change the depth of the mixed layer, and the changing sound speed profiles will affect sound transmission [Urick, 1984].

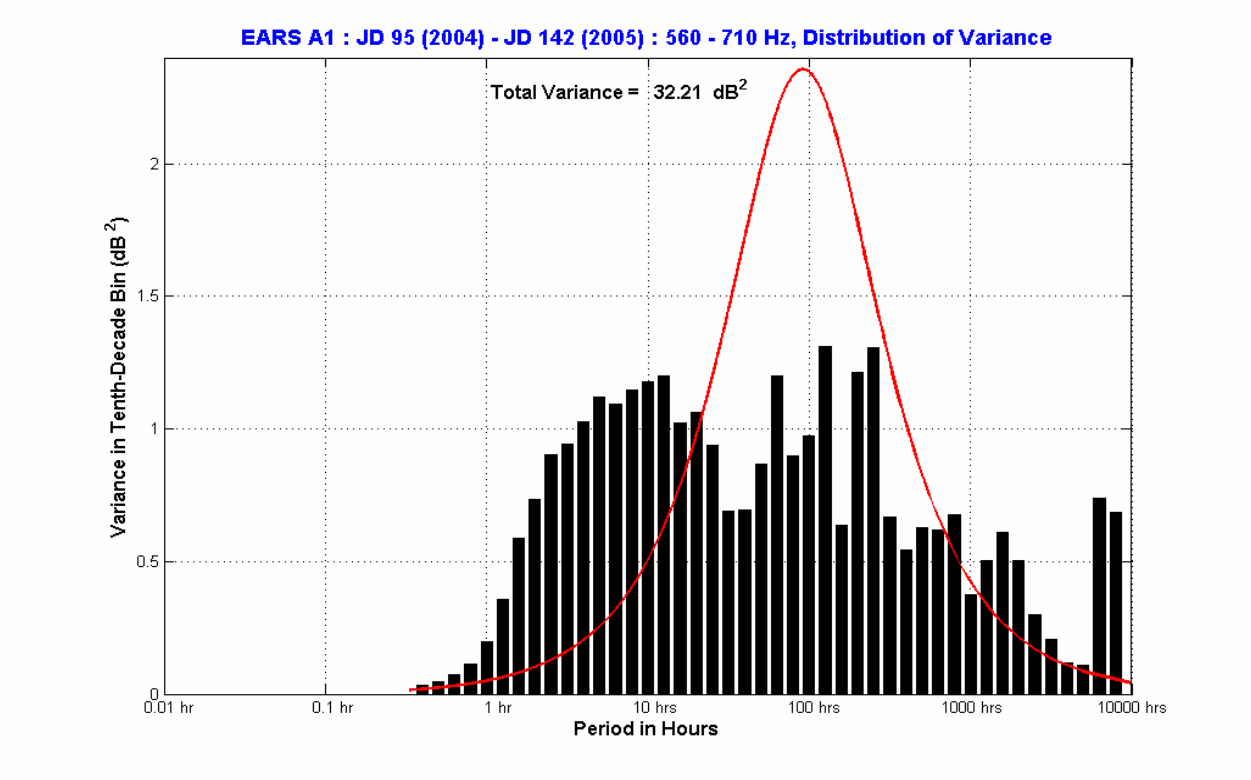

Figure 5.19 Distribution of variance at 630 Hz for entire time period.

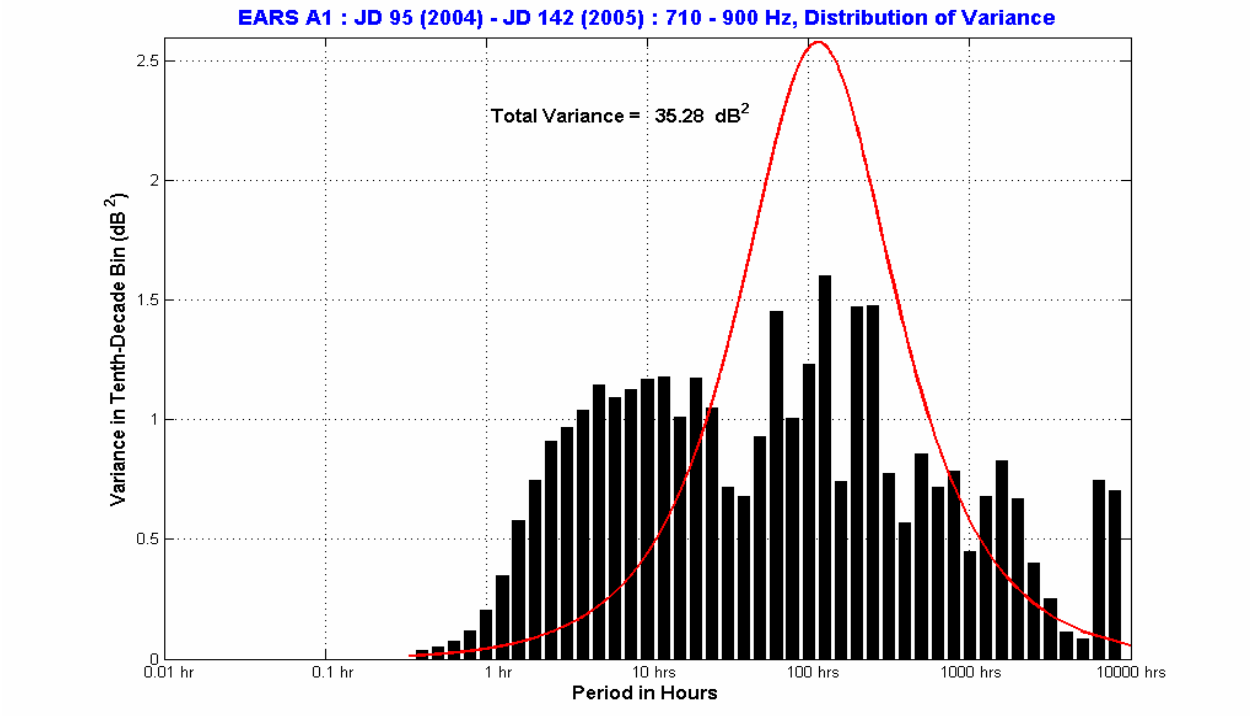

Figure 5.20 Distribution of variance at 800 Hz for entire time period.

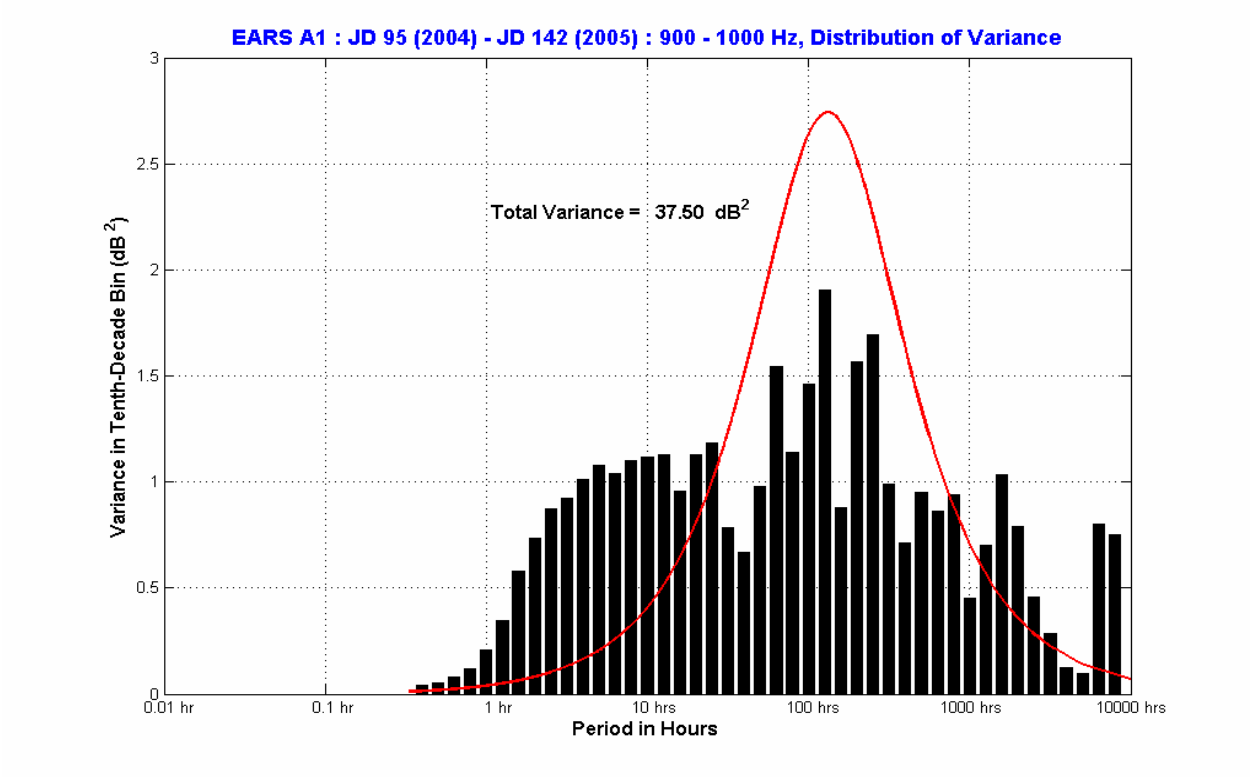

Figure 5.21 Distribution of variance at 950 Hz for entire time period.

The 50, 100, and 200 Hz bands are approximately fit by a 1st order Gauss-Markov process (Figures 5.15 to 5.17), suggesting that shipping noise may be modeled accurately by a 1st order Gauss-Markov process. All 3 bands have exponentially-decaying autocorrelation functions. The fit is very good at 50 Hz and gets progressively worse at 100 Hz and 200 Hz. But the higher frequency bands don't fit a 1st order Gauss-Markov process[7] at all, suggesting that weather bands are more complicated. There appear to be multiple noise processes involved in the weather bands.

The lowest frequency band at 25 Hz also does not fit a 1st order Gauss-Markov process. Rather than exponential, its autocorrelation function is sinusoidal, with a period of 8 hours. The 25 Hz time series has a strong peak in its fluctuation spectrum at a period of 8 hours, as can be seen in Figure 5.14. The cause of this 8 hour noise cycle at 25 Hz is being investigated, but it does not appear to be due to shipping or weather.

[7] None of the 8 frequency bands fit a 2nd order Gauss-Markov process, either.

Table 5.3 shows the properties of some autocorrelation and power spectral density functions [Li, 1999]. A random process modulated by a sine wave with angular frequency ω_0 has a sinusoidal autocorrelation with the same frequency. A random process containing a sinusoid with angular frequency ω_0 has a sinusoidal autocorrelation with the same frequency and peaks in its PSD at $\omega = \pm \omega_0$.[8] Plotted versus period, the 25 Hz band has a strong peak at period $T_0 = 2\pi / \omega_0 = 8$ hours.[9]

Random Process	**Autocorrelation Function**	**Power Spectral Density**
$X(t)$	$R(\tau)$	$S(\omega)$
$X(t)\cos(\omega_0 t + \theta)$	$R(\tau)\cos(\omega_0 \tau)$	$\frac{1}{2}[S(\omega+\omega_0) + S(\omega-\omega_0)]$
$A\cos(\omega_0 t + \theta)$	$\frac{1}{2}\langle A^2\rangle\cos(\omega_0 \tau)$	$\pi/2\langle A^2\rangle[\delta(\omega+\omega_0) + \delta(\omega-\omega_0)]$
1st order Gauss-Markov process	$\sigma^2 \exp(-\beta\lvert\tau\rvert)$	$2\beta\sigma^2(\omega^2 + \beta^2)^{-1}$

Table 5.3 Properties of some autocorrelation and power spectral density functions.

[8] Here $\delta(\omega)$ represents the Dirac delta function.

[9] In Table 5.3, A and θ are random but ω_0 is nonrandom (i.e., it has a fixed value). The quantity β is the reciprocal of the coherence time: β^{-1} = coherence time. The expression $\langle A^2\rangle$ represents the time-average of the random amplitude A squared. The quantity σ^2 is the variance of the random process.

Chapter 6
Threshold Crossing Statistics

The monthly time series for each of the frequency bands has been analyzed for peaks and troughs. This is done in order to determine how often and for how long it is noisy or quiet as a function of frequency and month. The following quantities are computed for the peaks and troughs: peaks/troughs per day, peak/trough duration (time above/below a specified threshold), and peak/trough inter-arrival time (the interval between peaks/troughs). Two types of thresholds are investigated. One is an absolute threshold for each frequency band and month: the 10^{th} percentile for troughs and the 90^{th} percentile for peaks. The second is a relative threshold, based on a six hour running average of the data and the monthly standard deviation in each frequency band.

The number of peaks in a month is computed by counting the number of times the data in a time series exceeds the 90^{th} percentile during the month. The duration of each peak is computed by subtracting each up-threshold-crossing time from its corresponding down-threshold-crossing time. The average number of peaks per day is computed by dividing the total number of peaks in a month by the number of days in that month. The average peak duration for a month is computed by adding the durations of each peak for that month and dividing by the total number of peaks.

The inter-arrival times (IAT) between peaks are computed by subtracting the up-threshold-crossing time of each peak from the up-threshold-crossing time of the peak immediately following the peak being analyzed. The average IAT for peaks during a month is computed by adding the IATs for each pair of peaks during the month and dividing by the total number of intervals.

Similarly, the number of troughs in a month is computed by counting the number of times the data in a time series go below the 10^{th} percentile during the month. The duration of each trough and the IAT between troughs are computed in a similar fashion to the duration and IAT of the peaks.

The absolute threshold method (based on the 10^{th} and 90^{th} percentiles) works well for stationary data. But during the course of a month, the data are not stationary. The mean values

in different frequency bands fluctuate in response to storms, hurricanes and changing shipping patterns.

The non-stationarity of the data over the course of a month is addressed by using a relative threshold method. For each frequency band and month, a six hour running average of the time series is computed. The actual time series (with a data point every ten minutes) is then compared to the local mean value of the data (based on looking three hours forward and three hours backward). If the time series exceeds a threshold above the six hour mean, that period is counted as a peak. Similarly, if the time series goes lower than a threshold below the six hour mean, that period is counted as a trough. The threshold is based on the standard deviation (σ) computed for the month and frequency band under consideration. The threshold is set at 0.6745σ for peaks and at -0.6745σ for troughs.[1]

In higher frequency bands, the noise due to weather dominates and determines the average ambient noise background level at a given time. But a ship passing close to a hydrophone can easily surpass this background noise level while the ship is nearby. Ship passages can easily be seen on a spectrogram. (Appendix A contains the monthly spectrograms from April 2004 to May 2005.) Thus, the peaks in higher frequency bands are usually an indicator of nearby ships.[2]

This is also easily seen in higher frequency band time series data. Appendix C contains monthly plots of the power in the 900 to 1000 Hz band. The black curve is the average power computed every 10 minutes. The red curve is the six hour running average of the 10 minute samples (the black curve). For reference, the monthly mean level, the 10^{th} percentile and the 90^{th} percentile monthly levels are also indicated on each plot. In this frequency band, the six hour running average (the red curve) is highly correlated with weather. The peaks of the 10 minute samples (the black spikes) on top of the red curve usually represent nearby ships. (The six hour average tends to "average out" the ships but leaves the weather features intact.)

The hurricane month of September 2004 presents a good example. Figure 6.1 shows the spectrogram for September 2004. Three hurricanes were recorded by the EARS buoys that

[1] The numerical factor 0.6745 is determined from the 25^{th} and 75^{th} percentiles for a Gaussian distribution. 25% of the data in a Gaussian distribution exceed the mean value plus 0.6745σ; 25% of the data fall below the mean value minus 0.6745σ [Li, 1999].

[2] Peaks in higher frequency bands may also be caused by intense rain and wind activity during extreme weather events [Newcomb, Snyder et al., 2007].

month: Frances, Ivan[3] and Jeanne. Figure 6.3 shows a comparison of the acoustic data in the 900 to 1000 Hz band and the wind speed data recorded at NDBC buoy 42003. To make the comparison, the EARS data were averaged over one hour to match the averaging interval of the wind speed data, and then both data sets were normalized (zero mean, unity variance).[4] The correlation is excellent. There is an obvious time lag near day 14, because Ivan passed by the weather buoy before it passed by the EARS buoys. Even with this time lag, the correlation coefficient for these two time series is 0.77.

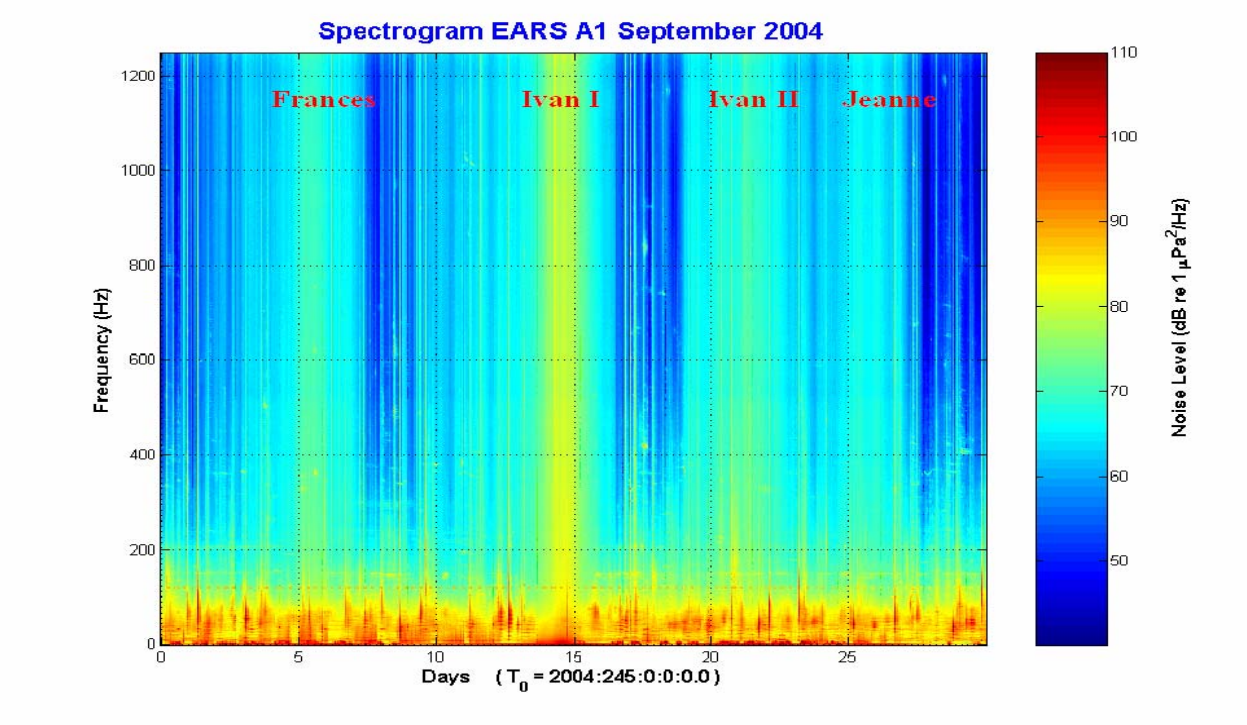

Figure 6.1 Spectrogram for September 2004.

[3] Ivan was actually recorded twice. Ivan passed by the EARS buoys once, went ashore near the Alabama-Florida border, moved into the Atlantic, then remnants came back into the Gulf of Mexico a second time. See Figure 6.2. [http://fermi.jhuapl.edu/hurr/04/ivan/index.html]

[4] For each data set, the data were put in standard normalized form: the mean value was subtracted from each data point, and then the result was divided by the standard deviation.

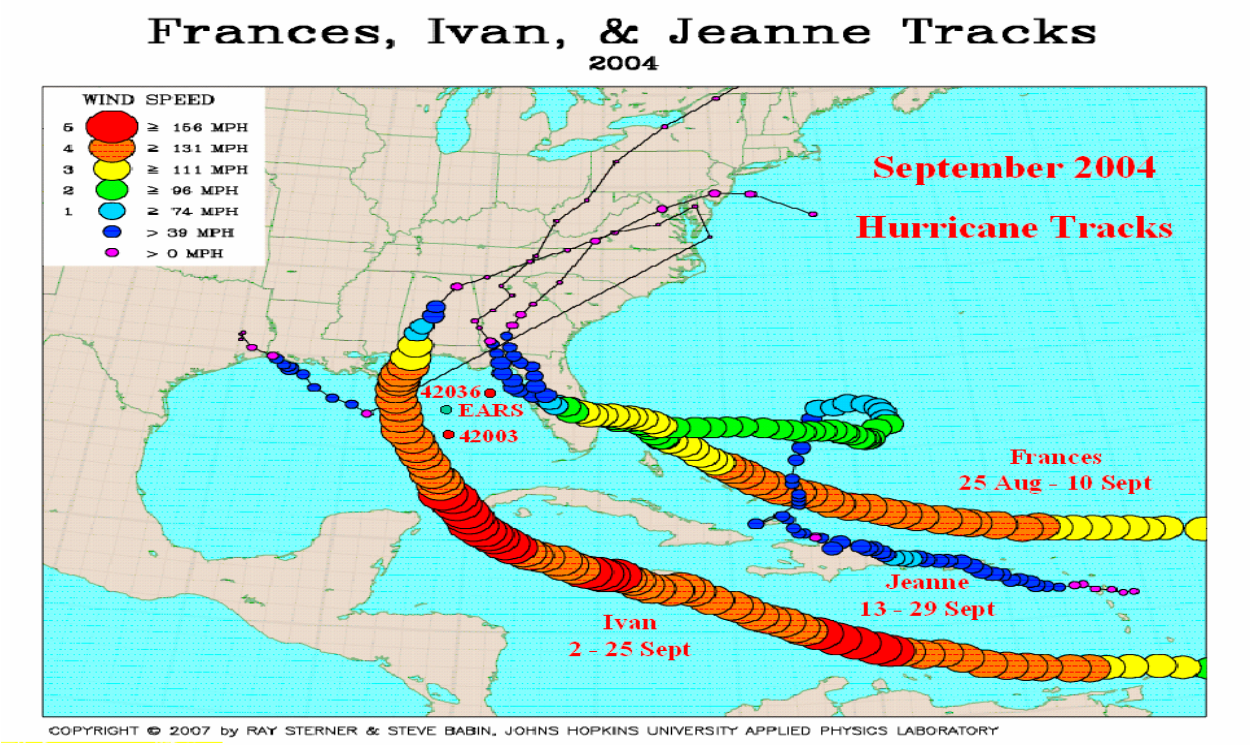

Figure 6.2 September 2004 hurricane tracks.

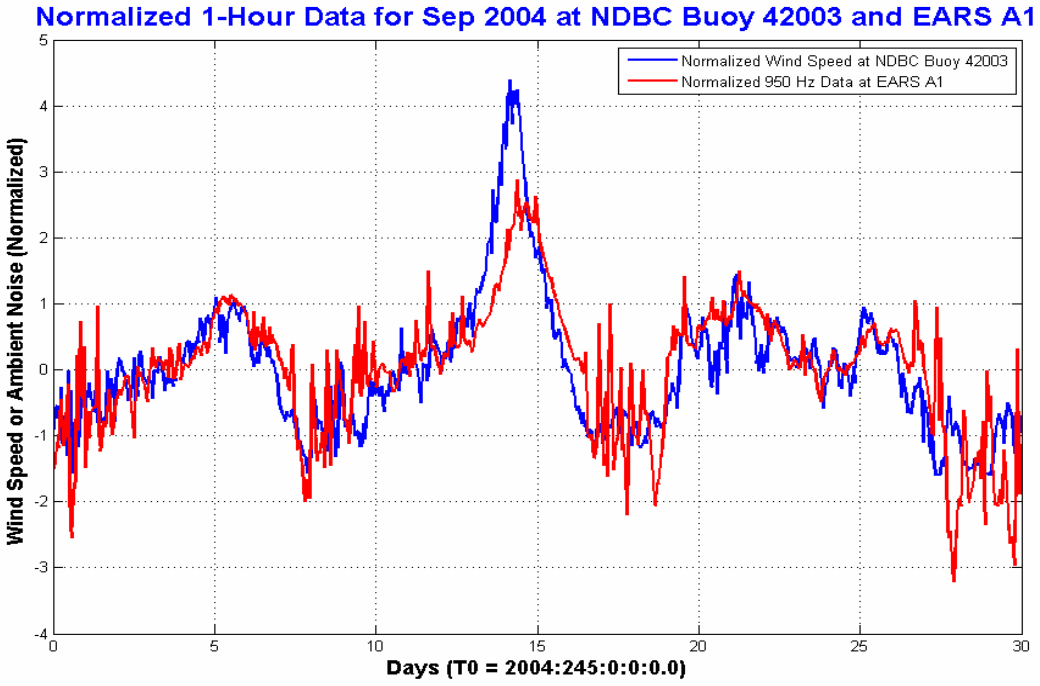

Figure 6.3 September 2004 wind speed and 950 Hz comparison.

Figure 6.4 shows the September 2004 power (10 minute average) in the 900 to 1000 Hz band for the entire month. Figure 6.5 shows the peaks for the entire month, the result after the six hour average is subtracted from the 10 minute data. The red line is the threshold of 0.6745σ. All of the peak threshold crossing statistics (peak duration and IAT) are computed from the points of intersection of the peaks with this threshold.

Similarly, Figure 6.6 shows the troughs for the entire month, the result after the six hour average is subtracted from the 10 minute data. The red line is the threshold of -0.6745σ. All of the trough threshold crossing statistics (trough duration and IAT) are computed from the points of intersection of the troughs with this threshold.

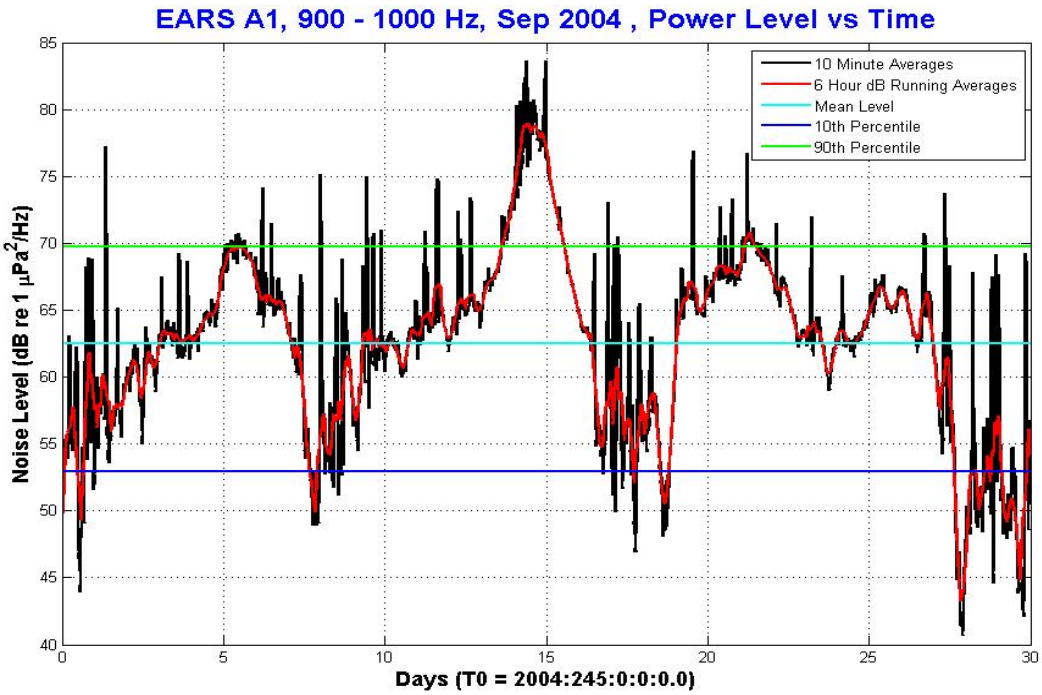

Figure 6.4 September 2004 power at 950 Hz for 30 days.

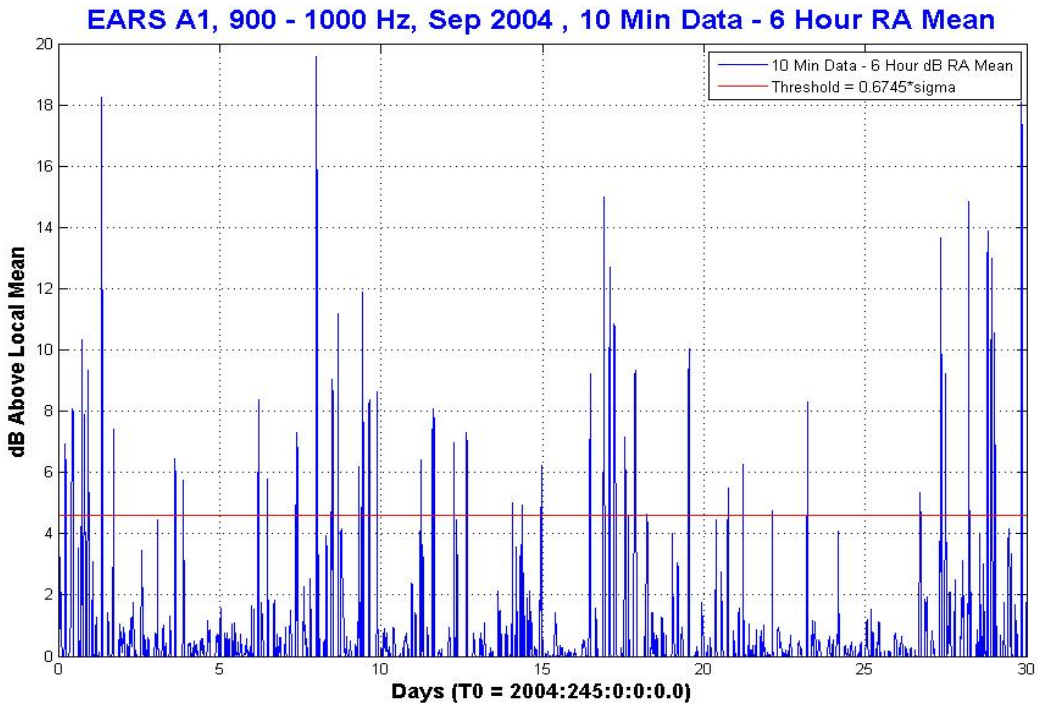

Figure 6.5 September 2004 peaks at 950 Hz for 30 days.

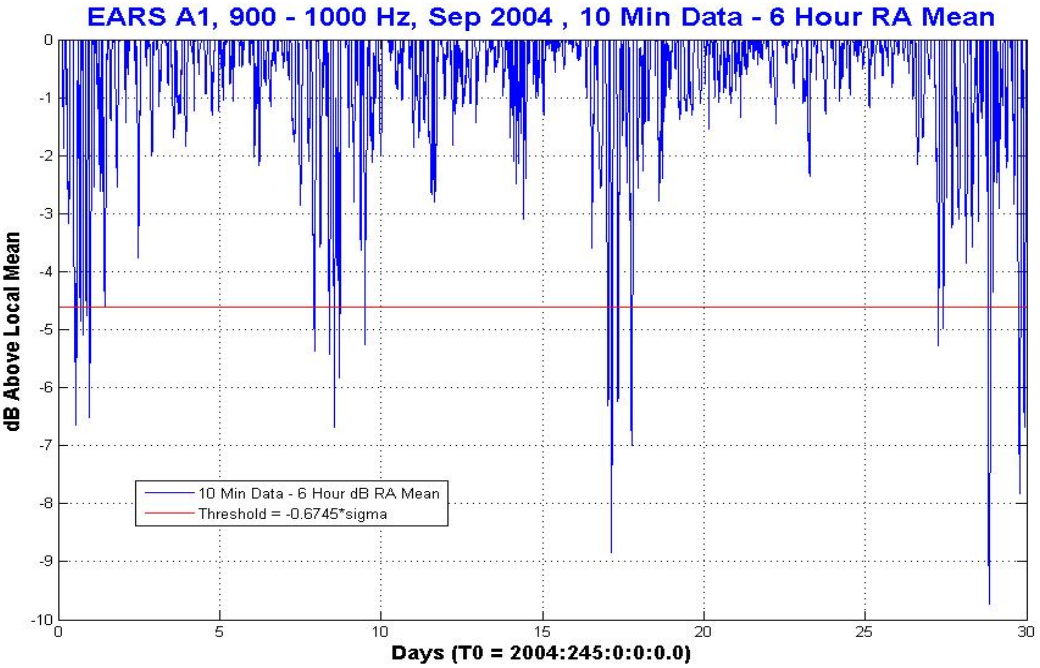

Figure 6.6 September 2004 troughs at 950 Hz for 30 days.

The next three plots are magnifications of Figures 6.4 through 6.6. In particular, they are 5 day magnifications, looking at days 5-10 of September 2004, during the passage of Hurricane Frances. Figure 6.7 is the 5 day magnification of Figure 6.4 (power at 950 Hz), Figure 6.8 is the 5 day magnification of Figure 6.5 (peaks), and Figure 6.9 is the 5 day magnification of Figure 6.6 (troughs).

As can be seen from Figure 6.7, there are 6 main peaks that exceed the 90th percentile threshold, and about 13 if the very small ones between days 5 and 6 are included. There are about 6 troughs that fall below the 10th percentile threshold, including some very small ones. The six hour average method for the same 5 day period yields about 12 peaks above the threshold of 0.6745σ (Figure 6.8), and 5 troughs below the threshold of -0.6745σ (Figure 6.9).

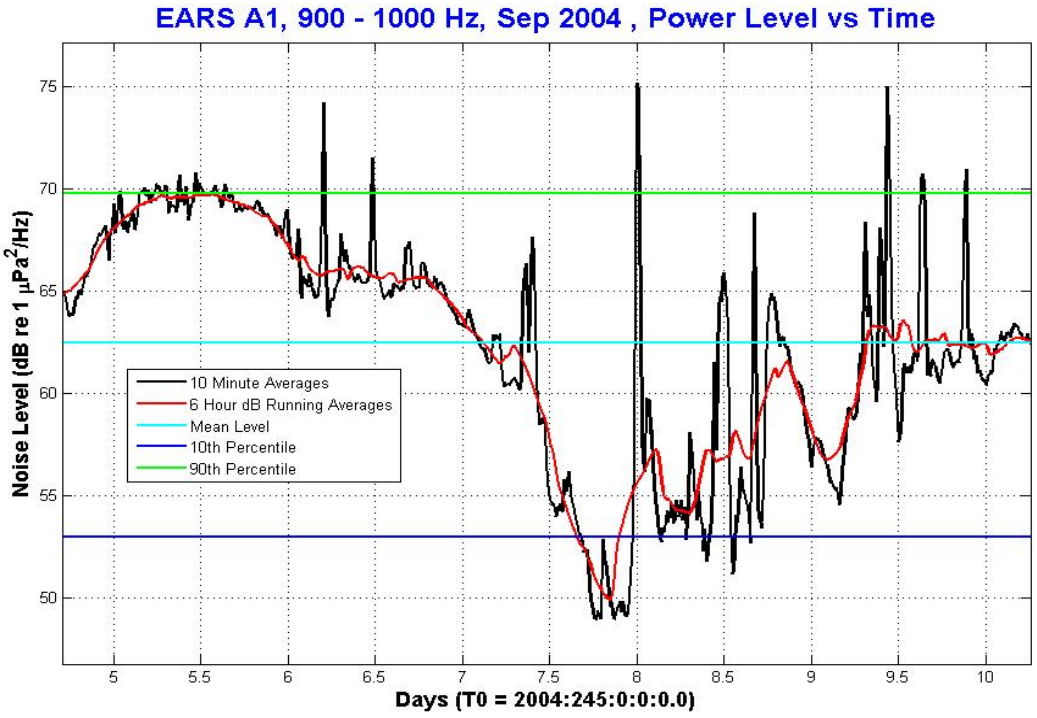

Figure 6.7 September 2004 power at 950 Hz for 5 days.

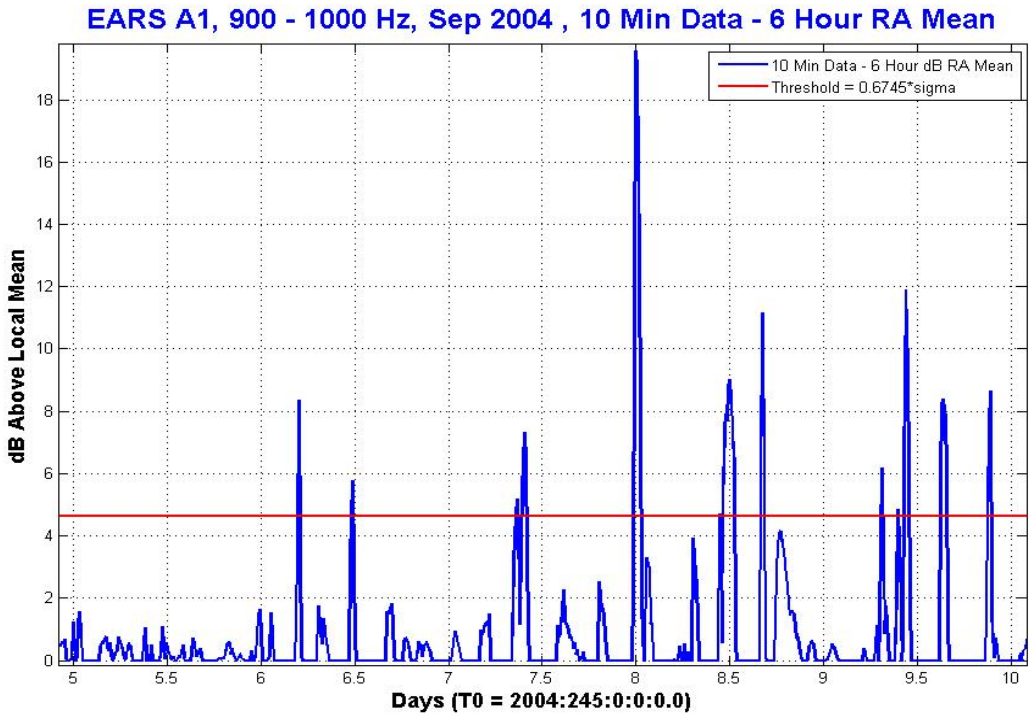

Figure 6.8 September 2004 peaks at 950 Hz for 5 days.

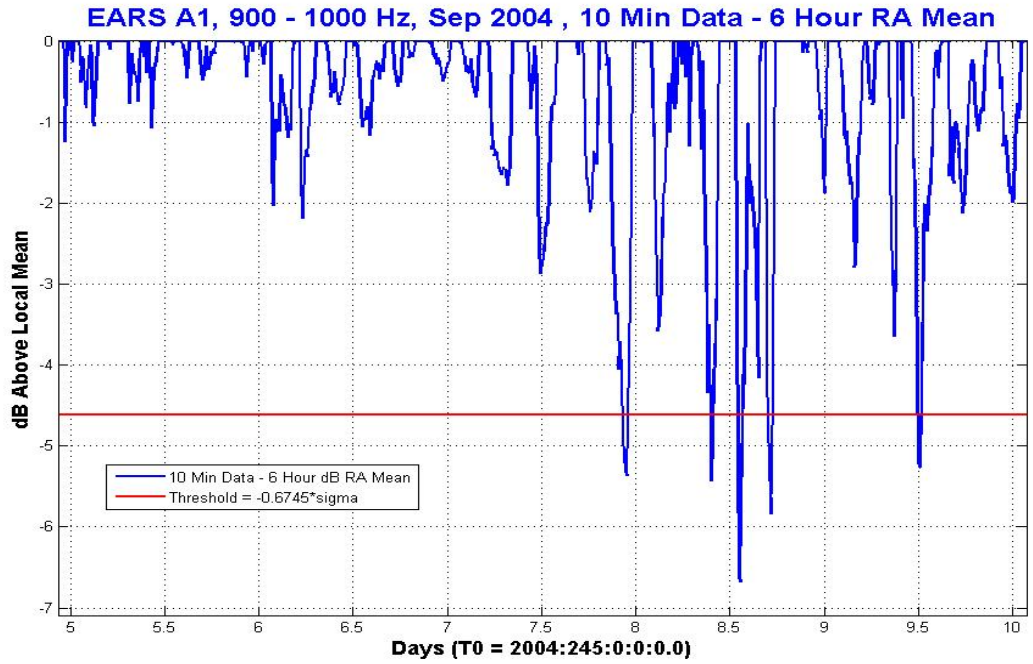

Figure 6.9 September 2004 troughs at 950 Hz for 5 days.

For the entire 14 month data set, as a function of frequency, the peaks per day have high values at 25 Hz and at 200 Hz (Figures 6.10 and 6.11). Figure 6.12 shows the average number of peaks per day using both methods (absolute and relative thresholds) for the two highest frequency bands analyzed, 800 and 950 Hz. Both methods show a high value during August 2004, although the relative threshold shows a higher value (about 4.2 peaks/day at 950 Hz versus about 3.2 peaks/day for the absolute threshold). Both methods show a sharp drop in peaks/day during September 2004. As was stated previously, the peaks in higher frequency bands are usually an indicator of nearby ships. August 2004 was a relatively mild month with an average wind speed of 7.8 knots. It would make sense for a relatively high number of ships to pass in close proximity to the EARS buoys during good weather. But September 2004 was a stormy month, with three hurricanes pushing the average wind speed to 15.0 knots.

It would make sense for a much smaller number of ships to be detected during a month with such intense hurricane activity. The shipping estimate picked up again in October, after the hurricane season had passed the busier summer months. During some months both methods (absolute and relative) gave similar estimates for nearby shipping activity, but in general the relative method yielded slightly higher estimates.

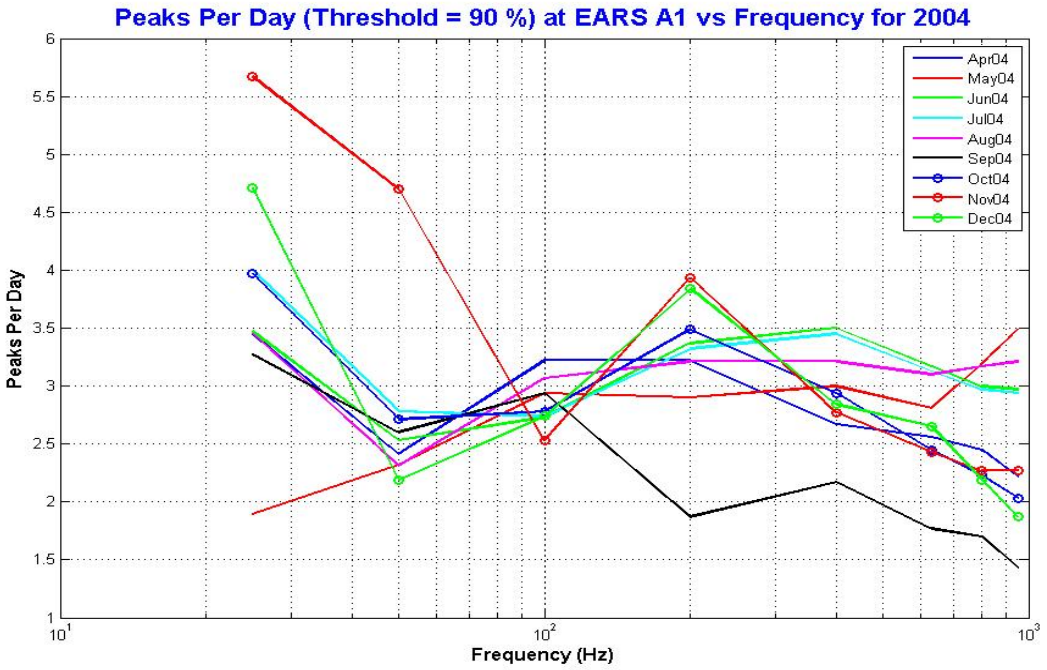

Figure 6.10 Peaks per day (90%) vs. frequency for 2004.

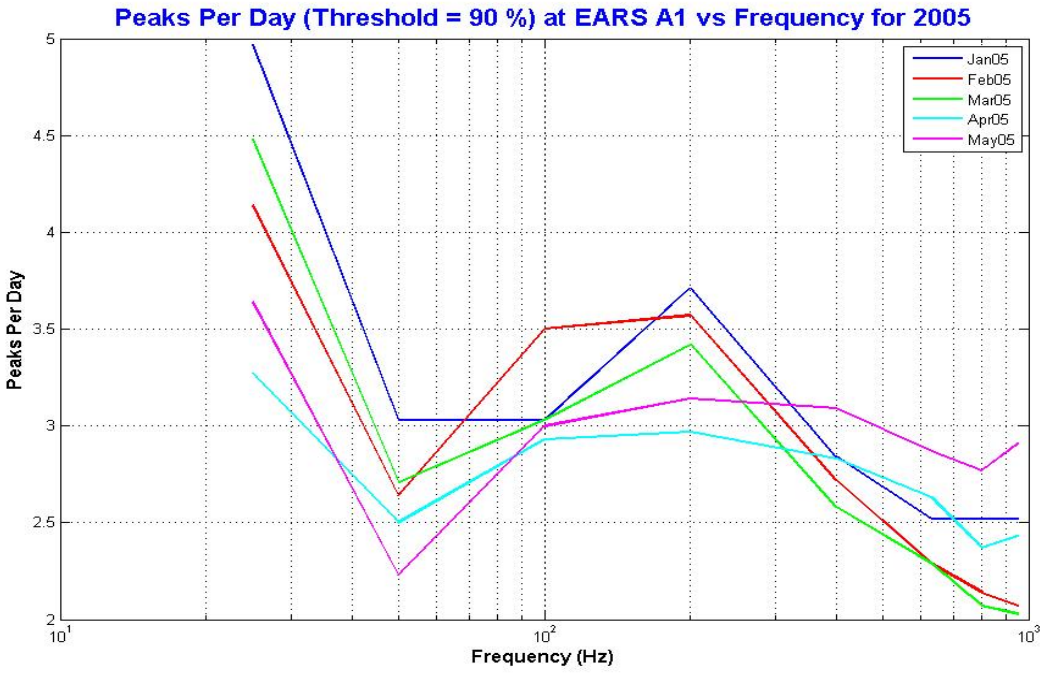

Figure 6.11 Peaks per day (90%) vs. frequency for 2005.

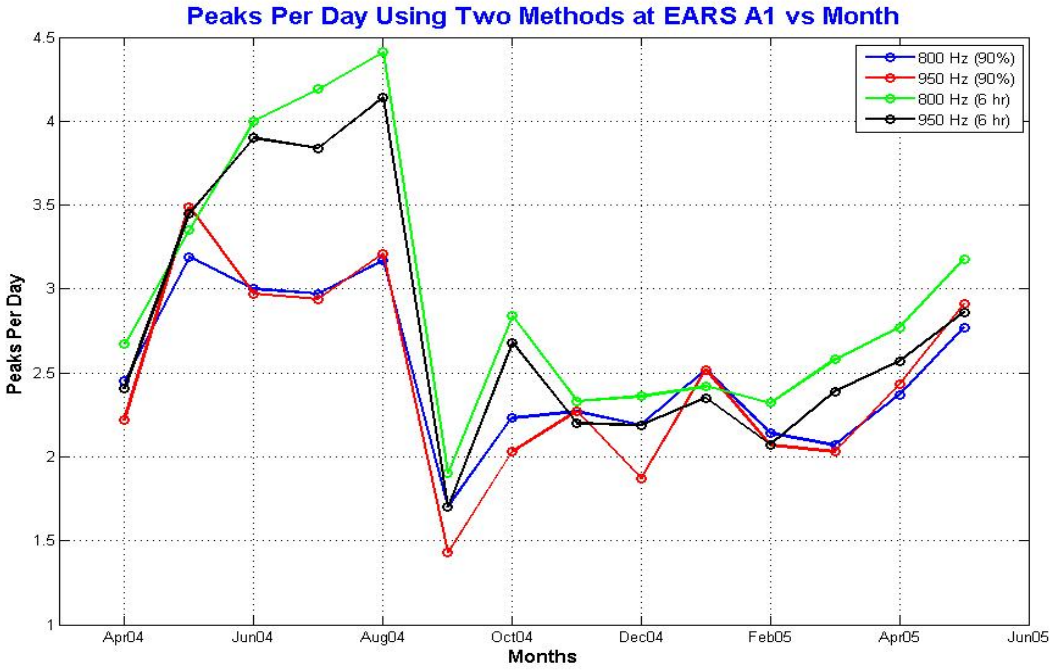

Figure 6.12 Peaks per day vs. month using both methods.

Figures 6.13 and 6.14 show the average peak duration for both methods. In general, the average peak duration using the 90th percentile threshold is greater than the average peak duration estimated by the relative threshold. This is because the absolute threshold estimate included periods where the background noise remained high for long periods, such as during hurricanes. A good example is again found during September 2004. The 90th percentile method shows an increase in average peak duration for most frequencies during September. But the relative threshold estimate shows a decrease for most frequencies during September. This is because the relative threshold method uses a six hour average and thus does not include periods of long weather duration.

Fig. 6.15 shows the average peak IAT as determined by the relative threshold method. One feature that stands out is the sharp increase in peak IAT at higher frequencies during September 2004. Again, this appears to be due to intense hurricane activity. As was stated earlier, there are many fewer ships detected during September 2004, so it makes sense that the time between ships is high. At 950 Hz the average time between peaks (ships) is about 14.1 hours during September, while it has a low value of about 6.1 hours during a much calmer month such as June 2004.

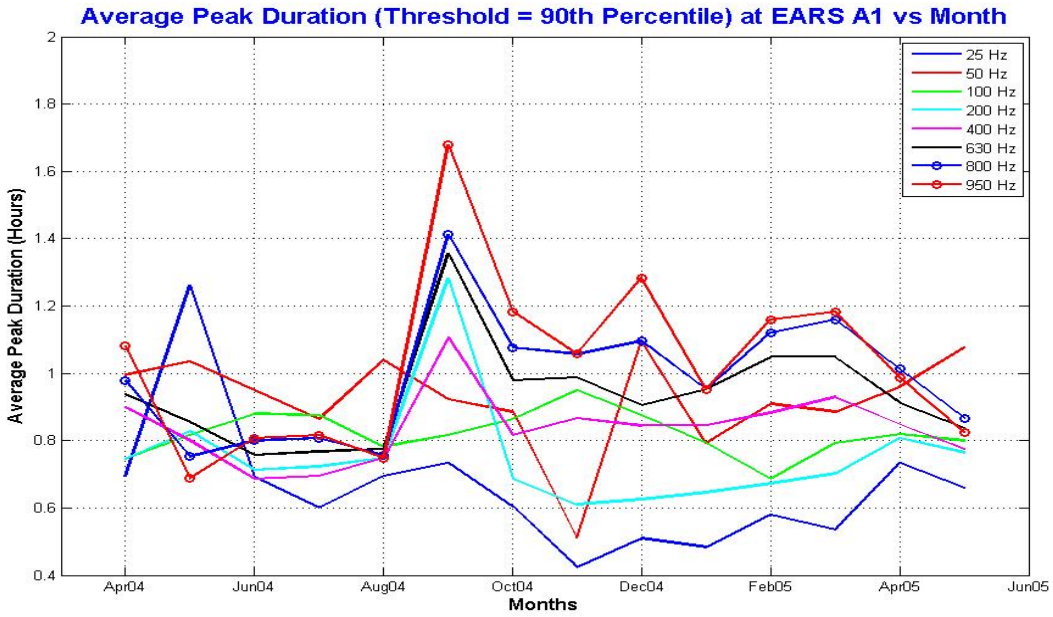

Figure 6.13 Average peak duration (90%) vs. month.

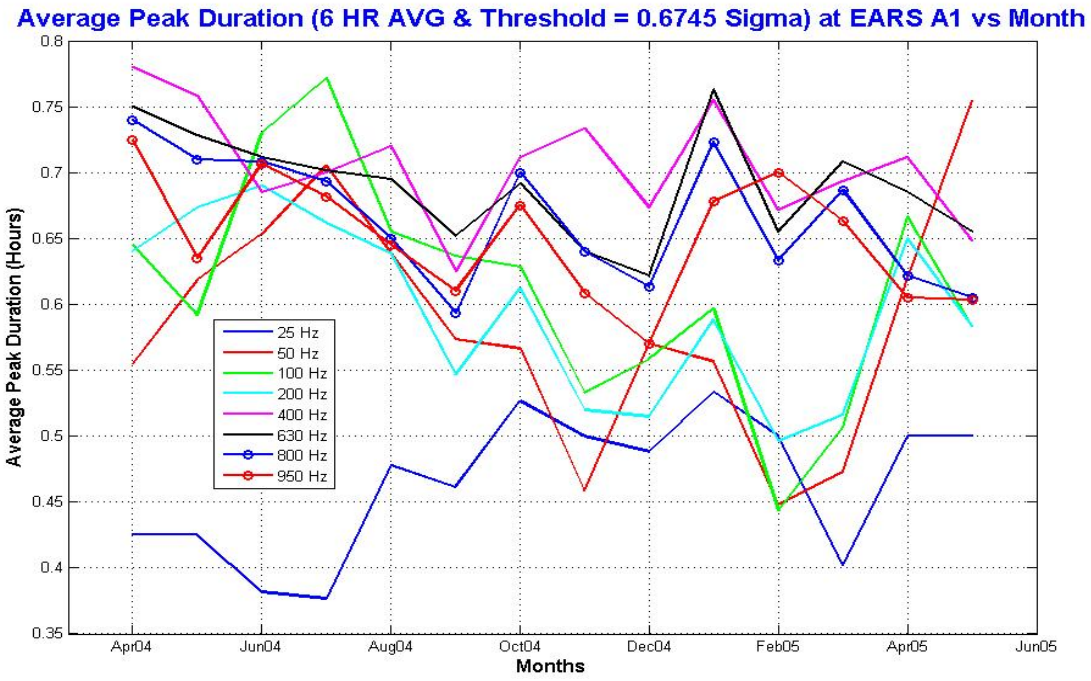

Figure 6.14 Average peak duration (6 hour avg) vs. month.

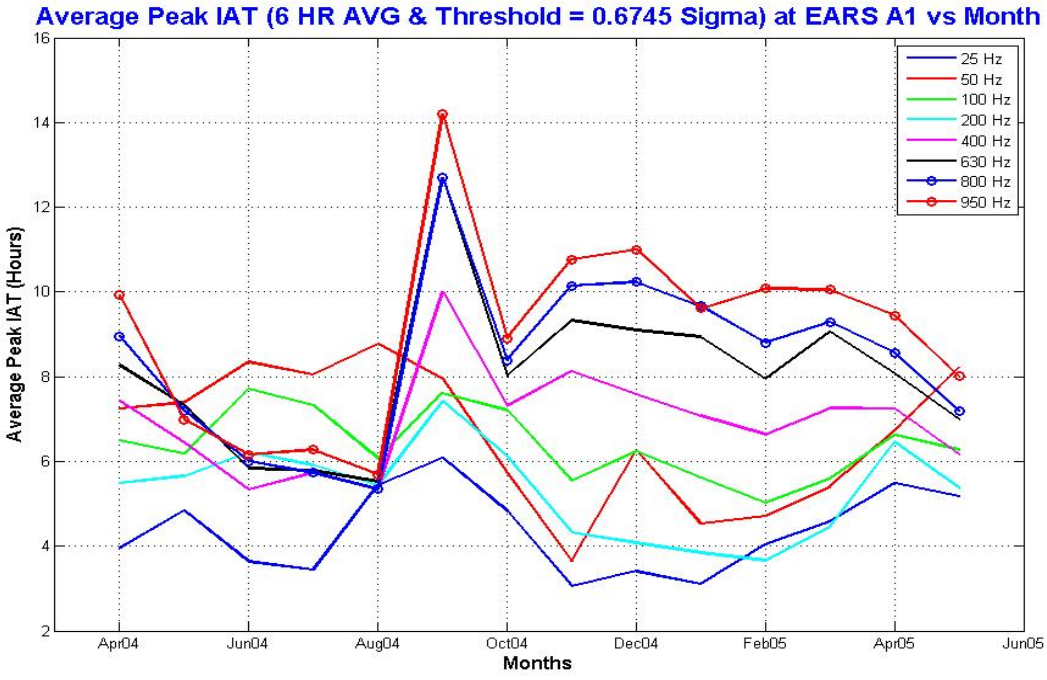

Figure 6.15 Average peak IAT (6 hour avg) vs. month.

As a function of frequency, the troughs per day have high values at 25 Hz and at 200 Hz (Figures 6.16 and 6.17). The number of troughs per day ranges from about 1 to 3.5 for the 10% threshold method (Figure 6.18) but approximately twice this range, about 1 to 7, for the six hour average method (Figure 6.19). Both methods show low values during the hurricane month of September 2004, especially in the upper frequency bands of 630-950 Hz. The noise level in the upper frequency bands stays high for long time periods during extreme wind conditions, so very few quiet periods should be expected. This was also evident in the average trough IAT (Figure 6.20). The average trough IAT ranges from about 4-35 hours for the six hour average method, with the highest values observed during September 2004 in the upper frequency bands of 400-950 Hz. The troughs during stormy conditions are few and far between.

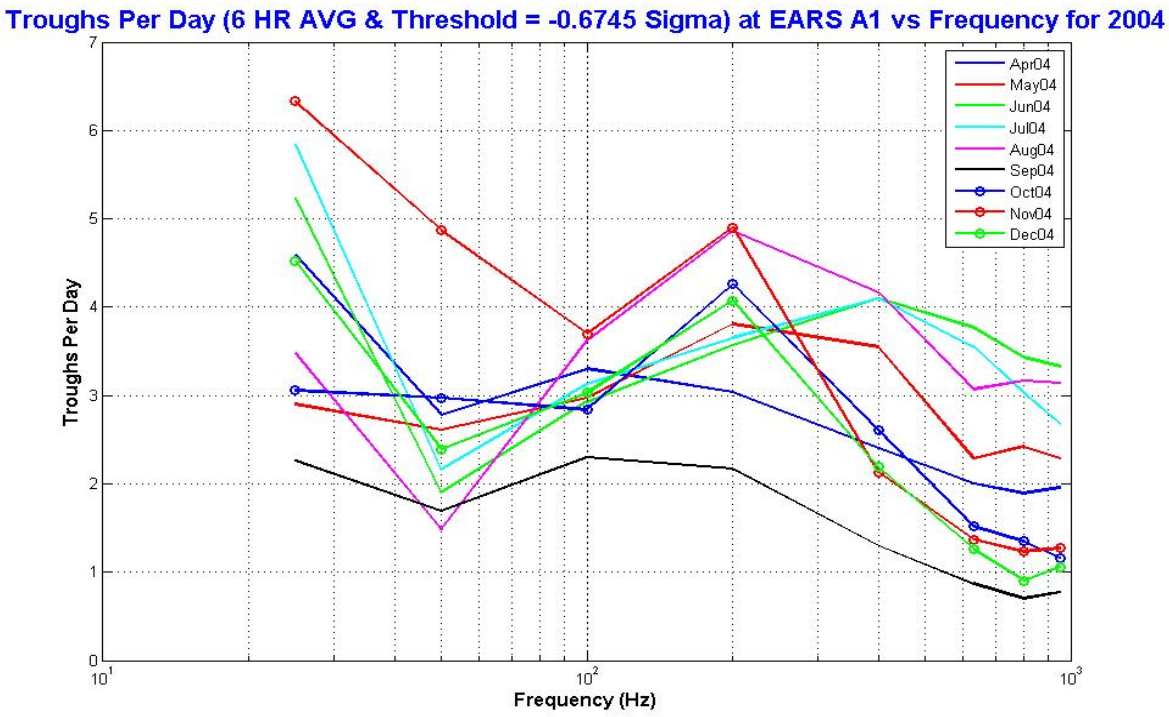

Figure 6.16 Troughs per day (6 hour avg) vs. frequency for 2004.

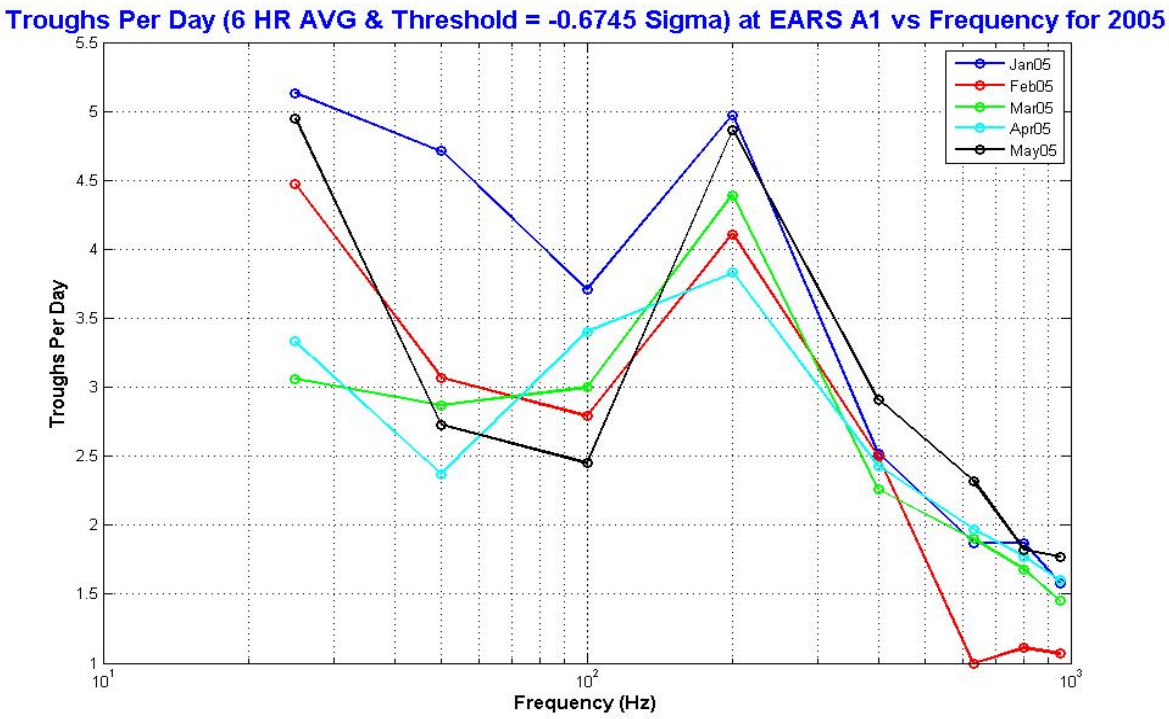

Figure 6.17 Troughs per day (6 hour avg) vs. frequency for 2005.

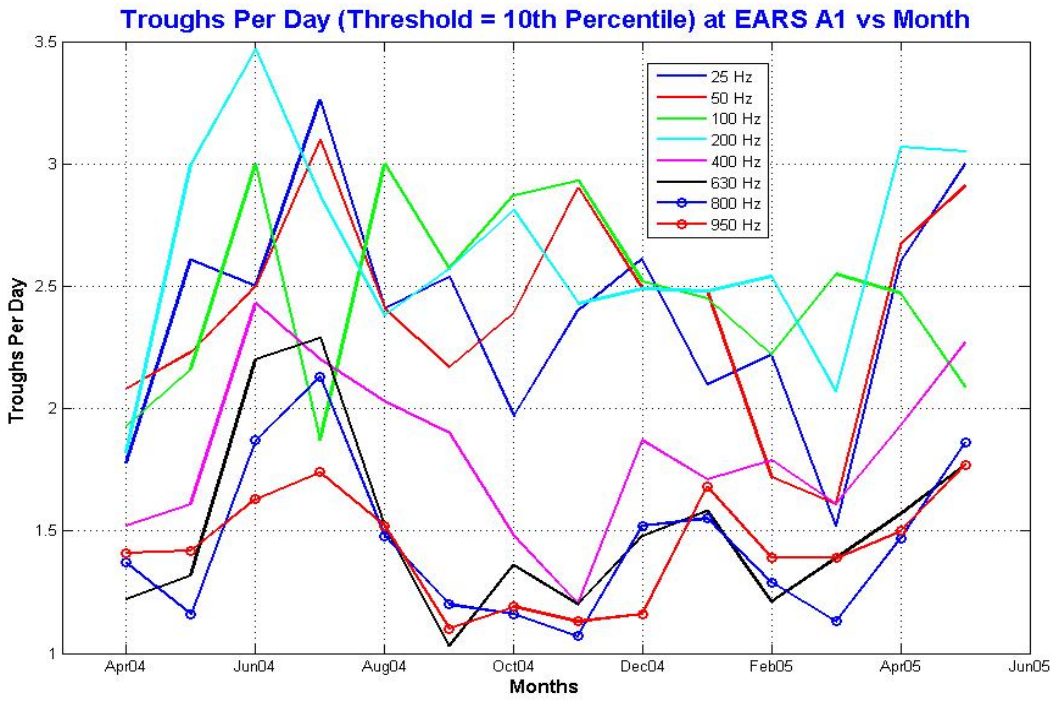

Figure 6.18 Troughs per day (10%) vs. month.

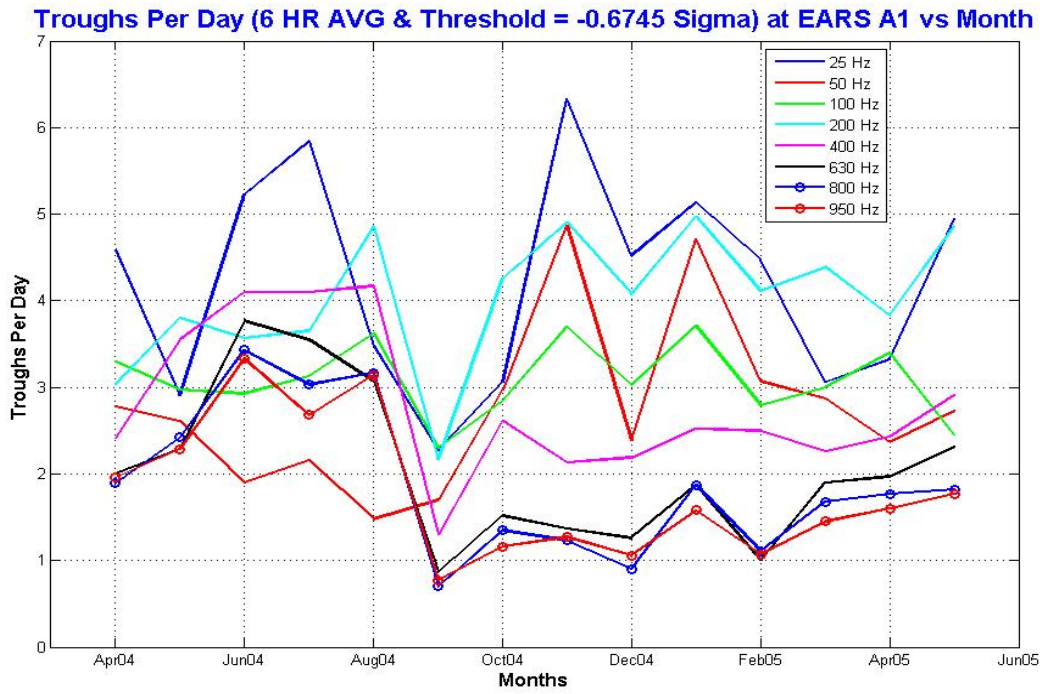

Figure 6.19 Troughs per day (6 hour avg) vs. month.

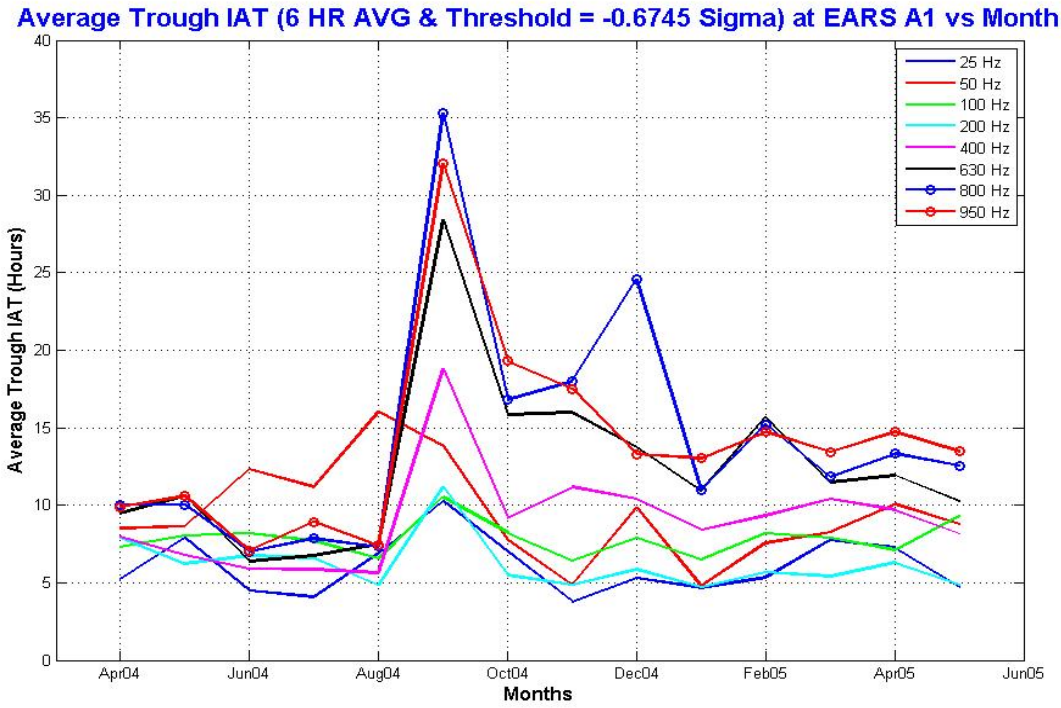

Figure 6.20 Average trough IAT (6 hour avg) vs. month.

Figures 6.21 and 6.22 show the average trough duration for both methods. In general, the average trough duration using the 10th percentile threshold is greater (about 0.7 to 2.3 hours) than the average trough duration estimated by the relative threshold (about 0.4 to 1.2 hours). The average trough duration is highest (2.3 hours) for the 10th percentile threshold at 630 Hz during September 2004, while it peaks at 1.2 hours at 630 Hz for the relative threshold method during the windy month of February 2005.

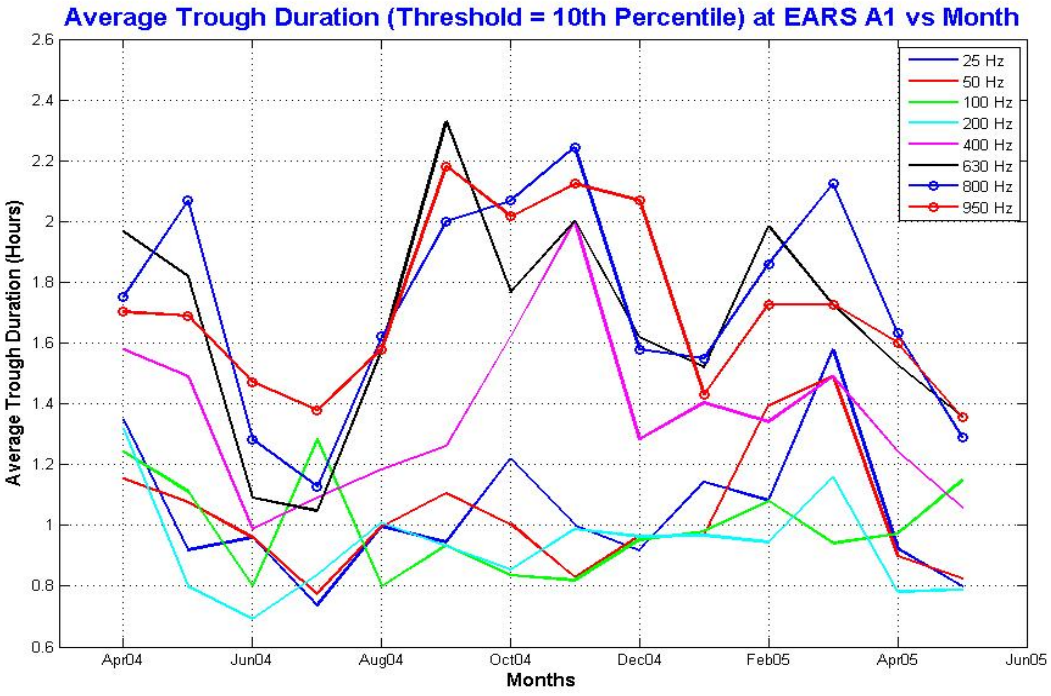

Figure 6.21 Average trough duration (10%) vs. month.

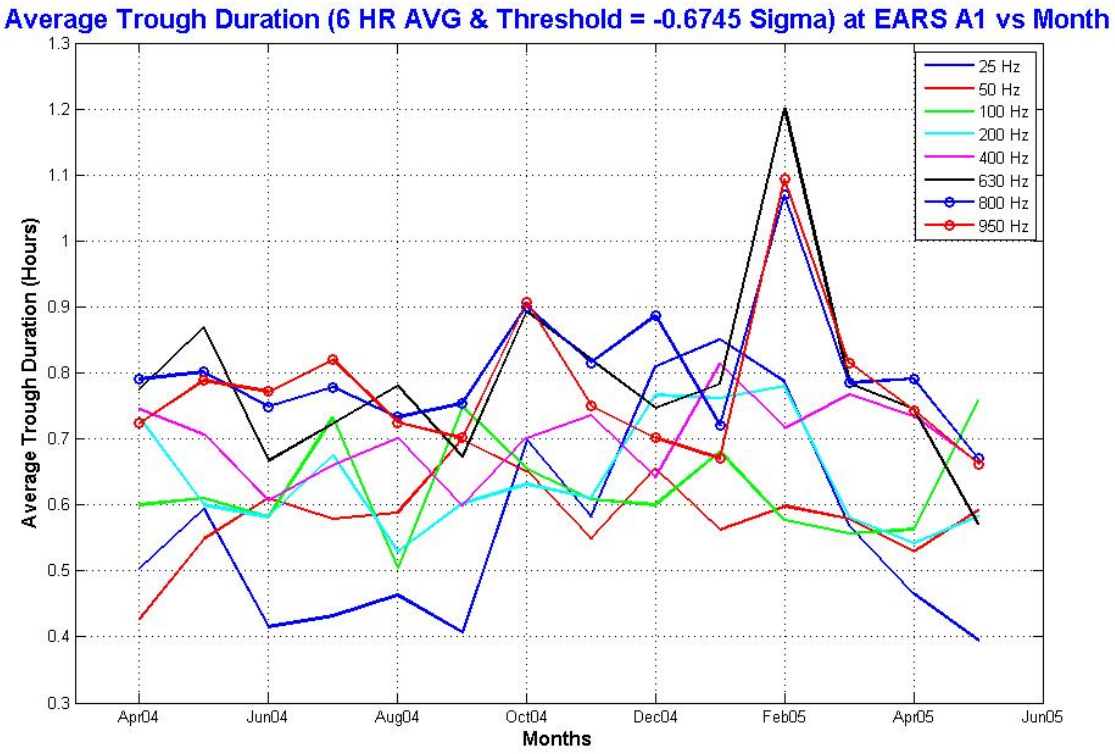

Figure 6.22 Average trough duration (6 hour avg) vs. month.

Chapter 7
Coherence

7.1 Spatial Coherence of the Noise Field

Spatial coherence is a measure of the degree to which noise levels at two places in the ocean are the same. Hydrophones placed at the two points will have identical outputs if the noise is perfectly coherent ($\rho = +1$). Conversely, if the time series measured at both locations are totally dissimilar ($\rho \approx 0$), the noise is called incoherent [Urick, 1984].

The spatial coherence between three hydrophones (each at approximately the same depth, 2935 m, and each in approximately the same water depth, 3200 m) is analyzed for hydrophone separations of 2.29, 2.56 and 4.84 km over a ten month period (August 2004 to May 2005). The three hydrophones are labelled A1, A3, and A6, with A1 in the center. Site A6 was 2.56 km to the west of A1, while site A3 was 2.29 km to the east of A1 (Figure 7.1). The ten month time series (with the average power computed every two minutes) are compared at the following eight frequencies in 1-Hz bands: 25, 50, 100, 200, 400, 600, 800 and 1000 Hz.

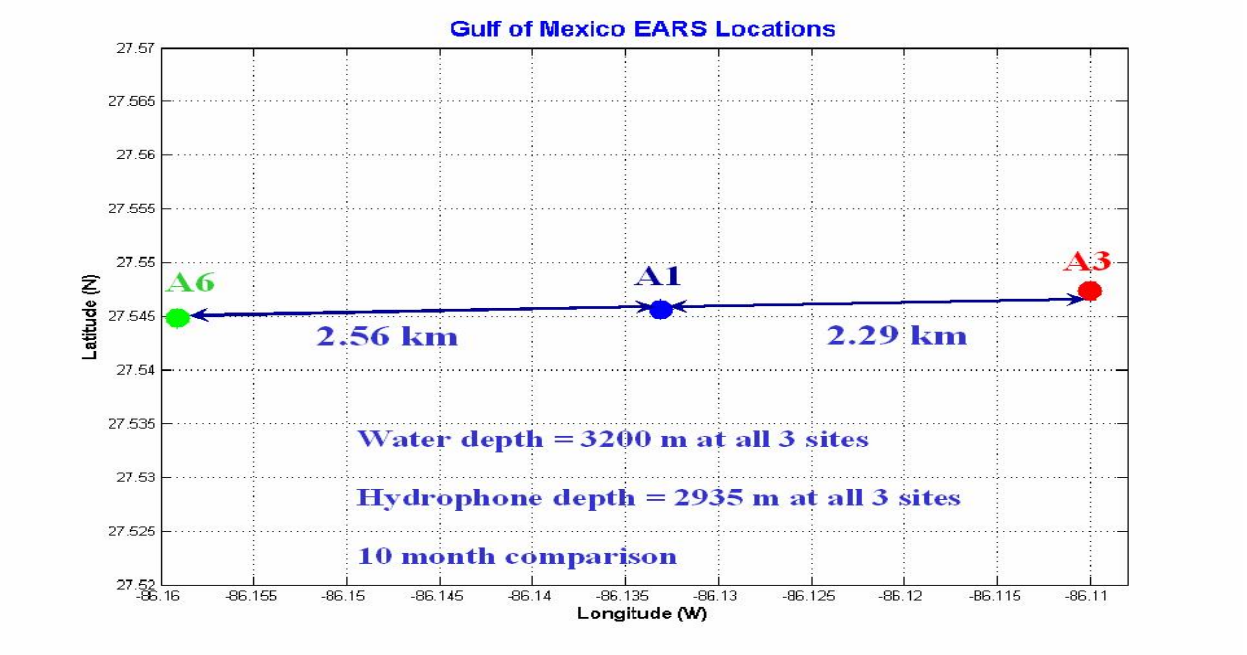

Figure 7.1 Gulf of Mexico EARS locations.

The 25 Hz time series at EARS site A1 is compared to the 25 Hz time series at EARS site A3 (2.29 km away) and at EARS site A6 (2.56 km away). In addition, the 25 Hz time series at EARS sites A3 and A6 are compared (4.84 km apart). This process is repeated for the other seven time series. The correlation coefficient is computed for each of the eight frequency bands for each hydrophone separation: 2.29, 2.56 and 4.84 km. In each case the correlation coefficient is always greater than 0.7; see Figure 7.2. The correlation coefficient is generally fairly high (0.85 to 0.93) at 25 Hz, decreases in the region 100-200 Hz, and then increases again in the region 400-1000 Hz. In general, the closer the hydrophone spacing, the higher the degree of correlation between the two time series. This analysis shows that the ambient noise field is highly coherent out to a distance of at least 4.84 km, the largest hydrophone separation available in this data set. It also shows how different noise sources affect the correlation between separated receivers. Figure 7.2 shows relative minimum values at 100-200 Hz, which is in the shipping band. This suggests that local noise sources, such as ships, are fairly loud and will be most correlated between separated receivers at the lowest frequencies. But this correlation will fall off at a faster rate as a function of distance than weather noise and will depend on the relative

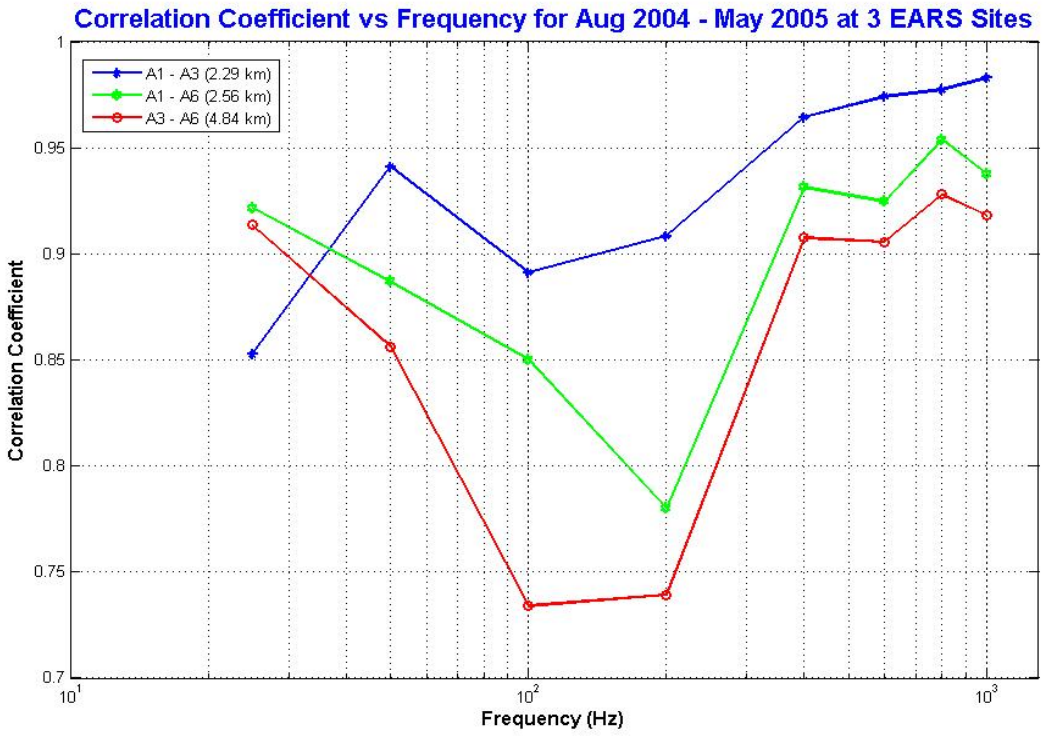

Figure 7.2 Correlation coefficient vs. frequency at 3 EARS sites.

noise levels produced by both nearby and distant shipping. The correlation values in the region 400-1000 Hz (in the weather band) are all high, above 0.9 for all three hydrophone separations. This suggests that weather noise is highly coherent, by this measure, over large distances.

7.2 Temporal Coherence of the Noise Field

The temporal coherence of the noise field at one site (A1) is analyzed by computing the autocorrelation of each fourteen month time series. The time for the autocorrelation to fall to e^{-1} of its central (zero-lag) value is called the coherence time. (Some authors call this the correlation time or the decorrelation time.) The coherence time is a measure of the effective width of the autocorrelation function, or how long a time series is coherent with itself. It is also a measure of the time scale of the noise fluctuations in a given frequency band [Urick, 1982].

The coherence time is computed for each of the eight time series. Figure 7.3 shows the autocorrelation function for the fourteen month time series at 50 Hz. The computed coherence time at 50 Hz is 2.97 hours. Note the near exponential decay, which is characteristic of a 1st order Gauss-Markov process.

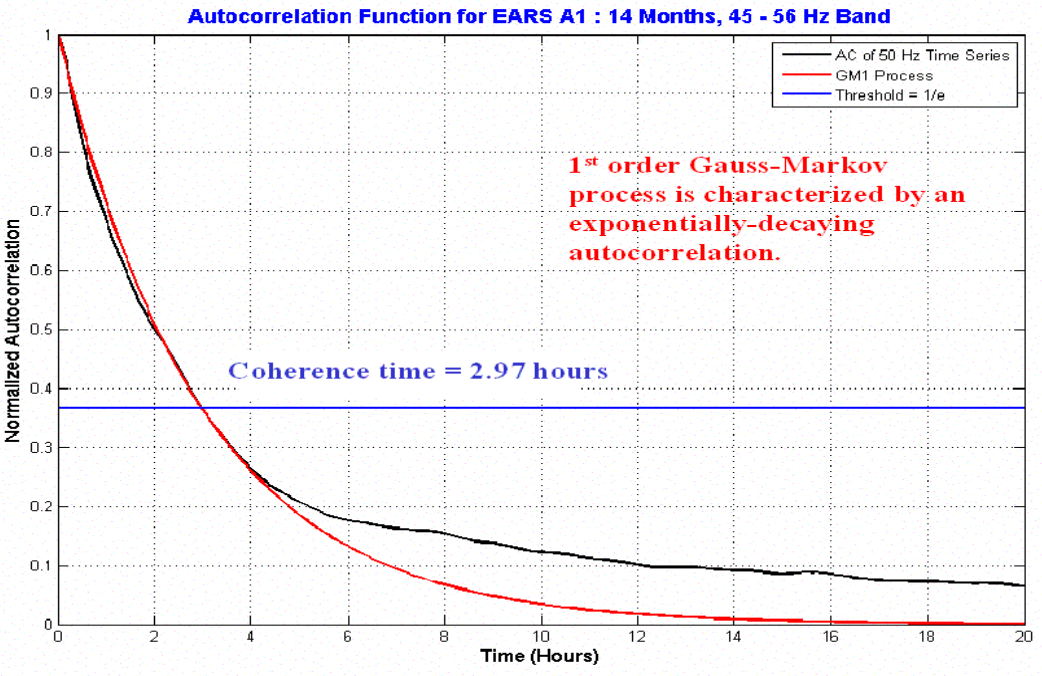

Figure 7.3 Autocorrelation function for 14 months at 50 Hz.

The coherence time results for all eight frequency bands are shown in Figure 7.4. The coherence time is low (2.52 to 3.71 hours) at low frequencies (25-400 Hz) but increases to 14.54 to 21.01 hours at high frequencies (630-950 Hz).

These values are understandable because of the dominance of shipping noise at low frequencies and of weather noise at high frequencies. As Urick points out, "The noise due to shipping varies more rapidly than the noise due to the wind" [Urick, 1984]. Perrone and King analyze acoustic data from Bermuda and the Grand Banks [Perrone and King, 1975]. They compute the autocorrelation time (the time for the autocorrelation function to fall to 0) and find it to be only 4-8 hours for shipping noise but 26-40 hours for wind noise.

The coherence times computed for the Gulf of Mexico data set (based on the time for the autocorrelation to fall to e^{-1} of its central value) are, as expected, somewhat shorter than the autocorrelation times (based on the time for the autocorrelation function to fall to 0) calculated by Perrone and King, but otherwise are in good agreement. The Gulf of Mexico data generally have exponentially decreasing-shaped autocorrelation functions as opposed to sinusoidally-shaped functions, so the e^{-1} calculation is more appropriate.

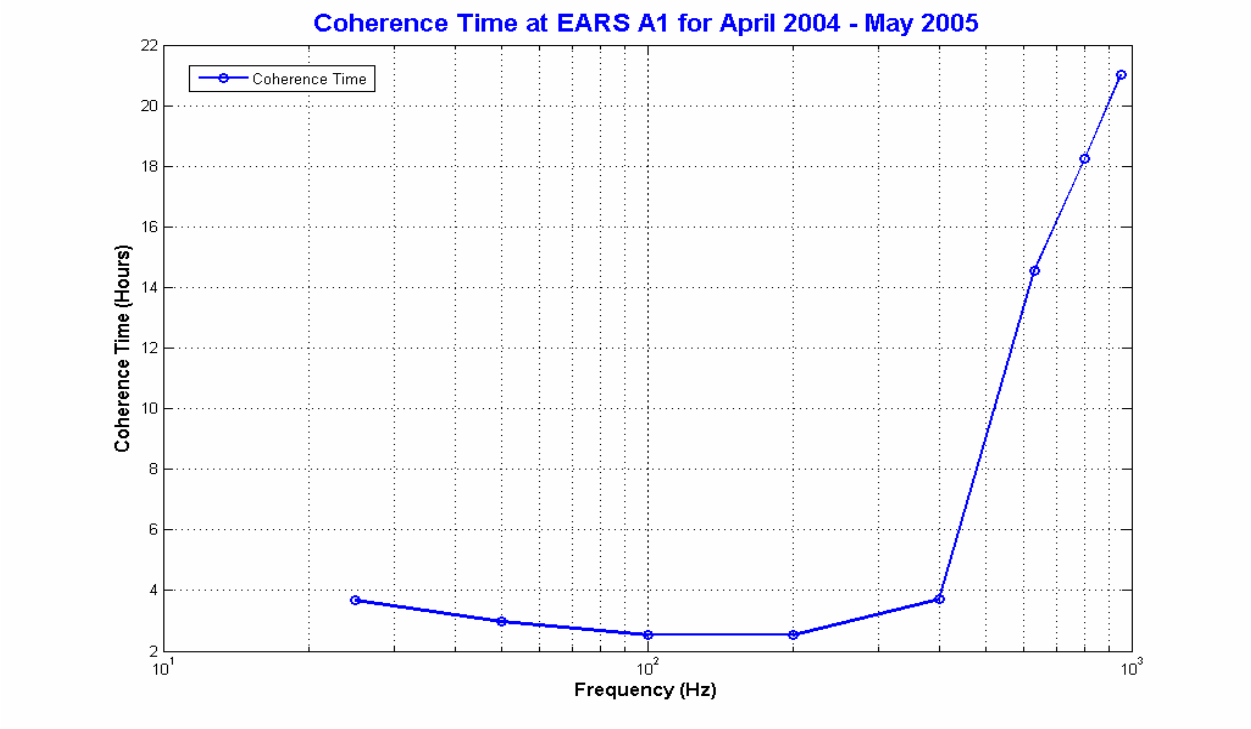

Figure 7.4 Coherence time at EARS A1 for 14 months.

7.3 Frequency Coherence of the Noise Field

The shape of the spectrum of ocean ambient noise is constantly changing, due to changes in the nature and the positions of the many sources that contribute to it, as well as the fluctuations in transmission associated with varying oceanographic conditions. One way to characterize the changes is to examine the statistics of the noise levels in a number of frequency bands across the spectrum. Frequency coherence calculations (also called frequency-frequency correlations) attempt to measure how changes in one part of the frequency spectrum are temporally correlated with those in other frequency regions [Nichols and Sayer, 1977]. There is a general tendency for the correlation of the levels in a given frequency band centered at f_1 with levels at various frequency bands centered at f_2 to fall off as the frequency spacing between f_1 and f_2 increases in either direction.

The correlation of the noise field at one site (A1) between the eight 1/3-octave bands frequency bands is computed. The coherence over the entire fourteen month period is investigated, comparing each of the eight time series to each other. The resulting correlation coefficients are plotted in Figures 7.5 to 7.12. Also displayed on each of these eight figures is a threshold (plotted in red) showing where the correlation coefficient is equal to 0.5.

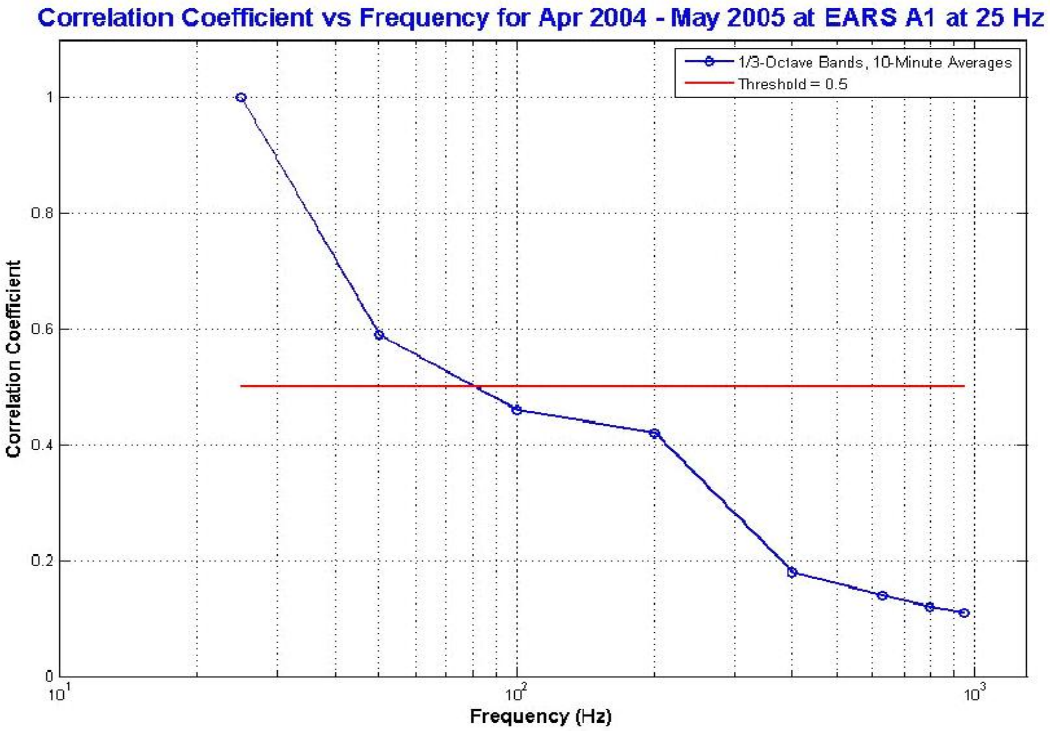

Figure 7.5 Correlation coefficient vs. frequency at EARS A1 for 14 months at 25 Hz.

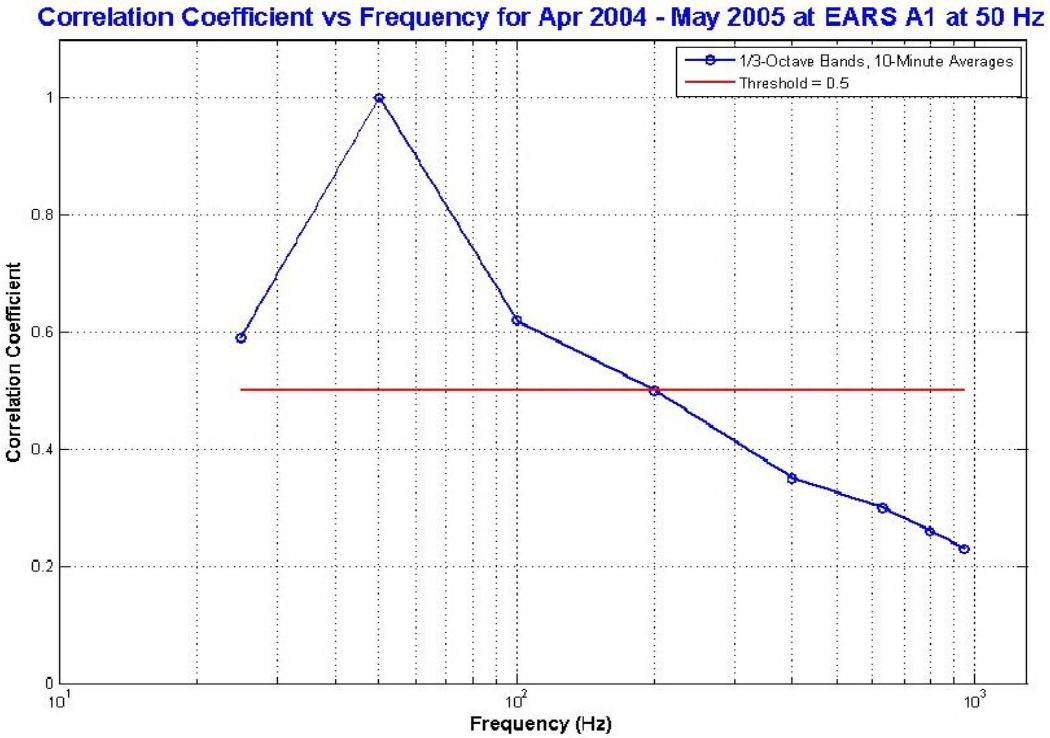

Figure 7.6 Correlation coefficient vs. frequency at EARS A1 for 14 months at 50 Hz.

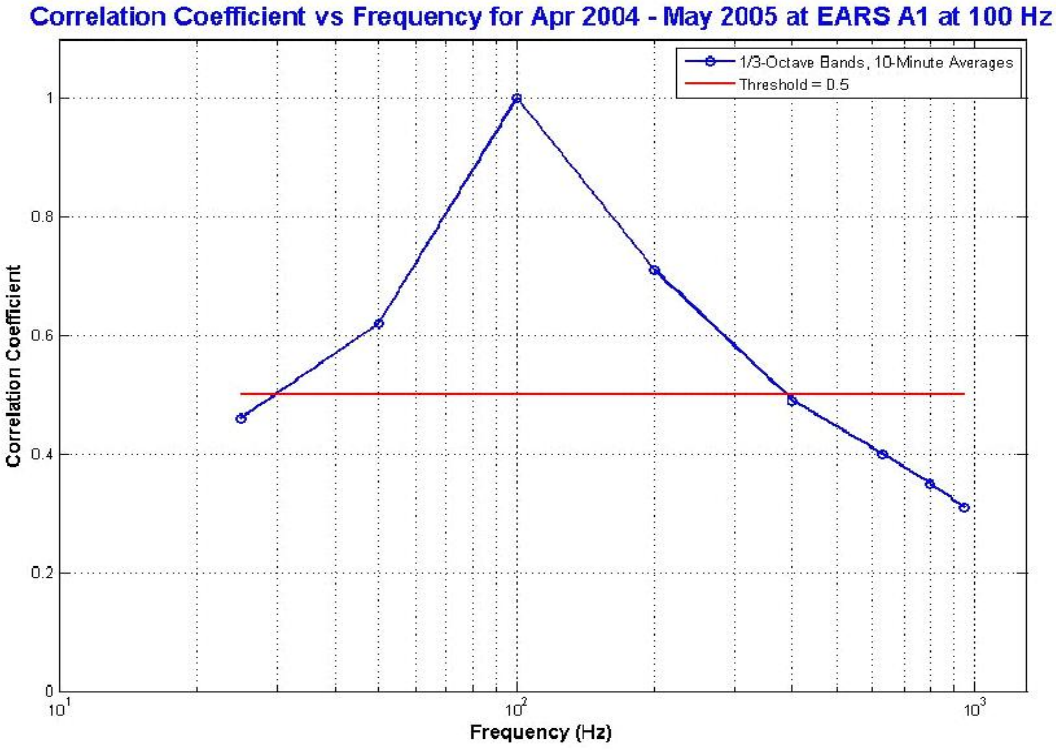

Figure 7.7 Correlation coefficient vs. frequency at EARS A1 for 14 months at 100 Hz.

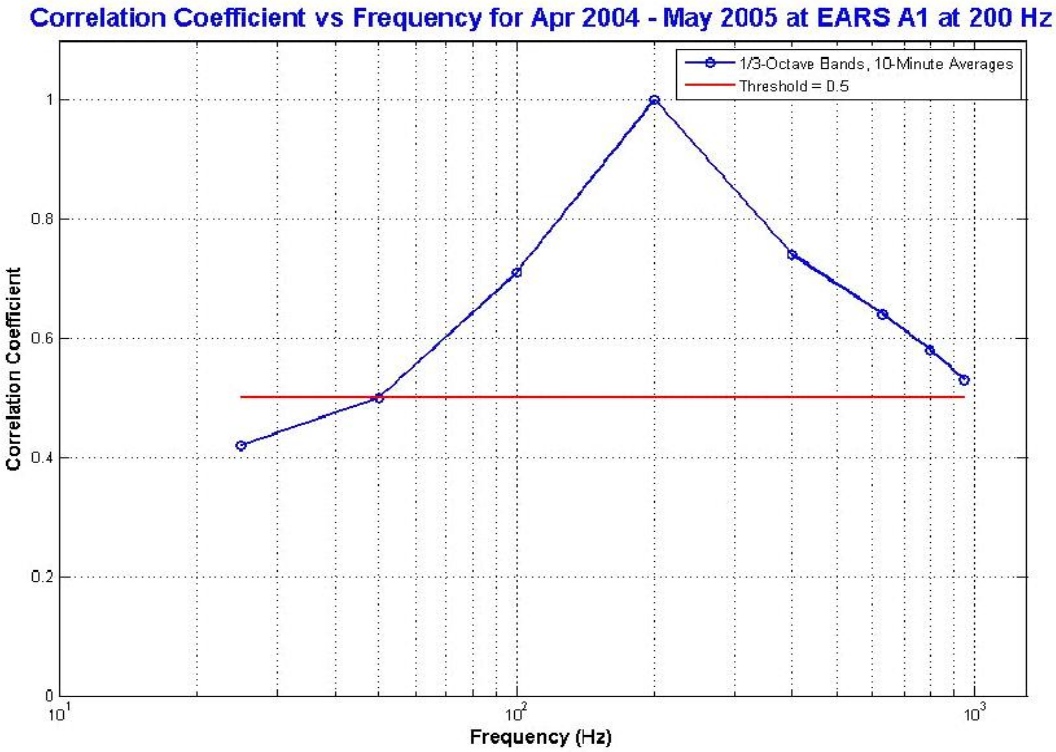

Figure 7.8 Correlation coefficient vs. frequency at EARS A1 for 14 months at 200 Hz.

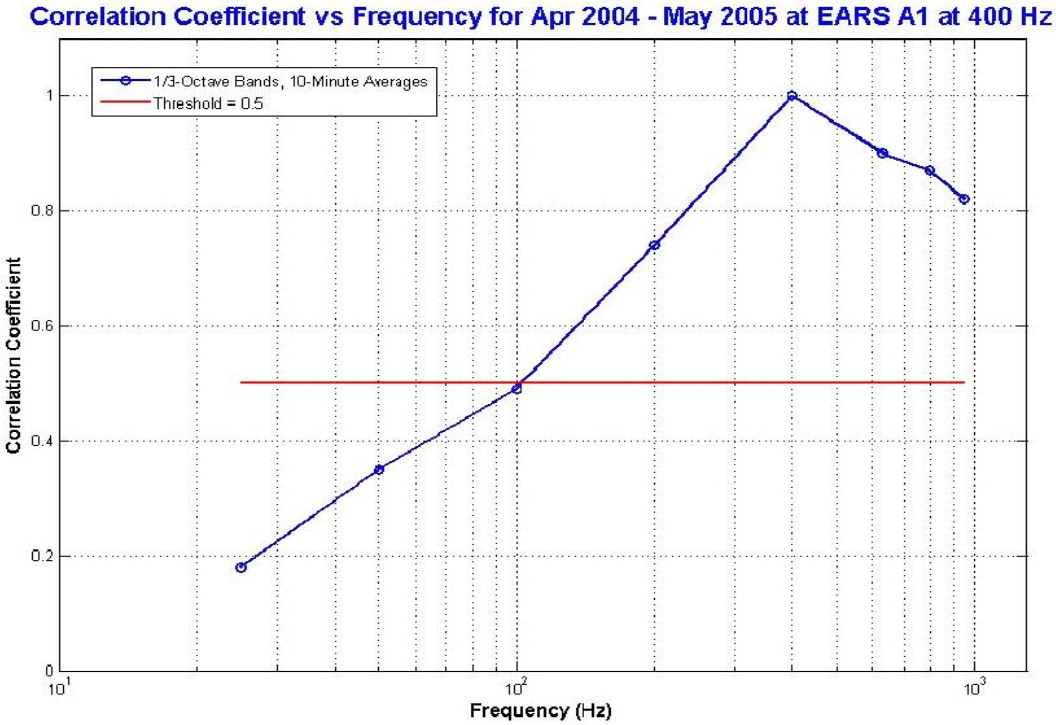

Figure 7.9 Correlation coefficient vs. frequency at EARS A1 for 14 months at 400 Hz.

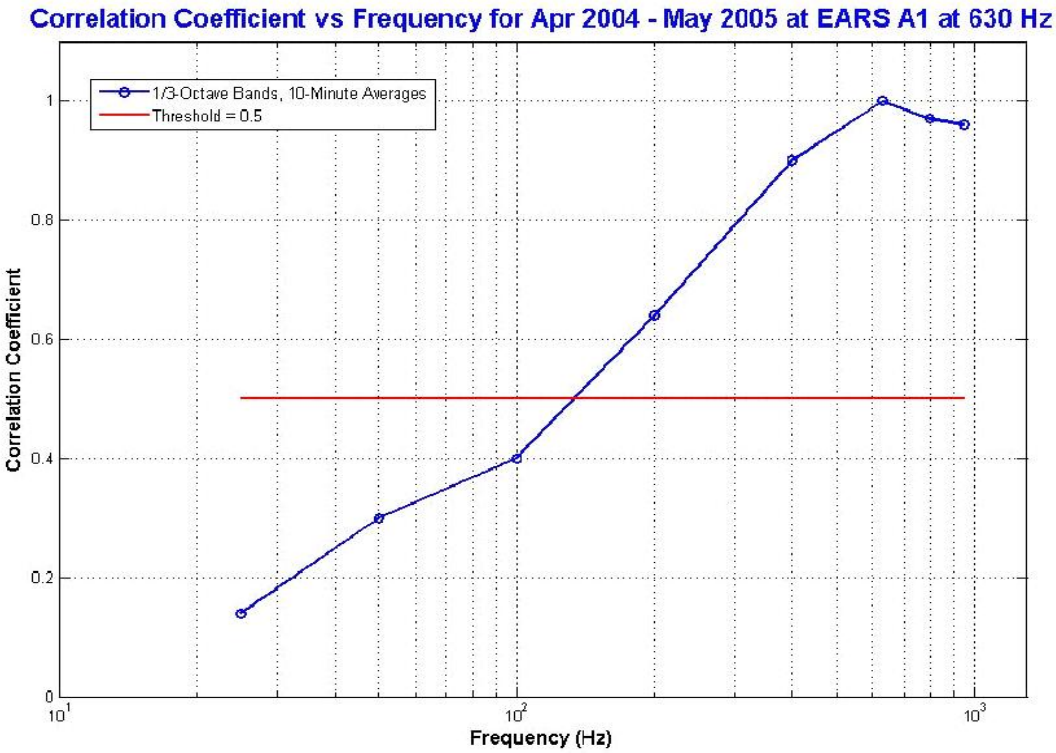

Figure 7.10 Correlation coefficient vs. frequency at EARS A1 for 14 months at 630 Hz.

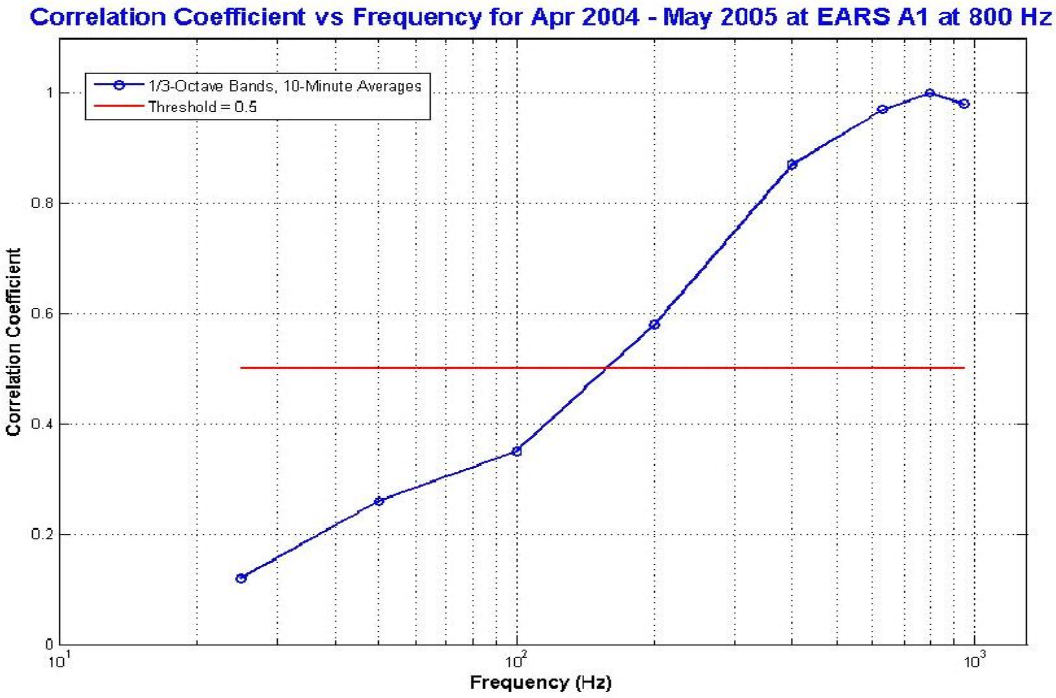

Figure 7.11 Correlation coefficient vs. frequency at EARS A1 for 14 months at 800 Hz.

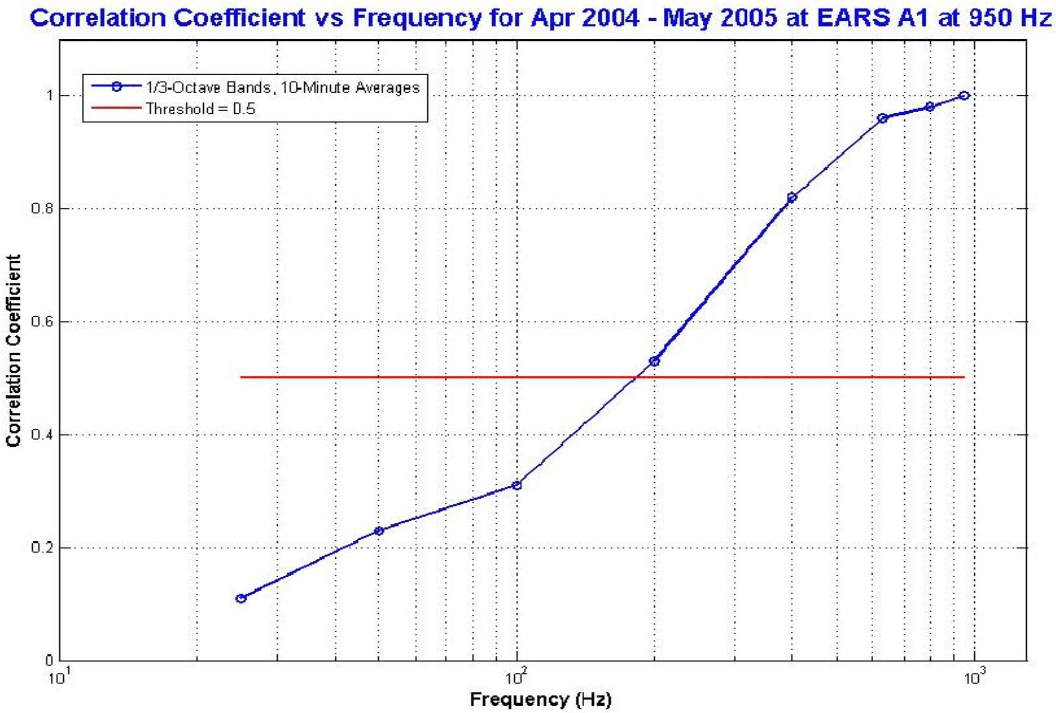

Figure 7.12 Correlation coefficient vs. frequency at EARS A1 for 14 months at 950 Hz.

Table 7.1 shows the frequency region for each 1/3-octave center frequency for which the correlation coefficient is greater than or equal to 0.5. This region ranges from 1.7 to 2.4 octaves (average = 2.1 octaves) to the left of the center frequency and from 1.7 to 2.0 octaves (average = 1.9 octaves) to the right of the center frequency for the octaves measured. This means, for example, that for this region in the Gulf of Mexico, a 1/3-octave time series measurement centered at 100 Hz will be well correlated ($\rho \geq 0.5$) with the 1/3-octave time series from about 30 Hz (1.7 octaves below 100 Hz) to about 400 Hz (2 octaves above 100 Hz). On average, the data in a time series at a particular center frequency are highly correlated with neighboring time series ranging from about 2 octaves below to 2 octaves above the center frequency.

F_c (Hz)	**Freq Band (Hz) with $\rho \geq 0.5$**	**Octaves Left or Right of F_C**
25	<25 to 80	1.7 (R)
50	<25 to 200	2.0 (R)
100	30 to 400	1.7 (L), 2.0 (R)
200	50 to >950	2.0 (L)
400	100 to >950	2.0 (L)
630	130 to >950	2.2 (L)
800	160 to >950	2.3 (L)
950	180 to >950	2.4 (L)

Table 7.1 Frequency band for which the correlation coefficient is ≥ 0.5.

Nichols and Sayer did a similar comparison during the month of February in deep water in the North Atlantic [Nichols and Sayer, 1977]. They use much narrower frequency bands (6 Hz wide) and a much shorter data duration (4.3 days) and look at a smaller frequency range of 5 to 150 Hz. Their results show that between any two frequency bands centered at f_1 and f_2, the correlation coefficient is 1.0 when $f_1 = f_2$ (by definition), but falls to about 0.5 for a ratio of one octave between f_1 and f_2. The Gulf of Mexico data thus showed a frequency coherence of twice the bandwidth of the North Atlantic data, with a ratio of two octaves between f_1 and f_2.

Chapter 8

Weather and Shipping Comparisons

The National Oceanic and Atmospheric Administration (NOAA), through the National Data Buoy Center (NDBC), operates a network of weather buoys in the Gulf of Mexico [National Data Buoy Center, 2007]. Two NDBC buoys close to the EARS buoys recorded wind speed and wave height data for the entire period the EARS buoys were recording. Station 42003 is located 260 nm south of Panama City, FL at a water depth of 3233 m; see Figure 8.1. The water depth at station 42003 is very close to the water depth in the vicinity of the EARS buoys, 3200 m. Station 42003 is located 89 nm south/southeast of EARS A1; the EARS buoys location and station 42003 are both in the Mexican Basin physiographic region in the eastern Gulf of Mexico, near the West Florida Escarpment. Station 42036 is located 106 nm west/northwest of Tampa, FL at a water depth of 55 m (on the West Florida Shelf). It is located 103 nm northeast of the EARS A1 location. The two NDBC buoys are 164 nm apart.

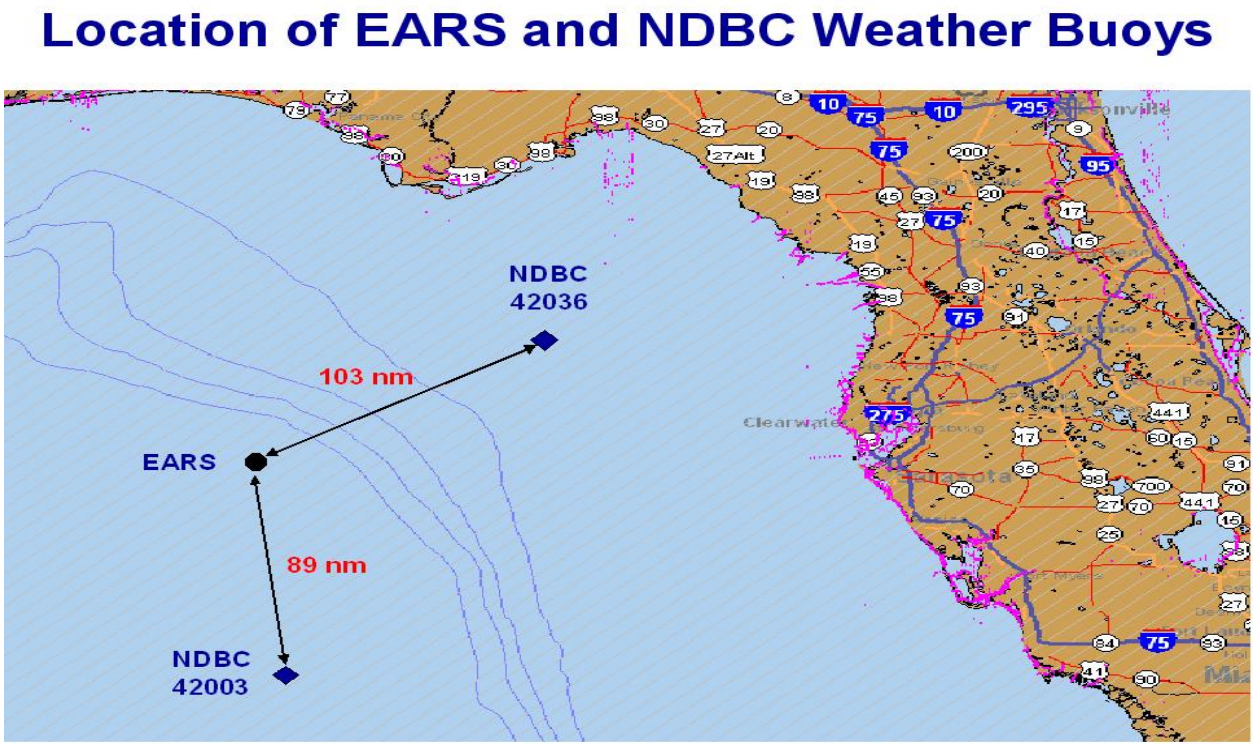

Figure 8.1 Location of EARS and NDBC weather buoys.

Both weather buoys report the wind speed values (in m/s) hourly. The wind speed values are computed as the scalar average of all the wind speed observations during an 8-minute sampling period. Both weather buoys also report the significant wave height values (in meters) hourly. The significant wave height values are computed as the average of the highest 1/3 of all the wave heights during a 20-minute sampling period. Figures 8.2 and 8.3 show the mean wind speed versus month and the mean significant wave height versus month, respectively, at each of the NDBC buoys. (Appendix D[1] shows the monthly significant wave height values every hour as reported by both weather buoys for the entire 14 month period.)

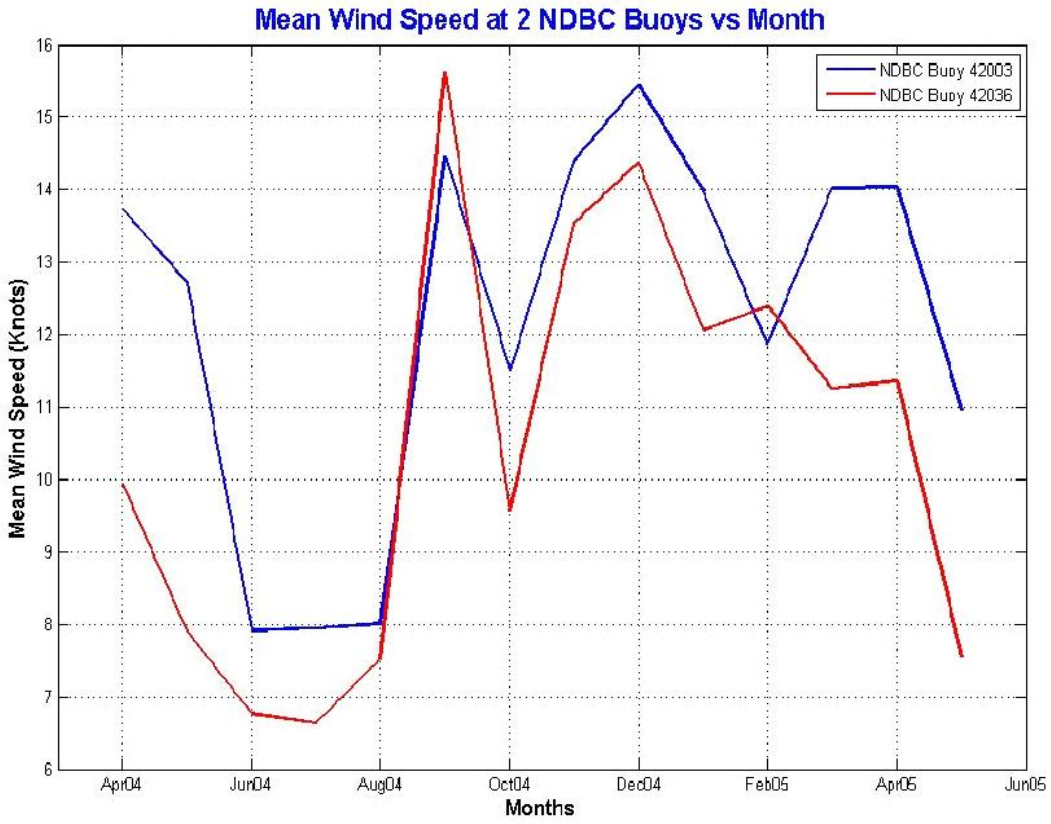

Figure 8.2 Mean wind speed at 2 NDBC buoys vs. month.

[1] In Appendix D, note that the wave height scale (the vertical scale) changes for each month. For example, the maximum wave height during June 2004 (Figure D.3) is slightly over 1.4 m. But the maximum wave height during Hurricane Ivan (September 2004, Figure D.6) is about 11.0 m.

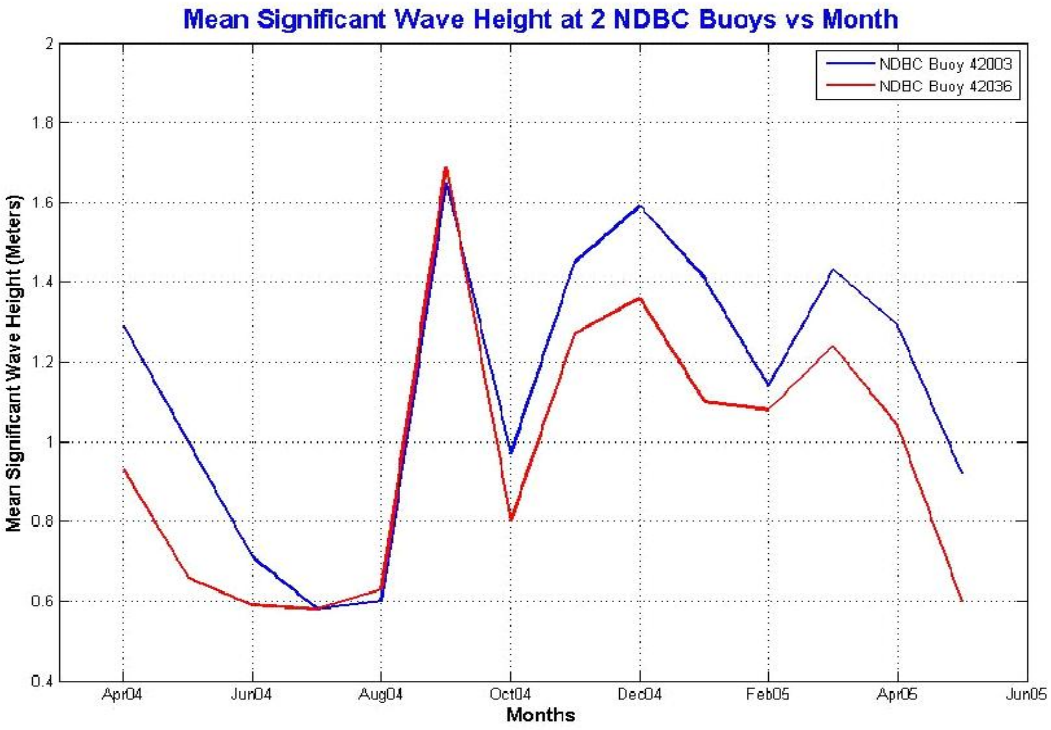

Figure 8.3 Mean significant wave height at 2 NDBC buoys vs. month.

Figures 8.4 and 8.5 show the wind speed and significant wave height standard deviation versus month, respectively, at each of the NDBC buoys. The values in each plot are generally low during May through August of 2004, peak during the hurricane month of September 2004, and then settle down again in October to higher values than those in May through August.

Figure 8.6 shows the coefficient of variation (sigma to mean ratio) at both NDBC buoys versus month. This dimensionless quantity, which is a measure of the amplitude fluctuation of a data set, is smallest for both weather buoys during May through June of 2004. Buoy 42003 had a narrow peak during September 2004 (much more pronounced for the waves than the wind), while buoy 42036 has a broader peak from July through October of 2004. The values for both buoys drop sharply during November 2004, matching the drop in the standard deviation and the spread of the ambient noise data seen at high frequencies (630 – 950 Hz) during November 2004 in Figures 4.13 and 4.15.

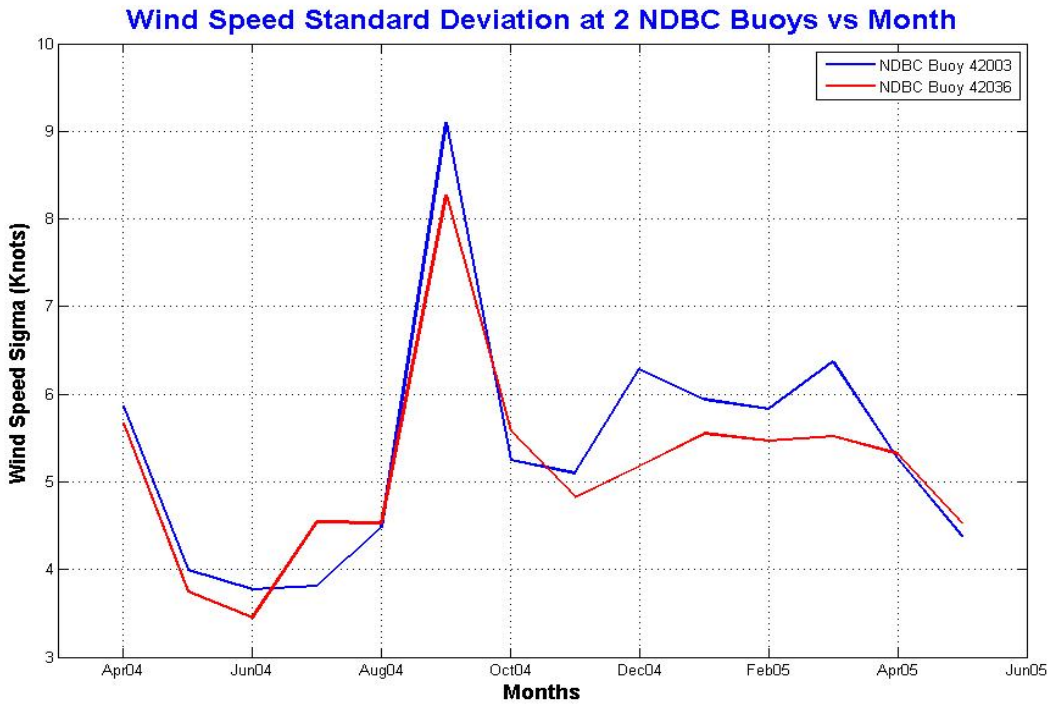

Figure 8.4 Wind speed standard deviation at 2 NDBC buoys vs. month.

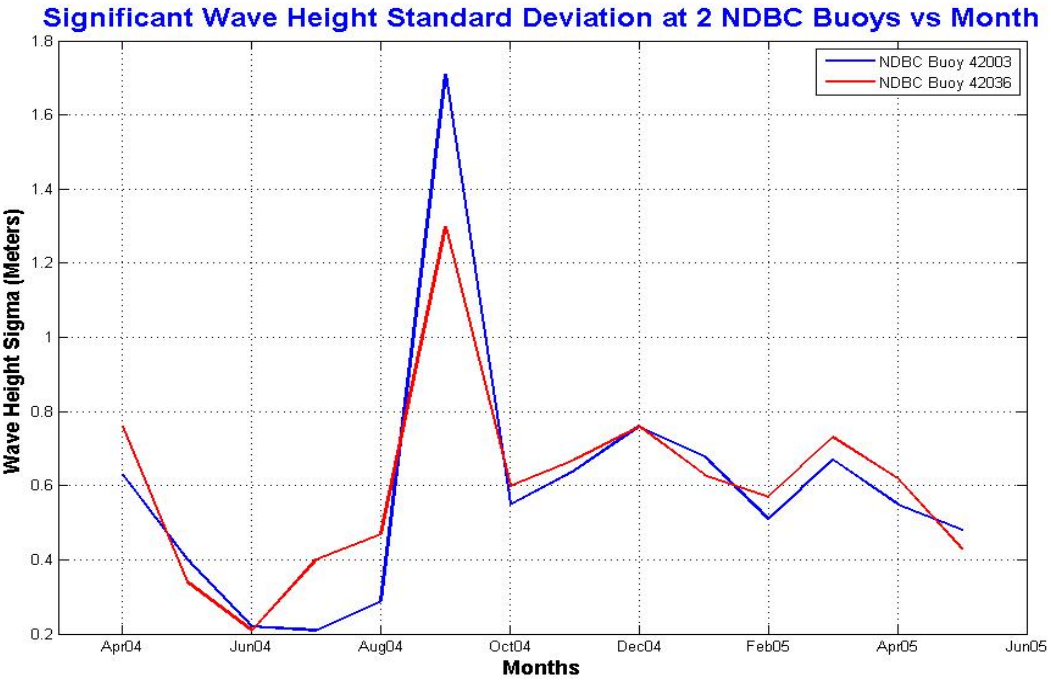

Figure 8.5 Wave height standard deviation at 2 NDBC buoys vs. month.

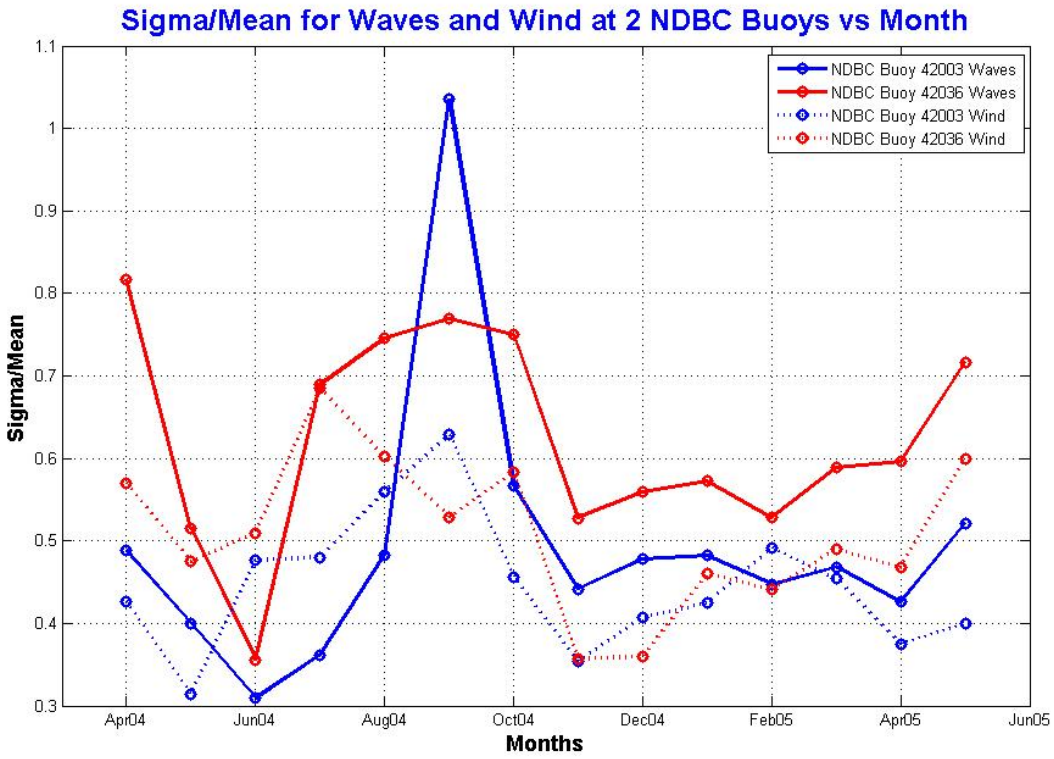

Figure 8.6 Coefficient of variation (sigma to mean ratio) at 2 NDBC buoys vs. month.

The Beaufort Wind Force (BWF) scale is used to assign numbers to wind speed ranges. A higher Beaufort number corresponds to a higher range of wind speeds. Table 8.1 illustrates the BWF scale with respect to wind speed and wave height [Urick, 1984].

BWF	Wind Speed (kts)	Wave Height (m)
0	<1	0 – 0.09
1	1-3	0.1 – 0.19
2	4-6	0.2 – 0.59
3	7-10	0.6 – 0.99
4	11-16	1.0 – 1.99
5	17-21	2.0 – 2.99
6	22-27	3.0 – 3.99
7	28-33	4.0 – 5.49
8	34-40	5.5 – 6.99

Table 8.1 The Beaufort Wind Force (BWF) scale.

The average wind speed over the 14 month period is 10.47 knots at NDBC buoy 42036 but slightly higher, 12.21 knots at NDBC buoy 42003. Since the EARS buoys were located approximately half-way between these two weather buoys, the estimated average wind speed in the vicinity of the EARS buoys over the entire 14 month period is the average of these two values, 11.34 knots. Similarly, the average significant wave height over the 14 month period is 0.97 m (3.2 ft) at NDBC buoy 42036 but slightly higher, 1.15 m (3.8 ft) at NDBC buoy 42003. The estimated average significant wave height in the vicinity of the EARS buoys over the entire 14 month period is 1.06 m (3.5 ft). These estimated average values (11.34 knots of wind and 1.06 m wave height) are right on the boundary of BWF3 (7-10 knots of wind, waves 0.6-0.99 m) and BWF4 (11-16 knots of wind, waves 1.0-1.99 m). So the estimated average Beaufort Wind Force at the EARS buoys over the entire 14 month period is BWF 3.5.

Table 8.2 shows the monthly average wind speed and wave height near the EARS buoys. The average wind speed column also includes the estimated average monthly Beaufort Wind Force in parenthesis. For example, the month of April 2004 has an average wind speed of 11.8 knots and an estimated average BWF of 4. Table 8.2 also includes the measured ambient noise at 800 Hz and the noise predicted at 800 Hz using Wenz curves and the average wind and wave data for each month. The measured noise values shown are the mean and median values computed over the 1/3-octave band centered at 800 Hz. As can be seen, there is excellent agreement between the predicted noise values and the measured noise values. The slight differences are probably due to the fact that the weather buoys were not collocated with the EARS buoys. As was mentioned previously, the two weather buoys were 89 nm and 103 nm away from the EARS buoys. Presumably a closer weather buoy would give a better estimate of the average BWF for each month.

Table 8.2 Average monthly wind speed, wave height and 800 Hz noise.

Month	Avg Wind Speed (kts)	Avg Wave Height (m)	Predicted Noise (dB)	Mean 800 Hz Noise (dB)	Med 800 Hz Noise (dB)
APR04	11.8 (4)	1.11	63	62.65	62.99
MAY04	10.3 (3.5)	0.83	61.5	60.35	60.77
JUN04	7.4 (2.5)	0.65	57	57.09	56.68
JUL04	7.3 (2.5)	0.58	57	57.96	57.59
AUG04	7.8 (2.5)	0.62	57	57.53	57.41
SEP04	15.0 (4)	1.67	63	62.97	63.72

OCT04	10.5 (3.5)	0.89	61.5	59.40	59.30
NOV04	14.0 (4)	1.36	63	63.27	63.10
DEC04	14.9 (4)	1.48	63	63.67	64.31
JAN05	13.0 (4)	1.26	63	63.28	63.93
FEB05	12.1 (4)	1.11	63	62.40	63.63
MAR05	12.6 (4)	1.34	63	62.16	62.58
APR05	12.7 (4)	1.17	63	62.96	63.60
MAY05	9.3 (3)	0.76	60	58.43	58.71
14 Months	11.3 (3.5)	1.06	61.5	61.05	61.67

Table 8.2 Continued.

The Gulf of Mexico is an area of high shipping activity, as is discussed in Chapter 3, so the expected shipping noise contribution is high. There is a major shipping lane that runs from the Straits of Florida and Cuba to New Orleans that passes near the EARS buoys; see Figure 3.1. Distant shipping is the major contributor to ambient noise in the band 20-200 Hz in most deep water areas [Ross, 1987]. The EARS buoys were located in deep water around 3200 m. Ross plots the estimated shipping contribution to deep water ambient noise as a function of shipping concentration, using four categories: remote, light, moderate and heavy shipping. Similarly, the Naval Oceanographic Office has plotted the estimated shipping contribution to deep water ambient noise as a function of shipping intensity, using nine categories: 1-2 (low), 3-4 (medium), 5-7 (high) and 8-9 (basins and chokepoints) [NAVOCEANO, 1999].

Figure 8.7 shows a comparison between the measured 14 month ambient noise values (mean and median) and predicted values based on the expected contributions of shipping and weather. Two curves are plotted for the expected shipping noise: shipping intensities 6 and 7, which correspond to high intensity [NAVOCEANO, 1999] and moderate to heavy [Ross, 1987]. The weather contribution is based on an average BWF[2] of 3.5 (half-way between BWF 3 and BWF 4). As can be seen from the figure, the measured levels at 25 Hz[3] and 50 Hz are closer to shipping intensity 7. The levels from 100-950 Hz closely fit a curve based on shipping intensity 6 coupled with a weather contribution of BWF 3.5.

[2] Wind speed on the 1946 Beaufort scale is defined by the empirical formula: $v = 1.625\, B^{3/2}$, where v is the wind speed in knots and B is the Beaufort scale number. Substituting an average $v = 11.34$ knots yields $B = 3.65$. [http://en.wikipedia.org/wiki/Beaufort_scale]

[3] In section 10.8 it is postulated that some of the noise at 25 Hz may be due to oil rig drilling activity to the west of the EARS buoys. So the noise level at 25 Hz may be modeled as shipping intensity 6 or 7 plus oil rig drilling noise.

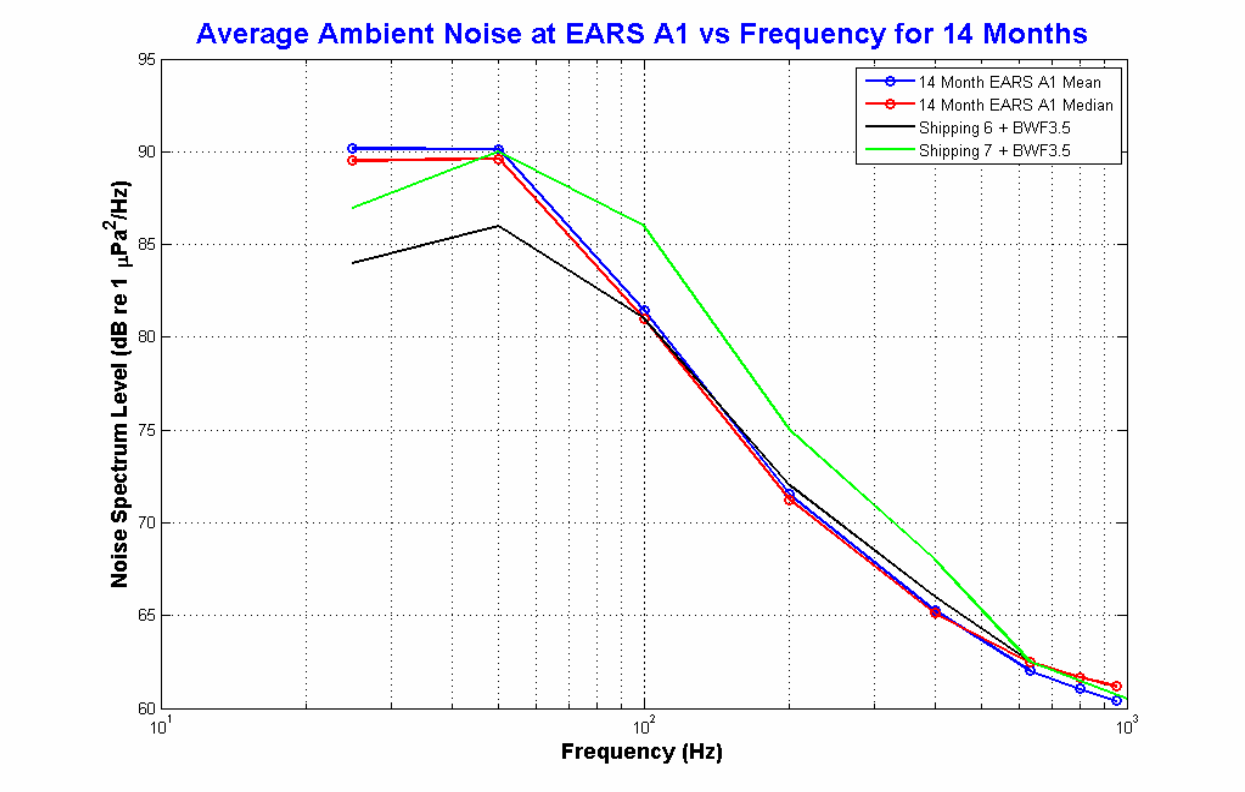

Figure 8.7 Measured and predicted noise for entire 14 month period.

Chapter 9
Day vs. Night Comparison

Some authors have found significant diurnal variability in ambient noise data. Wenz found a diurnal variability of 10-20 dB at one location [Wenz, 1961]. In one case the noise at 100 Hz was 15 dB louder at midnight local time than at noon local time. Many biological sounds have diurnal variation, with night noise levels 10-20 dB higher than day noise levels due to fish chorusing at night [McDonald, 2006]. Ambient noise in shallow water is characterized by a highly variable background of ship and biological activity with large changes between day and night. Day time shipping noise can be much higher near a busy harbor when more ships are present [Urick, 1984].

The EARS data are analyzed to see if any significant changes in noise level occur between day and night. Four months representative of the four seasons (July and October of 2004 and January and April of 2005) are selected for day versus night ambient noise comparisons. Local sunrise and sunset times at the EARS location were obtained from the U.S. Naval Observatory [U.S. Naval Observatory, 2007]. Average monthly hours of day/night were 57% day/43% night during July, 48% day/52% night during October, 45% day/55% night during January and 53% day/47% night during April. The data are separated into day and night periods for each month and the following statistical parameters are computed: the mean, standard deviation (sigma), and skewness.

Figure 9.1 shows the day and night data for July 2004 in the 900 to 1000 Hz band. The daytime periods are in blue and the nighttime periods are in red. (The same plot without the day and night periods separated is shown in Figure C.4.)

One factor affecting the statistics is the average monthly wind speed. July was a generally calm month, with an average wind speed of 7.4 knots (BWF 2.5). October was windier, with an average wind speed of 10.5 knots (BWF 3.5). January and April both had BWF 4, with average monthly wind speeds of 13.0 knots and 12.7 knots, respectively.

There is not a large difference between the mean day and mean night values for the four months analyzed (Figure 9.2). The mean day and night values never differ by more than 1.7 dB; the difference of the two values (mean day – mean night) is usually between +1.0 dB and -0.5 dB. The largest values (about -1.4 dB and -1.7 dB) occur during July at 800 and 950 Hz.

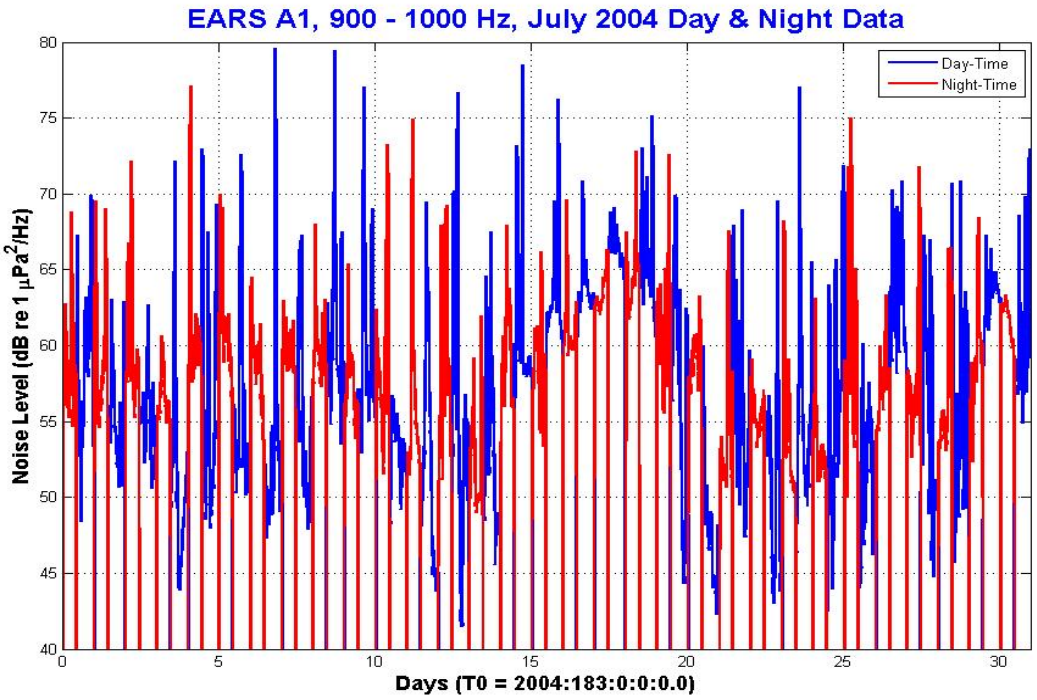

Figure 9.1 Day and night data for July 2004 at 950 Hz.

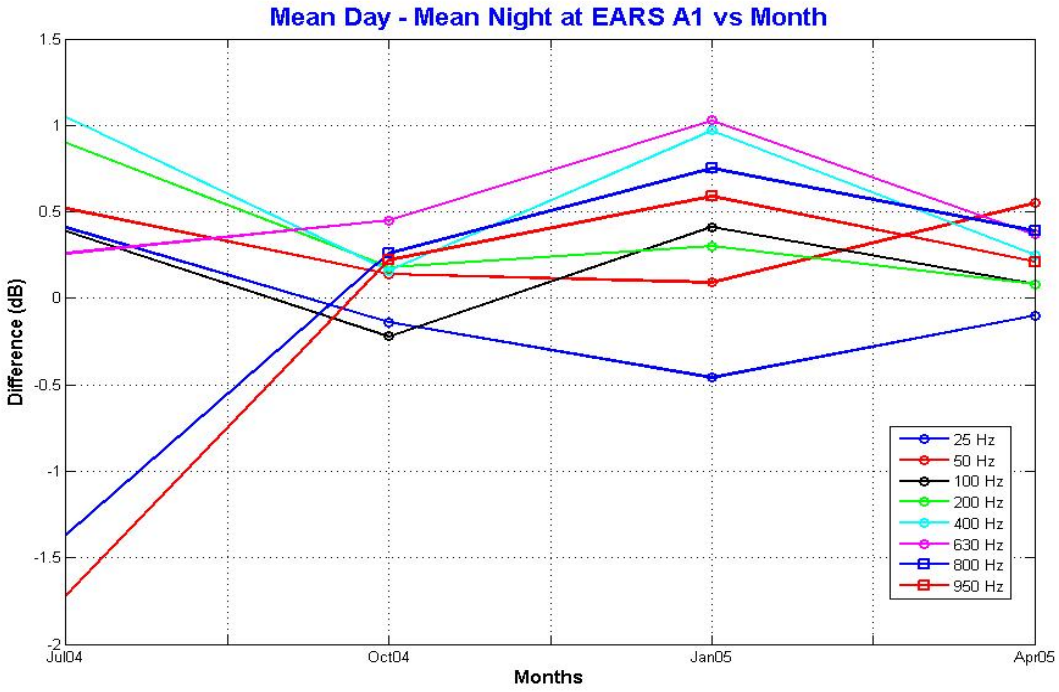

Figure 9.2 Mean noise day – mean noise night.

Overall day noise levels are slightly louder than night noise levels except at 25 Hz. The 25 Hz noise levels are higher at night for all months except July. All other frequency bands are louder during the day except for 100 Hz during October and for 800 and 950 Hz during July.

There is a small difference between day and night standard deviation (sigma) values. Most values of the difference, sigma day – sigma night, are between +0.5 dB and -0.5 dB (Figure 9.3). The largest values (+1.5 dB to +2.5 dB) occur during July for 630-950 Hz. Day standard deviations are generally higher (three out of four months) at 25, 50 and 200 Hz. Night standard deviations are generally higher (three out of four months) at 400 and 630 Hz. The night-time standard deviation is always higher at 100 Hz. The values at 800 and 950 Hz are evenly split: during half the months the day-time values are higher, and during half the months the night-time values are higher.

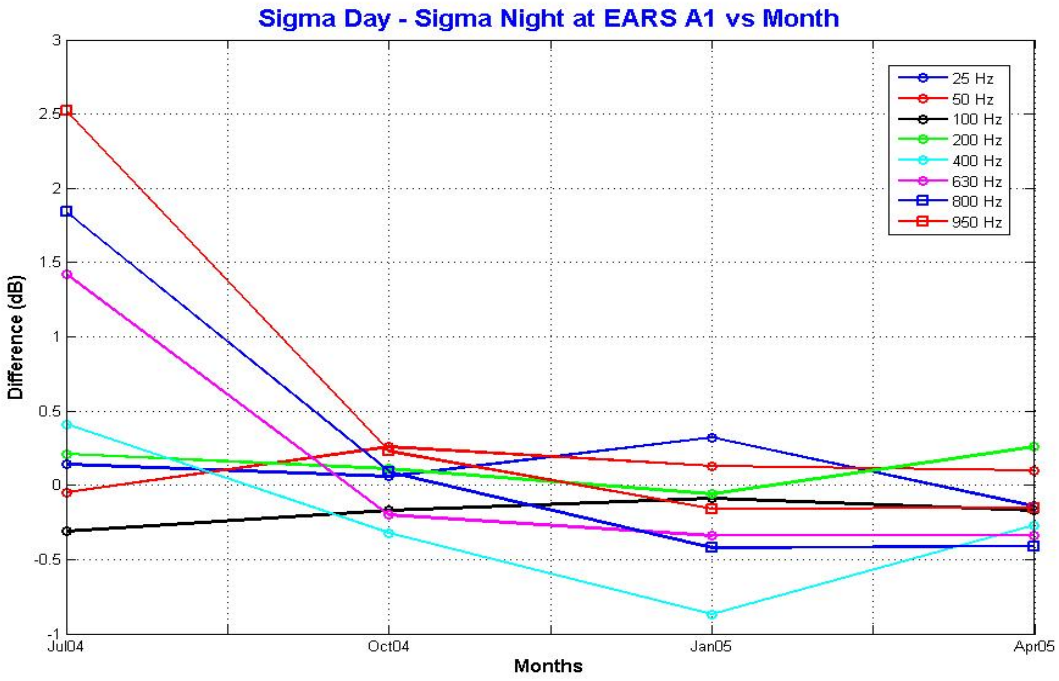

Figure 9.3 Sigma day – sigma night.

The day and night skewness values never differ by more than 0.8. Overall the night skewness values are higher (skewed towards peaks) than the day skewness values, but there are exceptions (Figure 9.4). Night skewness values are always higher at 950 Hz. Night skewness values are generally higher (three out of four months) at 100, 630 and 800 Hz. Day skewness values are generally higher (three out of four months) at 25 and 400 Hz. The values at 50 and 200 Hz are evenly split: during half the months the day-time values are higher, and during half the months the night-time values are higher. The generally higher skewness values at higher frequencies at night may be an indication of higher ship activity at night. The day and night skewness values have different signs at three times for certain frequencies: during October at 800 and 950 Hz and during January at 630 Hz. During October the overall monthly skewness at 800 Hz is -0.13 and at 950 Hz it is -0.19, and both frequencies show negative skewness (skewed towards troughs) during the day. But for both frequencies the night-time skewness is 0.04. This may have been caused by lower wind speeds at night (which would cause positive skewness) and higher wind speeds during the day (which would cause negative skewness). During January the overall monthly skewness at 630 Hz is -0.17 and the skewness during the night is also negative. But the skewness during the day is slightly positive (0.01).

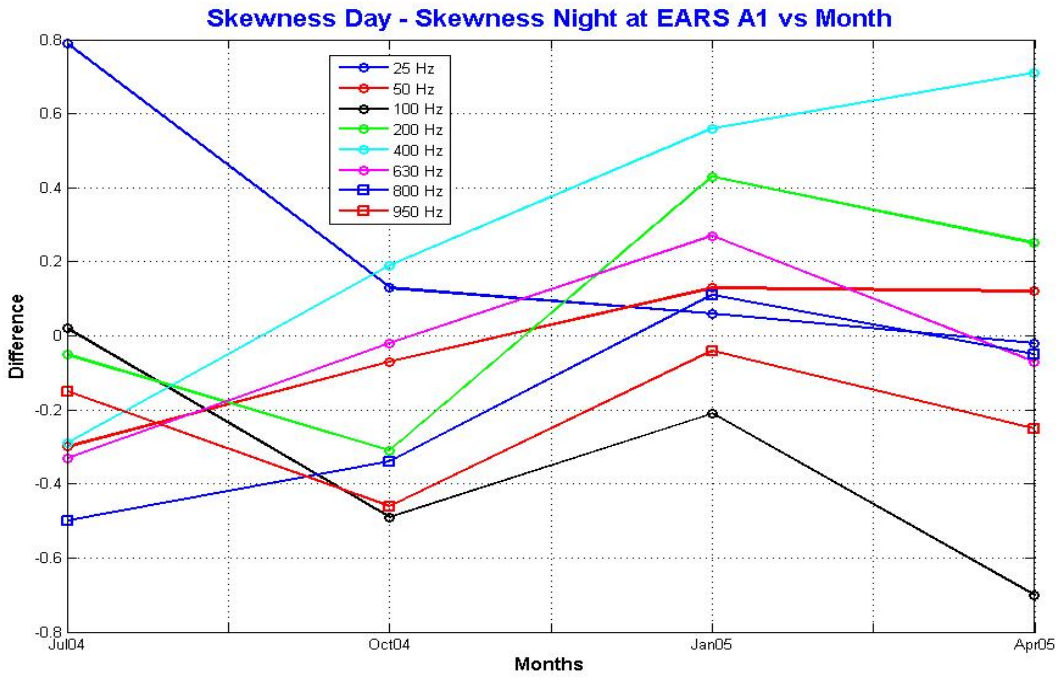

Figure 9.4 Skewness day - skewness night.

The overall monthly skewness from 630-950 Hz is positive during July and negative for the other three months. This is due to the average monthly wind speed for each month (low in July, high for the other three months).

In summary, there is not a significant diurnal variability of ambient noise observed in this data set. The biological activity in the region of the EARS buoys doesn't appear to have a diurnal pattern. Likewise, the shipping activity apparently has no significant preference for day or night periods either. This is not surprising, since the EARS buoys were located in deep water, far from ports.

Chapter 10
Summary and Conclusions

In this dissertation, long-term ambient noise data in the Gulf of Mexico are analyzed for statistical trends. Many interesting phenomena are observed. Section 10.1 contains a summary of the monthly statistics. The passage of four hurricanes during the summer of 2004 (three during the month of September) has a major impact on all of the statistical quantities measured, which are summarized in section 10.2. The statistics computed over the entire fourteen month period are discussed in section 10.3, followed by the threshold crossing results in section 10.4. The coherence of the ambient noise field is summarized in section 10.5. The comparison of day versus night noise data is discussed in section 10.6. Current research in this area is described in section 10.7. Section 10.8 discusses a proposed ambient noise model for this region of the Gulf of Mexico that is based on all of these observations. The chapter concludes with some suggestions for future work.

10.1 Monthly Statistics Summary

The monthly mean ambient noise values peak at 25 and 50 Hz, then decrease with increasing frequency out to 950 Hz. Most frequency bands appear to have a cycle of about one year, based on the monthly mean values. The low frequencies (25 – 100 Hz) peak during March 2005 and are least during the hurricane month of September 2004. High frequencies (400 – 950 Hz) are loudest during September 2004 and during the winter months of November, December and January due to high average wind speeds during these months. Conversely, the high frequencies are quietest during the summer months of June through August of 2004 due to low average wind speeds during these months.

The mean and median monthly values at each frequency never differ by more than 1.5 dB. The mean value is generally larger than the median value at low frequencies (25 - 400 Hz), which corresponds with those monthly time series having positive skewness. The median value is generally larger than the mean value at high frequencies (630 - 950 Hz), which corresponds with those monthly time series having negative skewness. This is always the case during months with high average wind speeds. The months of June through August 2004 have low average

wind speeds, which cause positive skewness and result in the mean values exceeding the median values at high frequencies.

The spread of the data (determined by subtracting the 10^{th} percentile value from the 90^{th} percentile value) is calculated for each 1/3-octave band. The data have the highest spread at the higher frequencies, especially from 630 – 950 Hz during July – October 2004 and May 2005. The spread is usually least in the region 100 – 200 Hz. The spread is smallest at high frequencies (400 – 950 Hz) during November 2004, which has low standard deviations over the same band of frequencies.

The standard deviation tends to be high at low frequencies (25 Hz), is least near 100 – 200 Hz, and increases to high values again at high frequencies (630 – 950 Hz). The highest standard deviations occur during September 2004 from 630 – 950 Hz due to the high wind speed variability during the hurricanes. The same pattern (although not as pronounced) is observed during May 2005.

The skewness tends to be low at low frequency (25 Hz), increasing to a maximum at 100 Hz, and then decreasing again at higher frequencies, with the lowest values at 950 Hz. The skewness is always positive (skewed towards peaks) from 25 - 400 Hz, except at 25 Hz during January – March 2005. Since shipping noise dominates low frequencies, the region 25 - 400 Hz is dominated by shipping peaks, which contribute to the high amplitude tails (louder decibel values) of a PDF and make the skewness positive.

Weather noise dominates high frequencies, so the region 630 - 950 Hz is dominated by weather. The average weather in a month determines the skewness in that month at higher frequencies. The skewness is usually negative (skewed towards troughs) from 630 - 950 Hz, especially in months with high average wind speeds. Of the 14 months analyzed, 11 months have average wind speeds of 9 knots or greater, and these months are generally negatively skewed in the region of 630 - 950 Hz. The skewness is positive from 630 - 950 Hz when the monthly average wind speed is low, such as occurred during June to August 2004 (when the monthly average wind speed ranged from 7.3 to 7.8 knots).[1] The most negative values of skewness at 630 - 950 Hz occur during February 2005, a very windy month with an average wind speed of 12.1 knots.

[1] In general, the skewness is positive when the mean is greater than the median and negative when the median is greater than the mean.

The kurtosis tends to be low at 25 Hz, peaks at 100 Hz and decreases again at higher frequencies. Values of kurtosis in the weather band of 630 – 950 Hz tend to be between 3 and 4, generally near 3 (the kurtosis of a Gaussian distribution). Conversely, the values of kurtosis in the shipping band of 25 - 200 Hz tend to be higher, reaching a maximum value of 9.5 at 100 Hz.

The coherence times range from a low value of about 1 hour to a high value of about 33 hours. The coherence time is generally low at low frequencies in the shipping band (25 - 400 Hz) year-round, and at higher frequencies in the weather band (630 - 950 Hz) when the average monthly wind speed is low (such as June through August of 2004). It is generally high at higher frequencies (630 - 950 Hz) when the average monthly wind speed is high. The highest values are observed during the hurricane month of September 2004 at all frequencies above 200 Hz, with the maximum being 32.66 hours at 950 Hz. During 2005 the highest values for coherence time are observed during May at higher frequencies; the peak value at 950 Hz is about 18 hours.

10.2 Hurricane Statistics Summary

The passage of three hurricanes during September 2004 has a major impact on all of the statistical quantities measured. Of all the months studied, September 2004 has the highest average wind speed and the highest average significant wave height. The ambient noise levels at high frequencies (400-950 Hz) are elevated, as expected, and are highly correlated with the wind and wave height data. The ambient noise levels at low frequencies (25-100 Hz) are depressed, perhaps an indicator of less shipping activity during extreme wind conditions. The fewest number of peaks per day (as well as troughs per day) are observed from 200-950 Hz during September, yielding the smallest estimate of nearby ships per day. The average time between peaks (as well as troughs) is maximum from 200-950 Hz.

The variability of the data is high at high frequencies (400-950 Hz) during September, as indicated by the standard deviation and the spread of the data (the difference between the 10^{th} and the 90^{th} percentiles). The skewness is positive from 25-400 Hz, which corresponds with the frequency range for which the monthly mean noise is greater than the monthly median noise. Likewise, the skewness is negative from 630-950 Hz, which corresponds with the frequency range for which the monthly median noise is greater than the monthly mean noise. The kurtosis

is high from 50-100 Hz, peaking at 100 Hz. The coherence time is maximum from 200-950 Hz, ranging from 10 hours at 200 Hz to 33 hours at 950 Hz.

10.3 Fourteen Month Statistics Summary

The fourteen month mean and median values in each frequency band never differ by more than 0.8 dB. The fourteen month mean noise is greater than the fourteen month median noise from 25-400 Hz, which corresponds with the frequency range of positive skewness. Similarly, the fourteen month median noise is greater than the fourteen month mean noise from 630-950 Hz, which corresponds with the frequency range of negative skewness. The skewness peaks at 100 Hz and is zero (Gaussian skewness) near 500 Hz.

The standard deviation is least at 100 Hz but increases at lower and higher frequencies. The kurtosis peaks at 100 Hz but is nearly 3 (Gaussian kurtosis) from 630-950 Hz. The coherence time is minimum at 100 Hz. The coherence time is less than 4 hours in shipping bands (25-400 Hz), but it is greater than 14 hours in weather bands (630-950 Hz).

The 25 Hz and 200 Hz bands match a Rayleigh PDF while the 50 Hz and 100 Hz bands match a Chi-Square PDF for the entire fourteen month period. In each case the first three moments of the PDFs match. None of the eight bands studied matches a Gaussian PDF, but interpolation between the 400 Hz and 630 Hz bands suggests that a band centered at 500 Hz would have come closest, having a skewness near 0 and a kurtosis near 3. The 50, 100, and 200 Hz bands approximately match a 1st order Gauss-Markov process, but, as already noted, none of these bands is actually Gaussian.

The fluctuation spectrum of each fourteen month time series is computed in order to see how variability is spread over long and short time scales. At low frequencies in the shipping band (25-400 Hz), most of the variability is in time scales near 10 hours. In the higher frequency bands dominated by weather processes (630-950 Hz), most of the variability is in time scales near 100 hours. The higher frequency bands still show variability near 10 hours, but more of the variance energy starts shifting to longer time scales as long period weather processes start to dominate short period shipping processes. All frequency bands show variability near a one-year period.

The 25 Hz band has a strong peak in its fluctuation spectrum at a period of 8 hours. This 8 hour cycle does not appear to be caused by shipping or weather, and is worthy of future research.

10.4 Threshold Crossing Statistics Summary

The frequency band of 900-1000 Hz is analyzed for shipping statistics. The estimate of ships per day is largest (3.0 to 4.5 ships/day) during the good weather months of May through August of 2004. The smallest estimate (about 1.5 ships per day) is observed during the hurricane month of September 2004.

The estimated average time between ships is about 9.1 hours for the entire data set, but it ranges from a minimum value of 5.7 hours during the calm month of August 2004 (ships are plenty) to a maximum value of 14.2 hours during the hurricane month of September 2004 (ships are few).

The estimated average ship duration (time above threshold) is about 39 minutes for the six hour average method and about 62 minutes for the 90^{th} percentile method.

10.5 Coherence Summary

The spatial coherence between three hydrophones is analyzed for hydrophone separations of 2.29, 2.56 and 4.84 km over a ten month period. The correlation coefficient is computed for each of the eight frequency band time series for each hydrophone separation. In each case the correlation coefficient is always greater than 0.7. The correlation coefficient is generally fairly high (0.85 to 0.93) at 25 Hz, decreases in the region 100-200 Hz, and then increases again in the region 400-1000 Hz. In general, the closer the hydrophone spacing, the higher the degree of correlation between the two time series. The ambient noise field is highly spatially coherent out to a distance of at least 4.84 km, the largest hydrophone separation available in this data set.

The frequency coherence is computed at one site over the entire fourteen month period in order to investigate how changes in one part of the frequency spectrum are temporally correlated with those in other frequency regions. Each of the eight 1/3-octave time series is compared to the others, and the regions where the correlation coefficient is greater than 0.5 are determined.

On average, the data in a 1/3-octave time series at a particular center frequency are highly correlated with neighboring time series ranging from about 2 octaves below to 2 octaves above the center frequency.

10.6 Day vs. Night Summary

Four months representative of the four seasons are analyzed for day versus night ambient noise comparisons. There is not a significant diurnal variability observed in this data set. The mean day and night ambient noise values never differ by more than 1.7 dB in the eight frequency bands studied.

10.7 Current Research

During the writing of this dissertation, the author and another NAVOCEANO employee started working on a process to automate the task of detecting and classifying several ambient noise sources in the EARS data from this data set [Orlin and Snyder, 2007]. In particular, the high correlation of EARS noise levels in the higher frequency bands with the nearby NDBC weather buoy data, especially during extreme wind and wave conditions, suggests that the periods with extreme weather should be relatively easy to identify (see Appendix D). Also, it seemed possible to further develop the work done in Chapter 6, where threshold crossing statistics are used to estimate monthly shipping statistics. A technique has been designed to look for peaks in multiple frequency bands. If a peak is identified in multiple frequency bands at the same time and it has the right characteristics, it is designated a ship.

The goal is to identify and classify these noise sources: nearby ships and significant weather events. Once these sources have been identified, they can be removed from the data set. This allows the shipping and weather statistics for a geographical region to be estimated from the acoustic data alone. This also allows an estimation of the baseline ambient noise for a region: the remaining background noise in an area after nearby shipping and high sea-state weather periods have been removed.

The method has been used successfully on one month of acoustic data from site A6[2] during January 2005 [Snyder and Orlin, 2007]. A total of 84 nearby ships were detected in 31 days, or an average of 2.71 ships per day. The average ship duration was 1.33 hours with an average time between ships of 8.55 hours (Figure 10.1). A total of 6 significant[3] weather events were detected. The average weather event duration was 2.59 days with an average time between weather events of 5.40 days.

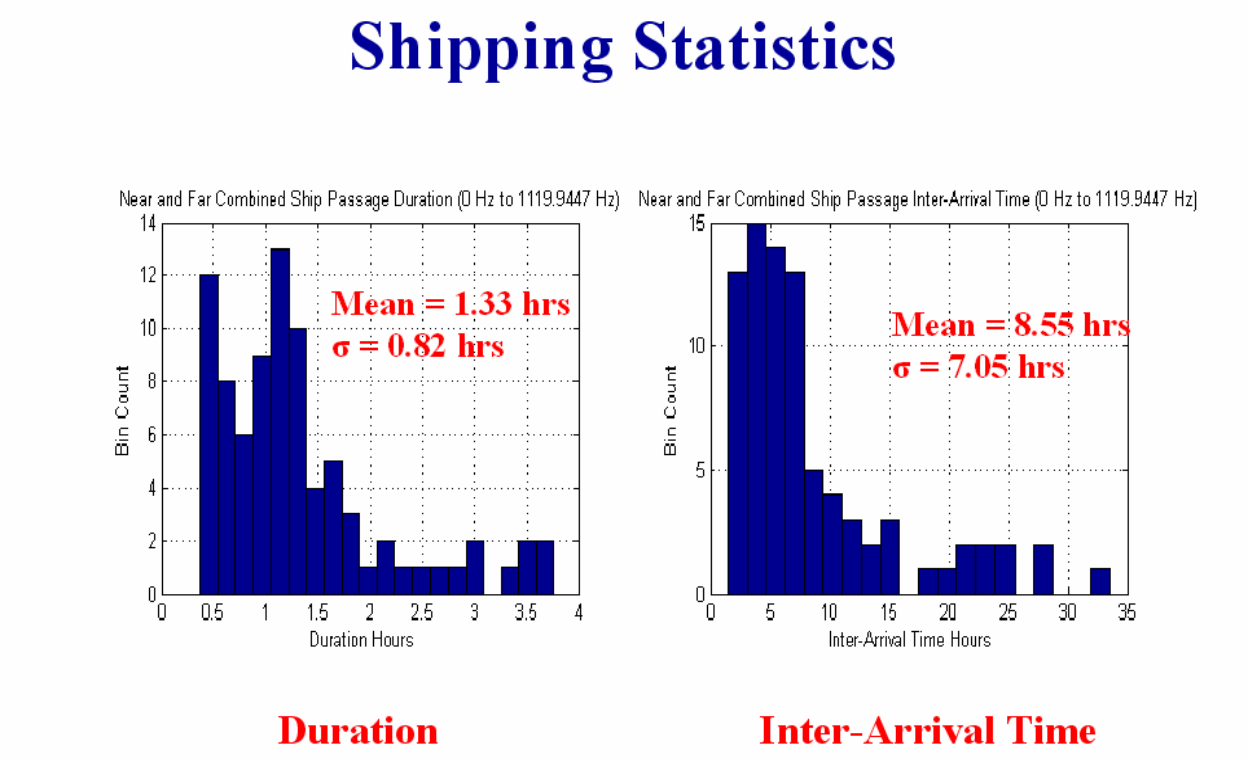

Figure 10.1 Shipping statistics for January 2005.

Periods containing shipping traffic as well as significant weather events are marked and removed from the data, and the first four moments of each resulting PDF are computed. This enables the values for the mean, standard deviation, skewness and kurtosis to be compared for the following 4 cases:

[2] The noise fields at sites A1 and A6 are very similar. Figures A.10 (January 2005 Spectrogram at A1) and C.10 (January 2005 Power at 950 Hz at A1) are very similar to the results obtained at site A6.
[3] Significant weather corresponds to time periods for which the wind speed is greater than 15 knots and/or the significant wave heights are greater than 1.5 meters. Figure D.10 shows the January 2005 Significant Wave Heights.

1) all of the data.

2) data with nearby shipping removed.

3) data with significant weather periods removed.

4) data with nearby shipping and significant weather periods removed.

The results are shown in Table 10.1. All of the effects listed are based on an average over eight 1/3-octave bands from 25-1000 Hz, except as noted in footnotes 4 and 5.

Noise Source	Effect on mean	Effect on standard deviation	Effect on skewness	Effect on kurtosis
Nearby shipping	+0.60 dB	+0.39 dB	+0.35	+0.89
Significant weather	-0.63 dB[4] +1.39 dB[5]	-0.32 dB	-0.26	+0.13
Nearby shipping and sig. weather	+1.78 dB	+0.61 dB	+0.13	+0.15

Table 10.1 Noise source effect on statistics

Additionally, the time series in the 50 Hz and 1000 Hz bands are compared for all four cases to see what effect the removal of different noise sources has on the correlation coefficient between a shipping band time series (50Hz) and a weather band time series (1000 Hz). The results are shown in Table 10.2.

Data set	Correlation Coefficient between 50 Hz and 1000 Hz	Comments
All data	0.14	2 bands have very little in common.
Data with nearby ships removed.	0.03	2 bands have nearby ships in common, but little else.
Data with significant weather removed.	0.37	2 bands have very little in common during sig. weather.
Data with nearby ships and significant weather removed.	0.15	2 bands correlate about the same when nearby ships and sig. weather are removed.

Table 10. 2 Noise source effect on correlation coefficient between 50 Hz and 1000 Hz

[4] This average is computed over 25-200 Hz.
[5] This average is computed over 400-1000 Hz.

Figure 10.2 shows the mean ambient noise for all 4 cases. Figure 10.3 shows the standard deviation for all 4 cases, while Figures 10.4 and 10.5 show the skewness and kurtosis, respectively, for all 4 cases. In each of these figures, the blue curve represents case 1 (all the data). The red curve represents case 2 (data with nearby shipping removed). The green curve represents case 3 (data with significant weather periods removed). The black curve represents case 4 (data with nearby shipping and significant weather periods removed).

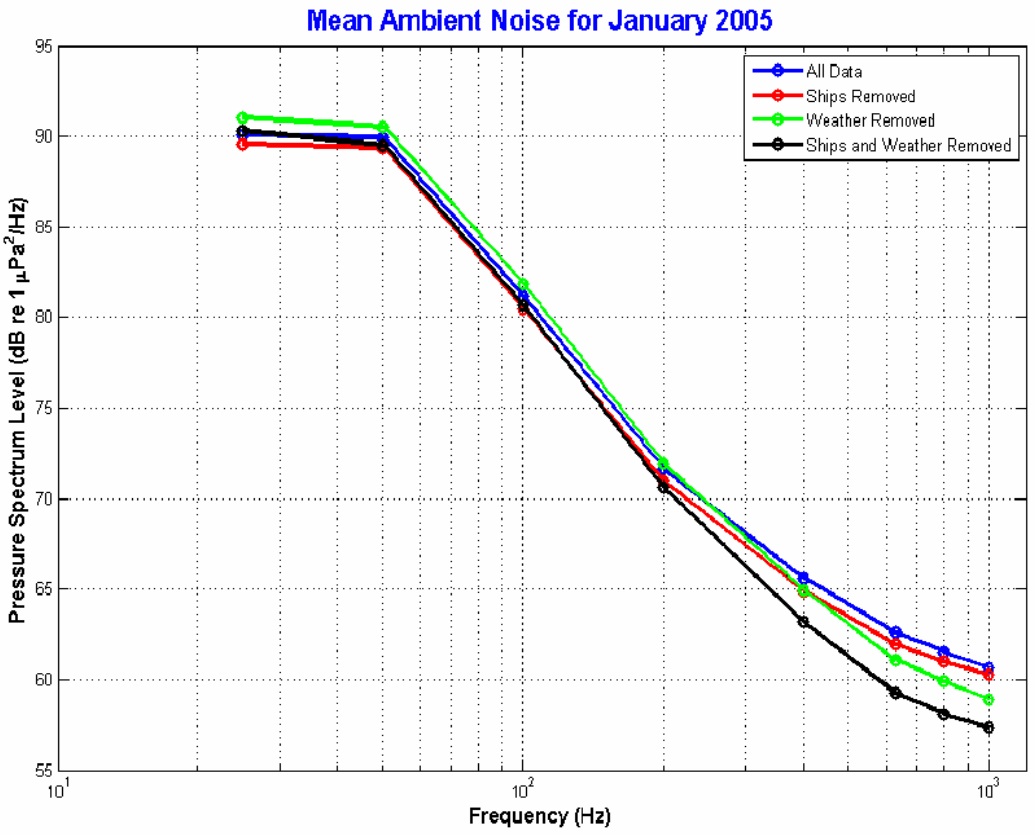

Figure 10.2 Mean ambient noise for January 2005.

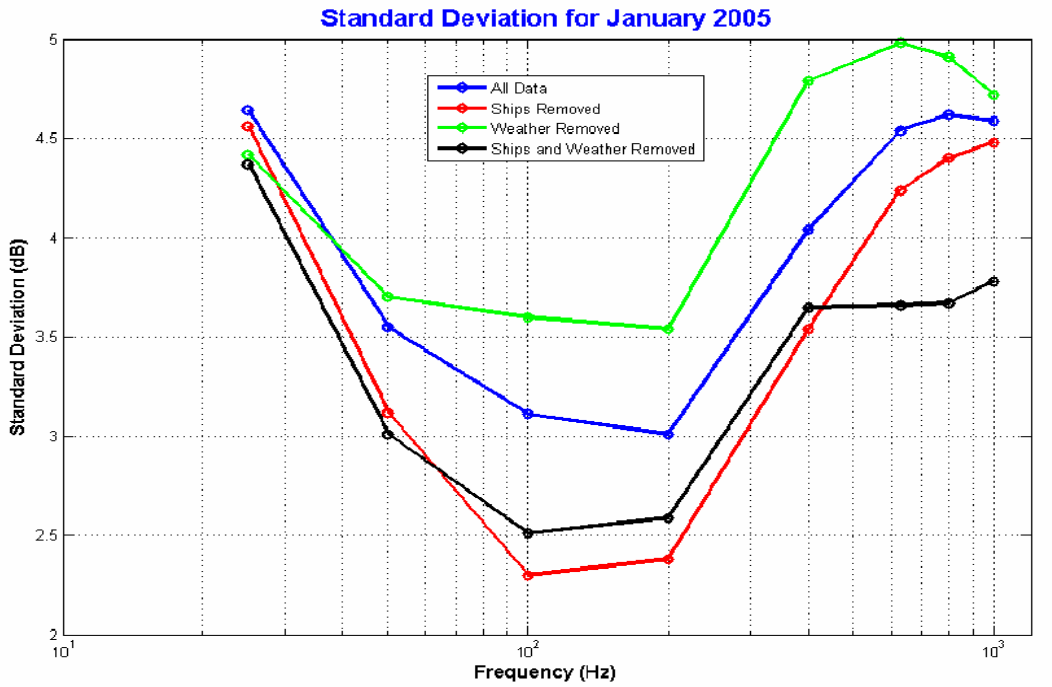

Figure 10.3 Standard deviation for January 2005.

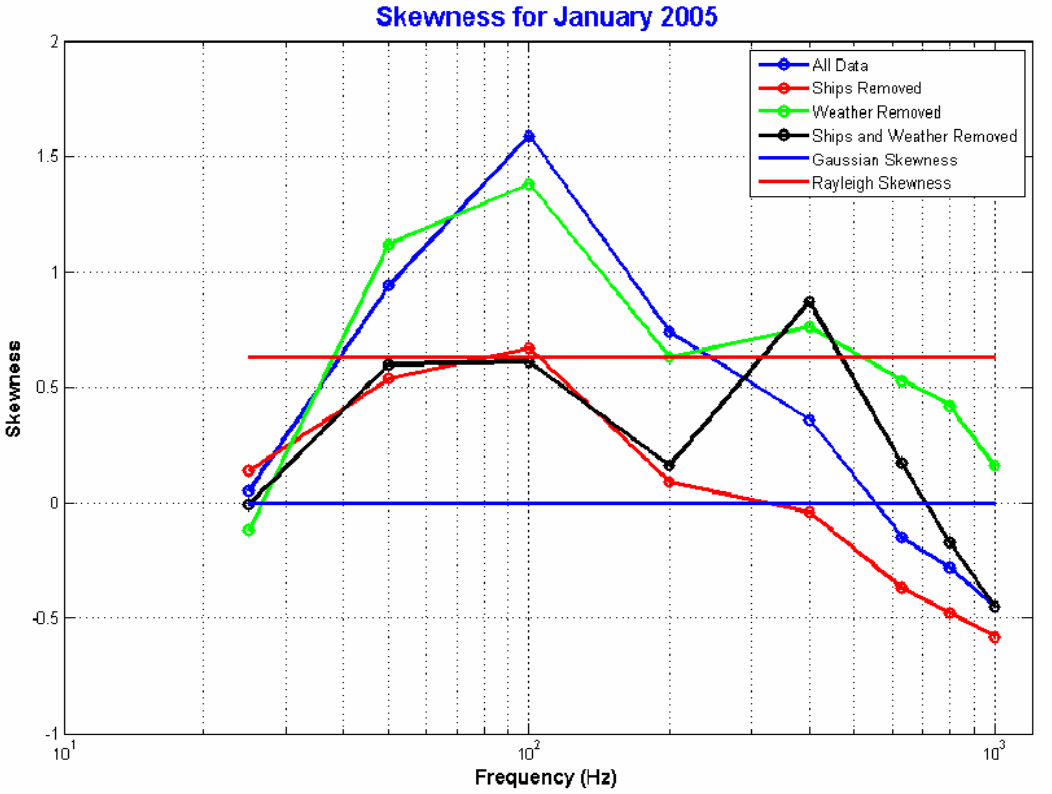

Figure 10.4 Skewness for January 2005.

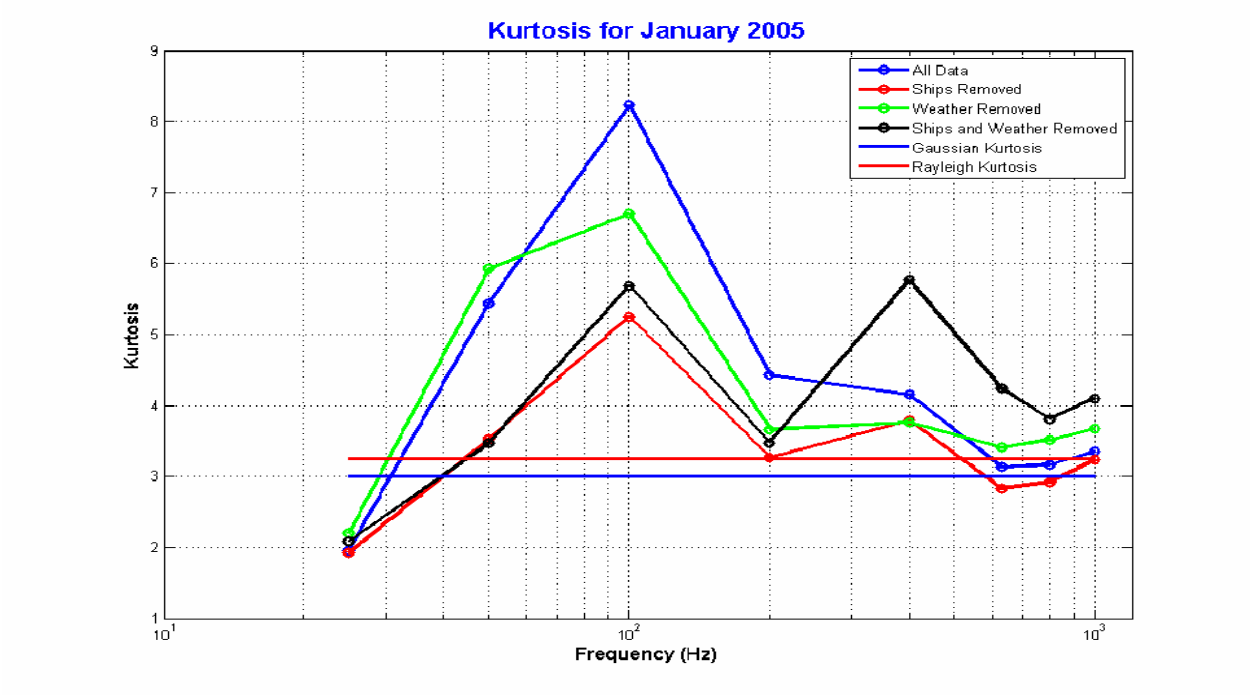

Figure 10.5 Kurtosis for January 2005.

Case 2 results: after nearby shipping traffic is removed, 85.3% of the original data remain. Since ships show up in time series as short duration spikes, removing them decreases all four moments. The mean decreases in all 8 bands, by an average amount of 0.60 dB. The decrease in the mean noise is almost constant with respect to frequency, ranging from 0.43 dB at 1000 Hz to 0.72 dB at 400 Hz. The standard deviation decreases in all 8 bands, by an average amount of 0.39 dB. The largest decreases in standard deviation are in the 50 – 400 Hz bands. Skewness decreases by an average amount of 0.35. (All bands show a decrease except for 25 Hz which shows a slight increase.) The largest decreases in skewness are in the 50 – 400 Hz bands. The kurtosis decreases in all 8 bands, by an average amount of 0.89. The largest decreases in kurtosis are in the 50 – 200 Hz bands.

Case 3 results: after removing significant weather but not shipping traffic, 55.0% of the original data remain. As compared to case 1, the mean actually increases from 25-200 Hz by an average amount of 0.63 dB but decreases from 400-1000 Hz by an average amount of 1.39 dB. Standard deviation increases by an average 0.32 dB. (All bands show an increase except for 25 Hz.) Skewness increases by an average amount of 0.26. (Three bands show a decrease while five bands show an increase. The biggest increases in skewness occur from 400-1000 Hz.)

Kurtosis decreases by an average amount of 0.13. (Three bands show a decrease while five bands show an increase. The biggest decreases in kurtosis occur from 100-200 Hz.)

Case 4 results: after nearby shipping traffic and significant weather are removed, 40.3% of the original data remain. The mean decreases by an average amount of 1.78 dB. (All bands show a decrease except for 25 Hz which shows a slight increase.) The largest decreases in mean noise are in the 400 – 1000 Hz bands. The standard deviation decreases in all 8 bands, by an average amount of 0.61 dB. The largest decreases in standard deviation are in the 630 – 1000 Hz bands. Skewness decreases by an average amount of 0.13. (Skewness decreases from 25 - 200 Hz but increases from 400 – 800 Hz, while 1000 Hz is unchanged.) The kurtosis decreases by an average amount of 0.15. (Three bands show a decrease while five bands show an increase. The biggest decreases in kurtosis occur from 50-100 Hz.)

Figure 10.6 shows a comparison of the average power in the 50 Hz and 1000 Hz bands during the time period of 21-31 January 2005. Also displayed are the monthly mean values at 50 Hz and 1000 Hz. Significant weather events occur between days 22-23.5 and between days 27.5-29. Note that during the periods of high sea-states, the noise levels at high frequencies are

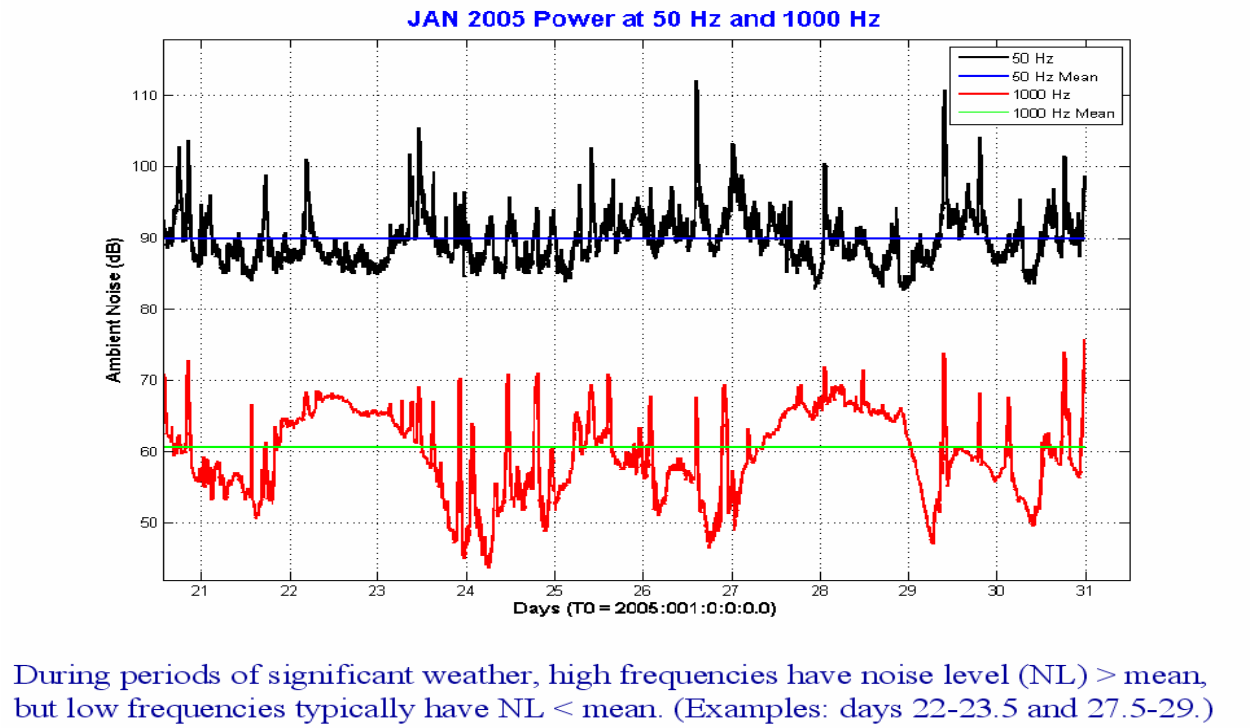

Figure 10.6 Average power at 50 Hz and 1000 Hz during January 2005.

driven high above their monthly mean value, while the noise levels at low frequencies are typically lower than their monthly mean value. Thus, when significant weather periods are removed from the data (case 3), low decibel values (below average) are removed at low frequencies while high dB values (above average) are removed at high frequencies. This explains the green curve in Figure 10.2, which shows the mean noise increasing from 25-200 Hz but decreasing from 400-1000 Hz after the significant weather periods are removed.

This effect can also be seen in Figures 10.7 and 10.8, which show the histograms for all 4 cases for 50 Hz and 1000 Hz, respectively. Note that when high sea-state periods are removed from the data (the green histograms or PDFs in both Figures), low dB values are removed at 50 Hz (the mean increased by 0.59 dB) while high dB values are removed at 1000 Hz (the mean decreased by 1.78 dB).

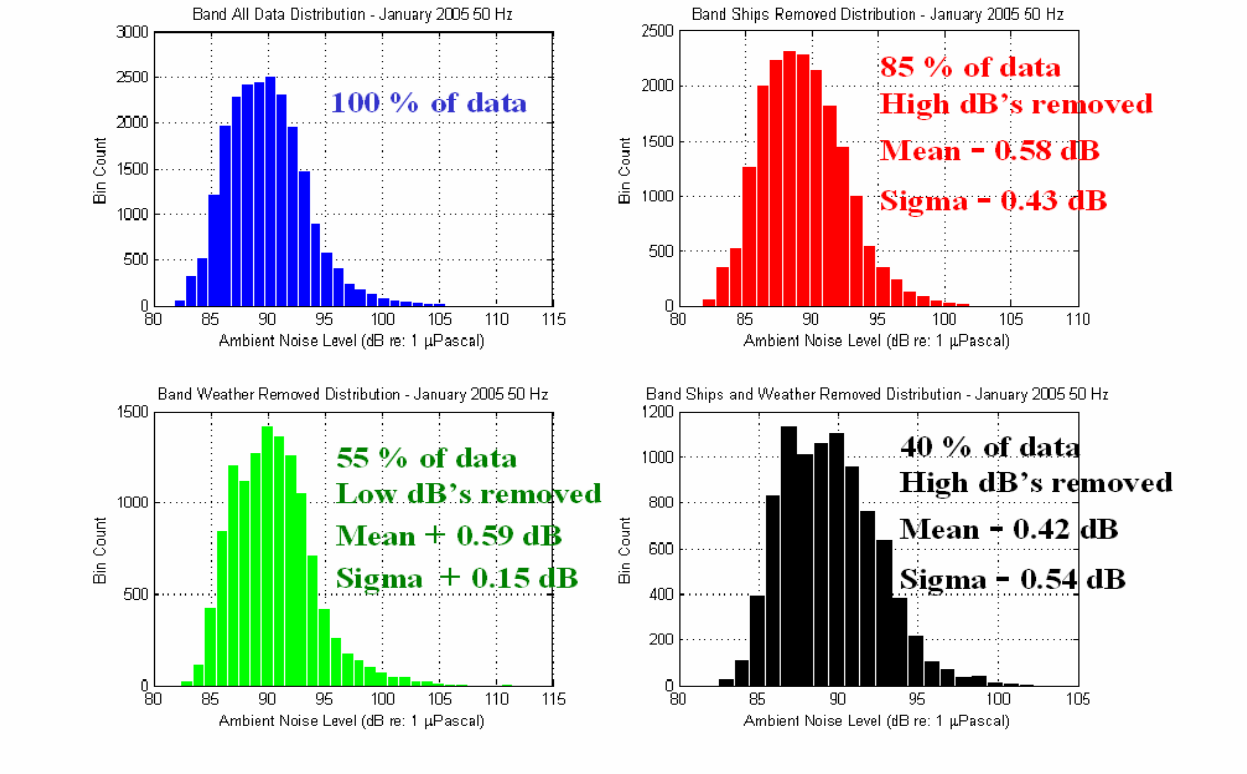

Figure 10.7 Histograms at 50 Hz for all 4 cases.

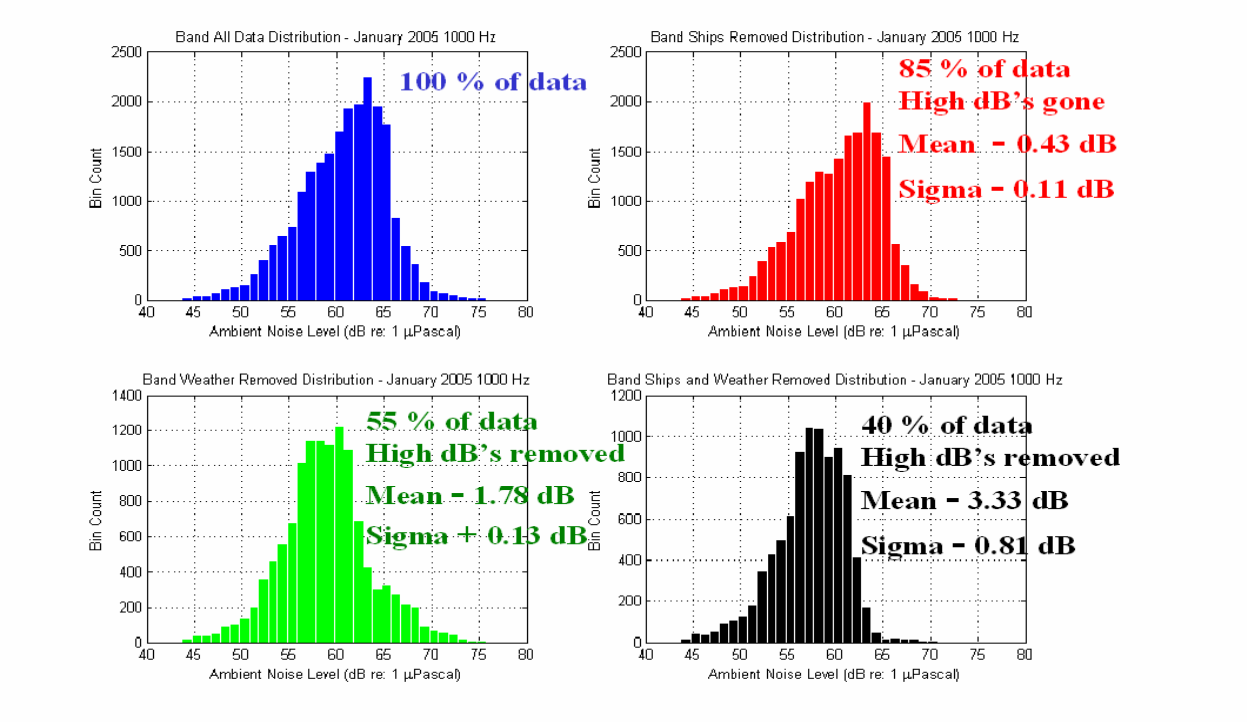

Figure 10.8 Histograms at 1000 Hz for all 4 cases.

This contrasts sharply with case 2 for which the nearby shipping traffic is removed. Figure 10.2 shows the mean noise levels when nearby ships are removed (red curve) just slightly below the mean noise levels for all the data (blue curve). As was mentioned previously, the "ships removed" mean level is on average 0.60 dB below the "all data" mean level.

The histograms for case 2 (the red histograms or PDFs in Figures 10.7 and 10.8) show the same result. When the nearby ships are removed from the data, high dB values are removed at all frequencies. The mean level decreases by 0.58 dB at 50 Hz and by 0.43 dB at 1000 Hz.

Case 4 represents the ambient noise baseline for January 2005: the minimum expected noise for this region in the Gulf of Mexico when nearby shipping and significant weather periods have been removed. Figure 10.2 (black curve) shows the mean noise decreasing from 50-1000 Hz when shipping and weather have been removed, with the largest decrease from 400-1000 Hz. The histograms for case 4 (the black histograms or PDFs in Figures 10.7 and 10.8) show the same result. When ships and significant weather are removed, the mean level decreases by 0.42 dB at 50 Hz but by 3.33 dB at 1000 Hz.

These results can be nicely summarized by plotting 4 sets of cumulative exceedance probability (CEP)[6] curves for each frequency band. The CEP for a given frequency band and a specific case 1-4 is related to the corresponding histogram (PDF) as follows: the integral of the PDF is the cumulative distribution function (CDF), then the CEP = 1 – CDF. The CEP displays the probability that the noise level in any 1/3-octave band will exceed any given threshold.

Figures 10.9 and 10.10 show the CEP for 50 Hz and 1000 Hz, respectively, for all 4 cases. The median values (50% probability) are also given on each figure. Figure 10.9 shows that the noise level at 50 Hz will exceed 80 dB 100% of the time for all 4 cases, while it will never get louder than 115 dB. But the median value for case 1 (all data) is 89.66 dB, meaning the noise level will exceed 89.66 dB 50% of the time. The median value for case 4 (ships and weather removed) is 89.29 dB.

Figure 10.10 shows that removing significant weather periods has a much greater impact at 1000 Hz than it does at 50 Hz. The median level decreases from 61.28 dB (all data) to 57.69 dB (ships and weather removed).

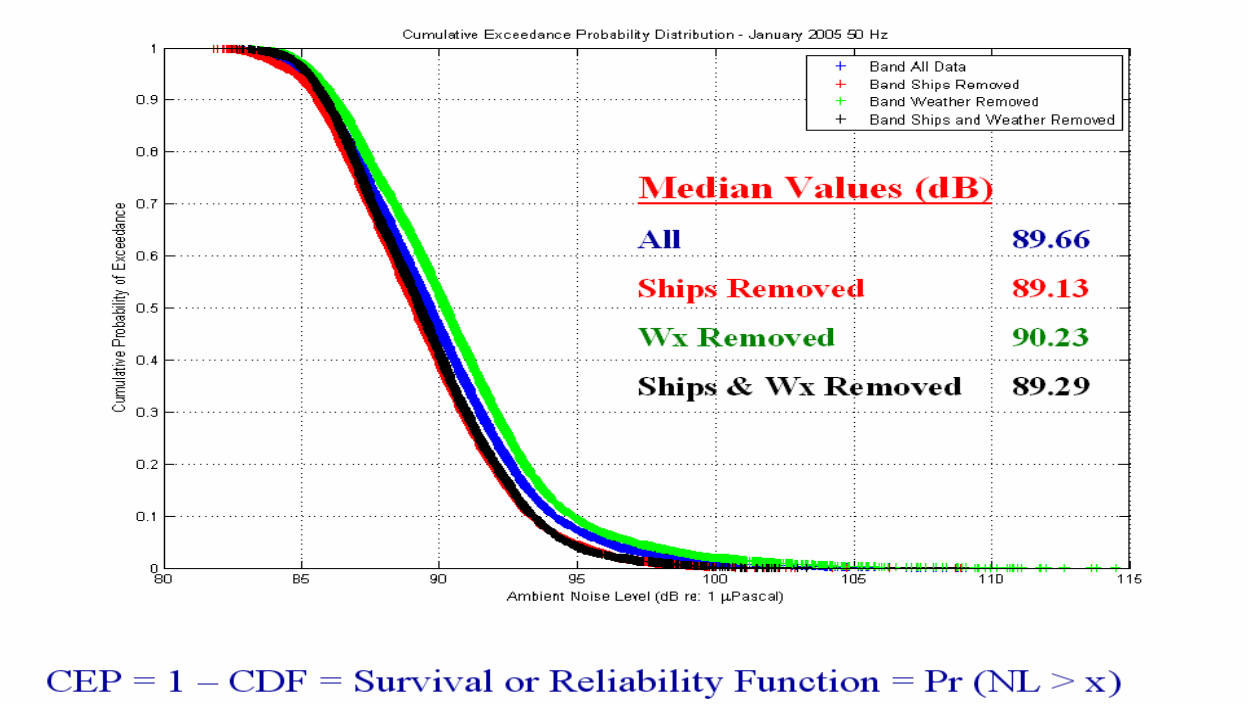

Figure 10.9 Cumulative exceedance probability at 50 Hz for January 2005.

[6] Some authors call the CEP the *survival* or the *reliability* function.

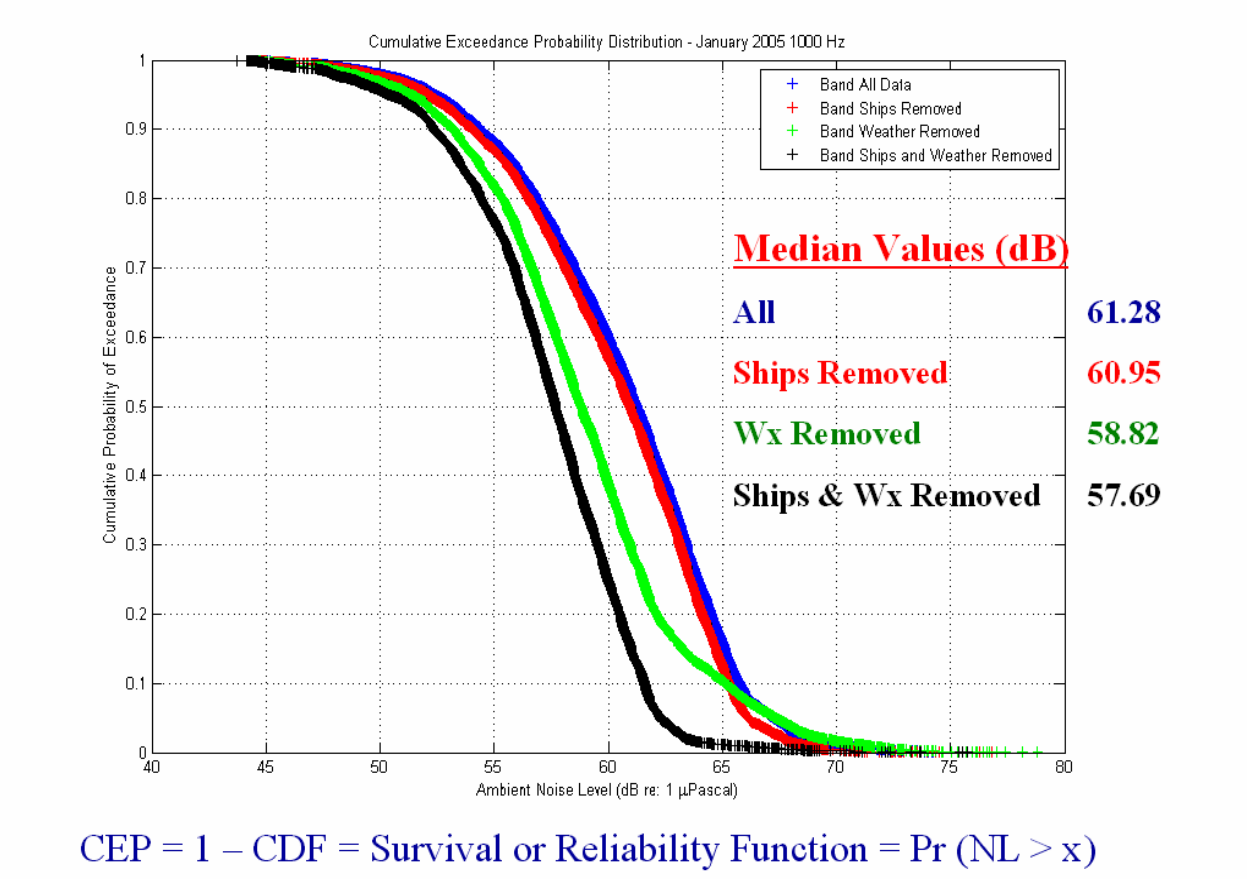

Figure 10.10 Cumulative exceedance probability at 1000 Hz for January 2005.

10.8 Ambient Noise Model

The results of this dissertation can be used to parameterize a proposed ambient noise model for this region in the Gulf of Mexico. The two dominant noise sources in the EARS frequency band are noise due to surface shipping and weather. For each of the eight 1/3-octave bands in the bandwidth of 10 Hz to 1000 Hz, assume the noise can be written as the sum of four noise processes (all functions of time and frequency):

$$TN(t,f) = DS(t,f) \oplus NS(t,f) \oplus W(t,f) \oplus B(t,f) \qquad \text{Equation 10.1}$$

$TN(t,f)$ = Total Noise time series in 1/3-octave band centered at frequency f (slowly varying time series with additive spikes due to nearby ships)

DS(t,f) = Distant Shipping noise time series in 1/3-octave band centered at frequency f

NS(t,f) = Nearby Shipping noise time series in 1/3-octave band centered at frequency f (time series containing short duration spikes)

W(t,f) = Weather noise time series in 1/3-octave band centered at frequency f

B(t,f) = Background noise time series in 1/3-octave band centered at frequency f

$\oplus$ denotes a power summation (necessary because all terms are expressed in dB)

All of the above noise processes have units of dB re 1 $\mu Pa^2/Hz$.

All of the noise processes are slowly varying except for the nearby shipping noise *NS(t,f)*. This is a time series which is usually zero, but can be modeled as the sum of delta-like functions. The nearby shipping noise time series *NS(t,f)* affects all eight frequency bands; it is never negligible. However, it is usually zero, except for a total of approximately 1.5 to 4.5 non-contiguous, one hour segments per day, on average.[7]

The distant shipping noise time series *DS(t,f)* dominates the low frequency bands (typically 50-200 Hz). In these bands, the weather noise time series *W(t,f)* is usually negligible. The distant shipping noise process typically has a peak period near 10-12 hours, as can be seen in the distribution of variance plots for 50, 100, and 200 Hz (Figures 5.15 through 5.17).

The weather noise time series *W(t,f)* dominates the high frequency bands (typically 630-1000 Hz). In these bands, the distant shipping noise time series *DS(t,f)* is usually negligible. The weather noise process typically has a longer period than the distant shipping noise process, but it depends on the weather. Low sea states cause *W(t,f)* to have a short period, while high sea states cause *W(t,f)* to have a long period. The weather noise process typically has peak periods near both 10 hours and again near 100 hours, as can be seen in the distribution of variance plots for 630, 800, and 950 Hz (Figures 5.19 through 5.21).

[7] On average, about 1.5 to 4.5 nearby ships were detected by the EARS buoy each day, with each ship having an estimated duration of about an hour.

There also appears to be a noise process with a period of about one year that affects all eight frequency bands, which can be seen in Figures 5.14 through 5.21.

The data in a 1/3-octave time series at a particular center frequency should be highly correlated with neighboring time series ranging from about 2 octaves below to 2 octaves above the center frequency.

The background noise time series *B(t,f)* is included to capture any noise sources not due to shipping or weather. In particular, it is needed at 25 Hz which has a noise source with a period near 8 hours, as can be seen in the distribution of variance plot for 25 Hz (Figure 5.14). This noise does not appear to be due to shipping or weather. It was present year-round but was strongest in the winter months of November through February, when the PDFs at 25 Hz were actually bimodal. It is postulated that this noise is produced by oil rig drilling activity to the west of the EARS buoys.

If the noise model is correct, some of the noise source parameters can be estimated. In particular, the mean and variance of the nearby shipping noise, the distant shipping noise and the weather noise can be estimated in special cases. Two results from statistics are useful here [Li, 1999]:

1) The mean of the sum of two or more random variables is the sum of the mean values of the random variables.
2) The variance of the sum of uncorrelated random variables is the sum of the variances.

For the proposed noise model, result 2) can be written as

$$\sigma_{TN}^2 = \sigma_{DS}^2 + \sigma_{NS}^2 + \sigma_W^2 + \sigma_B^2 \qquad \text{Equation 10.2}$$

For example, in a low frequency shipping band where both *B(t,f)* and *W(t,f)* are negligible, Equation 10.1 becomes $TN(t,f) = DS(t,f) \oplus NS(t,f)$

In terms of mean values, this becomes $\mu_{TN} = \mu_{DS} \oplus \mu_{NS}$

Equation 10.2 becomes $\sigma_{TN}^2 = \sigma_{DS}^2 + \sigma_{NS}^2$

In a high frequency weather band where both *B(t,f)* and *DS(t,f)* are negligible, Equation 10.1 becomes $TN(t,f) = NS(t,f) \oplus W(t,f)$

In terms of mean values, this becomes $\mu_{TN} = \mu_{NS} \oplus \mu_W$

Equation 10.2 becomes $\sigma_{TN}^2 = \sigma_{NS}^2 + \sigma_W^2$

The results of section 10.7 can be used here. The total noise field *TN(t,f)* corresponds to case 1 (all data). Case 2 (nearby ships removed) was also evaluated, so the values for the mean and the variance when nearby ships are removed is known. This allows the computation of the average noise level due to nearby shipping and the standard deviation due to nearby shipping at both 50 Hz and 1000 Hz for January 2005. The results are shown in Tables 10.3 and 10.4.

Frequency (Hz)	Mean TN (dB)	Mean DS (dB)	Mean NS (dB)	Mean W (dB)
50	89.94	89.36	80.91	NA
1000	60.68	NA	50.42	60.25

Table 10.3 Mean noise levels at 50 Hz and 1000 Hz.

Frequency (Hz)	Sigma TN (dB)	Sigma DS (dB)	Sigma NS (dB)	Sigma W (dB)
50	3.55	3.12	1.69	NA
1000	4.59	NA	1.00	4.48

Table 10.4 Standard deviations at 50 Hz and 1000 Hz.

Table 10.4 was calculated using Equation 10.2. Table 10.3 was calculated using Figure 10.11, which shows a power sum graph.[8]

[8] This graph shows how two noise sources (both expressed in dB) can be combined to find the sum in dB. The amount (in dB) to add to the higher level is given by $10*\log(1 + 10^{-x/10})$, where x is the positive difference (in dB) between the 2 levels [NAVOCEANO, 1999].

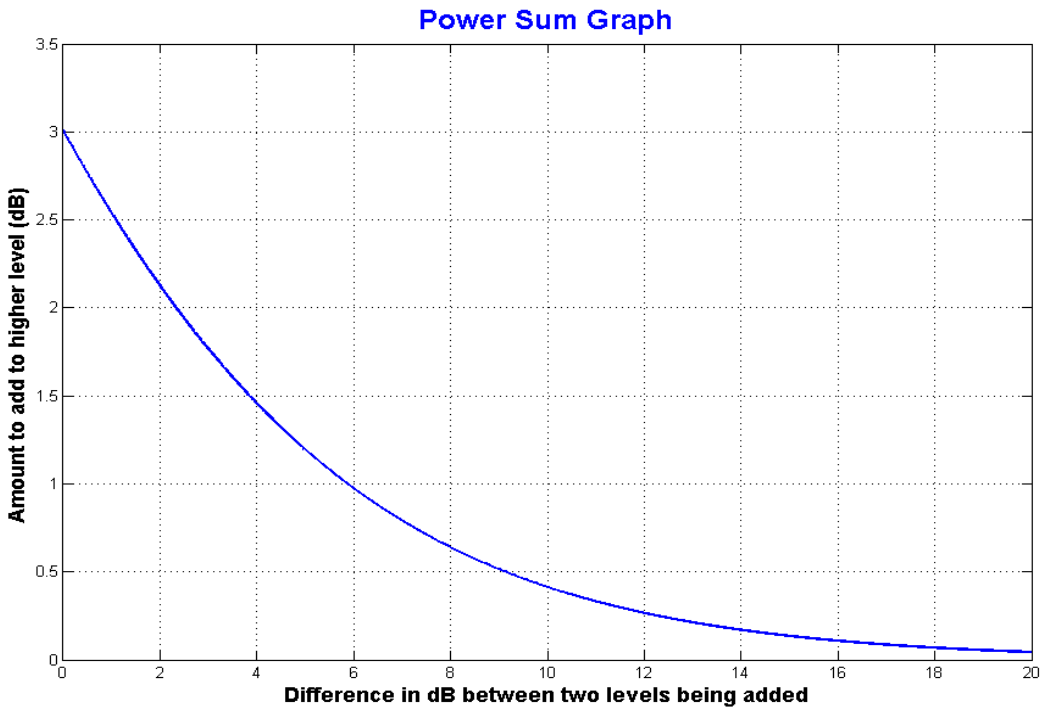

Figure 10.11 Power sum graph.

10.9 Future Work

In order to properly characterize the ambient noise in an area, long-term continuous data sets are necessary. Long-term data are needed to capture the complete variability including the seasonal and annual trends. Continuous data sets are needed to observe the ordered statistics such as coherence time and diurnal variability. Threshold crossing statistics, which can be used to analyze shipping and weather patterns for an area including duration and inter-arrival time, also require continuous data.

It would be very useful to be able to collect more long-term, continuous ambient noise data in the Gulf of Mexico. This fourteen month data set is a good start, but an even longer recording period would shed more light on the long-term trends. It would also be a good idea to collocate any future ambient noise buoys with weather buoys. This would allow that portion of the ambient noise field due to the weather to be determined very accurately.

In this dissertation, frequencies in the band 10 – 1000 Hz are analyzed. Information at frequencies above 1000 Hz would be of great interest. Also, of the eight 1/3-octave bands analyzed here, two of the bands need further investigation.

The 8 hour period present in the 25 Hz 1/3-octave band power spectrum deserves more attention. It was present year-round but was strongest in the winter months of November through February, when the PDFs at 25 Hz were bimodal. It is postulated that this noise is produced by oil rig drilling activity to the west of the EARS buoys. Some ambient noise measurements made in the vicinity of the oil rigs would be enlightening.

Also, the 100 Hz 1/3-octave band is very interesting. For the entire fourteen month period, the 100 Hz band has minimum standard deviation, minimum coherence time and minimum spatial coherence. But it has maximum skewness and maximum kurtosis. It would be of great value to see if this pattern is specific to this region of the Gulf of Mexico or if it is a fairly common or even universal feature of the ambient noise field.

References

Arase, E. and Arase, T. (1966). "Correlation of Ambient Sea Noise," J. Acoust. Soc. Amer., vol. 40, pp. 205-210.

Arase, T. and Arase, E. (1968). "Deep-Sea Ambient-Noise Statistics," J. Acoust. Soc. Amer., vol. 44, pp. 1679-1684.

Bannister, R. W., Denham, R. N., and Guthrie, K. M. (1979). "Variability of low-frequency ambient sea noise," J. Acoust. Soc. Amer., vol. 65, pp. 1156-1163.

Bracewell, R. (2000). *The Fourier Transform and its Applications*, 3rd Edition, McGraw-Hill.

Brockett, P., Hinich, M. and Wilson, G. (1987). "Nonlinear and Non-Gaussian Ocean Noise," J. Acoust. Soc. Amer., vol. 82, pp. 1386-1394.

Carey, W. M. (1986). "Measurement of down-slope sound propagation from a shallow source to a deep receiver," J. Acoust. Soc. Amer., vol. 79, pp. 49-59.

Dyer, Ira (1970). "Statistics of Sound Propagation in the Ocean," J. Acoust. Soc. Amer., vol. 48, pp. 337-345.

Dyer, Ira (1973). "Statistics of distant shipping noise," J. Acoust. Soc. Amer., vol. 53, pp. 564-570.

Evans, H., Hastings, N., and Peacock, B. (2000). *Statistical Distributions*, 3rd Edition, Wiley-Interscience.

Hall, T., Bradley, M. and Emery, L. (2004). "Software Design Description for the Dynamic Ambient Noise Model (DANM), Version 2.0", PSI Technical Report TRS-313, Planning Systems Incorporated, June.

Jobst, W. and Adams, S. (1977). "Statistical Analysis of Ambient Noise," J. Acoust. Soc. Amer., vol. 62, pp. 63-71.

Kinsler, L., Frey, A., Coppens, A., and Sanders, J. (1982). *Fundamentals of Acoustics*, 3rd Edition, Wiley.

Li, X. Rong (1999). *Probability, Random Signals and Statistics*, CRC Press.

Mathworks (2000). MATLAB Signal Processing Toolbox User's Guide, Mathworks Inc.

McDonald, M. A., Hildebrand, J. A. and Wiggins, S. M. (2006). "Increases in deep ocean ambient noise in the Northeast Pacific west of San Nicolas Island, California," J. Acoust. Soc. Amer., vol. 120, pp. 711-718.

Medwin, H. and Clay, C. (1998). *Fundamentals of Acoustical Oceanography*, Academic Press.

National Data Buoy Center (2007). http://www.ndbc.noaa.gov.

Naval Oceanographic Office (NAVOCEANO 1972). "Environmental-Acoustics Atlas of the Caribbean Sea and Gulf of Mexico, Volumes I and II (Marine Acoustics and Marine Environment)", Special Publications SP-189I and SP-189II, Naval Oceanographic Office, Washington, D.C., August.

Naval Oceanographic Office (NAVOCEANO 1999). "Fleet Oceanographic and Acoustic Reference Manual", Reference Publication RP33, Naval Oceanographic Office, Stennis Space Center, MS, April.

Newcomb, J., Snyder, M., Hillstrom, W. and Goodman, R. (2007). "Measurements of Ambient Noise During Extreme Wind Conditions in the Gulf of Mexico," Oceans 2007 MTS/IEEE Proceedings, October.

Nichols, R. H. and Sayer, C. E. (1977). "Frequency-frequency correlations of ocean ambient noise level," J. Acoust. Soc. Amer., vol. 61(5), pp. 1188-1190.

Orlin, P. and Snyder, M. (2007). "An Heuristic Ocean Ambient Noise Classifier", Pacific Rim Underwater Acoustics Conference Proceedings, October.

Perrone, A. J. (1970). "Ambient Noise Spectrum Levels as a Function of Water Depth," J. Acoust. Soc. Amer., vol. 48, pp. 362-370.

Perrone, A. J., and L. A. King (1975). "Analysis technique for classifying wind- and ship-generated noise characteristics," J. Acoust. Soc. Amer. 58, 1186.

Peterson, A. and Gross, E. (1972). *Handbook of Noise Measurement, 7th Edition*. General Radio Company.

Pflug, L., Thompson, C. and Hall, T. (2004). "Dynamic Ambient Noise Model (DANM) Evaluation Using Port Everglades Data", NRL/FR/7185—04-10,064, Naval Research Laboratory, Stennis Space Center, MS.

Ross, Donald (1987). *Mechanics of Underwater Noise*, Peninsula Publishing.

Shooter, J. A., DeMary, T. E. and Koch, R A. (1982). "Ambient Noise in the Western Gulf of Mexico", Technical Report ARL-TR-82-15, Applied Research Laboratories, University of Texas at Austin, March.

Snyder, M., Orlin, P., Schulte, A. and Newcomb, J. (2003). "Ambient noise analysis of underwater acoustic data," presented at 145th Meeting of the Acoustical Society of America and abstracted in J. Acoust. Soc. Amer. 113(4), p.2320.

Snyder, M., and Orlin, P. (2007). "Ambient Noise Classification in the Gulf of Mexico", Oceans 2007 MTS/IEEE Proceedings, October.

Snyder, M., Orlin, P. and Eller, A. (2007). "Long-Term Ambient Noise Statistics in the Gulf of Mexico", Pacific Rim Underwater Acoustics Conference Proceedings, October.

Stoica, P. and Moses, R. (1997). *Introduction to Spectral Analysis*, Prentice Hall.

U.S. Naval Observatory (2007). http://aa.usno.navy.mil.

Urick, Robert J. (1977). "Models for the amplitude fluctuations of narrow-band signals and noise in the sea," J. Acoust. Soc. Amer., vol. 62, pp. 878-887.

Urick, Robert J. (1982). *Sound Propagation in the Sea*, Peninsula Publishing.

Urick, Robert J. (1983). *Principles of Underwater Sound, 3rd Edition*. McGraw-Hill.

Urick, Robert J. (1984). *Ambient Noise in the Sea*, Naval Sea Systems Command.

Wagstaff, R. A. (1981). "Low Frequency Ambient Noise in the Deep Sound Channel - The Missing Component," J. Acoust. Soc. Amer., vol. 69, pp. 1009-1014.

Wenz, G. M. (1961). "Some Periodic Variations in Low-Frequency Acoustic Ambient Noise Levels in the Ocean," J. Acoust. Soc. Amer., vol. 33, pp. 64-74.

Wenz, G. M. (1962). "Acoustic ambient noise in the ocean: spectra and sources," J. Acoust. Soc. Amer., vol. 34, pp. 1936-1956.

Wenz, G. M. (1972). "Review of Underwater Acoustics Research: Noise," J. Acoust. Soc. Amer., vol. 51, pp. 1010-1024.

Wirsching, Paul H., T. L. Paez, and K. Ortiz (1995). *Random Vibrations: Theory and Practice*, Dover Publications.

Appendix A

Monthly Spectrograms

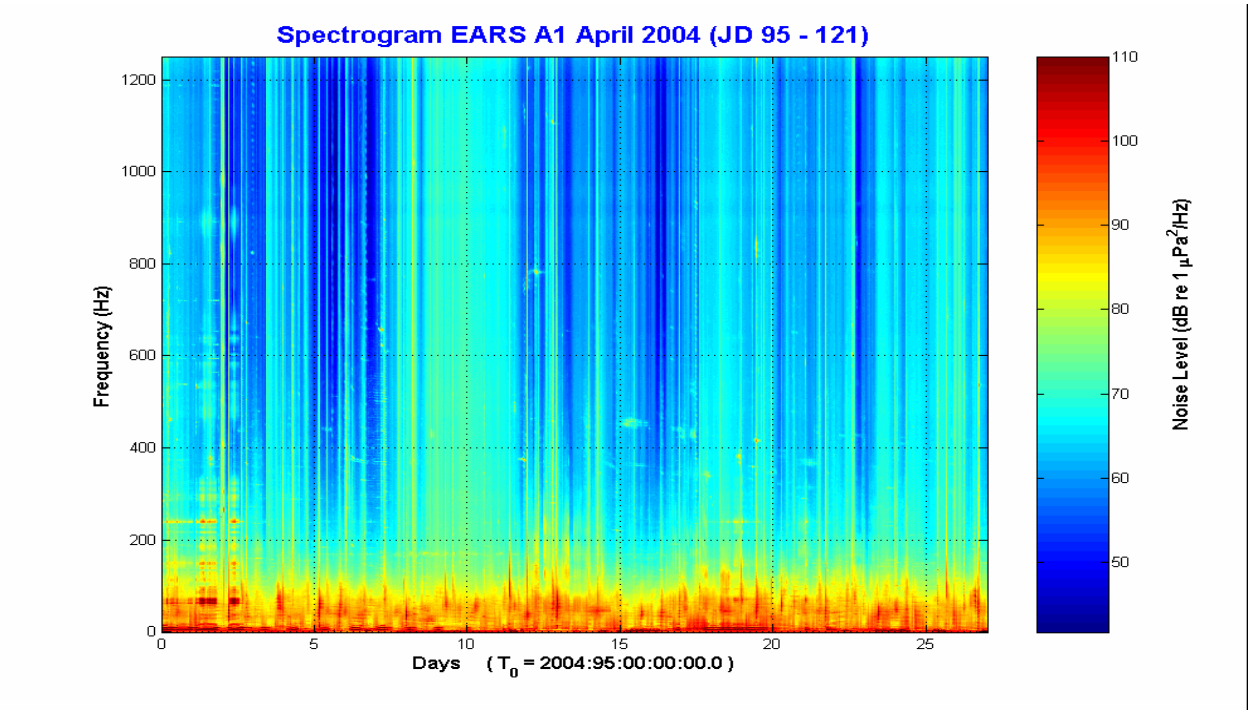

Figure A.1 April 2004 Spectrogram

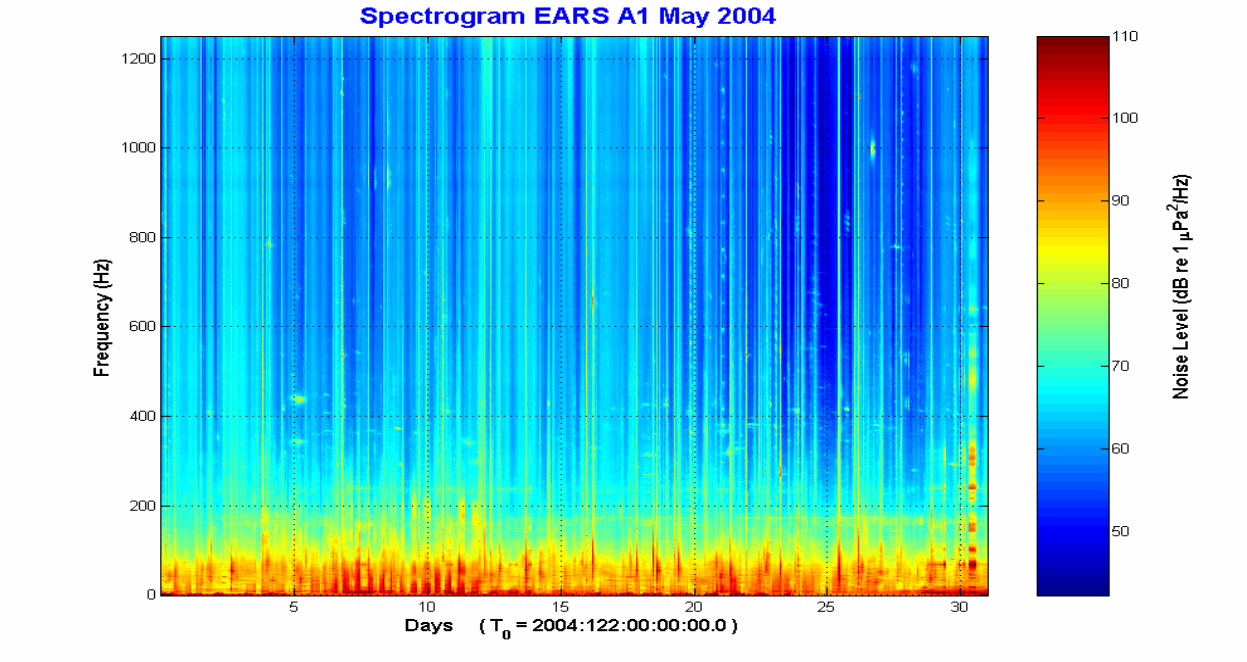

Figure A.2 May 2004 Spectrogram

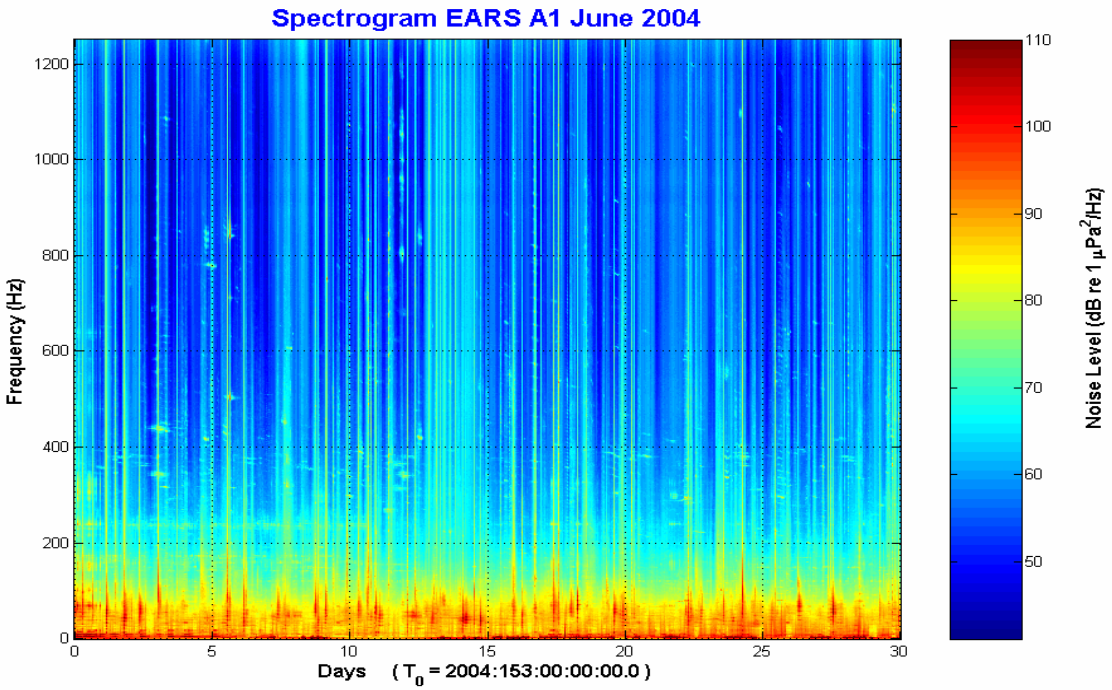

Figure A.3 June 2004 Spectrogram

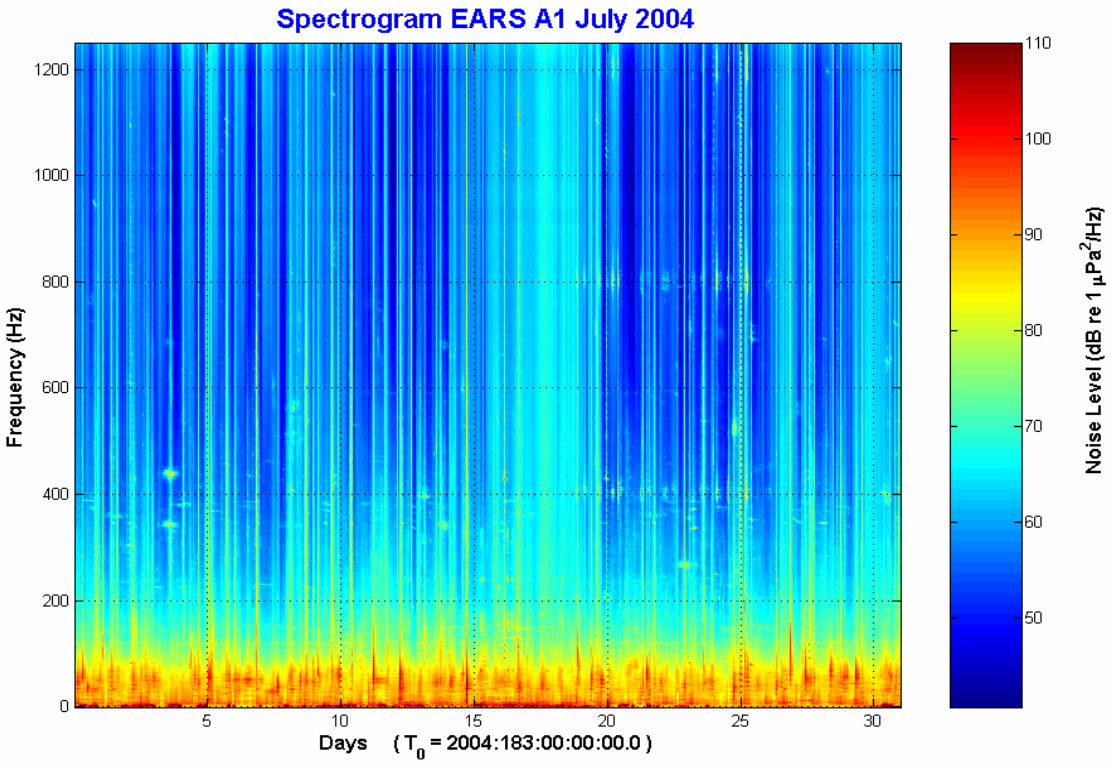

Figure A.4 July 2004 Spectrogram

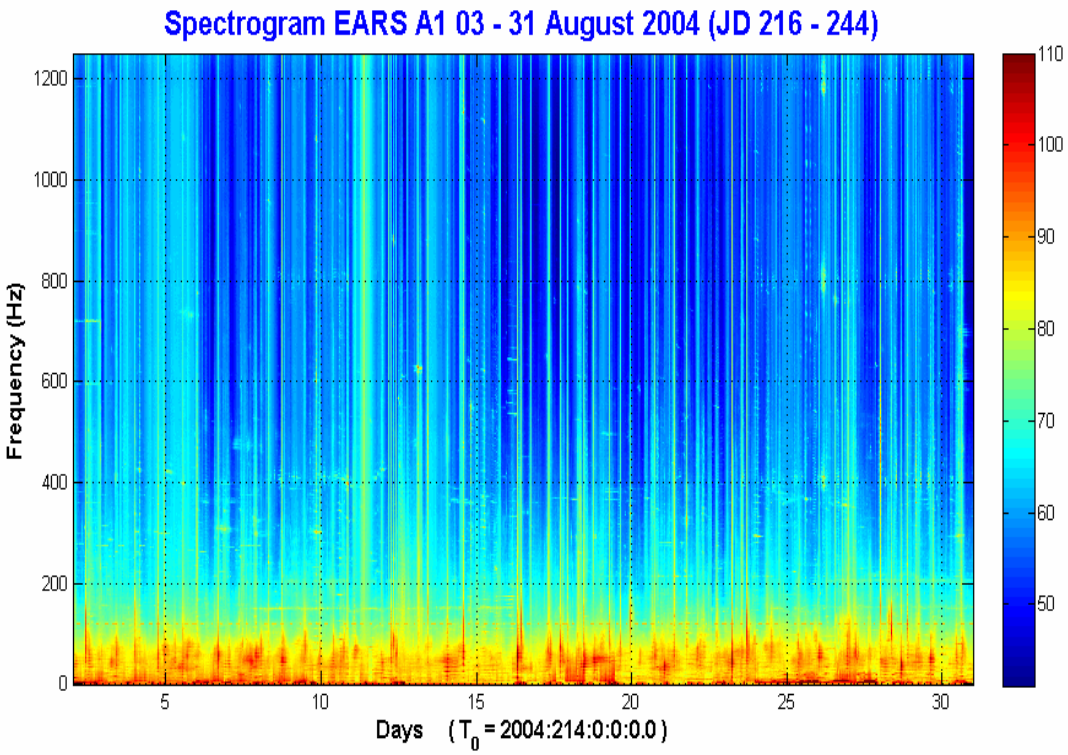

Figure A.5 August 2004 Spectrogram

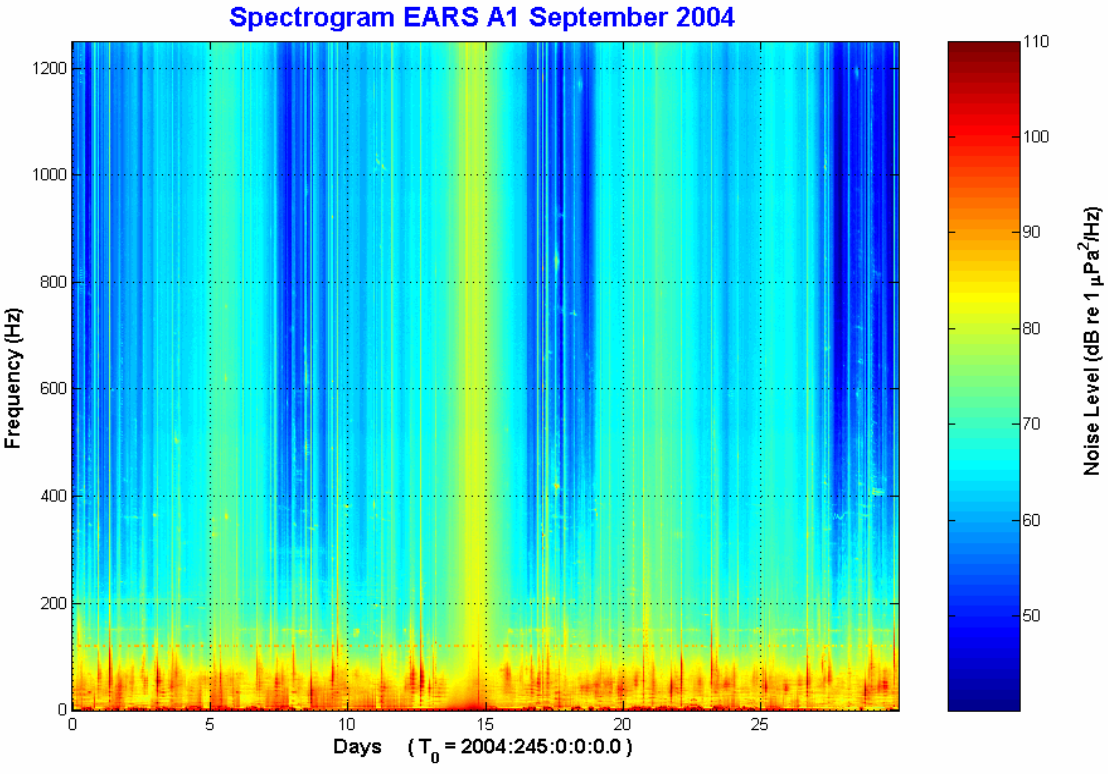

Figure A.6 September 2004 Spectrogram

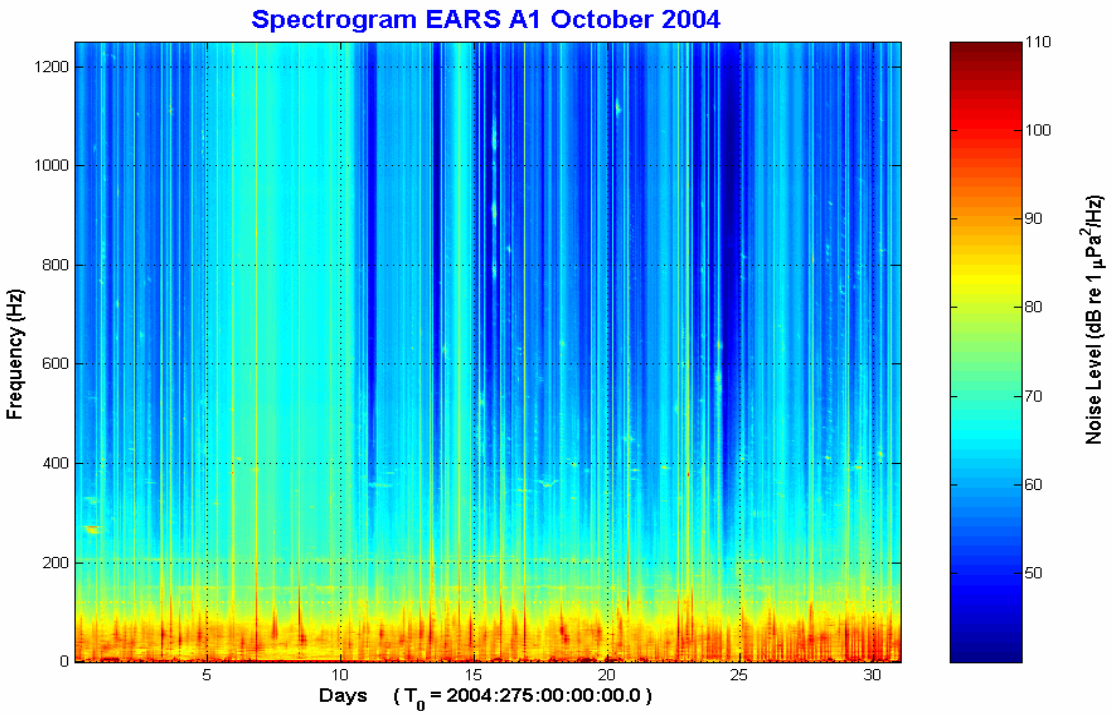

Figure A.7 October 2004 Spectrogram

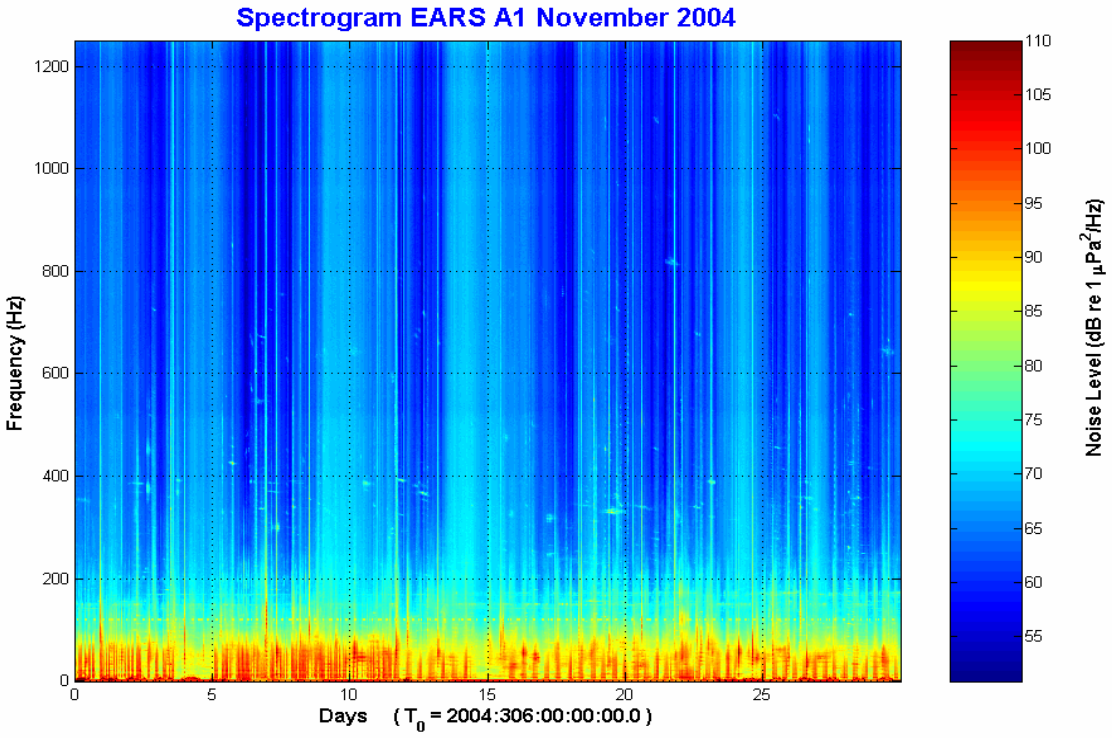

Figure A.8 November 2004 Spectrogram

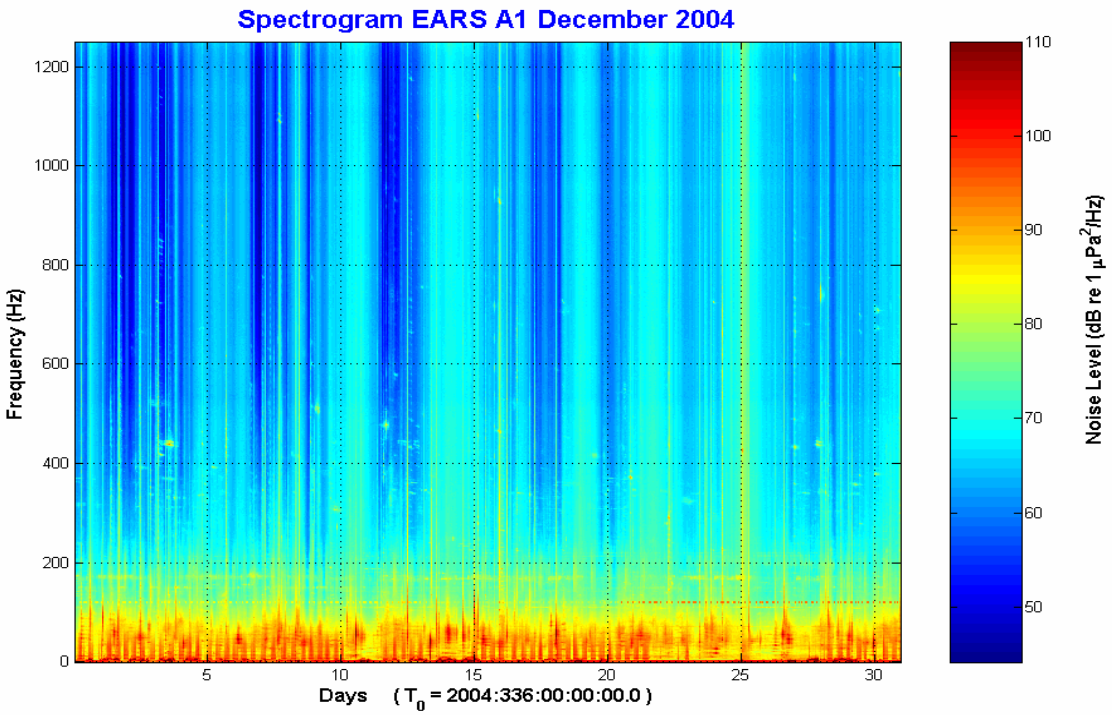

Figure A.9 December 2004 Spectrogram

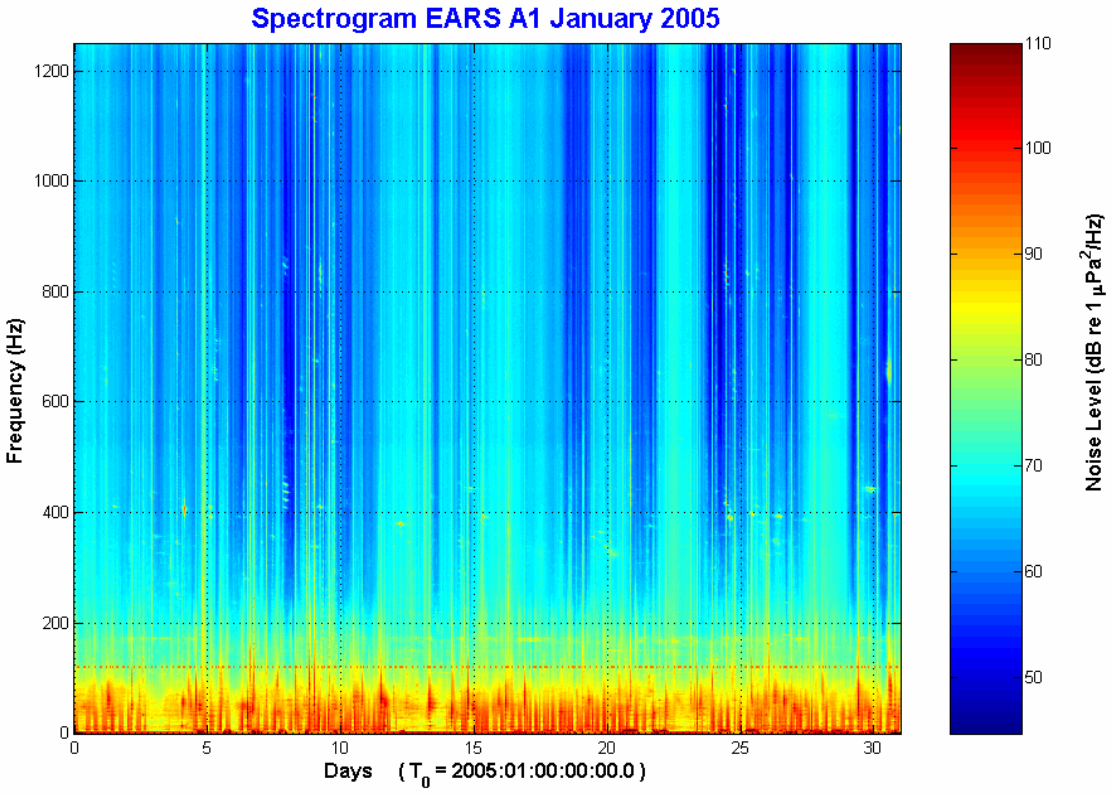

Figure A.10 January 2005 Spectrogram

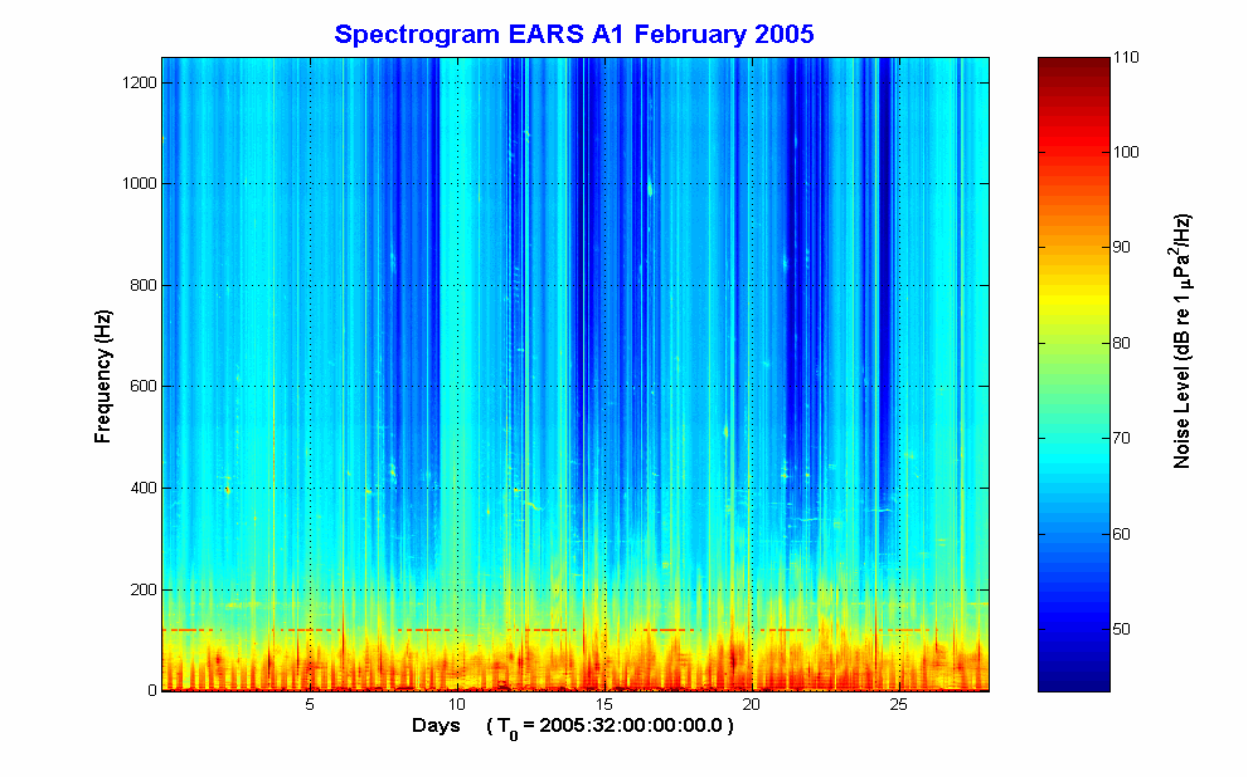

Figure A.11 February 2005 Spectrogram

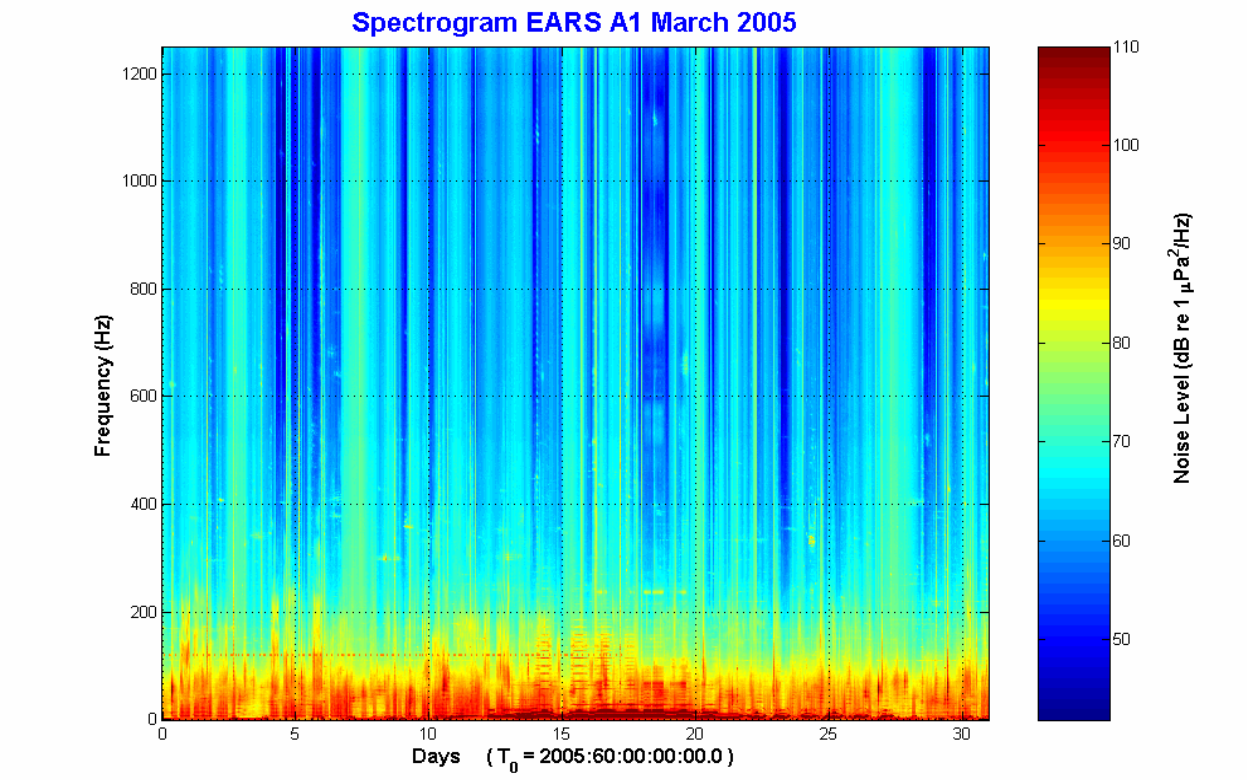

Figure A.12 March 2005 Spectrogram

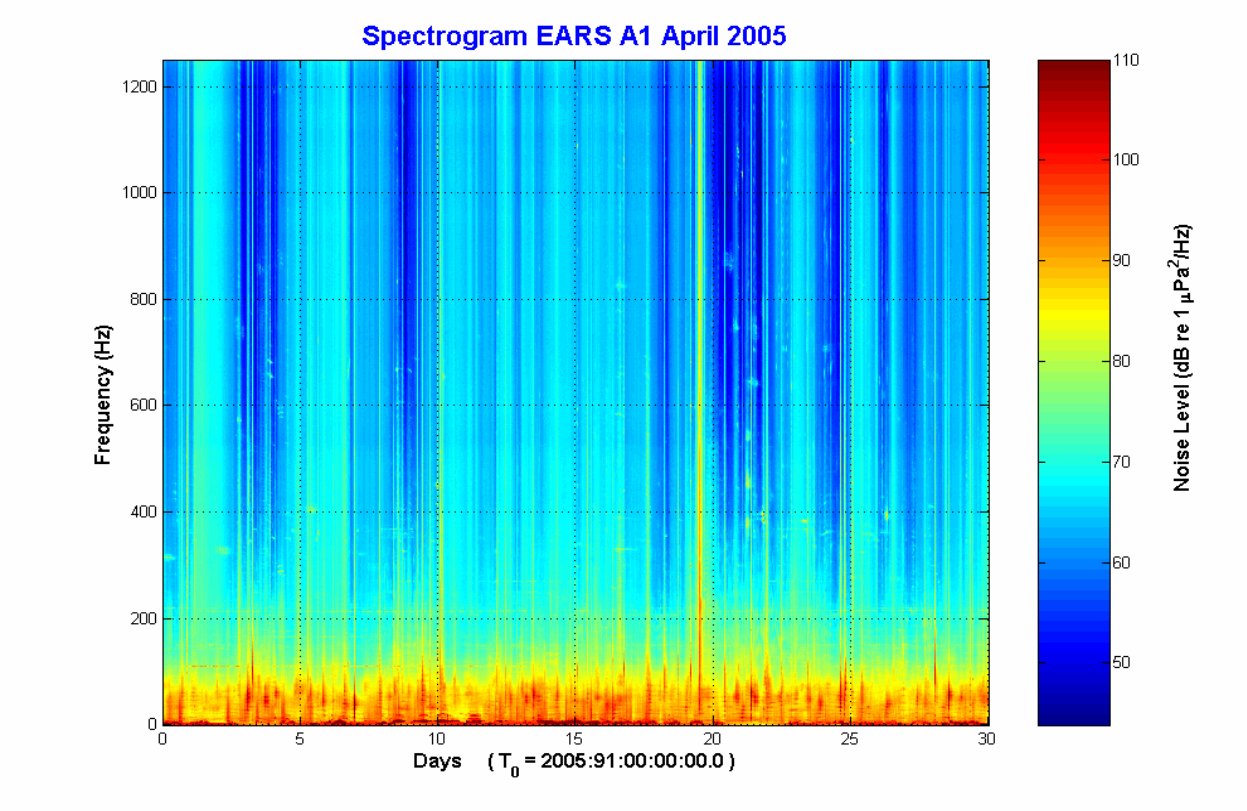

Figure A.13 April 2005 Spectrogram

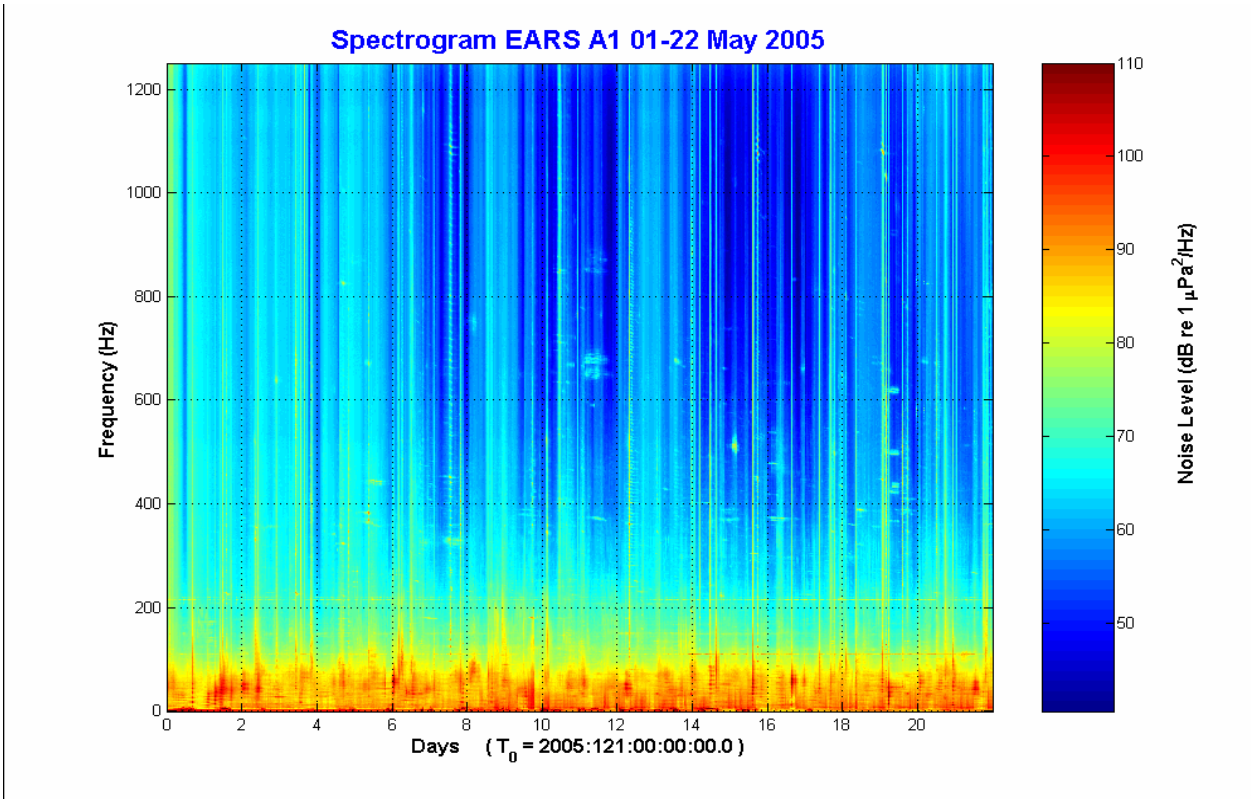

Figure A.14 May 2005 Spectrogram

Appendix B

Monthly Percentile Plots

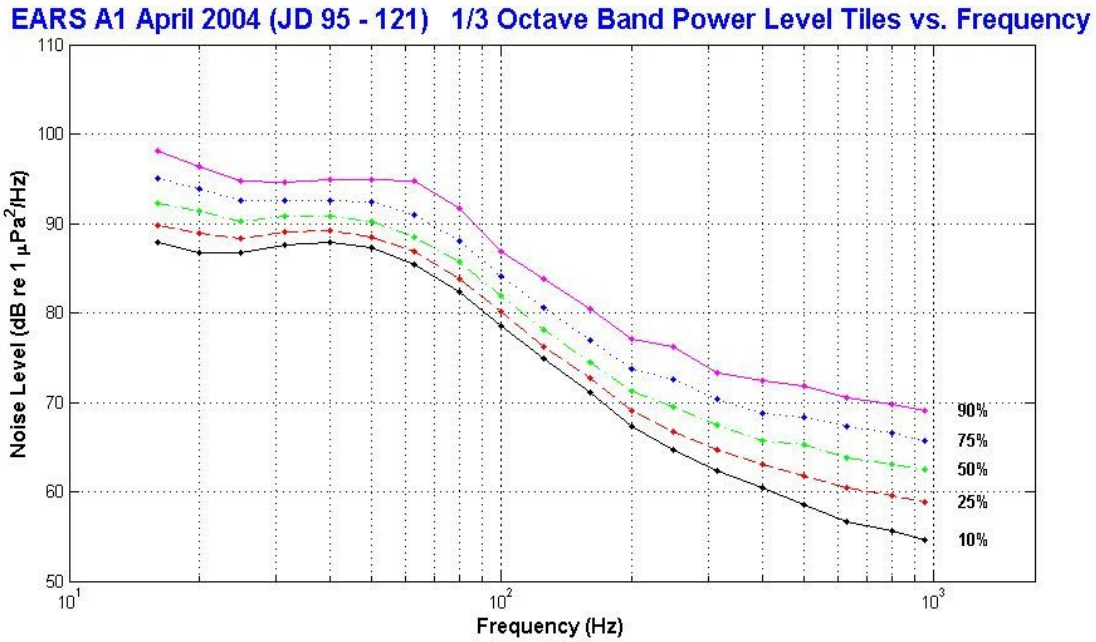

Figure B.1 April 2004 Percentile Plot

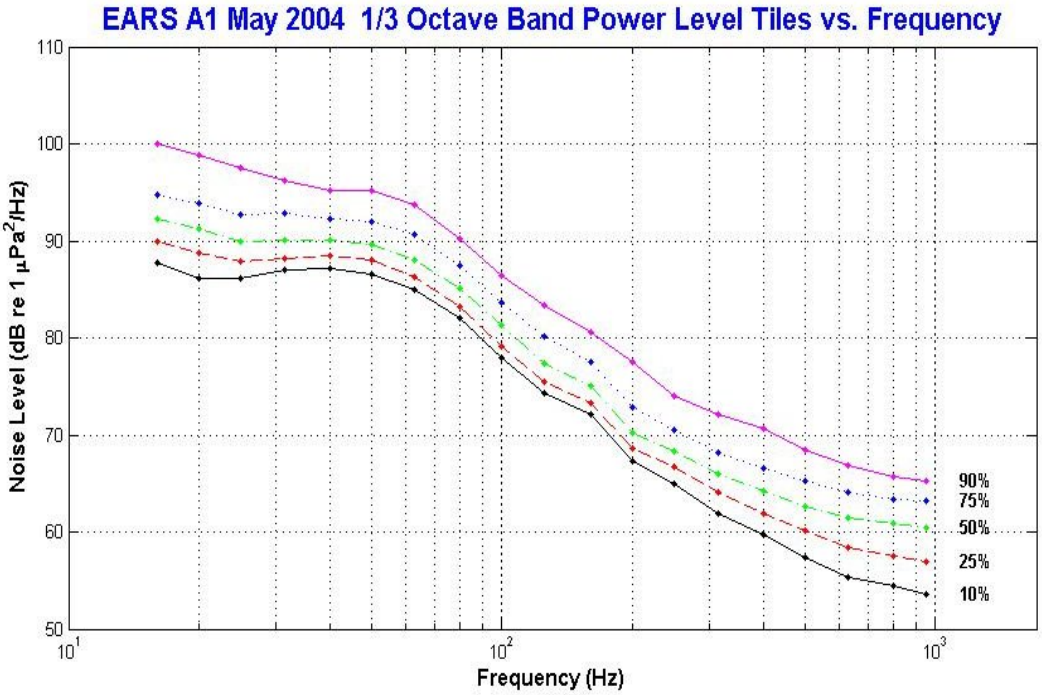

Figure B.2 May 2004 Percentile Plot

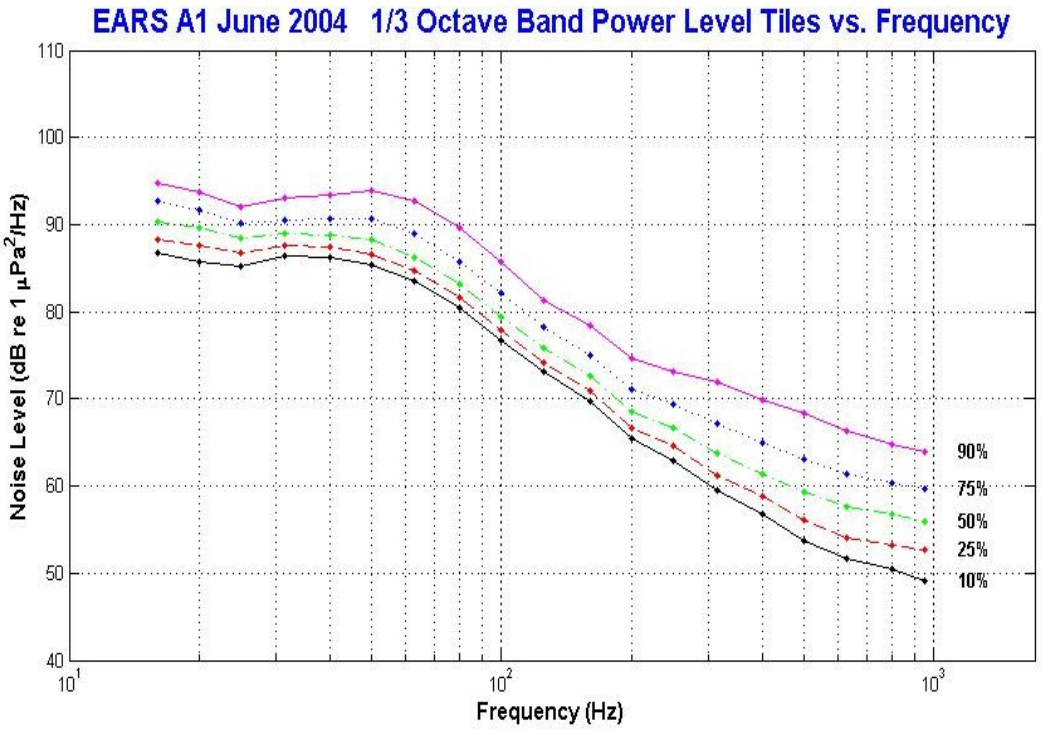

Figure B.3 June 2004 Percentile Plot

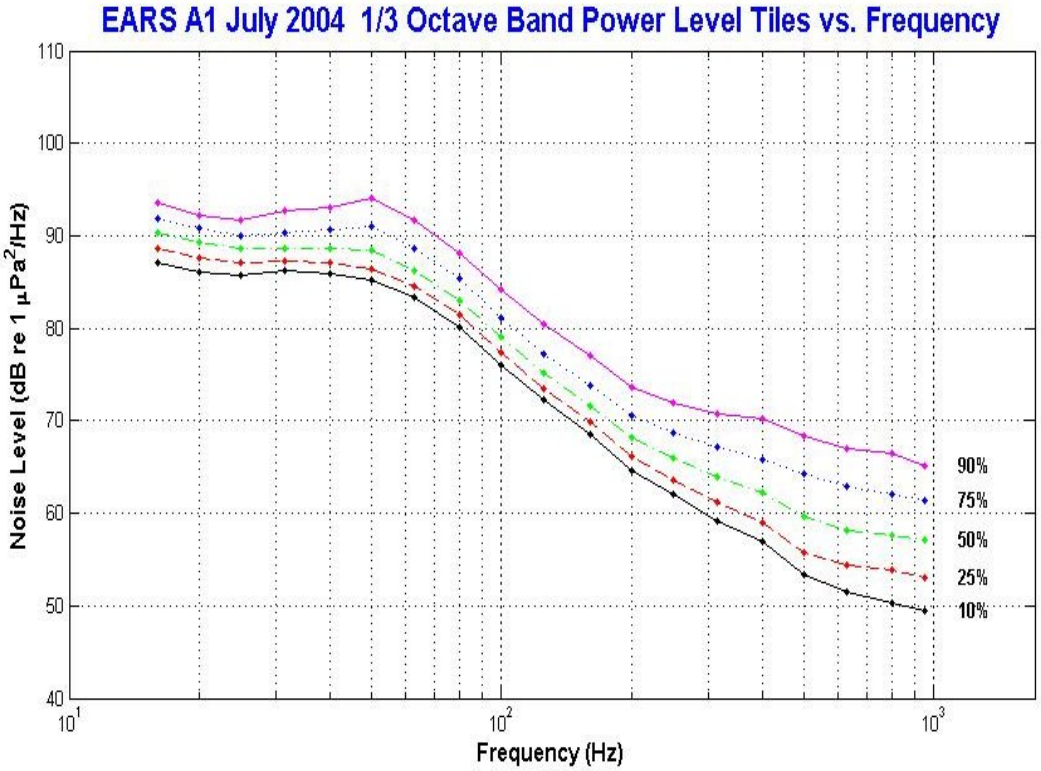

Figure B.4 July 2004 Percentile Plot

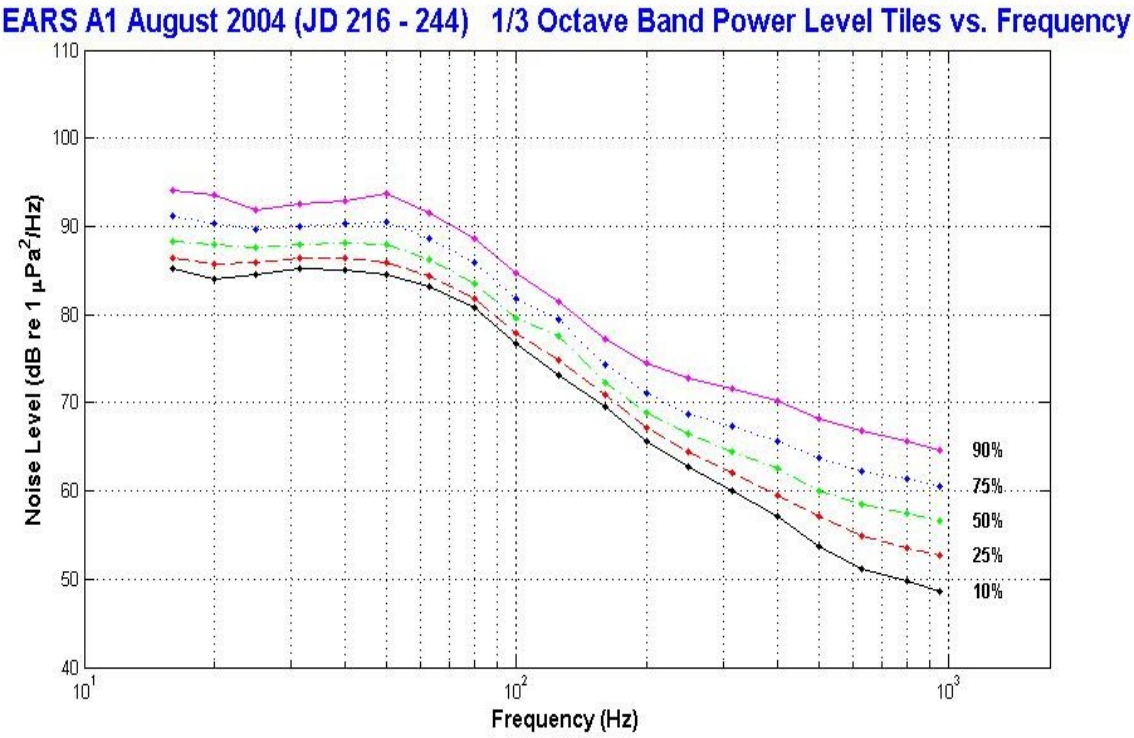

Figure B.5 August 2004 Percentile Plot

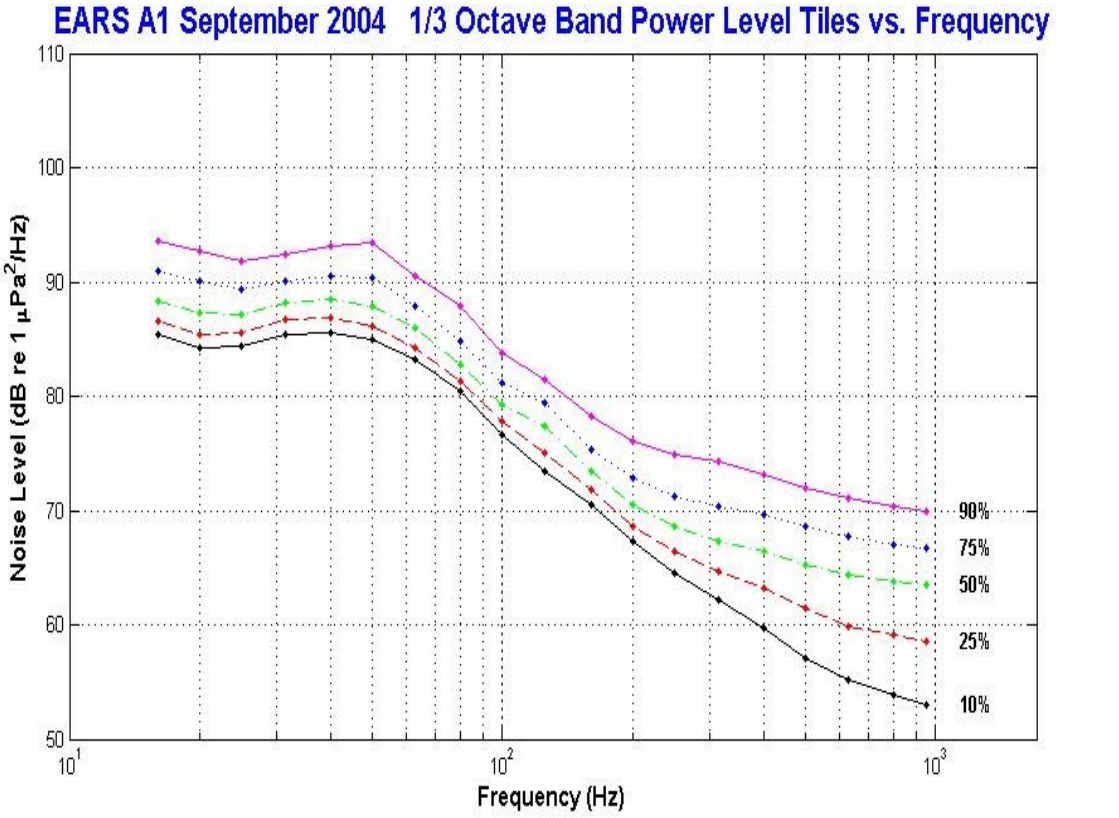

Figure B.6 September 2004 Percentile Plot

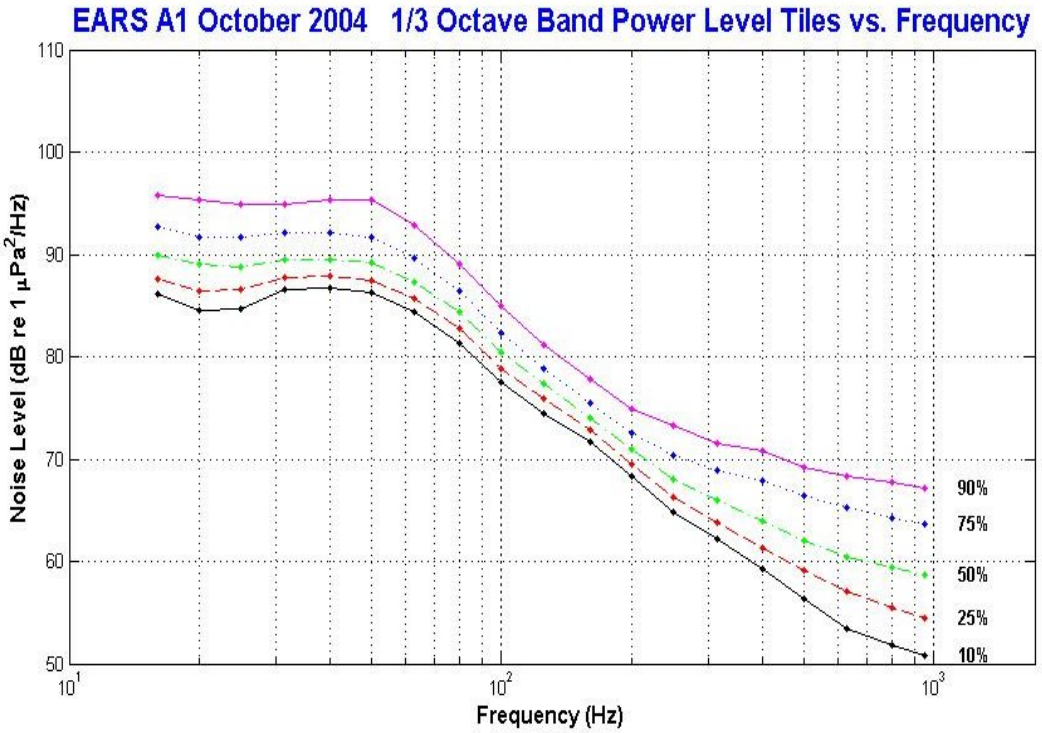

Figure B.7 October 2004 Percentile Plot

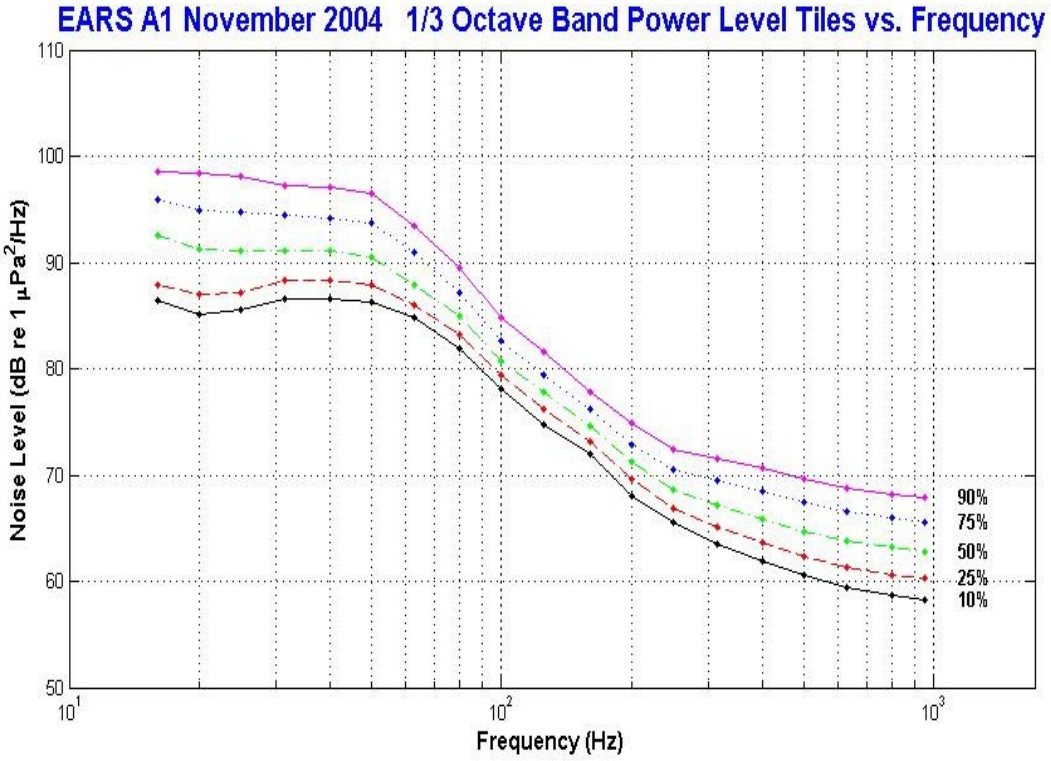

Figure B.8 November 2004 Percentile Plot

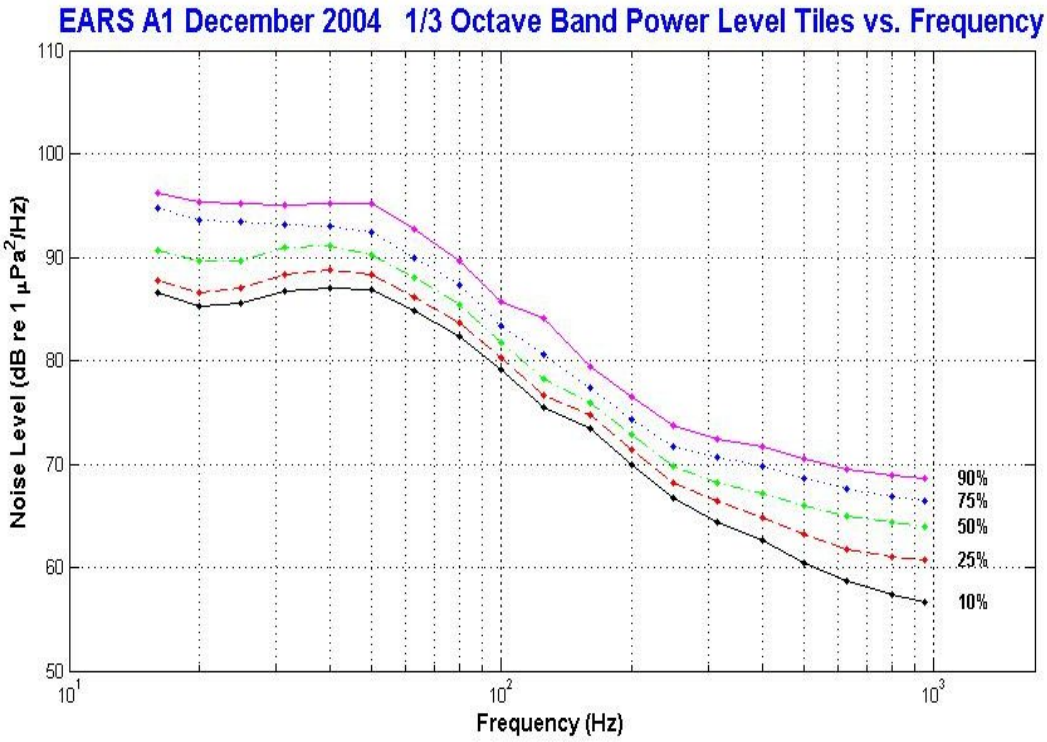

Figure B.9 December 2004 Percentile Plot

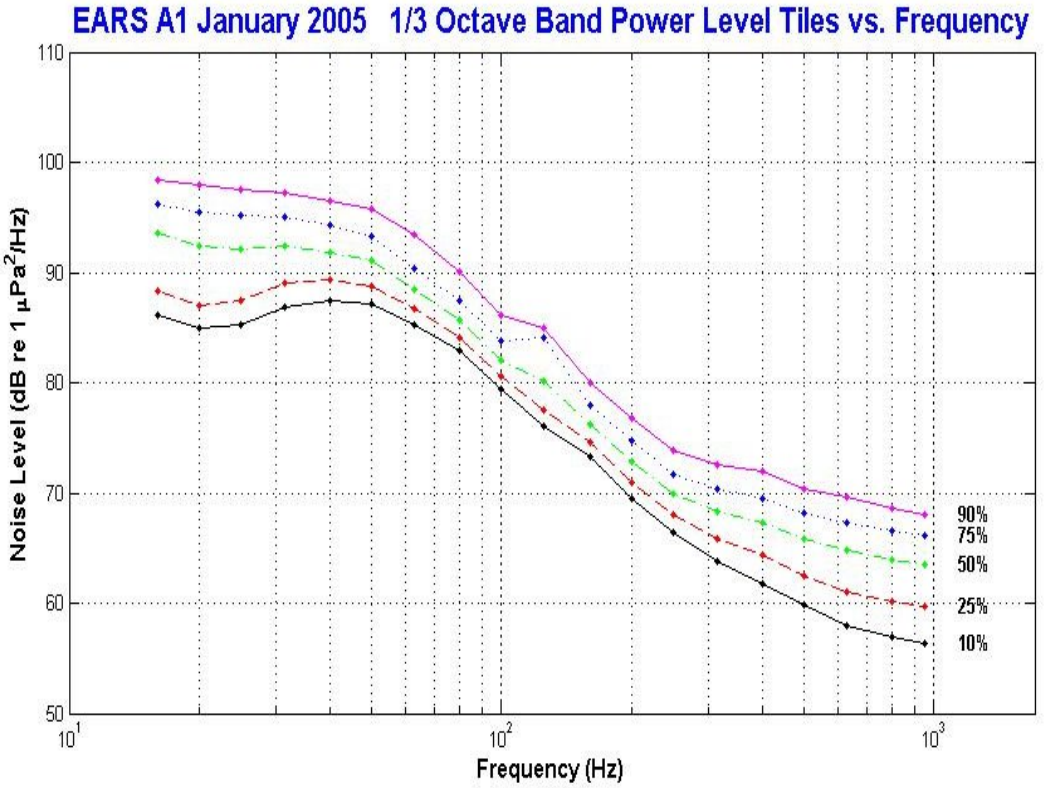

Figure B.10 January 2005 Percentile Plot

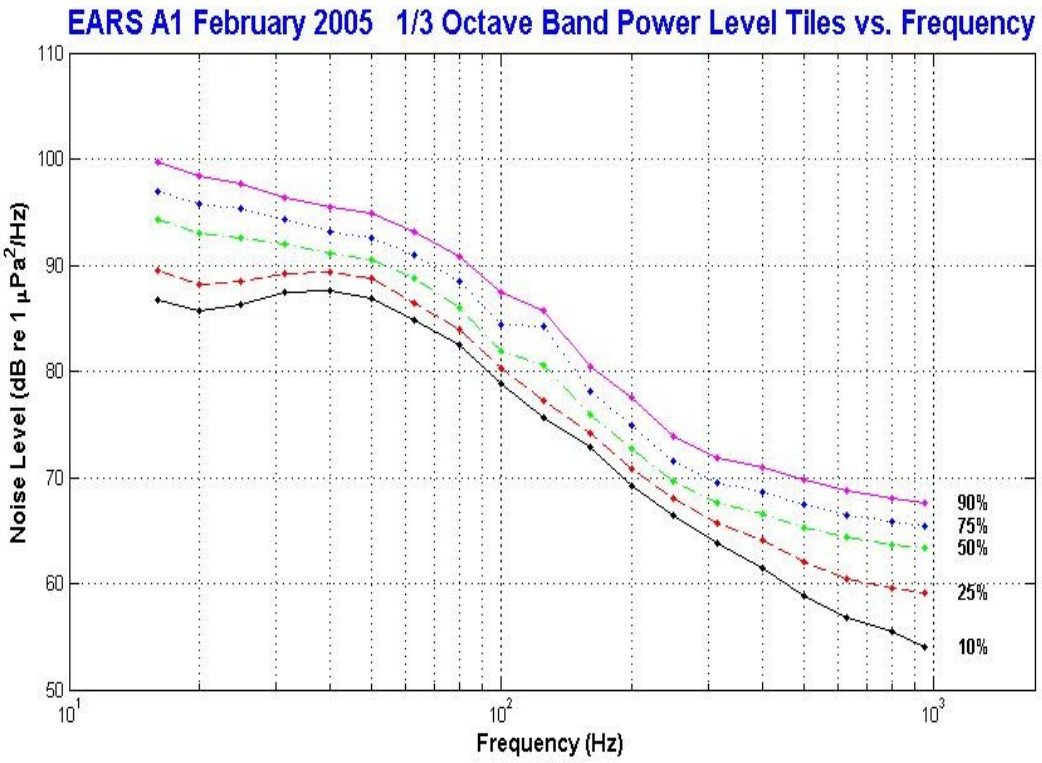

Figure B.11 February 2005 Percentile Plot

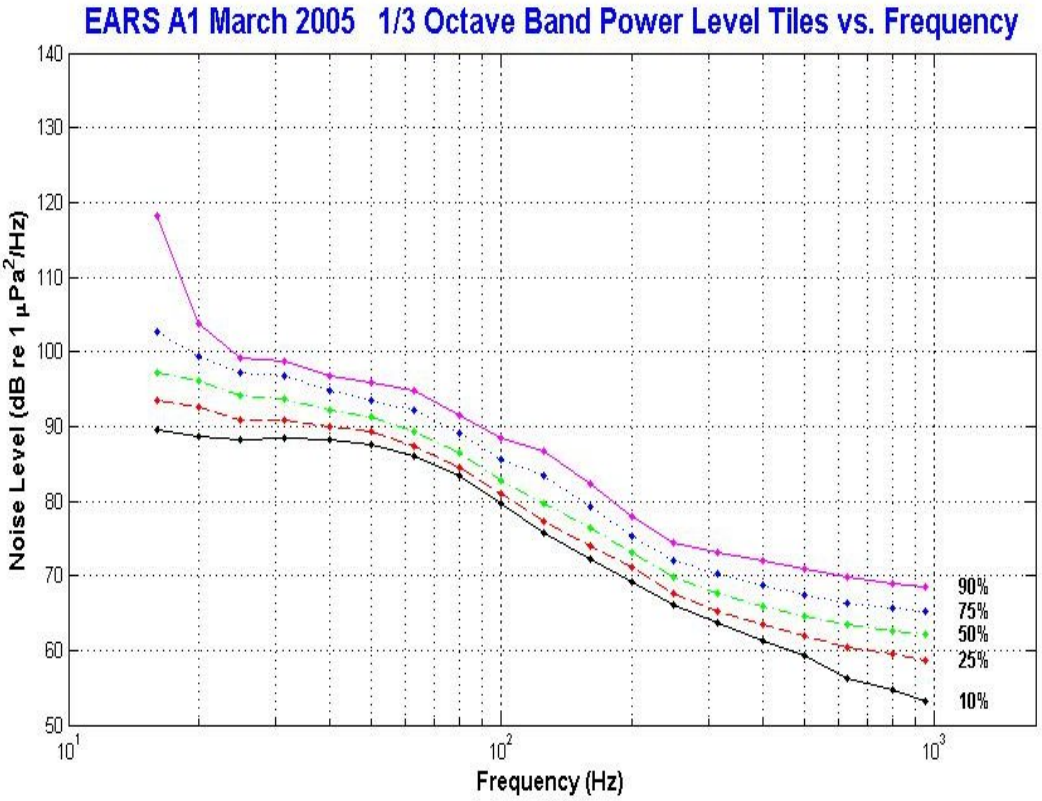

Figure B.12 March 2005 Percentile Plot

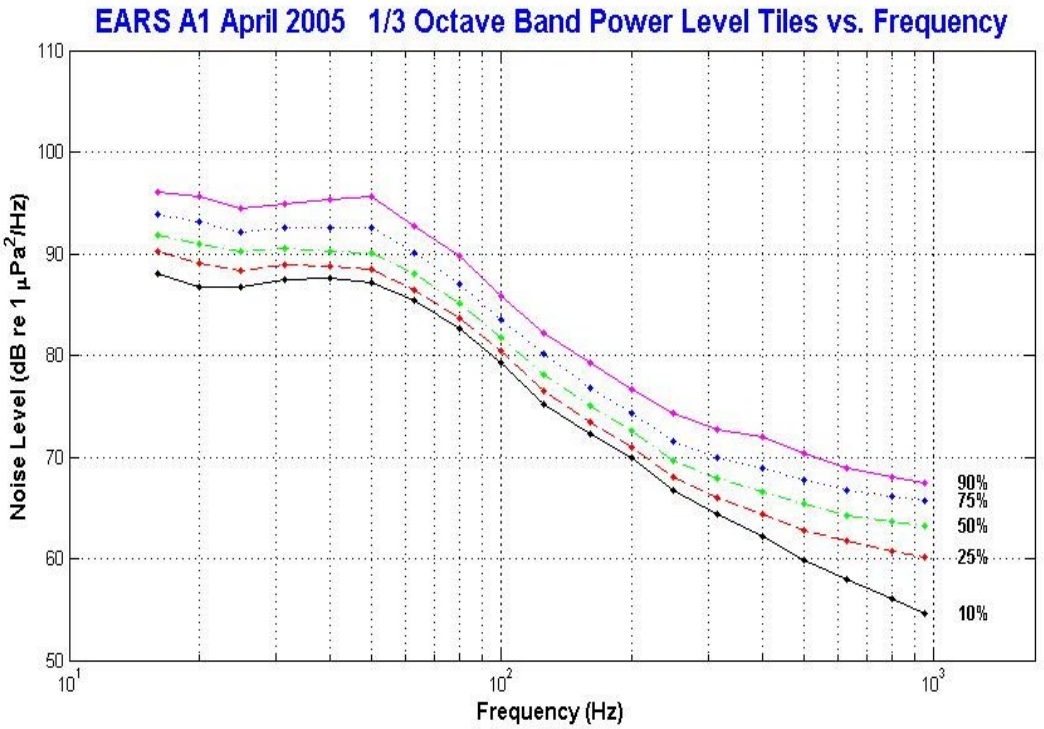

Figure B.13 April 2005 Percentile Plot

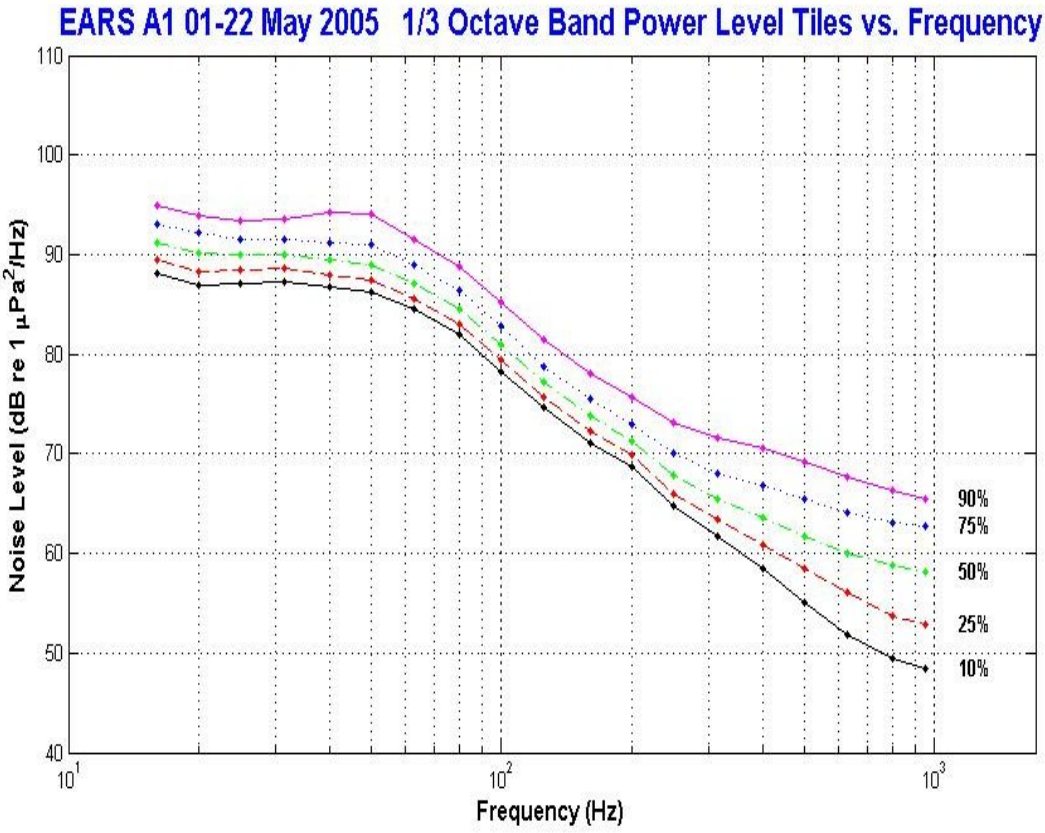

Figure B.14 May 2005 Percentile Plot

Appendix C

Monthly Power at 950 Hz

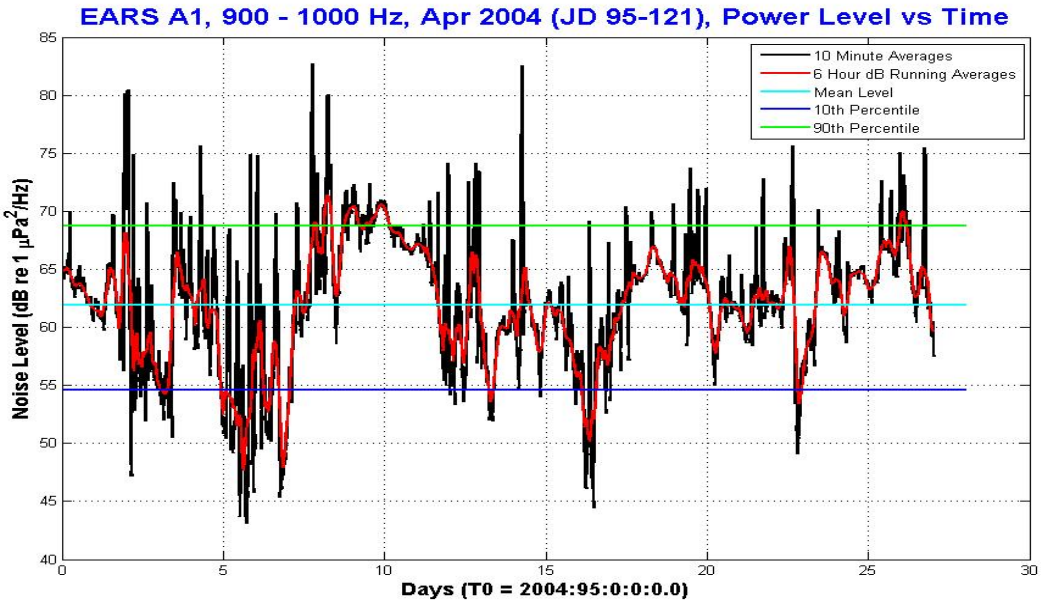

Figure C.1 April 2004 Power at 950 Hz

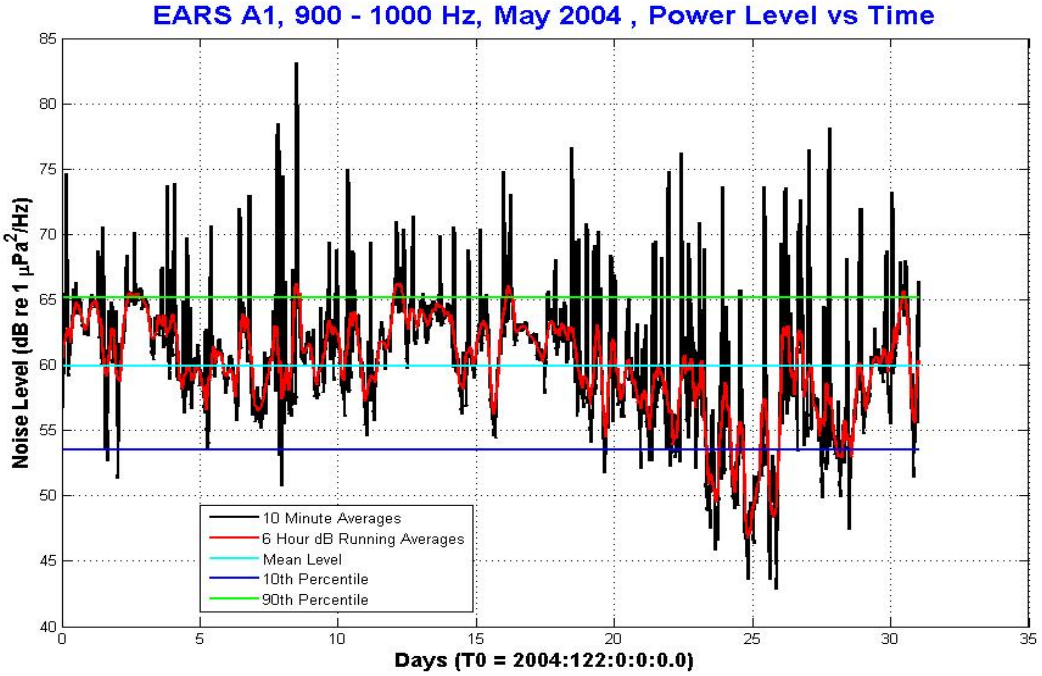

Figure C.2 May 2004 Power at 950 Hz

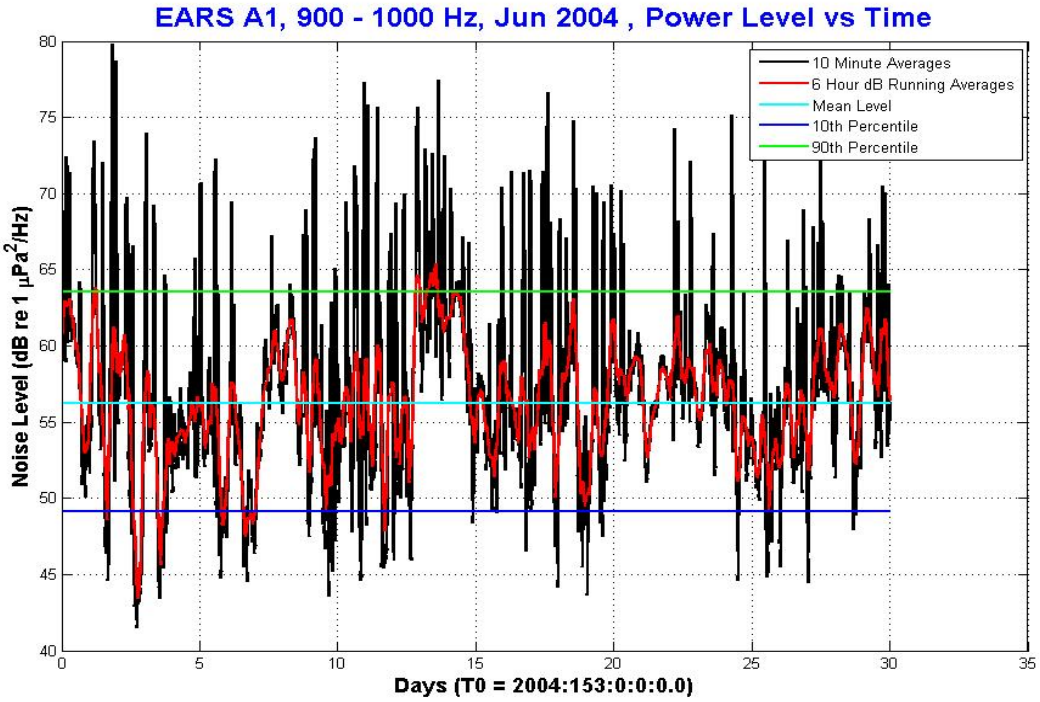

Figure C.3 June 2004 Power at 950 Hz

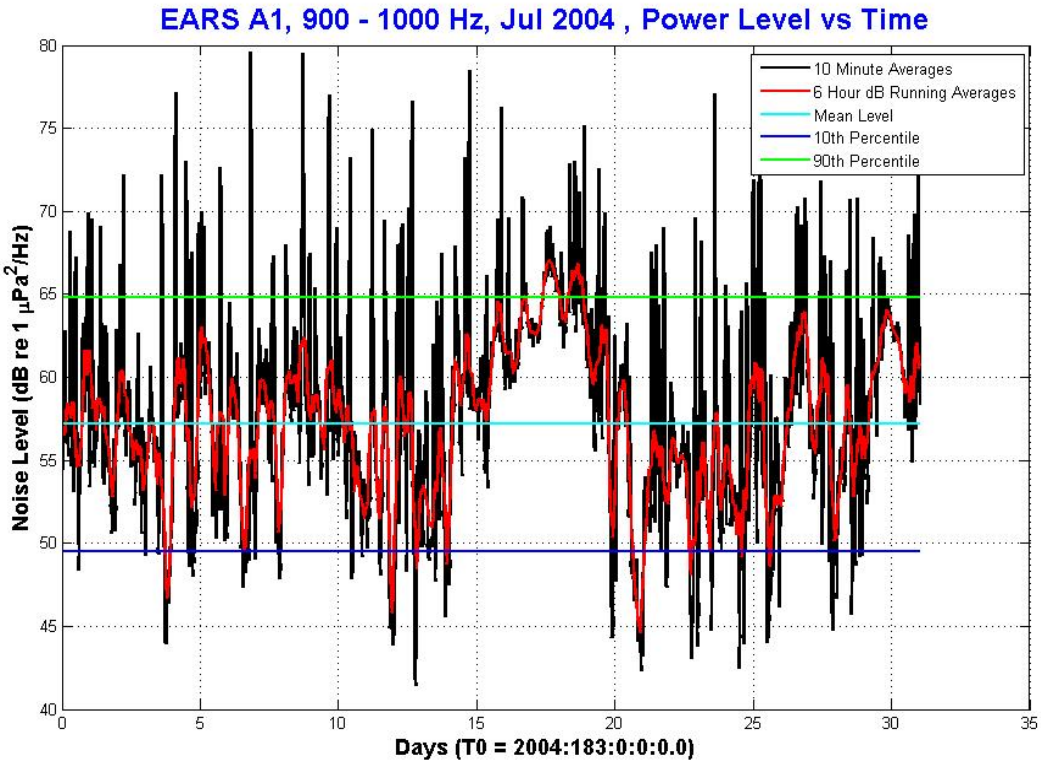

Figure C.4 July 2004 Power at 950 Hz

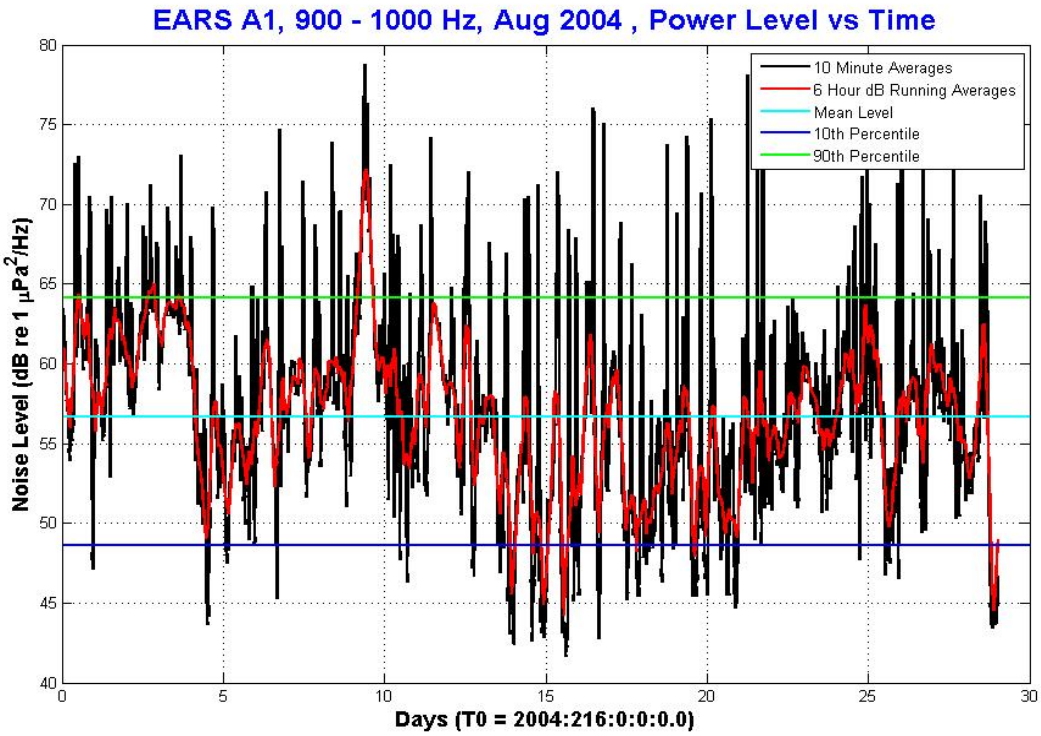

Figure C.5 August 2004 Power at 950 Hz

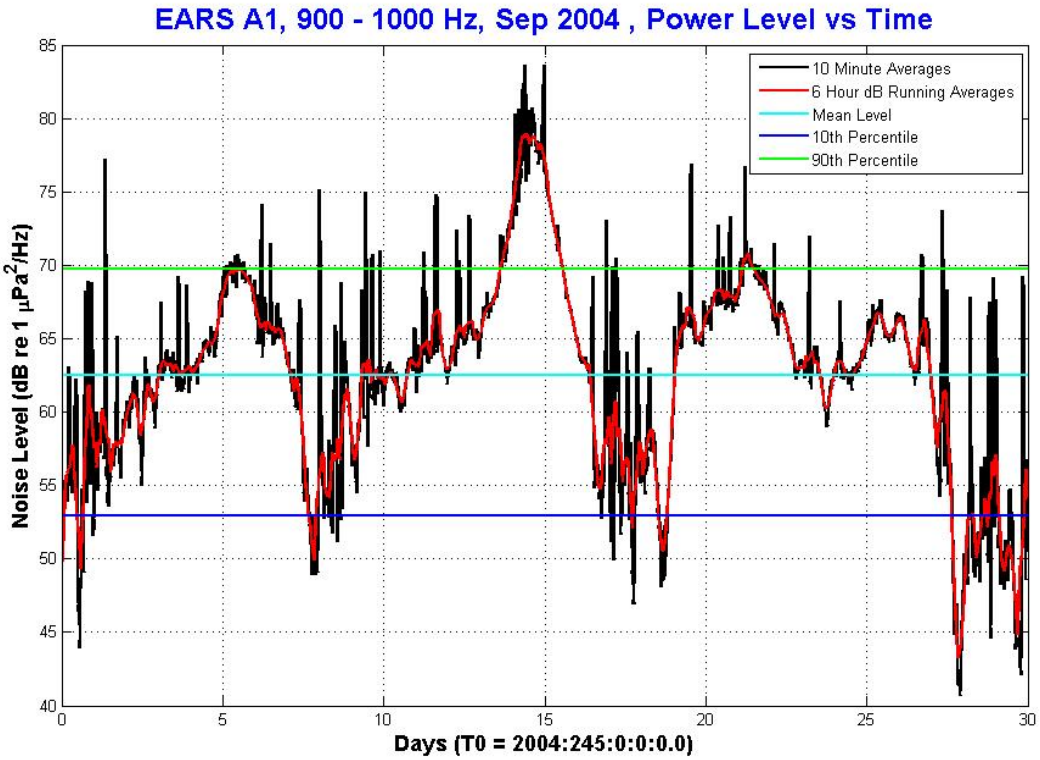

Figure C.6 September 2004 Power at 950 Hz

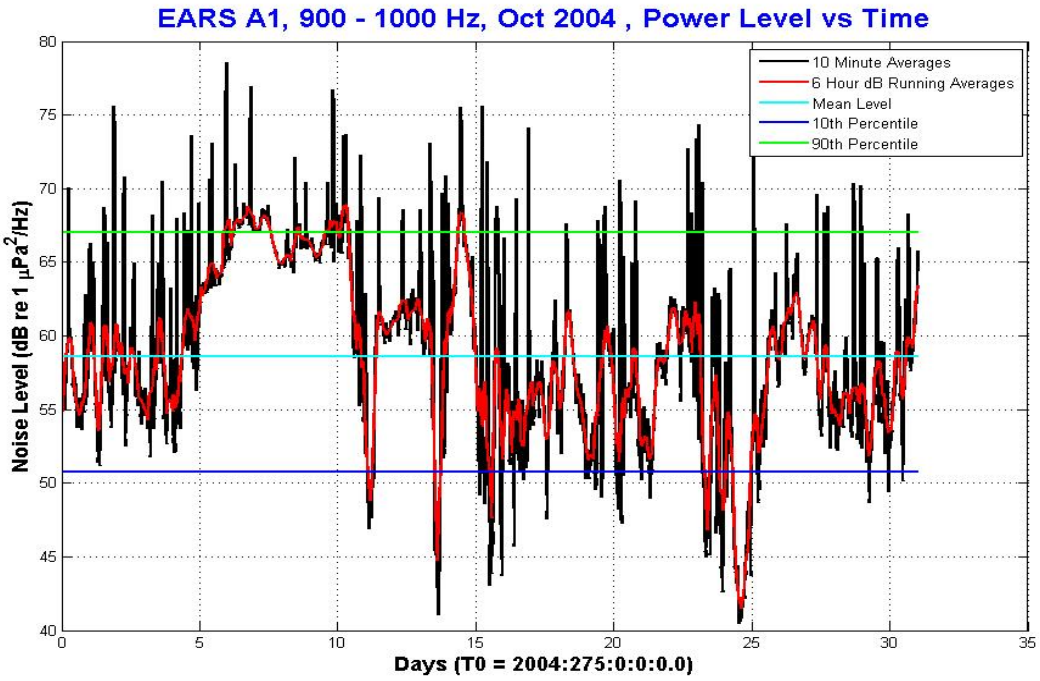

Figure C.7 October 2004 Power at 950 Hz

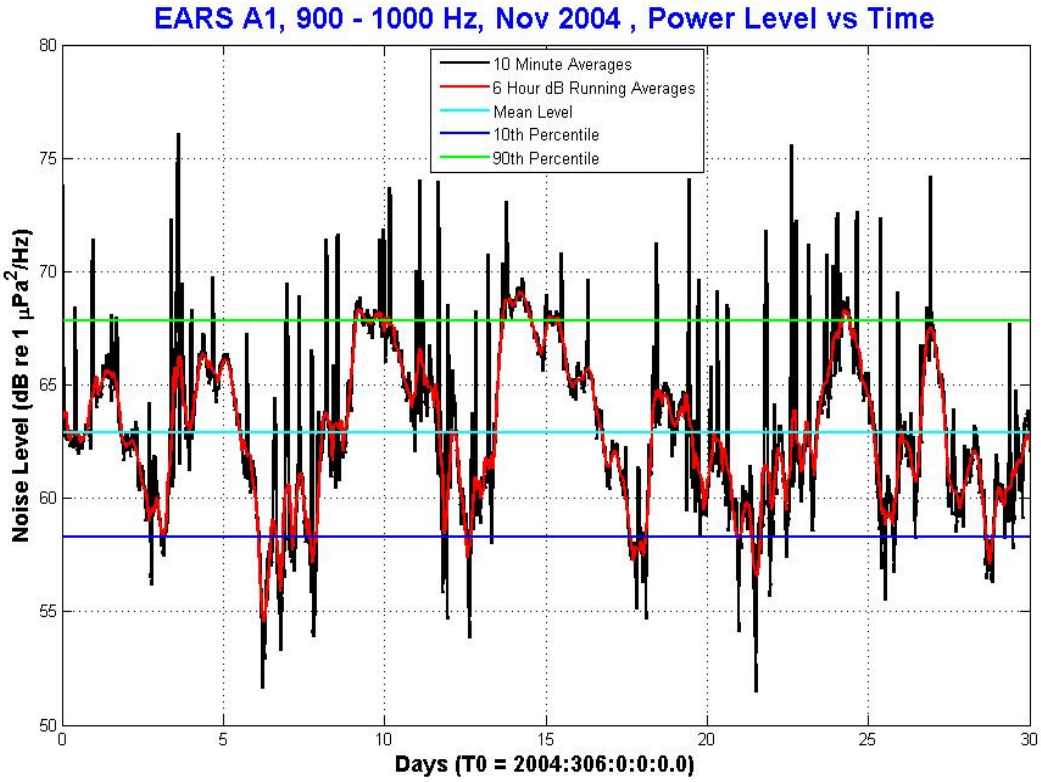

Figure C.8 November 2004 Power at 950 Hz

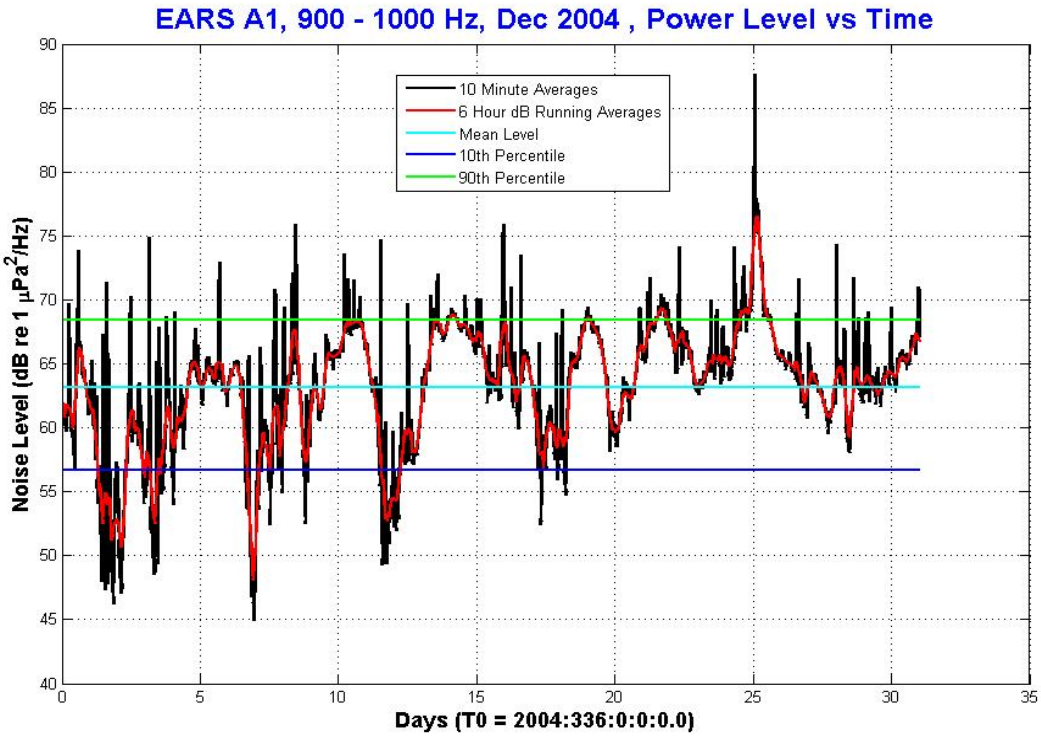

Figure C.9 December 2004 Power at 950 Hz

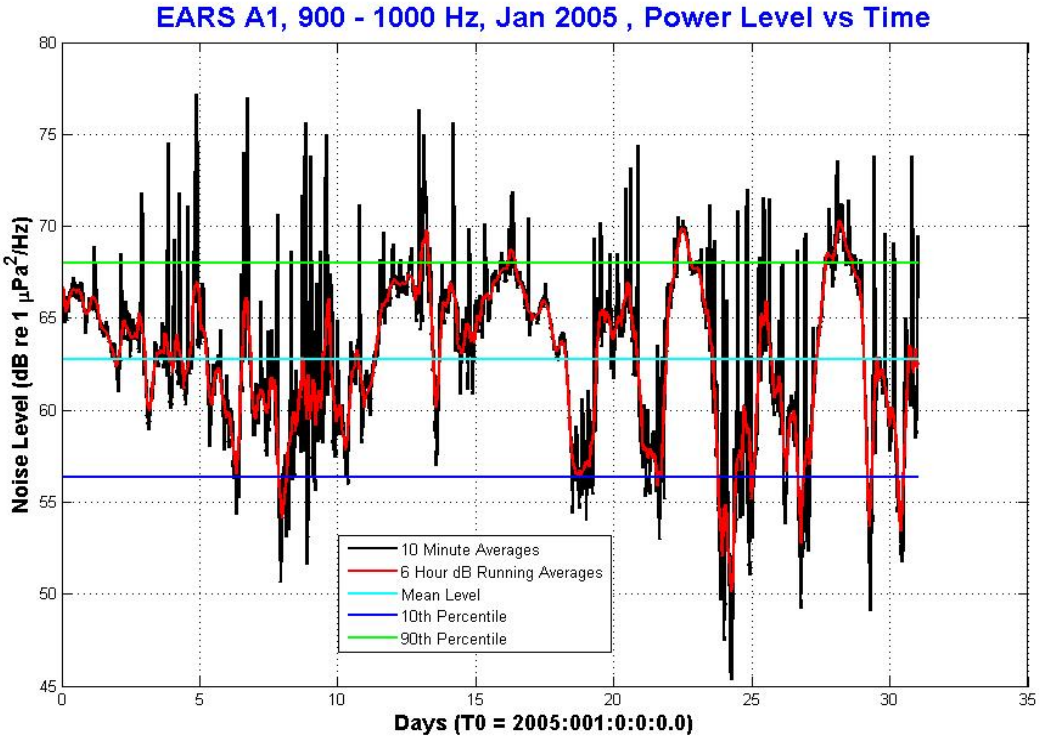

Figure C.10 January 2005 Power at 950 Hz

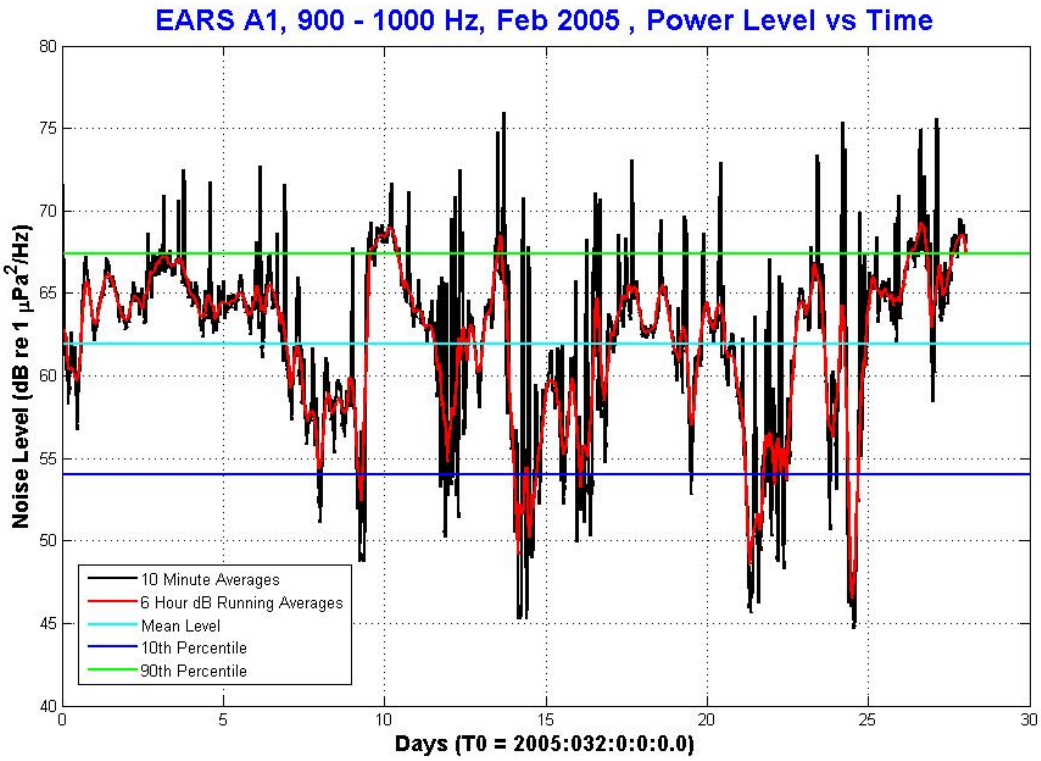

Figure C.11 February 2005 Power at 950 Hz

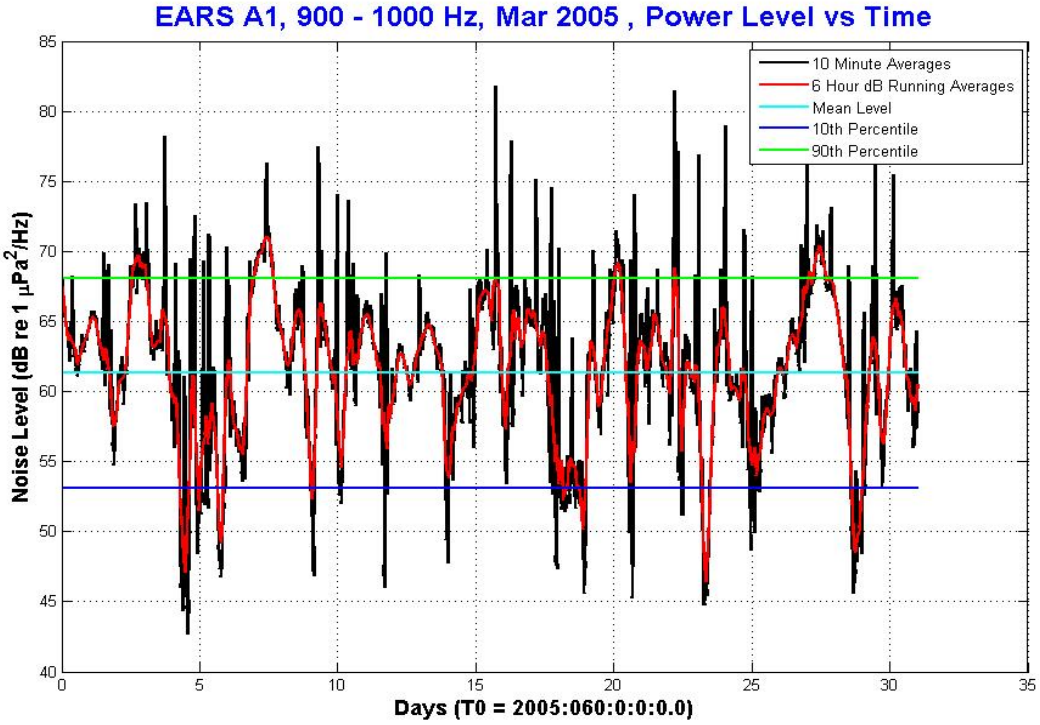

Figure C.12 March 2005 Power at 950 Hz

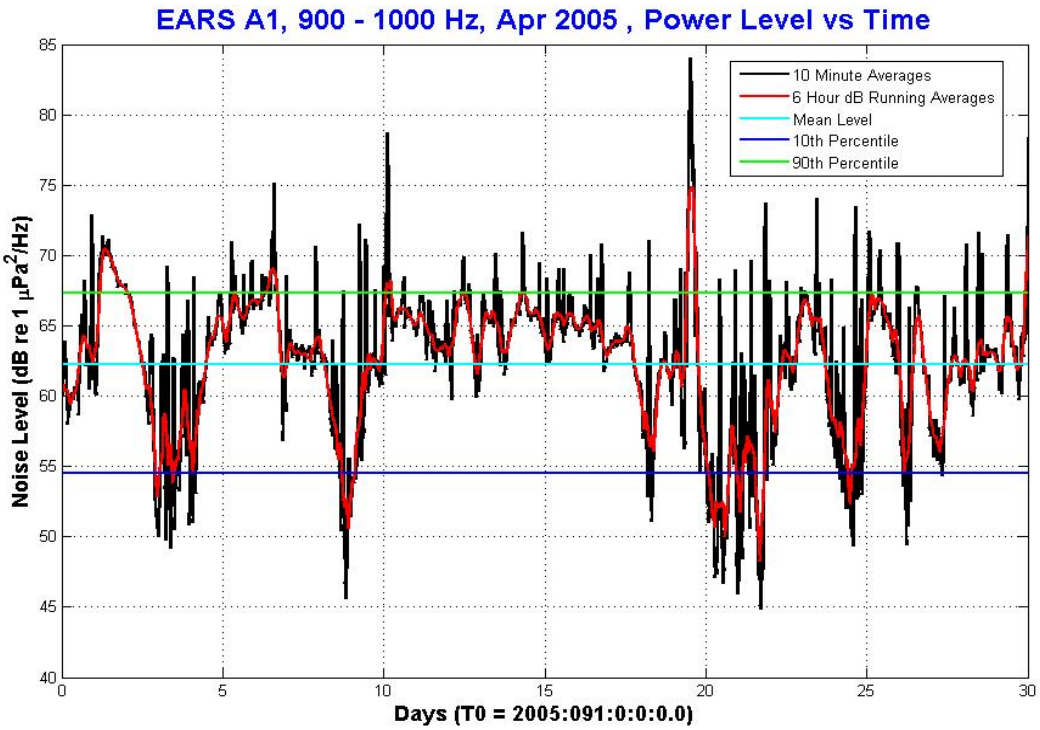

Figure C.13 April 2005 Power at 950 Hz

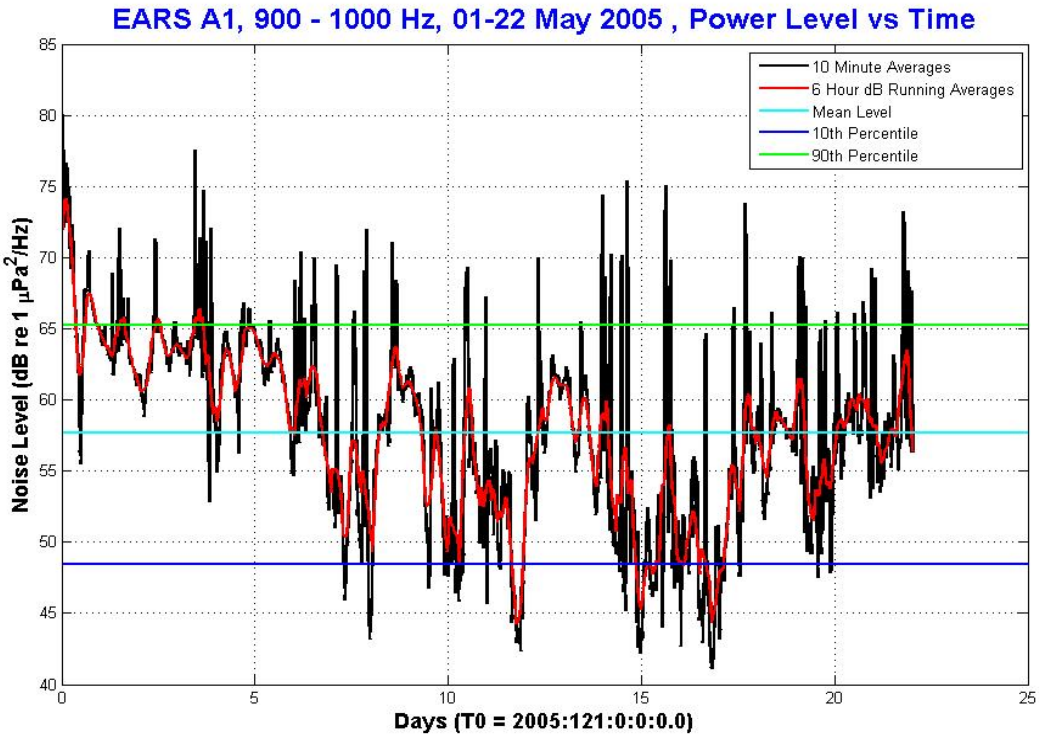

Figure C.14 May 2005 Power at 950 Hz

Appendix D

Monthly Significant Wave Heights

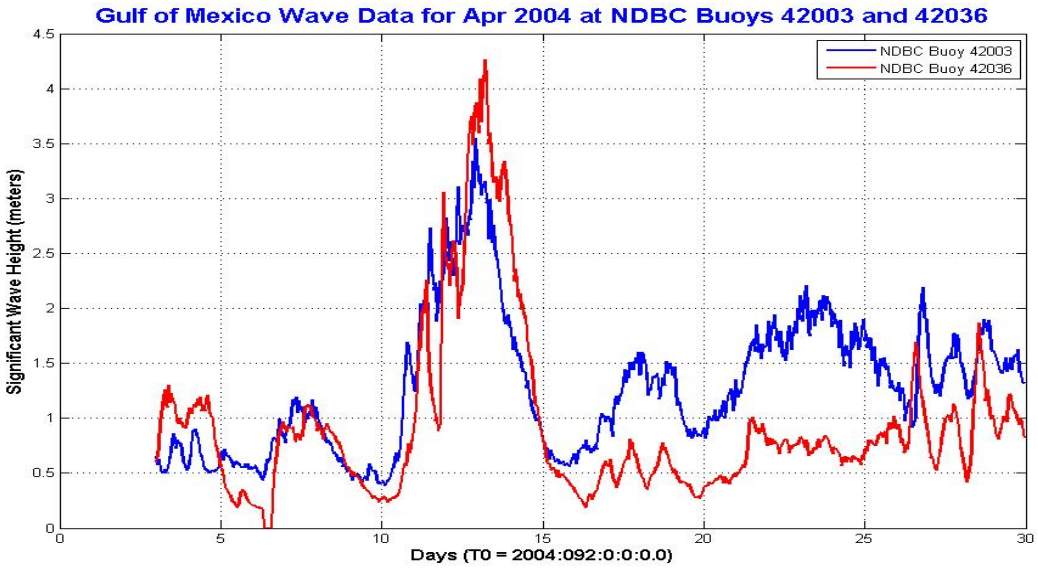

Figure D.1 April 2004 Significant Wave Height

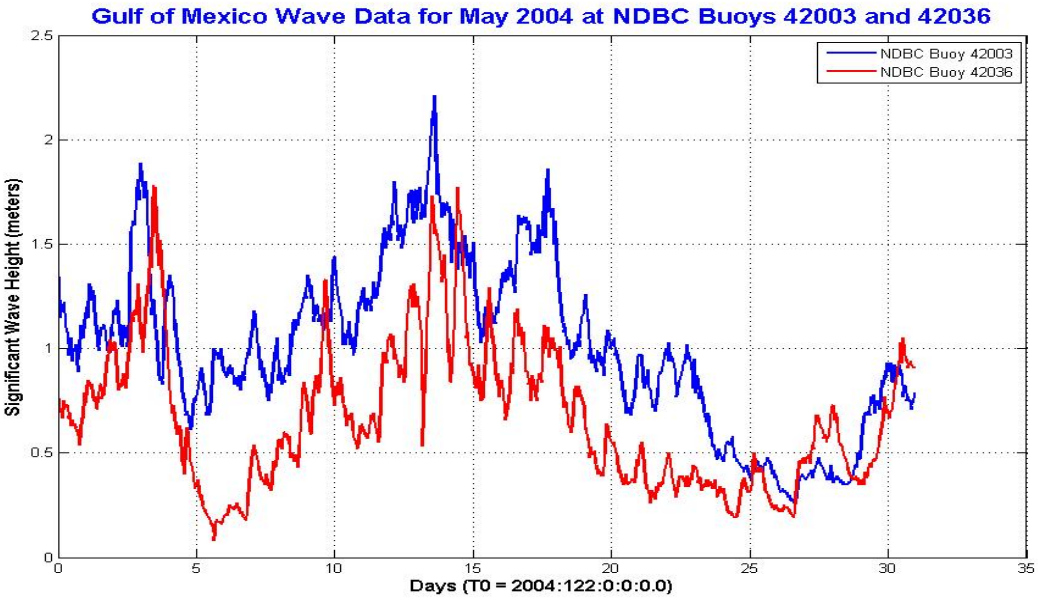

Figure D.2 May 2004 Significant Wave Height

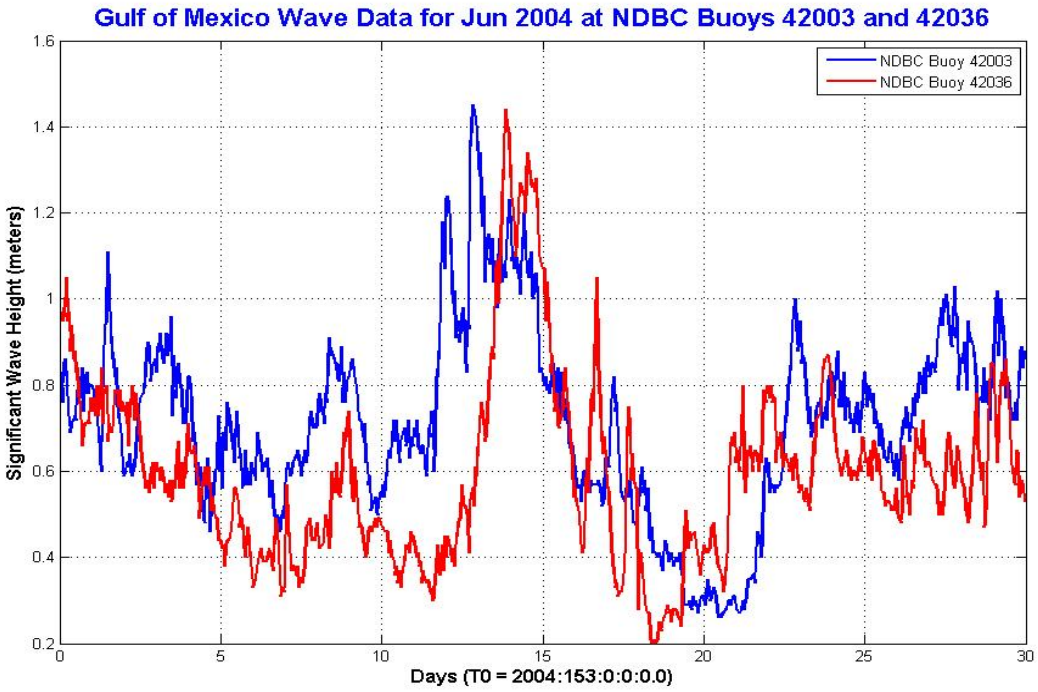

Figure D.3 June 2004 Significant Wave Height

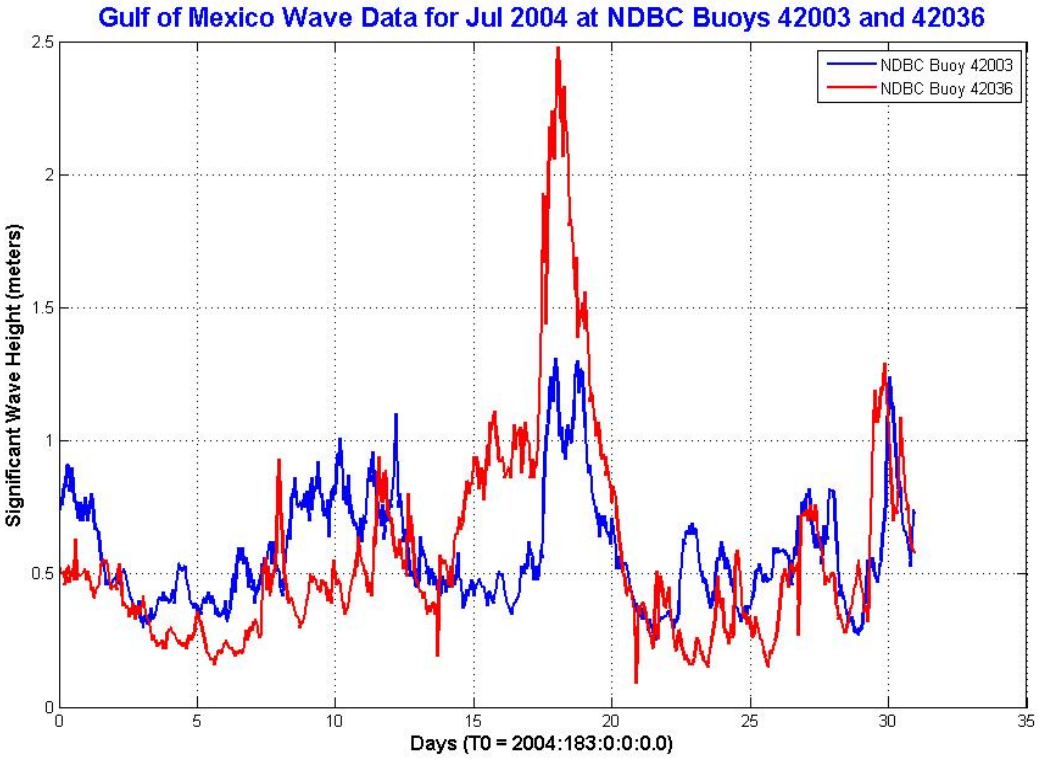

Figure D.4 July 2004 Significant Wave Height

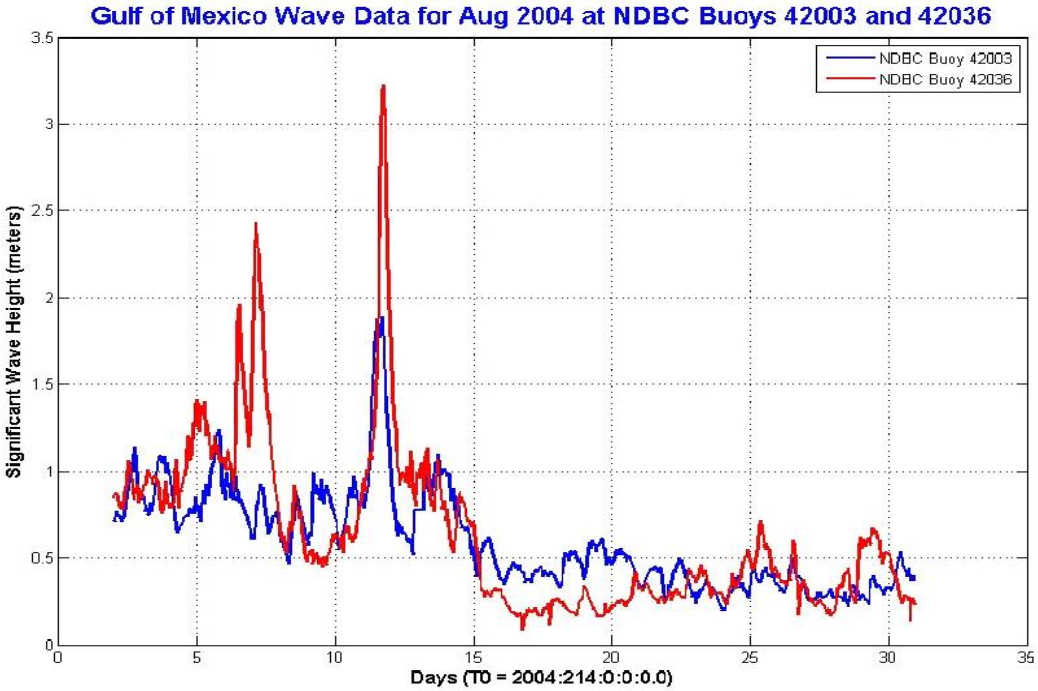

Figure D.5 August 2004 Significant Wave Height

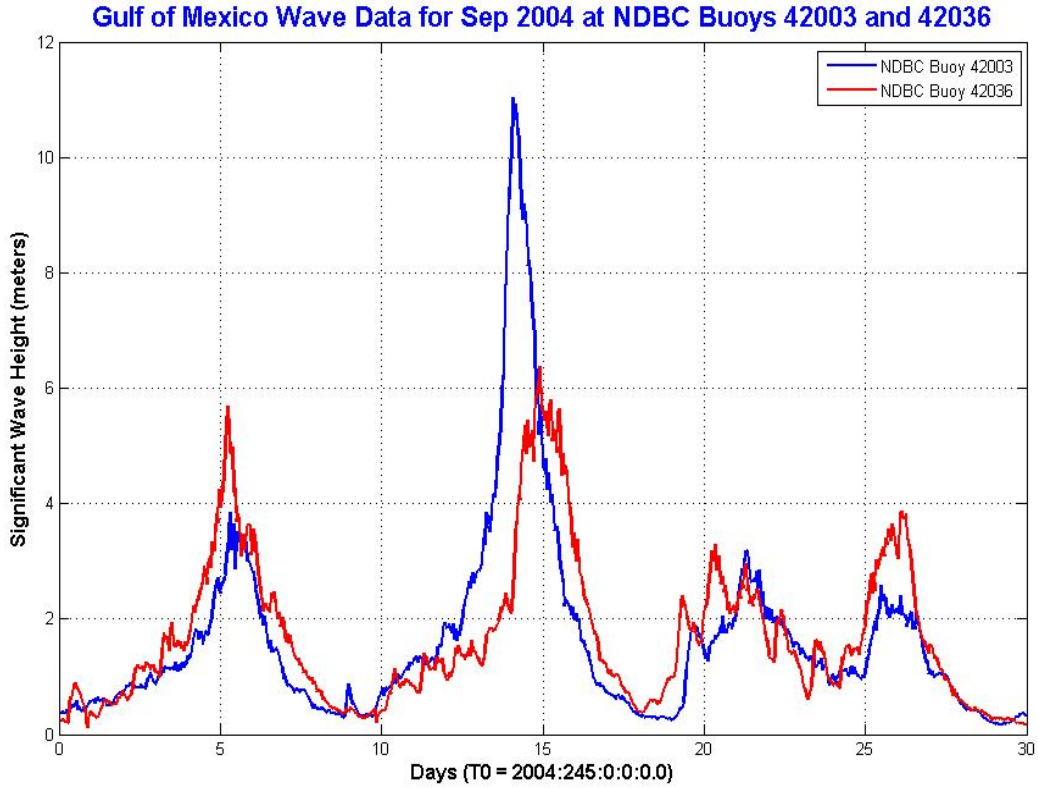

Figure D.6 September 2004 Significant Wave Height

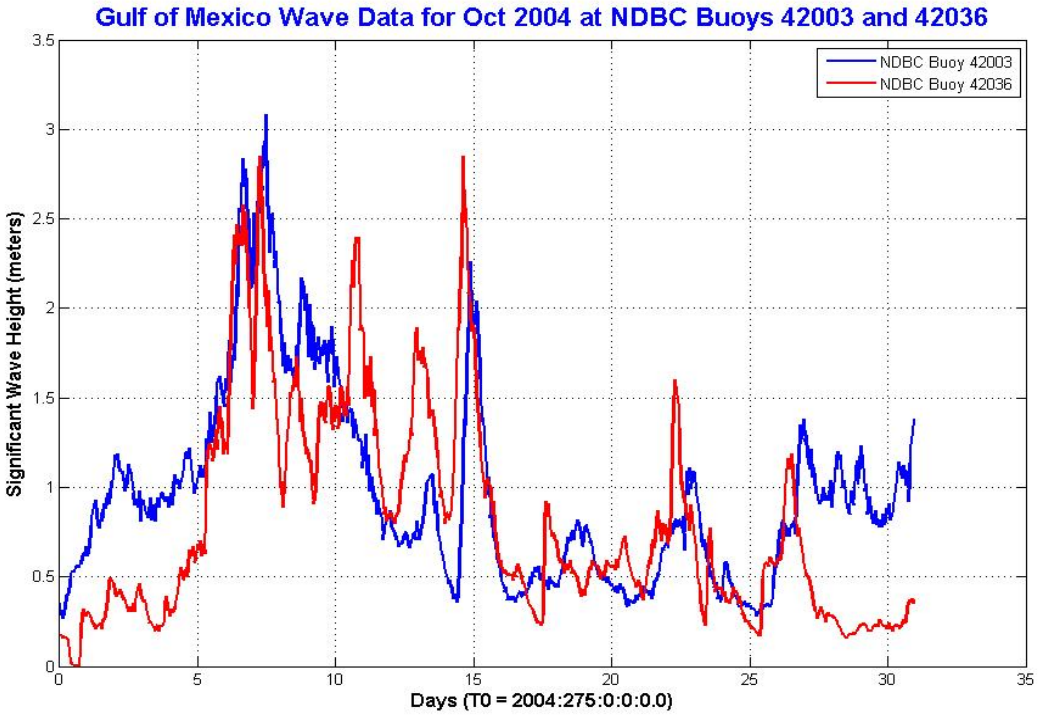

Figure D.7 October 2004 Significant Wave Height

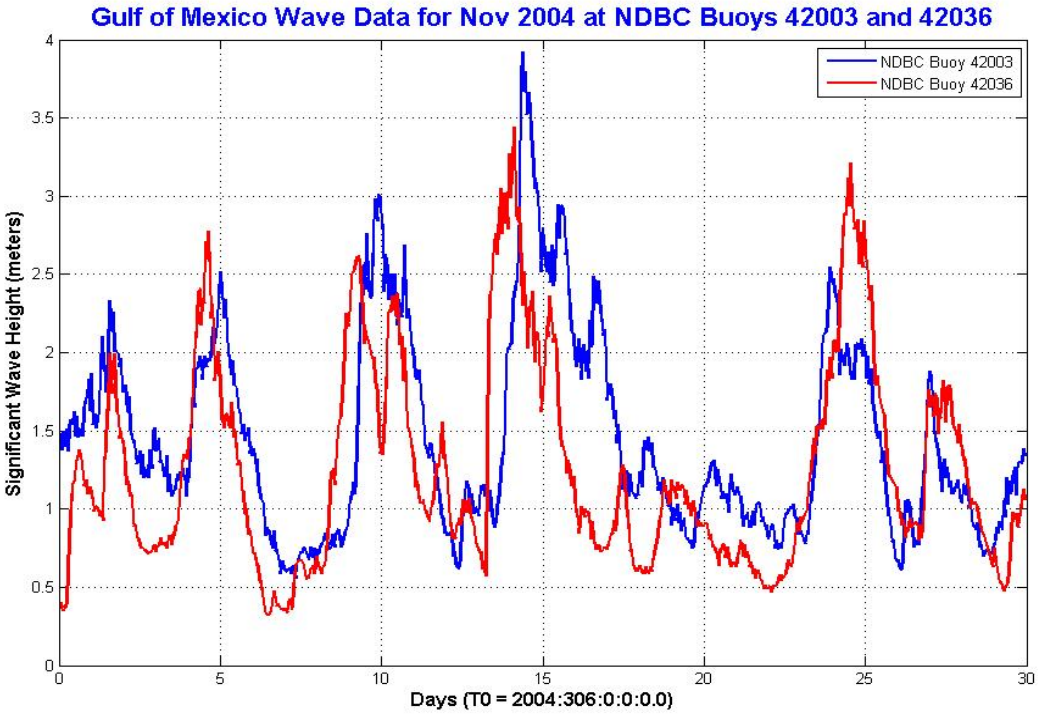

Figure D.8 November 2004 Significant Wave Height

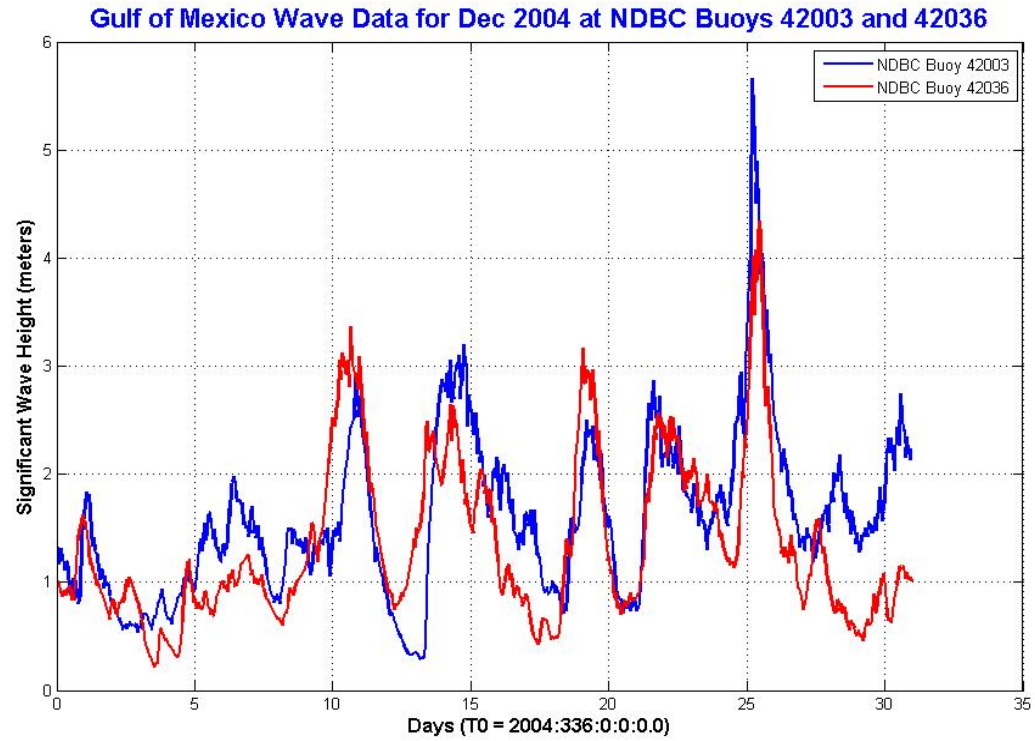

Figure D.9 December 2004 Significant Wave Height

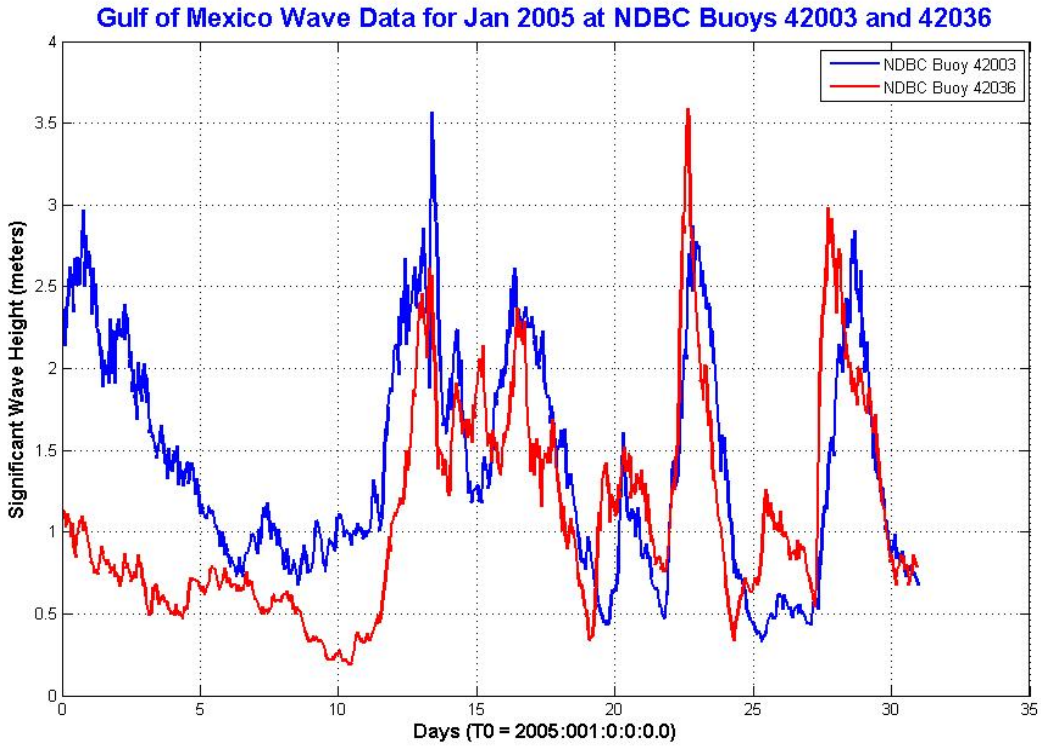

Figure D.10 January 2005 Significant Wave Height

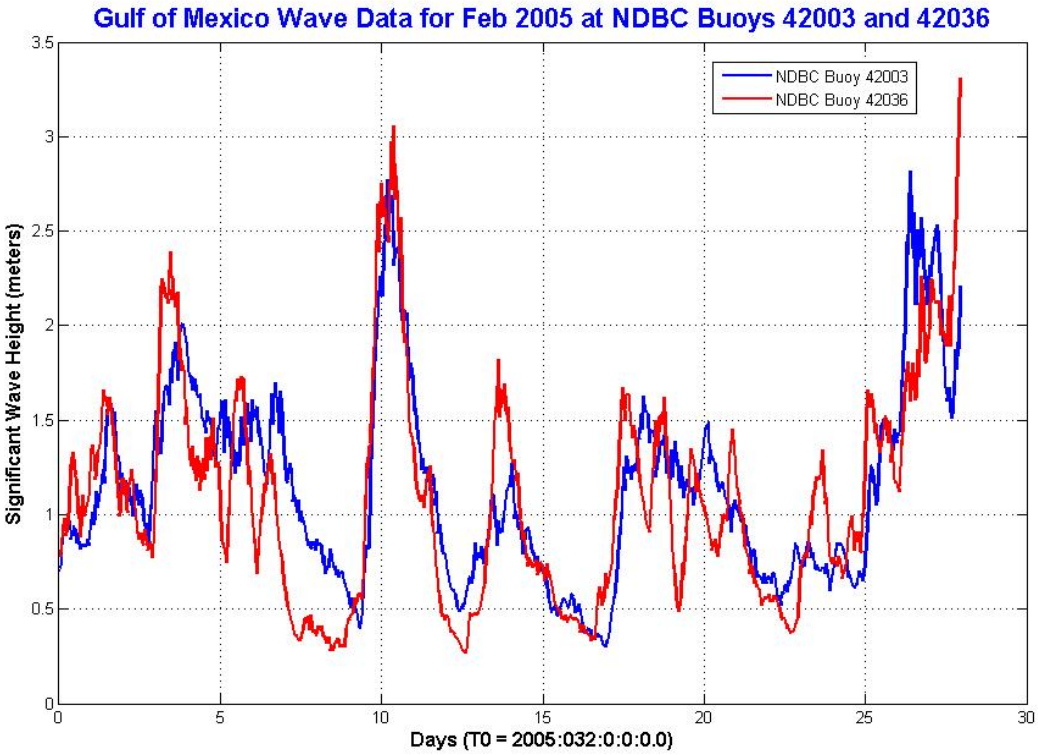

Figure D.11 February 2005 Significant Wave Height

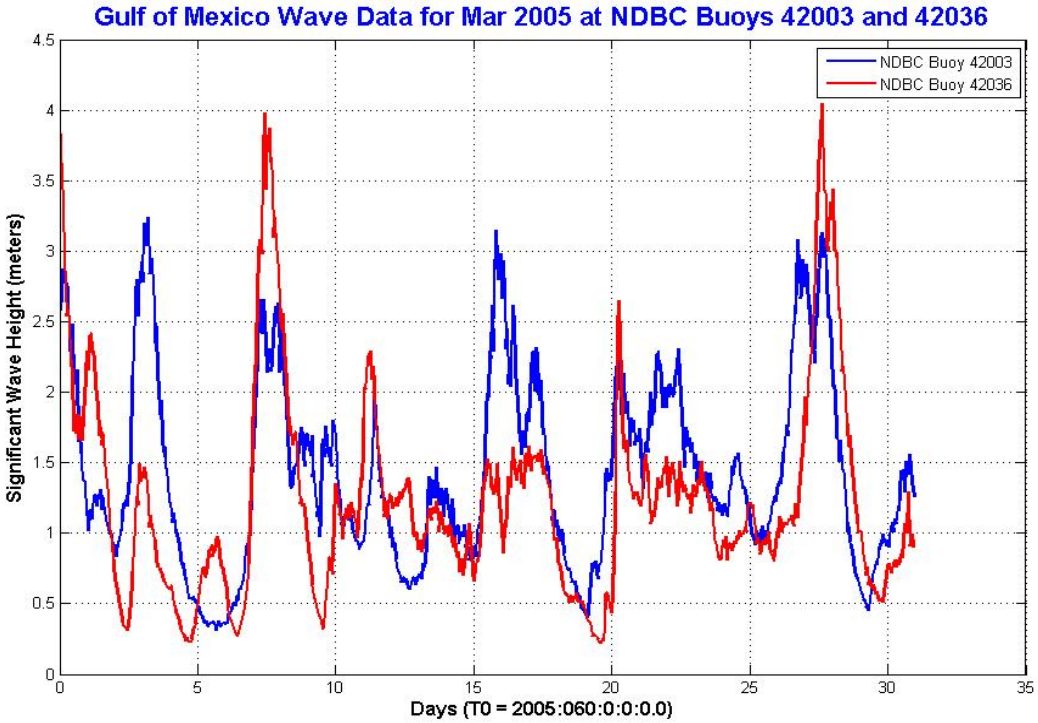

Figure D.12 March 2005 Significant Wave Height

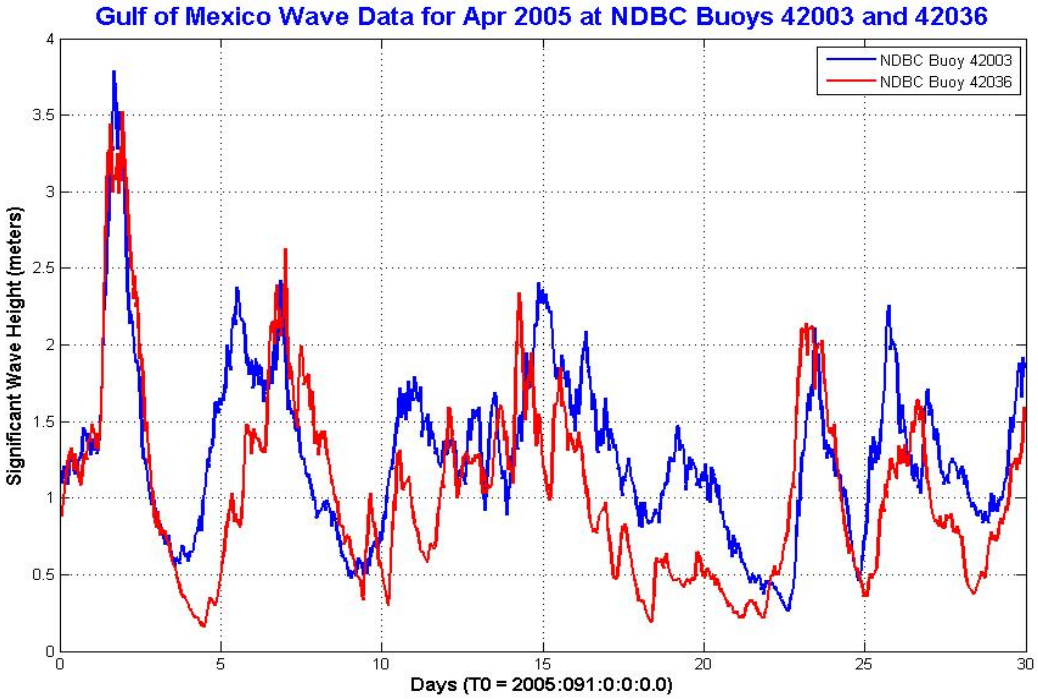

Figure D.13 April 2005 Significant Wave Height

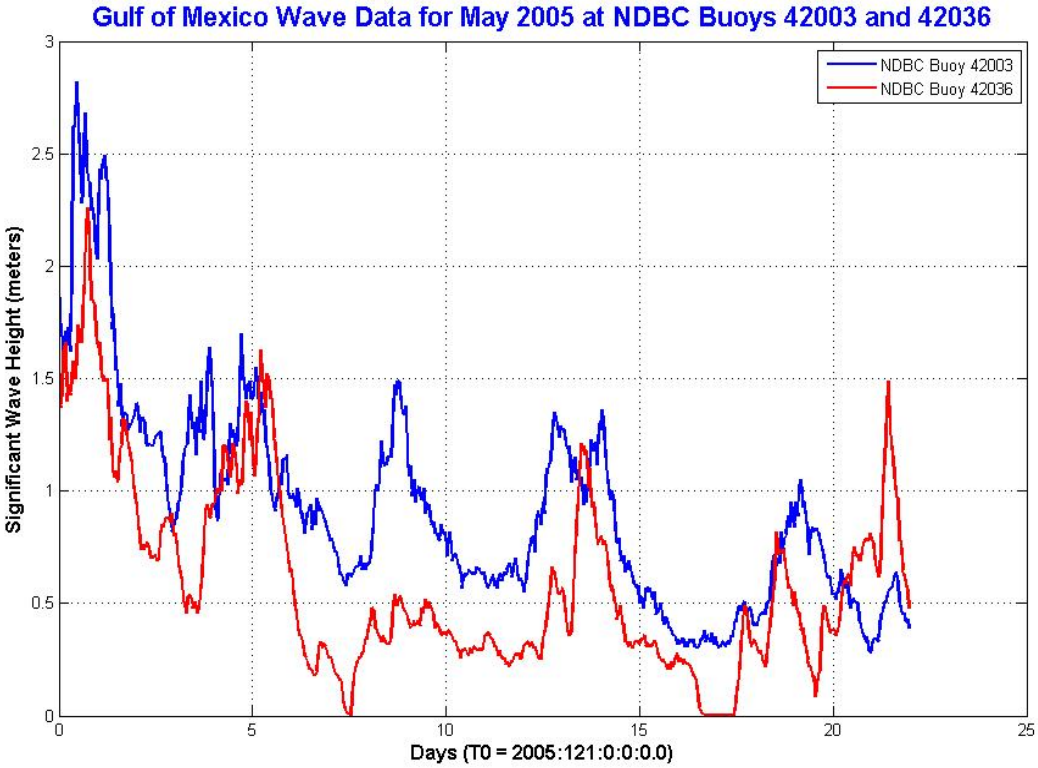

Figure D.14 May 2005 Significant Wave Height

Appendix E

Copyright Permission

-----Original Message-----
From: Steven Babin [mailto:steven.babin@jhuapl.edu]
Sent: Monday, October 29, 2007 15:35
To: Snyder, Mark A CIV N62306 [Mark.A.Snyder1@navy.mil]
Cc: sterner@tesla.jhuapl.edu; susan.furney@jhuapl.edu
Subject: Re: Request To Use Hurricane Track Images for Dissertation

Dear Mark,

Thank you for your request. That sounds like very interesting work!
You have our permission providing the copyright remains on the images.

Which track images did you want? Ray revised the track map software
but we haven't had time to update all the maps. If you let us know
which ones you want, we can use the new software that we believe
makes better looking maps. As an example of the new map, see
http://fermi.jhuapl.edu/hurr/07/humberto/Humberto.png
Compare this with an older version at
http://fermi.jhuapl.edu/hurr/06/ernesto/ernesto.gif
Please let us know what you think of these versions.

Thanks again for asking,

Steve

On Mon, 2007-10-29 at 16:22, Snyder, Mark A CIV N62306 wrote:

> Dear Steven Babin and Ray Sterner,
>
> I am a graduate student at the University of New Orleans. I am
> trying to finish a dissertation on ambient noise in the Gulf of Mexico.
> I have some acoustic data collected during 2004 and 2005. In
> particular, I have acoustic recordings from the summer of 2004
> during the passage of four hurricanes. I would like to request the use
> of one or more of your hurricane track images in my dissertation.
> I talked to Susan Furney and she said I could email you directly.
>
> Thank you for your consideration of my request.
>
> Sincerely,
>
> Mark A. Snyder
> Naval Oceanographic Office
> Stennis Space Center, MS 39522

Appendix F

Statistical Definitions

Autocorrelation function $R(\tau)$ of a random process $X(t)$: $R(\tau) = E[X(t+\tau)X(t)]$

$R(\tau)$ is the inverse Fourier transform of the power spectral density $S(\omega)$:

$$R(\tau) = \int_{-\infty}^{\infty} S(\omega) e^{+i\omega\tau} d\omega$$

Coherence time is the time for the autocorrelation function of a time series to fall to e^{-1} of its central (zero-lag) value. The coherence time is a measure of the effective width of the autocorrelation function, or how long a time series is coherent with itself.

Correlation coefficient ρ of two random variables X and Y is

$\rho = \frac{\text{cov}(x,y)}{\sigma_x \sigma_y}$ = normalized covariance, where

$cov(x,y) = E[(X - \mu_x)(Y - \mu_y)]$ = covariance of the two random variables X and Y

σ_x = standard deviation of the random variable X

σ_y = standard deviation of the random variable Y

Since ρ is normalized, $-1 \leq \rho \leq +1$

Expected value of the random variable $X = E[X]$ = mean value of $X = \mu_x$

Kurtosis = $\frac{1}{n} \sum_{i=1}^{n} \left(\frac{x_i - \mu}{\sigma} \right)^4$

Kurtosis is the fourth standardized moment = fourth central moment divided by the fourth power of the standard deviation. Kurtosis is a measure of how outlier-prone or how "peaked" a PDF is. The kurtosis of the normal distribution is 3. Distributions that are more outlier-prone than the normal distribution have kurtosis greater than 3 and are called leptokurtic; distributions that are less outlier-prone than the normal distribution have kurtosis less than 3 and are called platykurtic. Higher kurtosis means more of the variance is due to infrequent extreme deviations, as opposed to frequent modestly-sized deviations.

Mean is the sample average: mean = $\mu = \frac{1}{n} \sum_{i=1}^{n} x_i$

Median is the 50th percentile of a sample. Half of the sample values will fall below the median. The median is a robust estimate of the center of a sample of data, since outliers have little effect on it.

Percentile – The point x_n that satisfies $P\{X < x_n\} = n\ \%$ is called the $n\ \%$ percentile value of the distribution of the random variable X. For example, 10% of the values in a distribution will fall below the 10th percentile value x_{10}, while 90% of the values in a distribution will fall below the 90th percentile value x_{90}.

Power spectral density $S(\omega)$ of a random process X(t) is the Fourier transform of the

autocorrelation function $R(\tau)$: $S(\omega) = \frac{1}{2\pi} \int_{-\infty}^{\infty} R(\tau) e^{-i\omega\tau} d\tau$

Random process X(t) is a continuous function of time.

Skewness = $\frac{1}{n} \sum_{i=1}^{n} \left(\frac{x_i - \mu}{\sigma} \right)^3$

Skewness is the third standardized moment = third central moment divided by the cube of the standard deviation. Skewness is a measure of the asymmetry of the probability density function (PDF) around the sample mean.

If skewness is negative, the data are spread out more to the left side of the mean than to the right. In a negatively skewed distribution, the left tail is longer than the right. (The mass of the distribution is more concentrated on the right side of the PDF.)

If skewness is positive, the data are spread out more to the right side of the mean than to the left. In a positively skewed distribution, the right tail is longer than the left. (The mass of the distribution is more concentrated on the left side of the PDF.)

The skewness of the normal distribution (or any perfectly symmetric distribution) is zero.

Spread of the data is defined as the range of the data (in dB) from the 10th percentile to the 90th percentile.

Standard deviation = $\sigma = \sqrt{\frac{1}{n-1}\sum_{i=1}^{n}\left(x_i - \mu\right)^2}$

The standard deviation (sigma) is the square root of the second moment of the sample about its mean = square root of the variance. The "*n*-1" normalization yields an unbiased estimate of the sample standard deviation.

Time series x_i $i = 1, 2, 3, \ldots n$

The time series x_i is the sampled form of the continuous process X(t).
In this document, the time between samples is usually 10 minutes.
A thirty day month has approximately n = 4320 data points.
The entire fourteen month period has n = 59,365 data points.

Variance = second moment of the sample about its mean = $\frac{1}{n-1}\sum_{i=1}^{n}\left(x_i - \mu\right)^2$ = $E[(X - \mu)^2]$

= $E[X^2] - \mu^2 = \sigma^2$

The "*n*-1" normalization yields an unbiased estimate of the sample variance.

Vita

Mark Alan Snyder was born in DeKalb, Illinois in 1959. He received his B.S. in Engineering Physics from the University of Illinois in 1981. After completing his B.S. he worked as a geophysicist for Shell Oil Company in New Orleans. He received his M.S. in Applied Physics from the University of New Orleans in 1986. For the past twenty-three years he has worked as a physicist/oceanographer for the Naval Oceanographic Office (NAVOCEANO). He currently works in the Ocean Projects Department at NAVOCEANO.